UNIVERSITY OF LIVERPOOL

Intracellular Trafficking and Regulation of Variant B Cystatin C in Retinal Pigment Epithelial Cells

Thesis submitted in accordance with the requirements of the University of Liverpool for the degree of Doctor in Philosophy

Alessandro Riccio

November 2016

Abstract

Cystatin C is an important inhibitor of lysosomal and extracellular cysteine proteases. It is synthesized as a precursor containing a signal sequence that targets the protein to the secretory pathway. In retinal pigment epithelial (RPE) cells, cystatin C is abundantly expressed and secreted, suggesting a critical role in the regulation of the proteolytic activity in the extracellular space, which, if altered, may contribute to diseases such as Age-related Macular Degeneration (AMD). An amino acid substitution in the signal sequence of the precursor cystatin C generates the variant B, which has been linked to an increased risk of developing AMD and Alzheimer's disease (AD). This mutation has been reported to affect protein trafficking, resulting in decreased secretion and mitochondrial mislocalization. Recently, however, both its disease association as well as the effect on the protein trafficking have been questioned. The main aim of my study was to further investigate the trafficking and secretion of the mutated cystatin C. Recombinant wild-type and variant B cystatin C constructs, untagged or linked to different tags (EGFP, FLAG, HA), were transfected into RPE cell lines. Intracellular localization was investigated by imaging and subcellular fractionation. Protein trafficking and secretion were examined by analysing protein release into the culture media and the use of inhibitors of the secretory pathway. In addition, glycosylation sites were engineered to monitor transition through the Endoplasmic Reticulum (ER) and Golgi apparatus. Constructs encoding the signal sequence linked to EGFP were also used to evaluate the targeting properties of the variant B signal sequence. In the second part of my study, the efficiency of signal sequence cleavage was investigated by analysing the levels and localization of the precursor fraction by immunoprecipitation and imaging. The presence of alternatively cleaved forms and glycosylation modifications was also analysed, using immunodetection, mass spectrometry and deglycosylation treatments. In the last part, mechanisms of protein regulation, including degradation, internalization, dimerization were investigated to identify possible differences between the wild-type and variant B proteins. Interacting proteins were identified by mass spectrometry. My results showed no major differences in trafficking and regulation between wild-type and variant B proteins. Only the EGFP-tagged constructs resulted in mistrafficking to mitochondria, and this was the case for both cystatin C forms, suggesting that EGFP is not a suitable tag to study cystatin C and excluding mitochondrial mislocalization as a factor contributing to disease association. There were also no differences in secretion, regulation and interaction partners between wild-type and variant B. However, precursor processing for the variant B was slightly less efficient, resulting in a slightly higher fraction of non-processed precursor protein and an alternatively cleaved, possibly O-glycosylated form. The mutation in the signal sequence therefore appears to affect the precursor processing rather than targeting. These forms may accumulate over-time generating proteolytic imbalance and protein aggregates, which ultimately may lead to cellular dysfunction and degeneration associated with AMD and AD. Interestingly, inhibition of the ubiquitin-proteasome system or the autophagy-lysosome pathway, which become functionally impaired during aging and disease, led to a decrease or increase of cystatin C protein levels, respectively, suggesting a possible involvement in the altered levels of cystatin C in the structural and functional changes seen in age-related conditions.

Doctor of Philosophy Declaration

I hereby declare that this dissertation is a record of work carried out in the Institute of Ageing and Chronic Disease at the University of Liverpool and Institute of Molecular and Cellular Biology at the A*STAR in Singapore during the period from November 2012 to November 2016. The dissertation is original in content expect where otherwise indicated.

November 2016

(Alessandro Riccio)

Acknowledgements

I sincerely express my gratitude and appreciation to everyone whose contribution either directly or indirectly has helped in the eventual realisation of this work.

First of all, I would like to thank Dr Walter Hunziker, Prof Malcolm Jackson and Dr Luminita Paraoan for providing me this great opportunity to do my PhD at the University of Liverpool in collaboration with the A*STAR institute of Singapore. It has been the most challenging experience I have ever faced but also the greatest in my life that allowed me to develop professionally and also as a person.

I am extremely grateful to Dr Walter Hunziker who has been my main supervisor, my guide and mentor for those four years of my PhD. His knowledge and constructive criticism as well as his integrity and honesty inspired and motivated me to overcome all the obstacles often involved in a doctorate degree in science. His fundamental role led to the completion of my PhD.

I would also like to express my gratitude to Dr Simon Tew, who guided me in the last part of my PhD, whose expertise and valuable advices added considerably to my thesis. His encouragement and involvement during the last year of my PhD have proven invaluable.

Moreover, I am utterly grateful to all the members of the WH lab at the IMCB in Singapore, for their assistance during my PhD. Of those members special thanks go to Safiah, Jaya, Alicia, Wan Lu and Choon Peng, always supportive and encouraging friends. I would also like to use this opportunity to thank all my friends and housemates during my stay in Singapore, who made my experience there unique and unforgettable. Special thanks to Teresa, Dana, Anna, Trini, Elena, Dominic and Aled.

I would also like to thank all my colleagues, PhD peers and friends in the departments of EVS and MSB at the IACD in Liverpool, who helped and supported me during my last year of PhD. Without them I could not have achieved this goal. There would be so many to mention but special thanks goes to Joe, Sam, Michele, Ifigeneia and Tiago. Their help and moral support was priceless. I would also like to acknowledge Karen and Lee for their emotional encouragement.

I would like to extend my gratitude to all my friends in Italy and around the world who, even physically far, they have been always present for me. Among them a special thanks to Pamela, for her constant encouragement during all my PhD.

Finally, I would like to express my deepest gratitude to my family who played an indispensable part in the successful completion of this project, for their encouragement, motivation, love and profound understanding.

Esprimo la mia piu profonda gratitudine ai miei genitori e alla mia famiglia, per il costante incoraggiamento, amore e per aver sempre creduto in me.

Table of Contents

List of Tables

List of Figures

List of abbreviations

AD	Alzheimer's disease
ALP	Autophagy-lysosome pathway
AMD	Age-related Macular Degeneration
APP	Amyloid precursor protein
ATP	Adenosine triphosphate
Aβ	β-amyloid
BFA	Brefeldin A
BiP	Immunoglobulin-heavy-chain binding protein
BrM	Bruch's membrane
BSA	Bovine serum albumin
CMA	Chaperone-mediated autophagy
CMV	Cytomegalovirus
CNV	Choroidal neovascularisation
CQ	Chloroquine
CSF	Cerebrospinal fluid
CysC	Cystatin C
DAPI	4',6-Diamidino-2-Phenylindole
DC	Differential Centrifugation
DMEM	Dulbecco's modified Eagle's medium
DMSO	Dimethyl sulfoxide
dNTP	Deoxynucleoside triphosphate
ECL	Enhanced chemilumininescent
ECM	Extracellular matrix
EDTA	Ethylenediaminetetraacetic acid
EGFP	Enhanced green fluorescent protein
EndoH	Endoglycosidase F
ER	Endoplasmic Reticulum
ERAD	Endoplasmic Reticulum-associated degradation
ERGIC	ER-Golgi intermediate compartment

FBS	Fetal bovine serum
GAPDH	Glyceraldehyde 3- phosphate dehydrogenase
GFP	Green fluorescent protein
GFR	Glomerular filtration rate
GTP	Guanosine triphoshate
HA	Human influenza hemagglutinin
HRP	Horseradish peroxidase
Hsp	Heat shock protein
IFN	Interferon
IL	Interleukin
IRF8	Interferon regulatory factor 8
LMP	Lysosomal membrane permeabilization
LP	Leader peptide (signal peptide)
LPS	Lipopolysaccharide
M6P	Mannose-6-phosphate
MACS	Magnetic separation of mitochondria
MEM	Minimum essential medium
MMP	Matrix Metalloproteinase
MVBs	Multivesicular bodies
MW	Molecular Weight
NEF	Nucleotide exchange factor
OST	Oligosaccharyl-transferase
PAGE	Polyacrylamide gel electrophoresis
PBS	Phosphate buffered saline
PCR	Polymerase chain reaction
PDI	Protein-disulfide isomerase
PFA	Paraformaldehyde
PNGaseF	Peptide N-glycosidase F
POS	Photoreceptor outer segment
qPCR	Quantitative Polymerase chain reaction
RPE	Retinal Pigment Epithelium

SAM	Sorting and assembly machinery
SDS	Sodium dodecyl sulfate
SNP	Single nucleotide polymorphism
SPC	Signal peptidase complex
SPP	Signal peptide peptidase
SR	SRP receptor
SRP	Signal recognition particle
TGN	Trans-Golgi Network
TIM	Translocase of inner membrane
TOM	Translocase of outer membrane
UPR	Unfolded protein response
UPS	Ubiquitin-proteasome system
VEGF	Vascular Eedothelial growth factor
YFP	Yellow fluorescent protein

Chapter 1 - Introduction

1.1. Cystatin superfamily

Cystatins represent a superfamily of reversible competitive inhibitors of cysteine proteases, which are enzymes responsible for the degradation of proteins as part of many biological mechanisms. Regulation of protease activity is fundamental for the maintenance of cellular homeostasis and impairment of the actions of cystatins contribute to many pathological conditions primarily characterised by accumulation of misfolded proteins and generation of insoluble aggregates such as neurodegeneration (Turk, Stoka & Turk 2008). Roles in cardiovascular diseases, osteoporosis, arthritis, and tumorigenesis, among others, have also been reported (Ochieng, Chaudhuri 2010, Turk, Stoka & Turk 2008).

Cystatins can be subdivided into three major families: stefins, cystatins and the kininogens. The type 1 family includes the intracellular inhibitors stefin A and B (also named cystatin A and B) that are non-glycosylated proteins lacking a signal sequence and disulphide bridge. On the contrary, members of the type 2 family are characterised by the presence of a signal peptide, which targets the proteins for secretion, two disulphide bonds in their structure and, in some of the members, glycosylation. Cystatin C, D, E/M, F, G, S, SA and SN belong to the type 2 family and, due to the signal sequence, are mainly localised extracellularly. Finally, the members of the type 3 family are large glycosylated intravascular proteins with two protease inhibitor domains (Ochieng, Chaudhuri 2010, Turk, Stoka & Turk 2008).

1.2. Cystatin C

Cystatin C, also originally known as γ-trace and post-γ-globulin and main member of cystatin type 2 family, is the most potent inhibitor of major lysosomal and extracellular cysteine-proteases such as the plant derived papain and the mammalian lysosomal cathepsins B, H, L and S as well as some lysosomal caspases, such as legumain (Barrett, Davies & Grubb 1984, Turk, Bode 1991). It interacts reversibly with its target proteases to prevent the binding of substrate to the enzyme by competitively binding to the enzyme active site (Nycander et al. 1998).

Human Cystatin C is encoded by the *CST3* gene located on chromosome 20p11.21 (Abrahamson et al. 1989). Three KspI single nucleotide polymorphisms (SNPs) have been identified within the gene, the first two occurring in the 5' untranslated sequence at positions -157 and -72 and the third at position +73 consisting of a G to A nucleotide substitution in the coding region of the transcript, which leads to an alanine to threonine amino acid substitution in the penultimate position of the signal peptide. Due to strong linkage disequilibrium between the three SNPs, cystatin C is present only as two haplotypes called variant A (wild-type) and variant B, whose allele frequencies have been shown in a Caucasian population to be 0.71 and 0.29 respectively, and frequency of the homozygote B/B genotype of 7.5% (Balbín, Abrahamson 1991, Balbín, Grubb & Abrahamson 1993).

Another variant form of cystatin C generated by a point mutation which results in a leucine to glutamine amino acid substitution at position 68 of the mature protein sequence, has been also identified. This variant is highly amyloidogenic and the cause of a pathological condition known as hereditary amyloid angiopathy (Wei et al. 1998).

1.2.1. Cystatin C Structure and mode of actions

Human cystatin C protein is a non-glycosylated, basic, low molecular weight protein, synthetized as a precursor of 146 amino acids containing a hydrophobic N-terminal signal sequence of 26 amino acids (MW 2.5 kDa) that targets the protein to the Endoplasmic Reticulum (ER). Here the signal sequence undergoes cleavage by a specific peptidase and the resulting mature form of cystatin C is directed from the ER to the Golgi apparatus and the secretory pathway (Paraoan et al. 2001, Paraoan, Grierson 2007). The mature active cystatin C is a monomeric protein thus consisting of 120 amino acid residues with a molecular mass of approximately 13.3 kDa, folding into five-stranded antiparallel β-sheets partially twisted around an α-helix, with two disulphide bridges at the C-terminus, typical of the type 2 cystatins (Bode et al. 1988, Kozak et al. 1999) (figure 1.1).

The peptidase-binding site is composed of three main regions essential for the cystatin C inhibitory action, which consists of two β-hairpin loops and the N-terminus of the mature protein (Figure 1.1). In the N-terminal segment a conserved amino acid sequence, consisting of Arg-Leu-Val-Gly at position 8-11, guarantees the optimal interaction with the target protease by increasing the binding affinity. One of the β -hairpin loops, consisting of five amino acid residues at position 55-59 (Gln-Val-Ile-Ala-Gly), is crucial for binding cysteine proteases and the second one, consisting of the Pro105-Trp106 region, is involved in tightly anchoring cystatin C to its target enzyme once the complex is assembled (Paraoan et al. 2010, Cimerman et al. 1999). The inhibitory mechanism of cystatin C consists of two steps: an initial weak interaction that involves the binding of the N-terminal region of cystatin C to its target, which results in a conformational change that leads to a tighter association with the inhibitor and renders the active site of the enzyme partially blocked (Nycander et al. 1998), therefore preventing access of substrates.

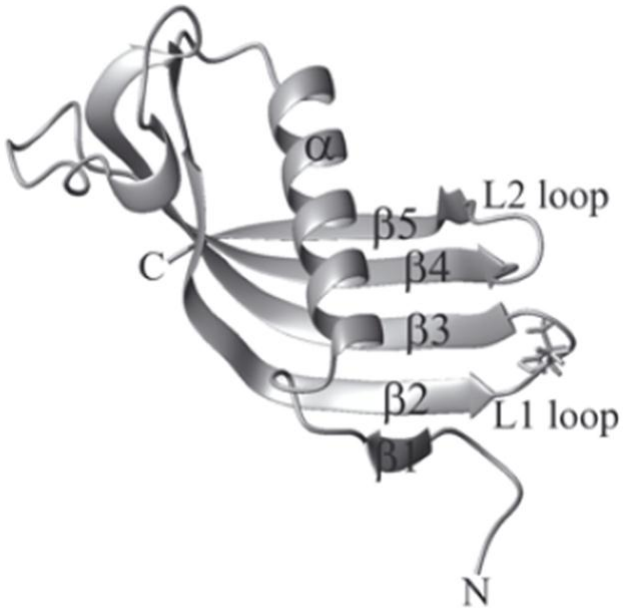

Figure 1.1 - Structure of cystatin C. It consists of five antiparallel β-sheets around a α-helix. The N-terminal region and the two hairpin loops L1 and L2 are critical for the inhibitory activity of cystatin C (Figure reproduced from (Szymańska et al. 2009)).

1.2.2. Cystatin C Regulation

Because of the presence of a signal sequence, active monomeric cystatin C is secreted into the extracellular environment where it acts as a protease inhibitor. In order to control its concentration and activity there are several mechanisms of regulation.

One mechanism that has been suggested to regulate cystatin C activity consists in its dimerization, which causes a complete loss of its protease inhibitory activity (Janowski et al. 2001). During intracellular trafficking, cystatin C has been demonstrated to form dimers through a process called three-dimensional domain swapping, which requires partial unfolding of the monomer followed by separation into two domains and subsequent exchange between two similarly unfolded molecules (Janowski et al. 2001, Janowski et al. 2005). In this conformation the inhibitory region of cystatin C is buried within the dimer interface, thus resulting in a loss of activity (Ekiel, Abrahamson 1996). This mechanism of dimerization has been hypothesized to regulate the level of active cystatin C in the cell. A study conducted in Chinese hamster ovary cells has reported that cystatin C can adopt this non-active dimeric conformation in the early part of its intracellular trafficking and then monomerizes shortly before secretion (Merz et al. 1997). Regulation of its dimer state has also been shown to play a role in the maturation of hematopoietic cells (Xu et al. 2014). Impairment of this mechanism can lead to an unbalanced proteolytic activity in the cell as well as an improper protein oligomerization leading to aggregation-related conditions. For instance, under condition of intracellular oxidative stress, an increase in the process of protein dimerization and oligomerization has been observed (Xu et al. 2014).

Regulation of cystatin C levels and activity also occurs through digestion by proteases. Its proteolytic digestion results in an N-terminal truncation of the protein, removing its inhibitory capacity. This can occur by the action of a number of different proteases, including the intracellular aspartic-cathepsin D, the serine-protease elastase and the extracellular matrix metalloproteinase 2 (MMP2)

(Abrahamson et al. 1991, Lenarčič et al. 1991, Dean et al. 2007, Laurent-Matha et al. 2012). Inactivation of cystatin C has also been shown to occur by one of its target enzymes through a non-inhibitory interaction with the extracellular cysteine-Cathepsin L, which cleaves 11 residues at the N-terminus of the protease inhibitor (Popovič et al. 1999).

Cystatin C is found predominately in the extracellular environment, consistent with the presence of the leader peptide responsible for targeting the protein to the secretory pathway. However, its target proteases belonging to the cysteine-cathepsin family mainly localize intracellularly in the lysosomes. Cystatin C is therefore also required inside the cell in order to regulate the intracellular proteolytic activity. For this reason its involvement in additional trafficking pathways has been investigated and it has been demonstrated that cystatin C can be subjected to internalization from the extracellular space via clathrin-dependent endocytosis (Kaseda et al. 2007, Ekström et al. 2008). Accordingly, cystatin C has been found also in endosomal-lysosomal cellular compartments, where it can inhibit cathepsin activities. For instance, exogenous cystatin C was shown to colocalize with cathepsin B and legumain in lysosomes after its uptake, causing a down regulation of their activities (Wallin, Abrahamson & Ekstrom 2013). Interestingly, cystatin C uptake can also occur in cells other than the ones that produced it, suggesting a paracrine role. This process has been shown to be particularly exploited by tumour cells (Wallin, Abrahamson & Ekstrom 2013, Wallin et al. 2010) as a protective mechanism to inhibit the degradation activity of cathepsins, which are involved in extracellular matrix degradation during cancer cell invasion and metastasis. Therefore, it was suggested that impairment of this cystatin C uptake might be crucial for the regulation of the proteolytic activity in both intracellular and extracellular environments (Wallin, Abrahamson & Ekstrom 2013, Wallin et al. 2010).

Cystatin C can also be alternatively secreted by a mechanism of exocytosis that involves the release of exosomes (Ghidoni et al. 2011b). Exosomes are 30-150 nm lipid-membrane vesicles generated in the endocytic pathway from late endosomes/multivesicular bodies (MVBs) (Raposo, Stoorvogel 2013). Exosomes transport a variety of molecules such as proteins, miRNA and lipids, and they are known to have roles in cell-cell communication, immune response/antigen presentation, removal of intracellular unwanted proteins or overload of damaged molecules, cell death, angiogenesis and inflammation (Raposo, Stoorvogel 2013). Once released into the extracellular environment, exosomes can be internalized by the same cell or by a secondary cell, or their content can be directly released into the extracellular space (Raposo, Stoorvogel 2013). Transport of cystatin C by exosomes may therefore represents an additional pathway of proteolysis regulation to maintain both intracellular and extracellular proteolytic balance. Interestingly exosomes have been found to be involved in different neurologic and degenerative conditions, such as Alzheimer disease and Age-related macular degeneration (AMD) (Ghidoni et al. 2011b, Wang et al. 2009, Joshi et al. 2015).

1.2.3. Functions of cystatin C

Cystatin C, initially identified in urine and cerebrospinal fluid (CSF), was later found to be ubiquitously expressed in a wide variety of human tissues and cell types, including kidney, brain, liver, placenta, pituitary glands, thyroid and alveolar macrophages (Turk, Stoka & Turk 2008). As a secreted protein it was particularly identified at significant concentrations in extracellular body fluids such as CSF, urine, blood serum, semen, saliva and tears, indicating that it performs a crucial role in the regulation of extracellular proteolytic activity. It was found to be highly expressed by the choroid plexus in the brain tissue and consequently secreted in the CSF, where it represents more than 90% of the total concentration of cysteine protease inhibitors (Cimerman 2007). Because of its presence in the blood plasma it is currently used in the clinic as a biomarker for kidney function, where it is a good indicator of glomerular filtration rate (GFR) due to its small molecular weight and easy detection (Shlipak et al. 2013).

Given its ubiquitous expression throughout the body, cystatin C may therefore play a general and crucial role in the regulation of protein degradation in the human body.

1.2.3.1. Protein degradation

Protein degradation is an essential cellular function that guarantees the turnover and removal of damaged or unnecessary proteins. The main cellular protein degradation systems are the ubiquitin-proteasome system (UPS) and the autophagy-lysosome pathway (ALP). Defects in either of these mechanisms of proteolysis can lead to several pathological conditions (Nedelsky, Todd & Taylor 2008).

The UPS system is the major mechanism for protein catabolism, responsible for the regulation of intracellular protein concentration and degradation of misfolded and damaged proteins. It therefore represents a quality control mechanism essential for cell survival (Amm, Sommer & Wolf 2014). The UPS mechanism of degradation consists of two steps: conjugation of a substrate protein with multiple ubiquitin molecules through a covalent bond, thus targeting the tagged protein to the proteasome, and the subsequent degradation in the catalytic core of the 26S proteasome (Hipp, Park & Hartl 2014, Vilchez, Saez & Dillin 2014). Additional roles identified for the proteasome system include regulation of gene transcription and antigen presentation (Lecker, Goldberg & Mitch 2006). The ALP is a mechanism that delivers cellular components to the lysosome for degradation and is mainly responsible for removal of damaged cell organelles, large protein aggregates, membrane proteins and extracellular endocytosed proteins. Different mechanisms are therefore involved in this pathway such as autophagy for cytoplasmic material, and endocytosis for exogenous and membrane components (Hipp, Park & Hartl 2014, Vilchez, Saez & Dillin 2014). In addition, autophagy has been shown to be involved in several crucial cellular mechanisms including apoptosis, protection against metabolic stress, DNA damage, defense against intracellular pathogens and antigen presentation (Eskelinen, Saftig 2009).

Autophagy can be classified into three types. Microautophagy involves the engulfment of cytoplasm into the lysosome. Chaperone-mediated autophagy (CMA) for proteins containing specific recognition sites that translocate across the lysosomal membrane with the help of chaperone molecules and specific lysosomal receptors. Macroautophagy is the main and more widely investigated mechanism and involves the formation of an isolated membrane called the phagophore that expands and engulfs the target substrate forming a double membrane structure, the autophagosome, which then fuses with the lysosome (autopagolysosome), where contents are degraded by the lysosomal enzymes (Nedelsky, Todd & Taylor 2008, García-Arencibia et al. 2010) (Figure 1.2).

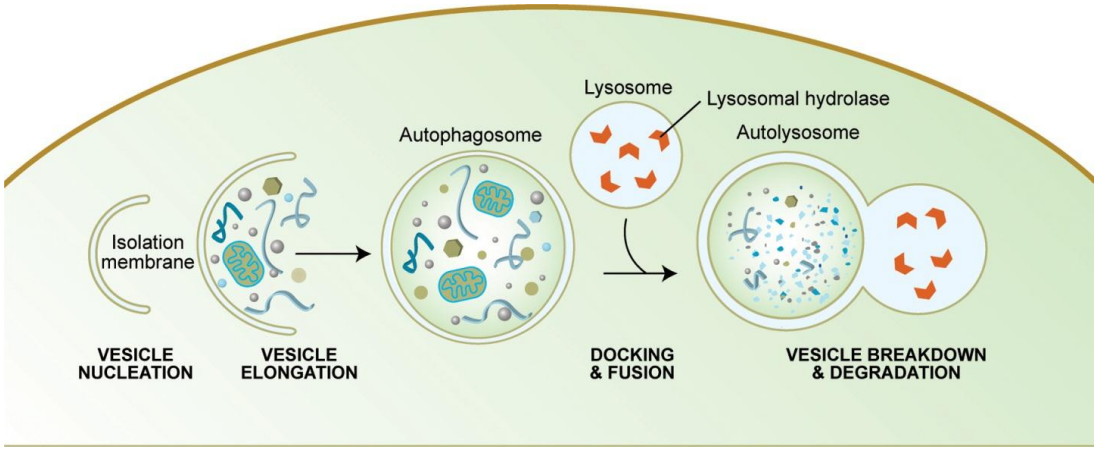

Figure 1.2 - Autophagy pathway. It begins with the formation of an isolation membrane (phagophore) that expands and engulfs the target substrates (e.g. proteins, aggregates, organelles). The resulting autophagosome fuses with the lysosome forming the autophagolysosome or autolysosome, where contents are degraded by the lysosomal hydrolases (figure from (Meléndez, Levine 2005)).

The other major route to the lysosome is the endocytic pathway, where extracellular material, cell membrane proteins and soluble molecules such as ligands bound to the cell surface are internalized in endocytic vesicles and directed to the lysosome for degradation (Doherty, McMahon 2009). Based on the size of the material engulfed into the vesicles, endocytosis can be divided in pinocytosis, for uptake of fluids and small solutes, and phagocytosis for engulfment of larger

particles, including cell debris, microorganisms and apoptotic cells. Different mechanisms have been described, depending on the composition and size of the vesicles: clathrin-mediated endocytosis, caveolae-mediated endocytosis, macropinocytosis and clathrin/claveolae independent endocytosis (Doherty, McMahon 2009). Briefly, the mechanism of endocytosis consists in the internalization of components from the plasma membrane into early endosomes where proteins can be sorted and either be sent back to the plasma membrane by the recycling endosomes or targeted to the lysosomes for degradation through the late endosomes. Late endosomes also contain proteases and lysosomal proteins and they have been reported to transport and exchange components with other organelles such as the trans-Golgi network (TGN), which provides newly synthesized lysosomal components and enzymes to the endosome-lysosomal system (Huotari, Helenius 2011).

The different mechanisms of autophagy and endocytosis described above eventually merge at the lysosome, where degradation of all kinds of macromolecules occurs thanks to the presence of a variety of hydrolases that include nucleases, lipases and proteases. Among the proteases involved in this process, cathepsins play a key role in protein degradation.

1.2.3.2. Cathepsins

Cathepsins represent the major family of proteases involved in protein degradation. They are subdivided in different groups known as cysteine-cathepsins (B, C, F, H, K, L, O, S, V, W, X), aspartic-cathepsins (D and E) and serine-proteases (A and G), depending on the amino acid residue found at the active site of the enzyme (Brix 2005). They are mostly endopeptidases, but some of them also show exopeptidase or dual endo/exopeptidase activity. The cysteine cathepsins represent the largest group and play the main role in the protein degradation in the lysosomes (Turk et al. 2012). Regulation of cathepsin activity is essential for lysosomal function as accumulation of undegraded material could lead to severe pathological conditions. Cystatin C represents their main endogenous inhibitor.

Cathepsins are synthesised as precursor pro-enzymes containing an N-terminal signal peptide responsible for targeting to the endoplasmic reticulum. After removal of the leader peptide by a signal peptidase, the partially folded pro-cathepsins undergo N-linked glycosylation in the ER and are then transported to the Golgi apparatus, where a further events of glycosylation occurs, including the addition of a mannose-6-phospate (M6P) that directs the protein to the trans Golgi network (TGN) upon binding to M6P-receptors. The enzyme-receptor complex exits from the TGN and fuses with late endosomes. Here the acidic pH causes dissociation of the pro-enzyme from the M6P-receptor and the resulting active protease is sent to lysosomes (Brix 2005, Turk et al. 2012). Active cathepsins are therefore found mainly in the lysosomes, where they are required for homeostatic protein turnover, but they have also been found in other intracellular vesicular compartments of the endosomal-lysosome system, such as trans-Golgi derived vesicles, transport vesicles, secretory vesicles, clathrin-coated vesicles and endosomes (Guha, Padh 2008, Repnik, Cesen & Turk 2013).

Functions within the endosomal-lysosome system include protein degradation and turnover, antigen processing during immune response, and processing/activation of pro-proteins and pro-hormones (Brix 2005).

In addition to their key function in the lysosomal system, cathepsins were also identified to play a role in different compartments such as cytoplasm and extracellular space, where they have been implicated in essential processes including apoptosis, inflammation, extracellular matrix (ECM) remodelling and angiogenesis. To fulfil these functions, cathepsins are required to exit from the lysosomal compartment (Turk et al. 2012, Repnik, Cesen & Turk 2013). Studies revealed that lysosomes are indeed also involved in the secretion of molecules by a mechanism known as lysosomal exocytosis (Jaiswal, Andrews & Simon 2002, Rodriguez et al. 1997). This secretory pathway consists in the fusion of the lysosome with the plasma membrane and the consequent release of lysosomal content extracellularly. In the extracellular environment cathepsins have been shown to be involved in ECM degradation and remodelling. Several components such as collagens, proteoglycans, fibronectin and laminins have been shown to be

targets for cathepsin cleavage (Turk et al. 2012). Furthermore, cathepsins have also been implicated in the process of angiogenesis, regulating levels of angiogenic factors and components of the vascular and epithelial membrane (Turk et al. 2012).

In addition, cathepsins have been shown to exert important roles within the cytosol such as involvement in apoptosis and inflammasome activation (Conus, Simon 2008). A prerequisite for cathepsin release into the cytosol is lysosomal membrane permeabilization (LMP), for example by stimuli such as reactive oxygen species (ROS), which are increased in oxidative stress conditions (Zdolsek, Svensson 1993). Active cathepsins released into the cytosol can then process other molecules. LMP has also been described as an early event of apoptosis and involvement of cathepsins in programmed cell death has been widely established. The pro-apoptotic Bcl-2 family member Bid was shown to be activated by cathepsins whilst, on the contrary, anti-apoptotic proteins Bcl-2 and Bcl-XL were shown to be inhibited (Droga-Mazovec et al. 2008, Repnik, Cesen & Turk 2013, Marques et al. 2013). Lysosome permeabilization and cathepsin activity has also been implicated in activation of the inflammasome, a multiprotein complex that initiates the inflammation process (Conus, Simon 2008, Tseng et al. 2013). Interestingly, in degenerating neurons, cathepsin release into the cytoplasm has been described after disruption of lysosomes, with deleterious consequences for the cells, thus indicating a role of these proteases in the cell degenerative process, possibly by activation of an abnormal inflammatory response and apoptosis.

1.2.3.3. Roles of cystatin C

Given its ubiquitous expression throughout the body and the several crucial roles played by its target enzymes, cystatin C is implicated in different key physiological functions and disease conditions.

As main inhibitor of cysteine-cathepsins, cystatin C plays an essential role in regulating the proteolytic activity within the endosomal-lysosomal system to ensure a proper protein turnover and maintenance of cellular homeostasis (Xu et al. 2015, Cimerman 2007). As previously described, uptake of cystatin C from the

extracellular environment occurs in different cell types in order to modulate intracellular cathepsin activity (Ekström et al. 2008, Wallin et al. 2010, Wallin, Abrahamson & Ekstrom 2013).

An important biological process involving cystatin C within the endosomal-lysosome system is antigen presentation occurring during the immune response in antigen-presenting cells such as the peripheral dendritic cells (Cimerman 2007, Xu et al. 2015). Cysteine-cathepsins have been widely reported to play a role in antigen presentation, being responsible of proteolytic degradation of pathogen proteins within the endosomal-lysosomal system to generate the immunogenic peptides that subsequently associate to MHC II to induce the immune response. However, conflicting results about the involvement of cystatin C in modulating cathepsin activities in MHC II antigen presentation have been reported (Cimerman 2007, Xu et al. 2015).

Cathepsins can be released from lysosomes upon membrane permeabilization and are implicated in the process of apoptosis. Consistently, upregulation of cystatin C expression was found to correlate with oxidative stress-induced apoptosis in cultured rat neurons, indicating a role in regulation of programmed cell death (Nishio et al. 2000). Cystatin C has also been reported to lead to neuronal cell death in vivo by up-regulation of caspase-3, which can be conversely inhibited by cathepsin B (Nagai et al. 2005). Furthermore, Liang et al. have shown that cystatin C induction of apoptosis in neuronal cells involves the decrease of anti-apoptotic Bcl-2 and increase of pro-apototic Bax and active caspase-9 protein levels via JNK-dependent pathway (Liang et al. 2011). In another study cystatin C was shown to trigger neurodegeneration through up-regulation and accumulation of the insoluble α-synuclein in neurons, which leads to apoptosis (Suzuki, Jin & Yazawa 2014). Conversely, protective and anti-apoptotic effects on neuronal cells have been also described, thus preventing cell death in vivo through inhibition of the activity of cathepsins (Nishiyama et al. 2005, Mori et al. 2016) and promoting neuronal regeneration (Kaur et al. 2010, Xu et al. 2005, Pirttilä et al. 2005). Furthermore, modulation of cell proliferation in normal and cancer cells by

antagonizing transforming growth factor-beta (TGF-β) signalling was also reported for cystatin C thereby promoting cell survival (Sokol, Schiemann 2004).

Several roles of cystatin C in the inflammatory process have been also described, including modulation of chemotactic activity and phagocytosis in neutrophils, activation of the complement cascade, involvement in the IFNγ signal transduction pathway, leading to nitric oxide production and release from macrophages and down-regulation of IL-10 (Xu et al. 2015, Cimerman 2007, Schulte et al. 2010).

Being primarily a secreted protein and given its high concentration in most body fluids, cystatin C is likely to play an essential role, along with its target cathepsins, in the maintenance of homeostasis and balance of proteins in the extracellular fluid and in the remodelling of extracellular membranes and structures. Regulation of proteolytic activity has been described to be involved in the preservation/remodelling of ECM in various human tissues and its impairment may result in disease conditions such as atherosclerosis, where arterial wall remodelling is dysregulated, and cancer, where ECM degradation facilitates tumour cell invasion and metastasis (Xu et al. 2015). Indeed, low levels of cystatin C were found to be associated with atheroma plaque formation, and cancer cell invasion was shown to be reduced by inhibition of the cystatin C targets cathepsin B and legumain (Keppler 2006, Wallin, Abrahamson & Ekstrom 2013).

Cystatin C in body fluids has been reported to vary under influence of many factors and in pathological conditions. Several stimuli such as cytokines, pathogens, growth factors, hormones, physicochemical damages and oxidative stress have been identified to affect cystatin C synthesis and secretion (Xu et al. 2015). For instance, reduction of the level of expression and secretion of cystatin C is caused by the presence of bacterial LPS as well as of inflammatory cytokines IFNγ and IL-6 (Xu et al. 2015). On the contrary, an up-regulation of its expression has been observed upon TGF-β stimulation, with exposure to oxidative stress and after induction of inflammatory IL-10 induced-IRF8 transcription factor (Xu et al. 2015). Alterations in

balance of cystatin C and its target cathepsins have been also associated with several disease conditions.

In conclusion, cystatin C is found in many compartments inside and outside the cell where it regulates cathepsin activity within the lysosomes as well as in other compartments including the extracellular space. Because cathepsins are involved in several physiological processes such as protein turnover, protein processing, tissue remodelling, antigen presentation, apoptosis as well as pathological conditions such as cardiovascular disease, cancer, inflammation and cell degeneration (Turk et al. 2012), it is essential that their activity is tightly regulated by their inhibitor.

1.3. Disease involvement of cystatin C

Cystatin C has been associated with several pathological conditions. Its involvement in neurodegenerative diseases has been particularly investigated given its high expression in brain tissue by neurons, astrocytes, endothelial and microglial cells, its presence at high level in the CSF and its involvement in brain development (Paraoan et al. 2010). Its involvement in Alzheimer's disease (AD) has been extensively described and it has been found to co-localise with β-amyloid precursors in the fibrils plaques generated in the brain of patients affected by AD (Levy et al. 2001, Mi et al. 2009). Other conditions where it has been implicated to play a role, as a consequence of its altered expression, are Parkinson's disease, multiple sclerosis, tissue-degenerative diseases such as osteoporosis and periodontisis as well as vascular diseases, like atherosclerosis and aneurysms, and cancer (Bengtsson, Nilsson & Jovinge 2008, Chen et al. 2015, Suzuki, Jin & Yazawa 2014, Xu et al. 2015, Schulte et al. 2010, Wilson et al. 2010).

In particular, changes in the level of cystatin C in CSF and plasma have been associated with various disease conditions. Increase of cystatin C level has been shown in several neurodegenerative diseases, brain injuries such as ischemia and epilepsy and cardiac injury, suggesting a protective role of the protease inhibitor (Zhong et al. 2013, Chen et al. 2015, Xie et al. 2010, Žerovnik 2009). Overall, it

indicates that preservation of the secretion level of cystatin C plays an important role in health and disease.

In addition, due to its propensity to self-assemble and form insoluble fibrils (Janowski et al. 2001, Tsiolaki et al. 2015), it has been implicated in aggregation-related degenerative conditions such as hereditary amyloidosis characterised by generation of amyloid deposits in the vascular walls causing severe angiopathy.

1.3.1. Amyloydogenic properties

As mentioned previously, cystatin C has been demonstrated to form inactive dimers and oligomers by a process known as three-dimensional domain swapping (Janowski et al. 2001). This tendency to form dimers can lead to protein aggregation causing the formation of amyloid deposits, which has been observed both in vitro under pre-denaturing conditions and in vivo where this process is particularly enhanced in the presence of an N-truncated form of cystatin C, as described in various neuropathologies (Nilsson et al. 2004, Janowski et al. 2004).

Amyloidogenic properties of cystatin C have been particularly observed in the case of the L68Q mutant cystatin C, a variant form responsible for a rare autosomal dominant form of amyloidosis called hereditary amyloid angiopathy, also known as Icelandic type that causes fatal cerebral haemorrhage (Wei et al. 1998, Calero et al. 2001, Rodziewicz-Motowidlo et al. 2006). Substitution of leucine by glutamine in position 68 seems to retain the inhibitory function of cystatin C but causes a decreased stability by disrupting the hydrophobic interaction network, thus leading to increased tendency for dimerization and aggregation in vitro and in vivo where generation of fibril deposits occurs in the brain vasculature (Wei et al. 1998, Rodziewicz-Motowidlo et al. 2006). In addition, these patients have shown a reduced level of cystatin C in the CSF, thus indicating an impaired trafficking of this variant form. However, Wei et al. (1998) have suggested that the reduced level in the CSF is due to an increased susceptibility of the variant to degradation by serine proteases in the extracellular space rather than a difference in level of secretion (Wei et al. 1998).

1.3.2. Neuroprotective roles

Despite its involvement in amyloidogenic and neurodegenerative diseases, cystatin C has also been described to have multiple neuroprotective roles (reviewed in (Gauthier et al. 2011, Mathews, Levy 2016)), through inhibition of its target enzymes, induction of cell proliferation and inhibition of apoptosis.

An important cellular protective mechanism is represented by the autophagy-lysosome pathway. Interestingly, cystatin C has been described to induce cellular autophagy via mTOR pathway inhibition, a mechanism that could be essential to increase lysosomal proteolytic clearance and remove accumulating detrimental substances or damaged organelles in pathological conditions. Through this mechanism, cystatin C protects neuronal cells against various stress conditions such as oxidative stress and starvation (Tizon et al. 2010b, Watanabe et al. 2014, Liu et al. 2013). Recently, reduced levels of cystatin C have been associated with autophagy dysfunction in atheroma plaques resulting in an increased atherosclerosis in mice (Li et al. 2016), thus further indicating an important role of cystatin C in the regulation of autophagy in pathological processes.

Furthermore, wild-type cystatin C was found to exhibit a protective role in Alzheimer's disease by binding soluble β-amyloid protein, thus preventing its aggregation and fibril formation in vitro and reducing cerebral β-amyloid plaque deposition in vivo (Mi et al. 2007, Sastre et al. 2004, Kaeser et al. 2007). It was also described to protect neuronal cells from amyloid toxicity by promoting neuronal cell survival (Tizon et al. 2010a). Another study has also reported a role of cystatin C in regulating β-amyloid levels, this time through its action on cathepsin B. However, in contrast to the above-mentioned works, it was the removal of cystatin C that played the protective role by increasing the cathepsin B-induced degradation of β-amyloid, thus indicating a neuroprotective role of cathepsin B rather than its inhibitor (Sun et al. 2008, Wang et al. 2012, Mueller-Steiner et al. 2006).

1.3.3. Cystatin C involvement in AD and AMD

Cystatin C's involvement in AD and other aggregation-related disease such as age-related macular degeneration (AMD) has been well investigated.

AD and AMD in particular are both age-related degenerative diseases that present many similarities, suggesting the involvement of common mechanisms in their pathogenesis. They are both characterized by aggregation and accumulation of extracellular deposits, i.e. amyloid plaques and drusen in AD and AMD, respectively, as a consequence of a dysregulation of the cellular proteolytic activity (Kaarniranta et al. 2011). Furthermore, these insoluble deposits show similarities in their composition and have been reported to trigger inflammation and impair essential cellular functions, leading eventually to cell degeneration (Kaarniranta et al. 2011). Some studies have suggested they share several genetic determinants (Logue et al. 2014) and pathogenic mechanisms (Ohno-Matsui 2011). Noteworthy, β-amyloid protein deposition was found in both senile plaque in the brain and drusen in AMD (Zhao et al. 2015, Feng, Wang 2016).

As mentioned before, Cystatin C has been implicated in AD. Low levels of serum cystatin C have been associated with AD and its levels in CSF correlate with amyloid-β peptide levels (Ghidoni et al. 2010, Sundelof et al. 2008, Sundelöf et al. 2010, Zhong et al. 2013, Ghidoni et al. 2011a). Cystatin C localizes and interacts with β-amyloid proteins in AD and has been reported to play a role in physiological conditions in promoting the proliferation of Neural Stem/Progenitor cells through stimulation of amyloid precursor protein expression (Hu et al. 2013). This therefore strongly indicates that there is an interaction between cystatin C and β-amyloid proteins. Cystatin C involvement in aging and AMD development has also been suggested (Kay et al. 2014, Klein et al. 2009) further indicating a protective role of cystatin C against age-related conditions (discussed in next sections). In addition, the CST3 polymorphism that generates the variant B cystatin C has been found to be associated with both AD and AMD diseases (Crawford et al. 2000, Finckh et al. 2000, Zurdel et al. 2002). Recent studies have further confirmed the variant B implication as a risk factor for late onset AD and exudative AMD (Hua et al. 2012, Butler et al. 2015).

In this study we focused on the role of cystatin C, and particularly of its variant B, in retinal pigment epithelial (RPE) cells and therefore in relation to AMD pathogenesis. However, given the similarities between these two conditions and the association of the CST3 polymorphism with both diseases, the biological effects of the mutated form are expected to be likely similar in both pathologies.

1.3.3.1. Cystatin C in AMD

Age-related macular degeneration (AMD) is a condition that affects a part of the retina called the macula, causing irreversible loss of the central vision and representing the leading cause of blindness in the elderly (Liu, Xie 2012). The macula is a specialized area of the neurosensitive layer of the retina that contains specific photoreceptors responsible for central vision (Jager, Mieler & Miller 2008). The retinal pigment epithelium (RPE) plays an important role in the AMD pathogenesis (Kinnunen et al. 2012). This highly specialized epithelial tissue, consisting of a monolayer of polarized cells, is the outermost layer of the retina, in contact apically with the photoreceptor layer of the neuroretina and basally with a basement acellular membrane called Bruch's membrane (BrM), which separates the retina from the vascularised choroid that consists of a network of blood vessels called choriocapillaries (Strauss 2005).

The RPE has many functions essential to the nourishment and maintenance of the functional integrity of the neuroretina. Functions include formation, along with the extracellular matrix BrM, of a protective blood-retinal barrier, that controls transport of nutrients and ions between the choroid and photoreceptors as well as removal of waste products. Other roles include the visual retinoid cycle, phagocytosis of spent photoreceptor outer segments (POS), absorption of light and anti-oxidant properties. Finally, RPE is involved in the secretion of several growth factors and proteins into both the apical and basal environments, including cystatin C, proteinases and angiogenic factors such as VEGF, thus playing a role in the regulation of the ECM composition of the BrM and of the choroidal vascularization,

as well as in the maintenance of the structural integrity of photoreceptors (Strauss 2005, Thumann, Hoffmann & Hinton 2006, Kay, Yang & Paraoan 2013). Given its roles, dysfunction of the RPE can lead to a severe visual impairment. AMD is characterized by pathological changes that involve primarily RPE dysfunction and degeneration, leading to subsequent dysfunction of photoreceptor cells in the macula region as well as affecting BrM composition and the underlying choriocapillaries (Kaarniranta et al. 2010, Klettner et al. 2013).

The early stage of AMD is characterised by the presence of drusen, yellow extracellular protein-lipid deposits, which accumulate between the RPE and the BrM and mainly consist of lipids such as unesterified and esterified cholesterol, phosphatidylcholine and fatty acids, and several other molecules such as apolipoproteins, advanced glycation end products (AGEs) and amyloid proteins (Gehrs et al. 2006, Jager, Mieler & Miller 2008). An increased formation and accumulation of lipofuscin also occurs within the lysosomes. Lipofuscin consists of undegradable polymeric granules composed of cross-linked protein and lipid-residues derived from inefficient lysosomal digestion. These granules are formed by oxidative stress and normally accumulate with age. Their presence decreases lysosomal enzyme activity and impairs autophagic clearance of damaged proteins, further contributing to proteolytic dysfunction (Gehrs et al. 2006, Jager, Mieler & Miller 2008). Advanced stages of AMD can be subdivided into two categories: geographic atrophy, also known as dry form, which is characterized by progressive atrophy of RPE, thickening of BrM and degeneration of photoreceptor cells; and exudative or wet AMD, characterised by an abnormal choroidal neovascularization (CNV) where the new forming leaky blood vessels penetrate through the BrM and the neuroretina causing serious damages of these layers, thus leading to rapid loss of central vision (Gehrs et al. 2006, Jager, Mieler & Miller 2008).

Impairment of proteolytic activity in RPE, resulting in drusen generation and increased accumulation of lipofuscin, is a hallmark of AMD pathogenesis. These events lead to activation of complement cascade, chronic inflammation and oxidative stress that contribute to RPE degeneration and subsequent photoreceptor loss (Gehrs et al. 2006, Jager, Mieler & Miller 2008).

Cystatin C is abundantly expressed in RPE and has been implicated in several of the processes that also characterize AMD. Alteration in the activity of its target cathepsins has been reported to affect ECM structure, the process of vascularization and to induce inflammatory and apoptotic processes, thus suggesting a role of the cystatin C-cathepsin axis in the pathogenesis of this degenerative disease (Turk et al. 2012, Repnik, Cesen & Turk 2013). Moreover, impaired autophagy and secretion of exosomes have been also implicated in drusen formation and AMD development (Wang et al. 2009). Dysregulation of autophagy has been particularly investigated for its involvement in RPE dysfunction suggesting a key role of this process in AMD pathogenesis (Wang et al. 2009, Kaarniranta et al. 2013, Mitter et al. 2014). Many of the pathological events that characterise AMD can therefore be associated with cystatin C. In agreement with the hypothesis of a key role played by cystatin C in the maintenance of retina integrity and functionality, Ahuja et al. have shown an imbalance in the activity of cystatin C and its target proteases in the retina of mice affected by retinitis pigmentosa, a condition characterized by retinal degeneration (Ahuja et al. 2008). In addition, the level of serum cystatin C has been found to associate with severe retinopathy in type 2 diabetes (He et al. 2013) and with the incidence of early AMD (Klein et al. 2009). To better understand cyatatin C association with AMD it is necessary to further explore its function in the RPE.

1.3.3.2. Cystatin C in RPE

In the eye cystatin C is present in a variety of tissues and detected at particularly high levels in the ciliary epithelium and in the retina (Wassélius et al. 2001, Wasselius et al. 2004). Within the retina, RPE cells have been described to predominantly express cystatin C transcripts (Paraoan, Grierson & Maden 2000) and constitutively secrete the protein into the extracellular environment (Paraoan et al. 2001). The role of the leader peptide in targeting the protease inhibitor to the secretory pathway in RPE cells was further confirmed by using a construct encoding the mature cystatin C lacking the signal sequence, which was no longer targeted to

the ER/Golgi pathway, thus presenting a diffuse distribution throughout the cytoplasm and nucleus of the cell (Paraoan, Grierson & Maden 2003).

In vitro analysis of Cystatin C secretion by RPE has shown it to occur on the basolateral side of the cell layer, suggesting a main role of this inhibitor in maintaining the proteolytic balance in the RPE underlying Bruch's membrane and vascularized choroid (Kay, Yang & Paraoan 2013). However, because cystatin C has also been shown to inactivate its target enzymes intracellularly, following re-uptake, it has been suggested that cystatin C in the intracellular compartment may be involved in the regulation of photoreceptor phagocytosis and degradation, an essential function of the RPE (Wassélius et al. 2001, Wassélius et al. 2005). Secretion of cystatin C has also been described to occur in RPE via exosomes (Locke et al. 2014). Both mechanisms of internalization and release by exosomes may play an important role in RPE cells to regulate the extracellular levels of cystatin C in order to maintain the correct balance between cystatin C and cathepsins in the ECM.

Given its abundance and functions, cystatin C has been suggested to play a role in the age-related changes that occur in RPE and BrM (Kay et al. 2014). A progressive decline of proteostasis has been widely established to occur with age, involving both UPS and ALP systems (Hipp, Park & Hartl 2014, Vilchez, Saez & Dillin 2014), thus reducing the capacity to prevent the accumulation of misfolded/damaged proteins and cytotoxic protein aggregates. In particular, in RPE cells phagocytosis and lysosomal degradative mechanisms can be impaired, resulting in decreased POS degradation and renewal with consequent photoreceptor dysfunction (Guha et al. 2014). Moreover, accumulation of intra-lysosomal debris such as lipofuscin and deposition of extracellular debris has been observed in senescent RPE cells, along with generation of reactive oxygen species (ROS), structural changes in BrM composition and altered vascularization (Guha et al. 2014). As a consequence, vision ability is impaired in the elderly. These age-related effects also characterize the onset of age-related maculopathy and AMD (Rakoczy et al. 2002). Interestingly, alterations in the expression of cathepsins and impairment in the lysosomal function were observed in RPE with aging (Glenn et al. 2009) as well as a decreased

expression and secretion of cystatin C (Kay et al. 2014), further indicating a crucial role of cystain C concentration in maintaining the proteolytic balance in the RPE and in contributing to RPE dysfunction in ageing and AMD.

1.4. Variant B

A variant form of cystatin C, homozygote for haplotype B, has been reported to be a risk factor for both AMD and AD development. The CST3 polymorphism implicated in such association consists in a G73A base change that results in an alanine (A) to threonine (T) substitution of the 25th amino acid residue (A25T) of the precursor cystatin C. This substitution resides within the signal sequence at the -2 position from the cleavage site (Figure 1.3) (Balbín, Abrahamson 1991, Balbín, Grubb & Abrahamson 1993). This CST3 polymorphism has been investigated for its association with exudative AMD in a case-control study in a Caucasian population and is significantly higher in patients (6.6%) compared to controls (2.3%) (Zurdel et al. 2002). The odds ratio for disease association with the homozygous CST3 genotype B/B is 2.97, nearly three-fold higher than the wild-type. In this study, A25T has been also suggested to be a recessive risk allele, since the heterozygote A/B did not correlate with the disease.

A genetic association for the variant B polymorphism has also been identified with late-onset Alzheimer's disease (Finckh et al. 2000, Crawford et al. 2000), suggesting a role of this protein in contributing to cell degenerative processes. Variant B association with AD has been more extensively investigated (Bertram et al. 2007, Hua et al. 2012) and, recently, these findings have been further supported by Butler et al., who have confirmed in a meta-analysis study the significant recessive effect of variant B genotype on both AMD and AD (Butler et al. 2015). The haplotype frequencies estimated are 76% for variant A and 23% for variant B, with a frequency of homozygote B/B genotype in AMD patients of 4.6%.

Interestingly, CST3 haplotype B has been also associated with other degenerative and aggregation-related neurological disorders such as the frontotemporal lobar degeneration, dementia in Lewy Body disease and parkinsonian form of multiple

system atrophy (Benussi et al. 2010, Maetzler et al. 2010, Urbizu et al. 2015), which further supports the role of variant B in proteolytic dysfunction and cell degeneration.

However, in conflict with the above-mentioned studies, there are many other works that have reported no association between the CST3 polymorphism and AD (Roks et al. 2001, Maruyama et al. 2001, Monastero et al. 2005, Nacmias et al. 2006, Wang et al. 2008). Further investigations are also required to confirm the association with AMD, since so far only two works have reported cystatin C association with exudative AMD (Zurdel et al. 2002, Butler et al. 2015), one of which is a meta-analysis that used data from the initial clinical study. Many genome-wide association studies have been also carried out and all of them have failed to identify CST3 among the loci associated with either AD or AMD (Butler et al. 2015). Therefore, the role of variant B cystatin C in disease pathogenesis still needs to be clarified.

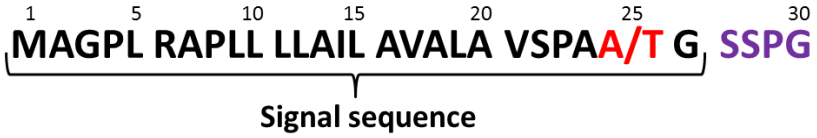

Figure 1.3 - Signal sequence of cystatin C. Amino acid sequence of cystatin C signal peptide (residues 1 to 26). Variant B is generated by Alanine to Threonine substitution on the 25th residue.

It is still not well understood how the variant B could cause an increased risk of developing AMD and AD pathologies. Several studies have investigated the mechanisms behind such association but so far inconclusive results were obtained. Since the A25T mutation occurs in the signal sequence of the precursor protein, it has been suggested that it does not affect any of the cystatin C domains involved in its inhibitory functions (Paraoan et al. 2004). However, an impairment in the intracellular trafficking of cystatin C variant B has been observed to occur in RPE cells in vitro by using EGFP-linked cystatin C constructs (Paraoan et al. 2004). Compared to the wild-type protein that was shown to localize in the ER/Golgi

apparatus and be normally processed for secretion in RPE cells, the variant B was mainly retained intracellularly, showing a diffuse intracellular distribution throughout the cytosol and nucleus and, in particular, an association with the mitochondria. As a consequence, a reduction in variant B cystatin C secretion into conditioned media by approximately 50% was also observed compared to the wild-type, thus indicating that variant B proteins are still partially processed in the ER and secreted from the cells, but due to the mutation likely a reduction in the efficiency of targeting and/or processing through the secretory pathway occurs for the variant protein (Paraoan et al. 2004). In another work by the same group, using a mutated variant of cystatin C linked to EGFP, it has been reported that the substitution of the amino acid alanine at the 25th position of the signal sequence with a serine, which has intermediate hydrophobic properties between alanine and threonine, results in an intermediate level of secretion between the wild-type and the A25T variant, as well as a localization to the ER/Golgi and mitochondria (Ratnayaka et al. 2007). This suggests that the change in the hydrophobicity is sufficient to interfere with the protein trafficking.

Therefore, regarding the variant B, it has been suggested that the substitution of the nonpolar alanine amino acid to a polar threonine residue, which significantly reduces the signal sequence hydrophobicity, is sufficient to interfere with the functionality of the leader peptide, preventing the proper targeting and/or processing of cystatin C through the secretory pathway, thus causing protein mistrafficking and decreased secretion (Ratnayaka et al. 2007). Given that a fraction of the protein is still secreted, Paraoan et al. have hypothesised that the signal sequence did not lose its targeting properties, but it may act as a weaker signal. The decreased hydrophobicity profile of the signal sequence could affect different steps (described in section 1.5.1), such as the signal-recognition process, thus partially blocking the protein targeting to the endoplasmic reticulum, or the interactions with the ER translocation channel, therefore preventing the translocation into the ER lumen, or the cleavage process by the signal peptidase (Paraoan et al. 2004). However, considering that the cleavage of the signal peptide would generate the same mature protein as that of the wild-type it has been

suggested that the variant B precursor protein is not entirely processed and as a consequence the whole precursor cystatin C with the signal peptide uncleaved may adopt an altered intracellular conformation that may incorrectly target the protein to the mitochondria (Paraoan et al. 2004).

Impaired secretion of variant B has been also described in B/B homozygous skin fibroblasts taken from AD donors, likely as a result of less efficient cleavage of the leader peptide in the case of the variant B (Benussi et al. 2003), thus supporting the hypothesis of a defective processing of cystatin C. Given the neuroprotective role of cystatin C in promoting cell survival and inhibition of β-amyloid deposition, they have suggested that the impaired production and secretion of cystatin C observed for the haplotype B might be responsible for the increased susceptibility to neurodegeneration (Benussi et al. 2003). In support of this hypothesis it has been observed that there is a reduction of cystatin C secretion in mice carrying a mutation in presenilin 2 gene, which is associated with familial AD (Ghidoni et al. 2007). The mutation seems to directly impair the trafficking of cystatin C causing intracellular accumulation and consequent reduction in secretion (Ghidoni et al. 2007), supporting a key role of cystatin C level in AD pathogenesis.

Interestingly, several studies in vivo have also reported association of the variant B haplotype with decreased levels of cystatin C in plasma and CSF in various pathologies, including neurological disorders and vascular diseases (Noto et al. 2005, Maetzler et al. 2010, Yamamoto-Watanabe et al. 2010, Åkerblom et al. 2014).

The CST3 polymorphism seems therefore to be associated with increased risk of developing both AMD and Alzheimer's disease through a reduction in the levels of cystatin C secretion in the extracellular fluids, as a consequence of a decreased efficiency or partial failure of signal cleavage.

In addition to these studies, Nilsson et al. (2009) have suggested that the intracellular cleavage of cystatin C variant B may occur at an alternative site,

between the 20th and 21st residue (Nilsson et al. 2009). In this study a O-linked glycan has been identified to be present in the variant B protein, likely residing on Ser27, Ser28 or on the mutated Thr25, therefore suggesting that the cleavage in the different position makes the six residues-longer mature protein able to undergo a O-linked glycosylation event, which may affect cystatin C functionality or stability. As described previously for the L68Q variant, this alternatively processed protein could be more susceptible to degradation and therefore the reduced levels in the extracellular compartment may result from a combination of a defect in cystatin C trafficking and an increased degradation of the secreted protein.

In contrast, a more recent study has shown no difference in secretion between the wild-type and variant B cystatin C in two different cell lines, ARPE19 and HEK-293T, and using different cystatin C constructs either untagged or tagged with GFP or FLAG tag (Nguyen, Hulleman 2016). Moreover, in this study they have shown that wild-type cystatin C can alternatively undergo signal sequence cleavage in two different sites, between the amino acids Gly26-Ser27, which represents the canonical cleavage site, and the second one between residues Ala20-Val21 that occurs at lower frequency. Interestingly, this alternative cleavage site was predicted to occur in the variant B by Nilsson et al. (2009) and, consistently, Nguyen and Hulleman have suggested that A25T protein has an increased probability to be alternatively cleaved at the 20th amino acid residue compared to the wild-type and the resulting processed protein consequently may be more likely to undergo O-glycosylation in the Golgi apparatus (Nguyen, Hulleman 2016). Furthermore, an additional study has also found association of haplotype B with increased risk of developing AD but no significant difference in the plasma level of variant B cystatin C compared to the wild-type was observed in AD patients (Chuo et al. 2007).

Based on the studies here described, the increased risk of developing AMD can therefore be due to the reduced level of cystatin C in the extracellular environment, which may affect the proteolytic balance in the extracellular space of the RPE (Paraoan et al. 2004). As described previously cystatin C is abundantly

present in this area where it may play an important role in the modulation of the proteolytic activity of cathepsin (Paraoan, Grierson & Maden 2000, (Paraoan et al. 2001). Its impaired secretion could therefore affect the ECM remodelling of the BrM and the angiogenesis balance in the underlying choroid. As mentioned before a decrease in cystatin C secretion from RPE has been also observed to occur with age (Kay et al. 2014) where it may contribute to the RPE dysfunction observed in aging. Therefore, the reduction in secretion observed for the variant B could accelerate the dysregulation of the proteolytic balance in the extracellular environment contributing even more to RPE dysfunction and AMD development (Kay et al. 2014).

In addition to the reduction in secretion, the intracellular accumulation of variant B and in particular its unusual association with mitochondria observed by Paraoan et al. may further contribute to RPE cell dysfunction, especially given that RPE cells are consistently rich in mitochondria, aligned with their high metabolic activity (Thumann, Hoffmann & Hinton 2006). Moreover, there is a large body of evidence that mitochondria alterations may play a role in AMD and other retinal pathologies (Feher et al. 2006, Nordgaard et al. 2008, Karunadharma et al. 2010, Jarrett et al. 2008) as well as in other degenerative diseases such AD and Parkinson (Eckmann et al. 2013, Moreira et al. 2010, Hirai et al. 2001) where proteins involved in such pathologies (i.e. β-amyloid precursor and α-synuclein) can be abnormally associated with mitochondria (Grant et al. 1999, Anandatheerthavarada et al. 2003, Anandatheerthavarada, Devi 2007, Liu et al. 2009, Devi et al. 2008, Devi, Anandatheerthavarada 2010).

Moreover, besides the impairment in secretion and intracellular mislocalization, an alternative mechanism through which the CST3 polymorphism increases the risk for the development of AD and AMD can be due to the alternative signal cleavage that generates a mature protein with six additional amino acids with increased propensity to undergo O-glycosylation. These additional residues at the N-terminus and/or the presence of O-glycosylation may affect cystatin C function, stability and regulation.

In conclusion, given the role of cystatin C and its target enzymes in processes such as inflammation, lysosomal function, autophagy, apoptosis, ECM remodelling, angiogenesis, all of which have been shown to be altered in AMD, there is a strong suggestion that there is a role for cystatin C in AMD pathogenesis. However, if and how the variant B of cystatin C alters the regulation of proteolytic balance is not well understood and controversial.

Therefore, further clarifying the molecular mechanisms underlying the trafficking, function and regulation of variant B will help us understand whether and how it contributes to the impairment of RPE function and to AMD development, and similarly to other degenerative diseases.

1.5. Protein Targeting and Trafficking

In all eukaryotic cells, proteins are synthesised on ribosomes and then can be targeted to cellular compartments, dependent upon specific signals present in the amino acid sequence of the protein. Generally, proteins targeted to the cytosol, nucleus, mitochondria, chloroplasts and peroxisomes are translated on "free" ribosomes in the cytosol and then transported to their target organelle (Kim, Hwang 2013, Barlowe, Miller 2013). Alternatively, proteins directed to the endoplasmic reticulum (ER), Golgi apparatus, lysosomes, plasma membrane and extracellular matrix or space are usually translated on ER-attached ribosomes and translocated into the ER before being directed to their specific cellular organelle. From the ER, proteins are transported to and across the Golgi apparatus and subsequently to the target intracellular compartment or extracellular space by vesicular transport (Figure 1.4). This ER-Golgi-vesicles route is generally known as the secretory pathway (Kim, Hwang 2013, Barlowe, Miller 2013).

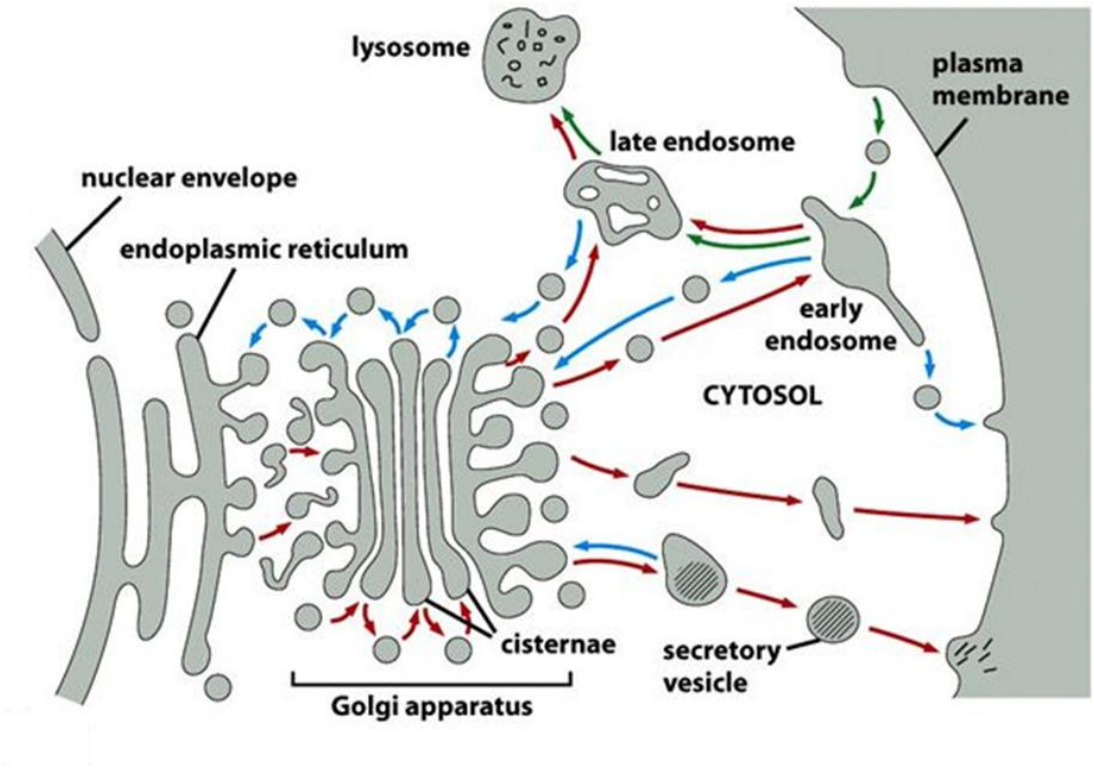

Figure 1.4 - Protein trafficking in the secretory pathway. Nascent proteins are targeted and translocated into the ER for their processing and folding. Proteins are subsequently delivered to Golgi apparatus, through the different Golgi compartments, where they can undergo post-translational modifications. Finally, proteins are sorted to the appropriate intracellular or extracellular destination. Endocytic pathway is also shown (Figure adapted from (Alberts et al. 2008)).

1.5.1. Secretory pathway

The secretory pathway consists of the transportation of both soluble and integral membrane proteins. Soluble proteins destined for secretion are mainly considered in this study, although some can also be delivered to intracellular organelles such as lysosomes by binding to mannose-6-phosphate receptors (e.g. cathepsins) (Braulke, Bonifacino 2009, Coutinho, Prata & Alves 2012). As mentioned above, the canonical pathway that leads to protein secretion comprises the ER, where proteins undergo process of co- or post-translational insertion, folding and modification, the Golgi apparatus, where further post-translational modification can occur, and the secretory vesicles, which ultimately will fuse with the plasma membrane thus releasing proteins outside the cell (Barlowe, Miller 2013). The trans compartment of the Golgi is, in addition, a major sorting compartment for delivery to intracellular

compartments such as lysosomes and different secretory compartments (e.g. luminal and serosal or dendritic and axonal in epithelial or neuronal cells, respectively, (Gu, Crump & Thomas 2001, Nejsum, Nelson 2009, Bradke, Dotti 1998)).

The main aspect investigated in this study is the role of signal sequences in ER targeting, translocation and processing of secretory proteins, which represent the first step of the canonical secretory pathway. Quality control and protein modifications, occurring along this pathway, will be also briefly discussed.

1.5.1.1. Translocation of nascent polypeptide chains across the ER membrane

Targeting and translocation of nascent polypeptide chains into the ER is a mechanism based on an amino-terminal signal sequence, also termed the leader peptide, within the nascent precursor polypeptide. This, together with transport components present in both cytosol and ER called molecular chaperones, permits targeting and translocation of proteins to the ER, where the signal sequence is cleaved from the protein. In the lumen of the ER, mature proteins are then subjected to folding and modifications, such as glycosylation, before being delivered to the Golgi apparatus (Barlowe, Miller 2013).

Translocation across the ER membrane can occur either co-translationally or post-translationally. The co-translational process begins when a hydrophobic signal sequence is translated during the protein synthesis, started on a free ribosome in the cytosol, and recognized by the signal-recognition particle (SRP). The ribosome-associated protein is thus targeted to the SRP receptor (SR) on the ER membrane in proximity of the ER translocation machinery (Walter, Blobel 1981, Görlich, Rapoport 1993) (Figure 1.5). Post-translational transport involves specific cytosolic chaperones necessary to maintain the fully synthetized polypeptide in an unfolded state, an essential condition for the protein to be able to cross the ER membrane. These chaperones belong to the heat shock proteins Hsp 70 and Hsp 40 families

(Chirico, Waters & Blobel 1988, Deshaies et al. 1988, Ast, Cohen & Schuldiner 2013).

Even though the mechanisms are not completely understood, in yeast it seems that generally the level of hydrophobicity of the signal sequence represents the main factor that determines which translocation pathway the protein will follow (Ng, Brown & Walter 1996, Hatsuzawa, Tagaya & Mizushima 1997). Secretory proteins with high hydrophobic signal sequences and integral membrane proteins typically make use of the SRP-dependent pathway, whereas a post-translational transport is preferred by proteins with soluble, less hydrophobic signal sequences (Ng, Brown & Walter 1996, Hatsuzawa, Tagaya & Mizushima 1997). In mammals one main feature that seems to characterize precursor proteins targeted for post-translational translocation is the length of the nascent polypeptide; if it contains less than 75-100 amino acid residues it seems not to be able to establish the proper interactions with SRP. Other characteristics are also suggested to play a role in signal sequence recognition, such as its orientation at the ribosomal surface, helical propensity and presence of N-terminal basic residues (Shao, Hegde 2011, Lakkaraju et al. 2012, Johnson et al. 2012, Peterson, Woolhead & Bernstein 2003).

Both of these mechanisms merge at the central component of the ER-membrane translocation machinery, the heterotrimeric Sec61 complex, or translocon, consisting of Sec61p associated with Sss1p and Sbh1p proteins in yeast, and named as Sec61α, Sec61β, and Sec61γ in mammalian cells. This complex forms an aqueous channel consisting of 10 transmembrane segments, which allow the passage of hydrophilic polypeptides across the ER membrane, and a lateral gate toward the lipid bilayer for integration of hydrophobic segments (Panzner et al. 1995, Görlich et al. 1992, Görlich, Rapoport 1993, Stirling et al. 1992). Various ligands interact with the Sec61 channel to promote protein translocation and to regulate its dynamics between the open and closed conformations. The major roles in this process are played by the precursor polypeptide itself, the ribosome and, at the ER lumen side, by the molecular chaperone Kar2 in yeast, a member of the heat shock protein 70 (Hsp70) family, or its equivalent in mammals BiP (immunoglobulin-heavy-chain binding protein) (Chirico, Waters & Blobel 1988, Craven, Egerton &

Stirling 1996, Panzner et al. 1995, Görlich et al. 1992). Binding of the chaperone to the nascent precursor protein at the luminal side guarantees an efficient and unidirectional transport across the ER membrane (Alder et al. 2005, Tyedmers et al. 2003).

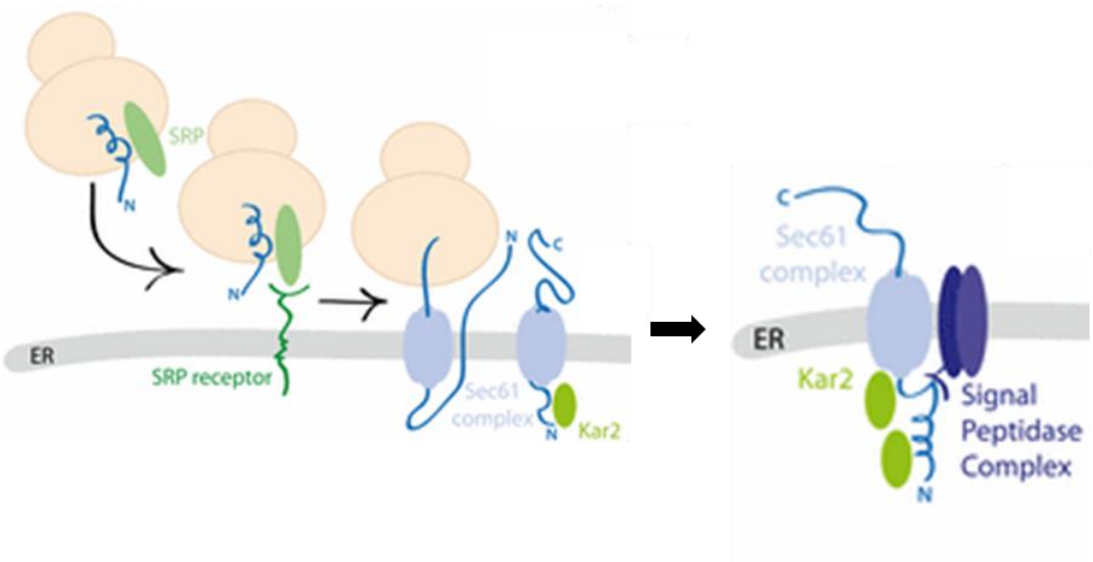

Figure 1.5 - Co-translational translocation of proteins to the Endoplasmic Reticulum (ER). It consists of SRP-mediated targeting of a nascent polypeptide chain-ribosome complex to the SRP receptor at the ER membrane, followed by translocation through the Sec61 complex into the ER lumen, with the assistance of Kar2 (or BiP) chaperone. The signal sequence is subsequently cleaved by the Signal Peptidase Complex, as soon as the cleavage site is exposed in the ER lumen (Figure adapted from (Barlowe, Miller 2013))

The prevalent mechanism reported in mammalian cells appears to be co-translational (Figure 1.5), involving most of the secretory proteins and many organellar and membrane proteins, whose biosynthesis occurs on rough ER-associated ribosomes simultaneously with their translocation into the membrane or lumen of the ER. Membrane proteins are inserted into the ER membrane unlike soluble, secretory polypeptides that are transported to the ER lumen (Barlowe, Miller 2013).

Once translation of mRNAs has started, the signal sequence of the nascent protein is bound by the cytosolic SRP as it is synthetized and emerges from the ribosome.

This usually occurs when the protein is about 70 amino acids long as 30 residues remain buried in the ribosome (Walter, Blobel 1981, Halic et al. 2004).

Signal sequences differ in length among the secretory proteins as well as in shape and amino acid composition. However, they usually consist of 16-30 amino acid residues, which present a similar tripartite structure consisting of a positively charged N-terminus, a main central hydrophobic region and C-terminal polar region containing the cleavage site (described in details in the next section) (Heijne 1983, von Heijne 1984, von Heijne 1985).

The SRP is a ribonucleoprotein composed of a 7S RNA component of 300 nucleotides and various protein subunits: Srp7p, Srp14p, Sec65p, Srp21p, Srp54p, Srp68p and Srp72p in yeast, or the equivalent SRP9, SRP14, SRP19, SRP54, SRP68, and SRP72 in mammalian cells (Brown et al. 1994, Halic et al. 2004, Nyathi, Wilkinson & Pool 2013). A major role is performed by the SRP54 subunit, which interacts with the ribosome, the signal sequence and with its receptor (SR) at the ER membrane, a heterodimer formed by α and β subunits (High, Dobberstein 1991, Zopf, Bernstein & Walter 1993, Nyathi, Wilkinson & Pool 2013). SRP normally binds to non-translating ribosomes with low affinity and the presence of the signal sequence at the exit site of the ribosome has been shown to increase its affinity for the ribosome (Flanagan et al. 2003, Halic et al. 2004).

After binding the signal peptide, the SRP binds its ER-membrane localized receptor, based on a GTP-dependent interaction between the SRP54 protein of the SRP and the α subunit of the SR (Nyathi, Wilkinson & Pool 2013). As a result, the ribosome-nascent chain-SRP complex is targeted to the Sec61 complex in the ER membrane so that the signal sequence can bind to the translocon, stimulating the initiation of the protein translocation across the ER membrane. The Sec61 complex undergoes a conformational change, thus opening the internal channel (Görlich et al. 1992, Rutkowski et al. 2003). The signal sequence seems also to mediate the ribosome association with the translocon, which facilitates stabilization and opening of the translocation complex (Nyathi, Wilkinson & Pool 2013, Rutkowski et al. 2003). Subsequently, the SRP-SR complex dissociates from the ribosome and the SRP is released in the cytosol, upon GTP hydrolysis, so that it can be used for a new

nascent precursor protein. The nascent chain inserts into the conducting channel of the translocon with the leader peptide ultimately assuming a loop conformation, with the N-terminus usually facing the cytosolic face and the C-terminus with the cleavage site facing the ER lumen (Shaw, Peter & Rose 1988, Goder, Spiess 2003). The polypeptide chain is now translated and simultaneously translocated into the translocation pore, a process driven by the hydrolysis of ATP. In yeast it has been widely reported that the ER chaperone Hsp70-type Kar2 binds to the growing chain on the luminal surface and then, again powered by the hydrolysis of ATP, releases the nascent chain (Craven, Egerton & Stirling 1996, Dierks et al. 1996). This cycle of binding and release of the nascent chain by Kar2 is essential for translocation to continue. The ATP needed for the luminal chaperones to fulfil their function is imported from the cytosol by an ATP/ADP translocase, called nucleotide exchange factor (NEF), located in the ER membrane (Craven, Egerton & Stirling 1996, Dierks et al. 1996). As mentioned earlier, the binding of Kar2/BiP to the incoming polypeptide ensures correct and unidirectional translocation, as movement through the translocation channel would otherwise be reversible (Tyedmers et al. 2003, Alder et al. 2005).

As soon as the cleavage site is exposed within the lumen, it is recognized and cleaved by the signal peptidase complex (SPC) located at the luminal side of the ER membrane. The SPC is an endoprotease consisting of four subunits: Spc1, Spc2, Spc3 and Sec11 (Evans, Gilmore & Blobel 1986). The latter contains the protease active site and is suggested to be located close to the translocation channel exit at the lumenal surface; Spc3 seems to be also essential for peptidase activity whereas Spc2 was reported to bind the Sec61 complex (Evans, Gilmore & Blobel 1986, Meyer, Hartmann 1997, Antonin, Meyer & Hartmann 2000).

The cleaved signal peptide is subsequently digested by the signal peptide peptidase (SPP), located within the ER membrane, and the resulting fragments are eventually released from the membrane into the cytosol, where they can be further processed or rapidly degraded in the proteasome (Lyko et al. 1995). The nascent protein continues its co-translational translocation and its process of maturation into the ER lumen, which includes events of modification. Specific enzymes present on the

luminal surface can add carbohydrates to the chain at specific residues of asparagine as soon as they emerge from the translocon (described in section 1.5.1.4). This represents a predominant protein modification known as N-linked glycosylation and operated by the oligosaccharyl transferase (OST) complex (Chavan, Yan & Lennarz 2005). Once translation is completed, the ribosomes are released, the C-terminus portion of the protein is also transferred into the ER lumen, the conducting channel of the translocon shuts, and the protein is subjected to a process of folding by the assistance of lumenal chaperones, such as BiP (Barlowe, Miller 2013). Lectins, such as calnexin and calreticulin, are crucial for the folding of glycoproteins through their interactions with sugars (Barlowe, Miller 2013). Further glycosylation events can occur within the ER after the protein is fully translated, consisting of subsequent modifications of the N-glycan attached previously as well as O-glycosylation (described below). Other modifications that can occur in the ER include the formation of disulphide bonds by the protein-disulfide isomerase (PDI) and the addition of a glycophosphatidylinositol (GPI) anchor (Barlowe, Miller 2013).

Post-translational translocation also occurs through the translocon complex but in a ribosome- and SRP-independent manner. In yeast and mammalian cells, precursor polypeptides entirely synthetized on unattached ribosomes in the cytosol are then targeted to the ER translocation machinery thanks to the interaction with cytosolic molecular chaperones, such as members of the Hsp70 and Hsp40 chaperone families, which maintain precursor proteins in an unfolded state and promote their binding with transport components in the ER membrane (Chirico, Waters & Blobel 1988, Deshaies et al. 1988, Ast, Cohen & Schuldiner 2013).

In this post-translation process, the Sec61 machinery is associated to another heterotrimeric complex at the ER membrane, the Sec63 complex, consisting of Sec63, Sec62 components (and additional Sec71, and Sec72 in yeast) (Deshaies et al. 1991, Panzner et al. 1995, Meyer et al. 2000). This Sec63 complex seems to act as a signal peptide receptor, binding the N-terminal signal sequence of the polypeptide and subsequently inducing a conformational change of the Sec61

channel in an open state to allow insertion of the protein into the ER membrane. As a result, the signal sequence can interact with cytosolic components of the Sec61 complex and be inserted in the translocation pore (Plath et al. 1998). Involvement of Sec62 and Sec63 has been actually reported also in the co-translational mechanism of certain precursor polypeptides in yeast and mammalian cells. For instance, in yeast, Sec62 and Sec63 were shown to interact with ribosomes and BiP to take part in the regulation of Sec61 channel conformation by binding to the ER luminal side of Sec61α and providing binding energy to the system (Brodsky, Schekman & Goeckeler 1995, Young et al. 2001). As mentioned above, the lumenal Hsp70-type chaperone Kar2 in yeast, or BiP in mammalian cells, is the other fundamental component that promotes the efficient protein import through the ER membrane. Once a hydrophilic region of the protein is inserted into the channel, the Kar2 chaperone is able to bind the polypeptide in an ATP-dependent manner, thus regulating and directing the protein import across the membrane (Craven, Egerton & Stirling 1996, Dierks et al. 1996). Kar2 chaperone has been also reported to interact with the luminal DnaJ domain of the Sec63 component and together they seem to tightly regulate the protein transport until it is completed (Brodsky, Schekman 1993, Panzner et al. 1995, Misselwitz et al. 1999, Matlack et al. 1999). As for the co-translational process, the N-terminal signal sequence, that initially remains inserted into the ER membrane facing the cytosol, is eventually removed by the ER membrane-associated SPC by endoproteolytic cleavage, thus permitting the protein release into the lumen.

Other components of the translocation machinery have also been described although their role is not fully understood. Examples are the translocating chain-associating membrane (TRAM), the translocon-associated protein (TRAP) complex, the ribosome-associated membrane protein RAMP4, and additional molecular chaperones (Voigt et al. 1996, Fons, Bogert & Hegde 2003, Shao, Hegde 2011, Johnson et al. 2012, Pool 2009).

1.5.1.2. Roles of the signal sequence

Signal sequences play several roles to ensure the efficient targeting, translocation and processing of nascent proteins (Hegde, Bernstein 2006). They usually consist of 16-30 amino acid residues located at the N-terminus of the respective protein. Although they do not display extensive homology in their amino acid sequence, they share similar features in the structure, which typically consists of three conserved domains, a positively charged N-terminus, a predominant hydrophobic core, and a C-terminal polar domain which contains the cleavage site for the signal peptidase (Heijne 1983, von Heijne 1984, von Heijne 1985). They are termed respectively n-, h- and c-region. These structural features are crucial to permit the efficient SRP recognition, translocation into the ER and cleavage of the precursor proteins (Nilsson et al. 2015).

The h-region is a 6-15 residue long domain fundamental for co-translational processing. As mentioned above, the hydrophobicity of the signal peptide is the main criterion that determines the translocation pathway of a nascent polypeptide, whether co-translational or post-translational (Ng, Brown & Walter 1996, Hatsuzawa, Tagaya & Mizushima 1997). High hydrophobic signal peptides usually characterize proteins that are directed to the SRP-dependent pathway. The h-region has been shown to be essential and sufficient for signal peptide recognition/binding by SRP. Moreover, mutations in this region have been also shown to affect protein translocation across the membrane. Indeed, the hydrophobicity has been described as having an effect on the orientation of the signal sequence within the translocon, influencing the N-terminus positioning towards the lumenal or cytosolic side and consequently affecting the protein orientation (Nilsson et al. 2015, Rosch et al. 2000).

The n-region is a short 1-5 residue hydrophilic domain that contains up to three positively charged basic residues, which have been described to facilitate the binding to SRP and the translocation across the membrane (Nilsson et al. 2015, Peterson, Woolhead & Bernstein 2003). Mutations in this region have shown to decrease the efficiency but not completely abolish the signal sequence recognition by SRP and the subsequent translocation, thus suggesting that the positive charged

amino acids mainly promote and guarantee the efficient interaction of the signal sequence with SRP and with the translocon components. Studies have reported that the positive charged residues contribute to the correct orientation of the signal sequence across the ER membrane, through a dynamic process that ultimately leads the positive N-terminus toward the cytosol (Nilsson et al. 2015, Kocik, Junne & Spiess 2012).

The c-region is a polar domain consisting of 4-7 residues, which include crucial amino acids required for the signal peptide cleavage. Residues at -1 and -3 positions, preceding the cleavage site, are particularly critical in regards to this. These positions are usually occupied by small and neutral residues, such as Ala, Gly, Cys, and Ser, leading to the formulation of the so-called (-1,-3) rule (Nothwehr, Gordon 1990, Auclair, Bhanu & Kendall 2012). Moreover, this region was also termed Ala-X-Ala motif due to the prevalence of Ala in such positions (Auclair, Bhanu & Kendall 2012). Other studies have also reported that the physical-chemical properties of the -1 residue and the length of the c-region are particularly important in defining the site of cleavage (Nothwehr, Gordon 1990, Auclair, Bhanu & Kendall 2012). Typically, the c-region also contains Pro or Gly residues, which are suggested to be important to impede the formation of a secondary structure (Nothwehr, Gordon 1990, Auclair, Bhanu & Kendall 2012). Structural features of this region are therefore critical for the efficient interaction with the active site of the signal peptidase.

The signal sequence has been described to influence the timing and efficiency of the protein translocation and cleavage. Consequently this affects the timing of post-translational modification, folding and ER exit of the proteins (Rutkowski et al. 2003, Hegde, Bernstein 2006). The signal sequence, through its hydrophobic domain, can reorient itself within the translocation channel, through its interaction with the translocon components Sec61α and Sec61β. This regulates its presentation to the processing machinery, providing access to the active site of the SPC and allowing subsequent N-linked glycosylation by the OST (Rutkowski et al. 2003, Hegde, Bernstein 2006). In the case of glycoproteins with N-glycosylation acceptor sites located close to the signal peptide, it has been shown that signal

sequence cleavage is a prerequisite for the efficient glycosylation modification (Chen et al. 2001).

1.5.1.3. Quality control of protein folding

In order to ensure the correct protein folding and assembly within the ER, proteins undergo a process of quality control (Hegde, Ploegh 2010). This is monitored by a system mainly consisting of ER chaperones, which associate with unfolded proteins to assist their maturation. Proteins that fail to assume the correct conformation are prevented from continuing along the secretory pathway. If this is the case, the quality control system acts to repair or remove these incorrect proteins (Tsai, Ye & Rapoport 2002, Hegde, Ploegh 2010, Buchberger, Bukau & Sommer 2010) (Figure 1.6).

The presence of misfolded proteins has been described to disrupt ER homeostasis, a condition called ER stress, which activates a signalling network known as the unfolded protein response (UPR) (Hegde, Ploegh 2010). Through activation of different signalling pathways, UPR leads to an increase in the chaperone concentration within the ER as well as of the cellular proteolytic system components, by up-regulation of their gene expression. The higher presence of chaperones is needed to restore the correct folding process. A simultaneous down-regulation of the global protein translation is also usually induced to facilitate the folding process machinery (Tsai, Ye & Rapoport 2002, Hegde, Ploegh 2010, Buchberger, Bukau & Sommer 2010).

In the case the chaperone-mediated folding continues to fail, proteins are recruited for proteasomal degradation in the cystosol, through a process called ER-associated degradation (ERAD). This mechanism consists of selective recognition of the misfolded substrate by the action of several factors. They typically include components of the ER processing machinery, including the chaperone BiP, calnexin, calreticulin, protein disulfide isomerase (PDI) and GRP94 (Tsai, Ye & Rapoport 2002, Hegde, Ploegh 2010, Buchberger, Bukau & Sommer 2010). Usually the substrate is recognised because of the exposure of structural elements not normally present in

the native protein, such as hydrophobic regions, erroneous post-translational modification and disulphide bonds formation. In the case of glycoproteins, for example, they can be targeted for degradation depending on the glycan composition, specifically modified by glycosidase/glycosyltransferase enzymes and recognised by the calnexin/calreticulin system. Glycans can act as signals to inform about the status of the proteins and either direct them to the target cellular compartment, if they are properly folded, or trigger the quality control system to assist their folding process, or delivering to ERAD (Tsai, Ye & Rapoport 2002, Hegde, Ploegh 2010, Buchberger, Bukau & Sommer 2010).

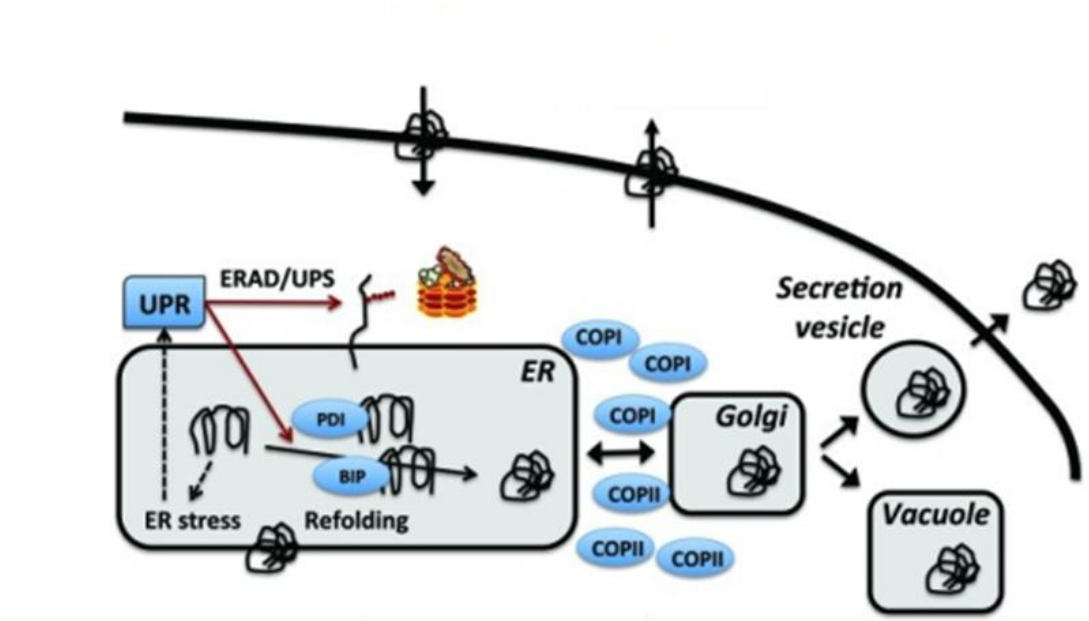

Figure 1.6 - Quality control of protein folding. It ensures that only proper folded proteins proceed along the secretory pathway. Otherwise, the presence of misfolfed proteins determines ER stress and induces the Unfolded Protein Response (UPR), which in turn activates ER chaperones (e.g. BiP) to facilitate the folding or the ERAD/ubiquitin proteasome system (UPS) pathway to degrade the protein (Figure adapted from (Nielsen 2013)).

Recognised substrates, in association with the ER chaperones, are subsequently delivered, through an ER transmembrane complex, to the cytosolic face of the ER membrane where an ubiquitin-ligase complex targets them for proteasomal degradation (Tsai, Ye & Rapoport 2002). A process of retro-translocation from the ER back to the cystosol is therefore required. The export machinery has not been

fully characterised but different complexes have been suggested to be involved in this process. These include the same complex involved in protein translocation to the ER (Sec61), the ubiquitin-ligase complex and members of the Derlin family (Tsai, Ye & Rapoport 2002, Hegde, Ploegh 2010, Buchberger, Bukau & Sommer 2010). As soon as proteins emerge at the cytosolic face of the ER membrane, they are subjected to polyubiquitination by the action of the catalytic subunit E3 ubiquitin-ligase. Proteins can then be released into the cytosol, via an ATP-driven mechanism, and recognized by proteasomal components for their degradation (Tsai, Ye & Rapoport 2002, Hegde, Ploegh 2010, Buchberger, Bukau & Sommer 2010) (Figure 1.6).

In addition to the ERAD system, misfolded proteins can sometimes proceed through the secretory pathway and be sent to lysosomes for degradation (Hegde, Ploegh 2010). Furthermore, in the case of an excessive accumulation of misfolded proteins, overwhelming the ERAD system or causing formation of protein aggregates in the ER, their degradation can occur through the autophagic pathway (Buchberger, Bukau & Sommer 2010). It is unlikely that large protein aggregates can be transported through the ER membrane export channel. The ERAD system is also involved in the "quantity" control to remove proper folded proteins when over-produced and unnecessary (Hegde, Ploegh 2010).

Finally, in case the degradative system is unable to remove the misfolded or aggregated protein, the UPR can induce the apoptotic pathway in order to remove the damaged cell (Kim et al. 2006). This, for example, occurs in degenerative diseases, characterised by accumulation of misfolded proteins, protein aggregates and a saturated/non-functional proteolytic system, where UPR ultimately leads to cell death (Rutishauser, Spiess 2002).

1.5.1.4. Protein maturation in the ER and Golgi apparatus

Once proteins have been folded and appropriately modified, vesicular transport allows them to be directed from ER to Golgi apparatus and subsequently to the cell surface for secretion (Barlowe, Miller 2013). Vesicles formation from donor

membranes requires the recruitment of cytosolic coat proteins, which differ based on the cellular route. Transport vesicles that bud off from the ER directed to the Golgi apparatus are COPII-coated. There is also a retrograde transport from Golgi back to ER, essential to retrieve escaped proteins that are misfolded or not fully processed, or proteins that are destined to reside in the ER. This transport is mediated by COPI-coated vesicles (Barlowe, Miller 2013, Nickel, Wieland 1998).

ER-originated COPII-coated vesicles merge together to form the ER-Golgi intermediate compartment (ERGIC). Subsequently, the cargo proteins are transported through the various cisternae of the Golgi stack, consisting of cis-Golgi, medial compartment, trans-Golgi and ultimately to the trans-Golgi network (TGN), where proteins are sorted and delivered to the appropriate destination i.e. the endosomal-lysosome system, the plasma membrane or the secretory granules (Barlowe, Miller 2013). In absence of other signals present within the protein sequence or acquired by post-translational modifications, proteins are usually directed for secretion through secretory vesicles that fuse with the plasma membrane, thus releasing their content in the extracellular space (Barlowe, Miller 2013).

Within the Golgi apparatus, cargo proteins can undergo extensive glycan processing as well as additional modifications including phosphorylation, sulfation, and proteolytic processing, which are usually necessary for the bioactivity, targeting or stability of the protein (Barlowe, Miller 2013). Among the different post-translational modifications, glycosylation represents one of the most important processes, which modulates both structural and regulatory functions of proteins by monitoring protein folding and targeting for degradation (Stanley 2011). Glycosylation is also often essential for protein targeted to specific cellular compartments, as occurs for lysosomal hydrolases such as cathepsins (described in section 1.2.3.2).

Main forms of glycosylation include N-linked and O-linked glycosylation, which consist, respectively, in the covalent addition of a glycan to the side-chain amino group of an asparagine (N) residue within the conserved Asn-X-Thr/Ser sequence (where X can be any amino acid expect Proline), and to the hydroxyl group (O) of a

serine or threonine amino acid (Stanley 2011). The O-linked glycans usually consist of simple oligosaccharide structures compared to the N-linked glycans, whose complexity varies among different glycopeptides. In both forms of glycosylation, sugar nucleotides are used as monosaccharide donors (Stanley 2011).

As described earlier, N-glycosylation typically occurs co-translationally. It begins in the ER with the addition of a precursor oligosaccharide to a nascent growing protein during its translocation into the ER lumen (Chavan, Yan & Lennarz 2005). The precursor oligosaccharide is synthesised and activated in the cytosol from sugar nucleotides and then transferred and linked to dolichol, which is a lipid carrier in the ER membrane (Stanley 2011). High energy is required for synthesis and transfer of an oligosaccharide. Its transfer to the protein is mediated by the transmembrane enzyme OST, as soon as the Asn-X-Ser/Thr acceptor site emerges into the ER lumen. The N-glycan is then further processed in the ER and then, once in the Golgi apparatus, can remain unmodified or undergo further changes. Specific modifications occur in the different Golgi compartments consisting in both removal and addition of specific sugar residues ultimately leading to formation of complex or hybrid N-glycans (Schedin-Weiss, Winblad & Tjernberg 2014, Stanley 2011).

O-glycosylation only occurs post-translationally by addition of a sugar molecule to Ser or Thr residues of a fully translated and folded protein (Stanley 2011). It can begin in the ER or alternatively in the cis-Golgi compartment. Transfer of the cytosolic precursor oligosaccharide is catalysed by an O-galactosaminyl-transferase (OGT), localised in both ER and cis-Golgi (Schedin-Weiss, Winblad & Tjernberg 2014, Stanley 2011, Steen et al. 1998). Subsequently, O-glycans are extended and modified in the other Golgi compartments by sequential removal and addition of different types of sugar residue, by the action of glycosidase and glycosyl-transferase enzymes. In the different Golgi compartments the glycan can be also modified by epimerases and sulfotransferases, thus adding different modifications. Furthermore, in some cases, the event of O-glycosylation can occur also in the cytosol and nucleus, where it has been reported to be involved in gene expression regulation or signal transduction (Schedin-Weiss, Winblad & Tjernberg 2014, Stanley 2011, Steen et al. 1998).

1.5.2. Alternative secretory pathways

A large number of soluble proteins are secreted from secretory vesicles fusing with the plasma membrane via the classical secretory pathway. However, many proteins are also released in the extracellular space via alternative mechanisms, which do not require ER and Golgi involvement. These so-called unconventional secretory pathways have been shown to be unaffected by the inhibitor of the classical ER-Golgi pathway, brefeldin A (BFA) (Nickel 2005). Mechanisms and functions of these alternative pathways are not entirely understood. In general, these proteins do not contain signal sequences, usually localize in the cytoplasm and can be secreted under physiological and pathological conditions (Nickel 2005).

Several unconventional pathways have been reported (Figure 1.7), including the lysosomal exocytosis and the secretion by exosomes. These two pathways consist of fusion to the plasma membrane of intracellular vesicles derived from the endosomal system, followed by release of the protein cargo into the extracellular space (Nickel 2005). In addition, cytosolic proteins can also be directly translocated, through a non-vesicular mechanism, from the cytoplasm across the plasma membrane into the extracellular space. This can occur by means of protein conducting channel (e.g. ATP-binding cassette (ABC) transporters) or through plasma membrane blebbing that consists in the shedding of membrane-derived vesicles (Nickel 2005).

Another alternative Golgi-independent pathway has been described particularly for membrane proteins, which consists in the direct protein transportation from the ER to the plasma membrane (Nickel, Rabouille 2009).

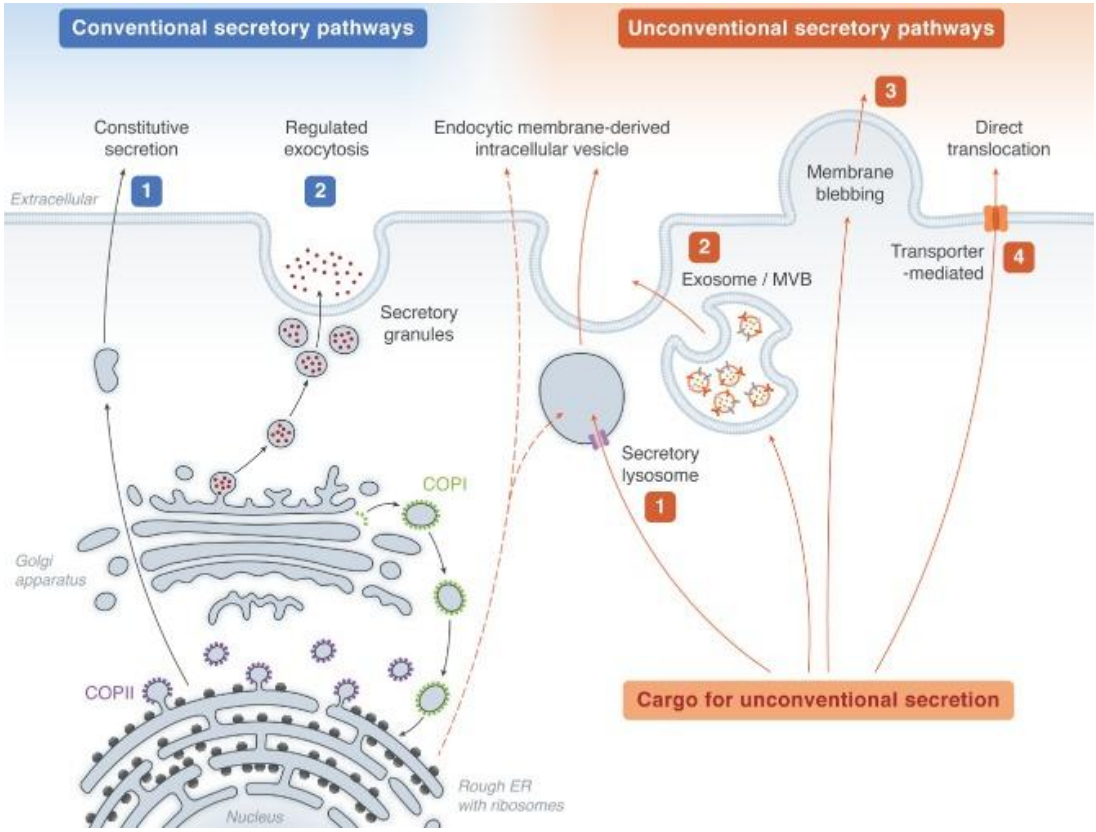

Figure 1.7 - Unconventional secretory pathways. As an alternative to the conventional secretory pathway (1, 2 in blue), a number of proteins is released in the extracellular space by several other ER-Golgi independent mechanisms, such as lysosomal exocytosis (1, in red), exosomes (2, in red), membrane blebbing (3), or transporter-mediated pathway (4) (Figure from (Bhattacharya, Prakash & Eissa 2014)).

1.5.3. Targeting to mitochondria

Protein transportation to mitochondria always occurs post-translationally, after the protein has been fully synthesised as precursor on cytosolic ribosomes (Kim, Hwang 2013). Subsequently, molecular chaperones are responsible for delivering the protein to the mitochondrial membrane for its subsequent translocation (Kim, Hwang 2013).

Mitochondria are complex organelles, consisting of two membranes, called outer and inner membrane, an intermembrane space and, more internally, the matrix. For this reason, mitochondrial import is a highly complex mechanisms consisting of multiple import machineries and targeting signals, depending on the compartment where the protein is destined to reside (Chacinska et al. 2009, Schmidt, Pfanner &

Meisinger 2010, Becker, Böttinger & Pfanner 2012). In general, the precursor protein contains a targeting signal, which leads the protein to the mitochondrial outer membrane. From here, additional signals can direct the protein to its specific intra-mitochondrial compartment (Chacinska et al. 2009, Schmidt, Pfanner & Meisinger 2010, Becker, Böttinger & Pfanner 2012). A variety of targeting and sorting signals is present to specifically target the protein to one of the several translocation machineries present in the mitochondria, in both the outer and inner membranes. Several cytosolic (e.g. Hsp70, Hsp90, MSF) and mitochondrial chaperones (e.g. small TIM chaperones) are also essential for the correct protein transportation.

The different import pathways characteristic for each mitochondrial compartment are extensively reviewed elsewhere (Chacinska et al. 2009, Schmidt, Pfanner & Meisinger 2010, Becker, Böttinger & Pfanner 2012) (Figure 1.8). The variety of targeting signals is briefly described below.

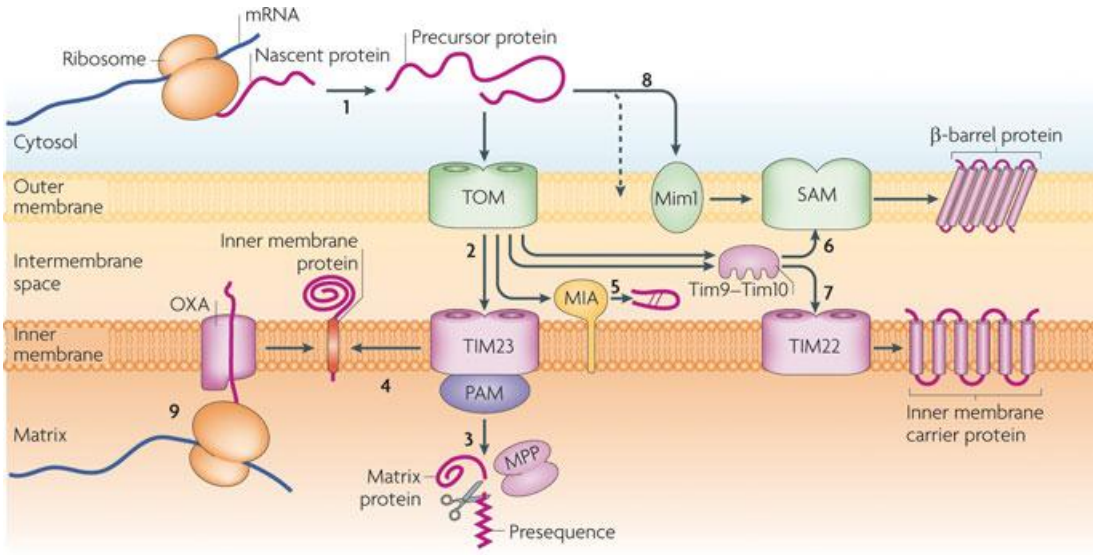

Figure 1.8 - Mitochondrial import pathways. They include several mechanisms depending on the protein properties and the submitochondrial compartment where the protein is destined to reside (i.e. outer membrane, intermembrane space, inner membrane, matrix). Further details are described in the section 1.5.3 (Figure adapted from (Schmidt, Pfanner & Meisinger 2010)).

Precursor proteins synthesised in the cytosolic ribosome contain targeting signals recognised by specific cytosolic chaperones and/or by receptors present in the mitochondrial outer membrane. These signals can be generally subdivided in cleavable N-terminal pre-sequences and non-cleavable internal signals. The first group is usually recognised by the specific receptors Tom20 and Tom22, which are part of the translocase of the outer membrane (TOM) complex. The second group is usually recognised by the receptor Tom70, also part of the TOM complex, with the assistance of cytosolic chaperones (Hsp70 and Hsp90) (Chacinska et al. 2009, Schmidt, Pfanner & Meisinger 2010, Becker, Böttinger & Pfanner 2012). However, both groups merge to the hydrophilic channel Tom40 for their translocation across the outer membrane, which therefore represents the common gate entry for the majority of the mitochondrial precursors. Subsequently, the different precursors engage specific pathways for each mitochondrial sub-compartment, depending on additional sorting signals present in the protein sequence (Schmidt, Pfanner & Meisinger 2010, Chacinska et al. 2009, Becker, Böttinger & Pfanner 2012).

The N-terminal pre-sequence usually consists of 10 to 60 amino acids forming an amphipathic, positively charged α-helix. Both its hydrophobic and charged surfaces are essential for recognition and binding by Tom receptors. In absence of any other signals, these precursors are subsequently targeted to TIM23 complex in the inner membrane. Then, with the cooperation of the import motor PAM, they are released in the matrix where the pre-sequence is proteolytically cleaved by the mitochondrial processing peptidase (MPP) and the mature protein subjected to folding with the help of mitochondrial chaperones (Schmidt, Pfanner & Meisinger 2010, Chacinska et al. 2009). Next to the pre-sequence, precursor proteins can possess an additional uncleaveable or cleavable hydrophobic sorting signal. In the first case it operates as a stop transfer signal to hold the protein in the mitochondrial inner membrane. In the second case, this signal is subsequently cleaved by the inner membrane peptidase (IMP), thus releasing the protein in the intermembrane space (Schmidt, Pfanner & Meisinger 2010, Chacinska et al. 2009).

The second group of mitochondrial targeted proteins contains non-cleavable internal signals, which therefore remain in the mature proteins. They can be

destined to the inner membrane, intermembrane space and outer membrane. Proteins directed to the inner membrane usually possess multiple internal signals which permit protein transfer from the TOM complex to the inner membrane TIM22 complex, with the help of small TIM chaperones in the intermembrane space. These signals usually consist of six transmembrane segments distributed along the protein sequence (Schmidt, Pfanner & Meisinger 2010, Chacinska et al. 2009, Becker, Böttinger & Pfanner 2012).

Internal signals for intermembrane space proteins are instead characterised by cysteine motifs, which allow formation of disulphide bonds between the precursor emerging from the TOM complex and the receptor Mia40, located in the inner membrane facing the intermembrane space (Schmidt, Pfanner & Meisinger 2010, Chacinska et al. 2009, Becker, Böttinger & Pfanner 2012).

Proteins targeted to the outer membrane can be subdivided in α-helical and β-barrel proteins, and they are always characterised by a non-cleavable anchor-targeting signal. For α-helical proteins, the targeting signal can be located at the N-terminus, C-terminus or in the middle of the protein sequence. This signal generally contains positively charged residues at the side of a hydrophobic α-helical transmembrane segment. Depending on its position within the sequence, different pathways are engaged. For example, these include the protein transfer through the intermembrane space, via small TIM chaperones, from the Tom40 to the sorting and assembly machinery (SAM) in the outer membrane. Alternatively, the protein insertion can occur through the mitochondrial import 1 (Mim1), which then also interacts with the SAM complex. This pathway therefore does not involve the main Tom40 channel. Differently, β-barrel proteins possess a β-strand at the C-terminus (β-signal), which is also recognized by SAM thus permitting protein insertion in the mitochondrial outer membrane (Schmidt, Pfanner & Meisinger 2010, Chacinska et al. 2009, Becker, Böttinger & Pfanner 2012).

Mitochondrial protein import is therefore a highly elaborated mechanism, necessary to guarantee the correct protein localization in the various sub-mitochondrial compartments and consequently the correct mitochondrial functionality.

Chapter 2 - Materials and Methods

2.1. Cell culture

2.1.1. Cell lines used

Several human immortalised RPE cell lines were used in this study, including ARPE19, D4O7 and hTERT-RPE1. In addition, HeLa cell line was used as additional control.

The ARPE19 cell line is an immortal, non-transformed line derived from a primary culture of human RPE cells that maintains RPE-specific structural and functional characteristics (Dunn et al. 1996). It possesses classic epithelial cobblestone morphology with intercellular junction forming stable polarized epithelial monolayers. These cells are therefore valuable tools for in vitro studies of retinal pigment epithelium (Dunn et al. 1996). For this reason, this cell line was mainly utilised in this work. Origin: American Type Culture Collection (ATCC).

D407 cells are a spontaneously transformed human RPE cell line that also retains many morphologic and metabolic characteristics of RPE cells (Davis et al. 1995). However, it has been reported the loss of some enzymatic activity, involved for example in the retinol cycle, and cytoskeletal polarization (Davis et al. 1995). This cell line was used for some of the studies due to the advantage of higher transfection rate and faster growth. Origin: Departmental stocks.

hTERT-RPE1 cell line is a human telomerase-immortalized RPE cell line derived from a 1-year-old person, obtained transfecting the RPE-340 cell line with the pGRN145 hTERT-expressing plasmid (Gong et al. 2014). This line has been reported to achieve a high degree of RPE functional maturation (Gong et al. 2014). This cell line was used as control in some imaging experiments. Origin: ATCC.

HeLa cell line is a widely used immortalised epithelial cell line derived from cervical cancer cells (Scherer, Syverton & Gey 1953). It was used as additional control for some imaging experiments. Origin: ATCC.

2.1.2. Maintenance of cells in culture

ARPE19, D4O7 and hTERT-RPE1 cells were cultured in Dulbecco's modified Eagle's medium (DMEM):Ham's F12 Nutrient Mixture (1:1) (GIBCO, 11330), supplemented with 10% fetal bovine serum (FBS) (Sigma, 2442) and maintained at 37°C in 5% CO_2.

HeLa cells were cultured in DMEM (Biopolis Shared Facilities, IMCB, A*STAR, Singapore) supplemented with 10% FBS, 2mM L-Glutamine (Gibco, 25030081), 1 mM sodium-pyruvate (Gibco, 11360070) and 1% (0.1 mM) non-essential amino acids (Gibco, 11140050).

All cells were grown in 75cm^3 culture flasks and routinely subcultured by trypsinization using the following procedure. The cell monolayer was washed with phosphate buffered saline (PBS) (Biopolis Shared Facilities, IMCB, A*STAR, Singapore), then incubated with Trypsin-EDTA (Biopolis Shared Facilities, IMCB, A*STAR, Singapore) at 37°C for 2-3 minutes to allow cells to detach from the surface. Pre-warmed complete media was then added to neutralise the trypsin, and the cell suspension centrifuged at 200 g for 3 minutes. The cell pellet was then resuspended in complete media and seeded into new flasks at 1:3-1:5 ratio depending on the cell line. Cell counting by haemocytometer was carried out if seeding a precise number of cells was required for experimental purposes.

All cells lines were tested for the presence of mycoplasma contamination using the LookOut PCR Mycoplasma Detection Kit (Sigma), following manufacture's guidelines.

Cell stocks were stored and cryopreserved in liquid nitrogen using freezing media (50% FBS, 40% complete media, 10% DMSO).

2.1.3. Transfection

Cell lines were transiently transfected with cDNA plasmids encoding the protein of interest (described in section 2.2), using the lipid-based reagent Lipofectamine LTX with Plus reagent (Thermo Fisher Scientific, 15338). This transfection reagent was mainly used in this study. However, TurboFect (Thermo Fisher Scientific, R0531), a

cationic polymer-based transfection reagent, was also occasionally used. Higher transfection efficiency was achieved using Lipofectamine.

Transfection methods were used following manufacturer's guidelines. Most of the experiments were carried out on cells seeded in 6-well plates. Cells in 24-well plates and 100 mm dishes were also used in some experiments.

Cells were seeded in 6-well plates the day before transfection at a density between $2.5x10^5$ to $5.0 x10^5$ cells per well (depending on the cells line) in order to have cells 70-80% confluent at the time of transfection. The next day the media of cells was removed and replaced with Opti-MEM reduced serum media (Thermo Fisher, 31985). The transfection mixture used for each well consisted of 2 µg of DNA and 9 µl of Lipofectamine (6 µl in the case of Turbofect). The media was then replaced 5 hours after transfection with fresh complete media. Analysis was typically performed after 24 hours for all the different experiments.

For transfections in different sized culture plates or dishes, the amount of DNA and reagent was scaled appropriately based on manufacturer's guidelines. In general, 0.5 µg of DNA was used for cells in 24 well plates and 10 µg for cells in 100 mm dishes with 3 and 30 µL of Lipofectamine, respectively.

2.1.4. Cell treatments

In this study cells were treated with a number of different reagents. These treatments were usually carried out on ARPE19 cells seeded onto 6-well plates, transfected or non-transfected with cDNA constructs. In the case of transfected cells, reagents were added to the culture the day after transfection.

a) Inhibition of the secretory pathway was performed by using different reagents which block protein trafficking at different steps of the pathway. Brefeldin A (BFA), which blocks protein transport from ER to Golgi (Klausner, Donaldson & Lippincott-Schwartz 1992), Monensin, which inhibits transport of proteins through the Golgi stack (Mollenhauer, Morré & Rowe 1990) and

Nocodazole, a microtubule-depolymerizing agent that affects the Golgi structure and the transport of secretory vesicles (Trucco et al. 2004, Thyberg, Moskalewski 1999). Cells were treated with BFA (Epicentre, B901MG), at a final concentration of 5 μg/mL, Monensin (BioLegend, 420701) at 5μM, Nocodazole (Merk Millipore, 487928) at 10 μg/mL. Cell lysates and conditioned media were collected 3 and 7 hours post-treatment.

b) Inhibition of protein synthesis was carried out using cycloheximide (Sigma, C7698 and C1988), an antibiotic that blocks the mRNA translation on ribosomes (Obrig et al. 1971). It was used at a final concentration of 200 μM and cell lysates and conditioned media collected at 2, 7, and 24 hours after treatment.

c) Inhibition of proteolytic systems was performed by using Chloroquine (CQ) and MG132 to suppress ALP and UPS, respectively (described in chapter 6.2). CQ (Sigma, C6628) and MG132 (Merk Millipore, 474790) were used at final concentrations of 25 μM and 5 μM, respectively. Cell lysates and conditioned media were collected 24-hours post-treatment. mRNA was also extracted from cells treated with MG132 (described below).

2.2. Cloning

2.2.1. Plasmid DNA constructs used

2.2.1.1. Existing constructs

The pCys-EGFP construct was used to express the wild-type full-length precursor cystatin C. The plasmid was developed cloning cDNA of cystatin C into a pEGFP-N3 backbone, as described previously in Paraoan *et al.* (2001) (Figure 1.1). The Ala25Thr_pCys-EGFP plasmid was used to express the variant B full-length protein. This construct was produced by site-directed mutagenesis as described in Paraoan *et al.* (2004).

Wild-type and variant B cystatin C are therefore expressed as fluorescently labelled fusion proteins easily detected in live cells by fluorescence microscopy. They will be called WT-EGFP and VB-EGFP.

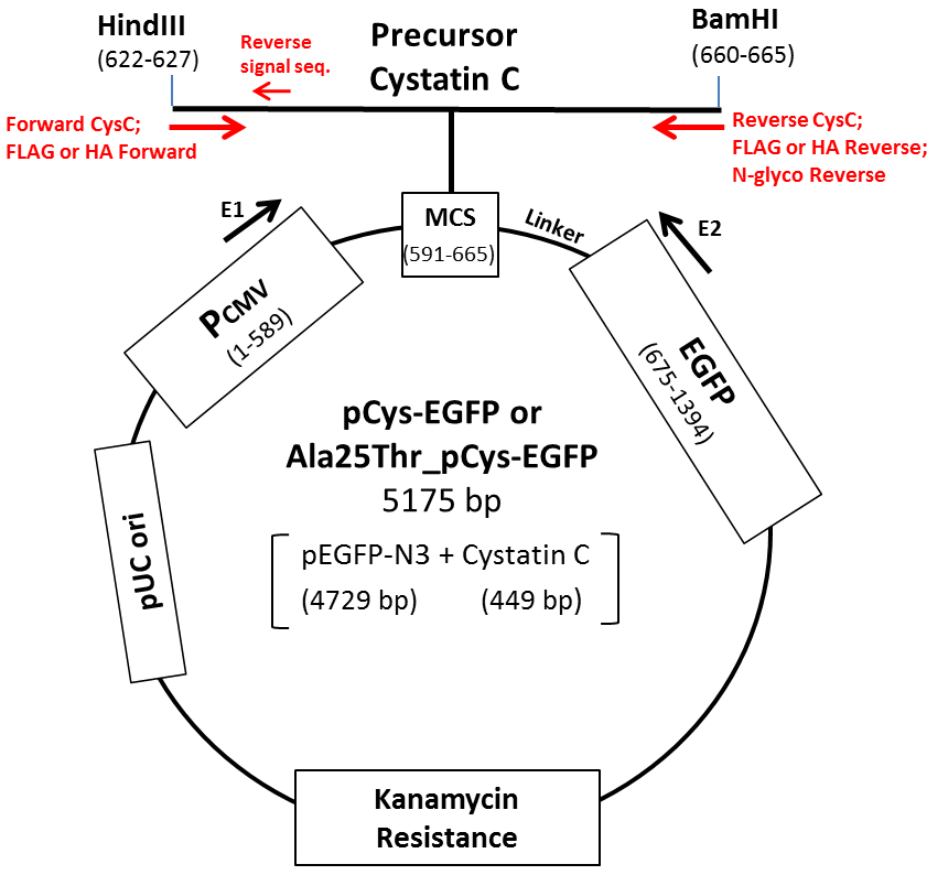

Figure 2.1 - Diagram of pCys-EGFP and Ala25Thr_pCys-EGFP constructs. Sequence encoding the wild-type or variant precursor cystatin C (449bp) was inserted into the

multiple cloning site (MCS, restriction sites HindIII/BamHI) of the pEGFP-N3 vector (4729 bp) (BD Biosciences Clontech). EGFP-linked cystatin C fusion proteins, separated by a 9 bp linker, are expressed in eukaryotic cells from a CMV promoter. Black arrows represent primers used for sequencing whereas red arrows represent the primers designed to develop the new constructs (see Table 1).

2.2.1.2. New constructs

Using the existing constructs as template (Figure 2.1 and Figure 2.2), new recombinant plasmids were generated (table 2) by designing specific primers (Table 1) in order to amplify and modify the sequence of interest. Restriction site sequences were included in all the primers: HindIII sequence in all the forward primers and BamHI in all the reverse primers (sequences shown in bold in Table 1). Start or stop codons were added when needed.

a) pEGFP-N3 based constructs

New EGFP-based constructs were engineered to express EGFP proteins fused to the leader sequence of the wild-type or variant B precursor cystatin C only. These constructs were named LPWT-EGFP and LPVB-EGFP respectively (Figure 2.3) and are used to further characterise the role of the signal peptide in the protein trafficking. Primers used for this purpose were designed in order to amplify only the signal sequence of cystatin C protein and are described in table 1 (Forward CysC and Reverse Signal Seq. primers).

b) pcDNA3-based constructs

Other constructs were obtained by subcloning the sequence of interest into the plasmid pcDNA3 that does not encode fluorescent proteins (Figure 2.4). In such constructs cystatin C is untagged or linked to small, non-fluorescent tags or N-linked glycosylation sites.

All the new constructs are shown in Table 2.

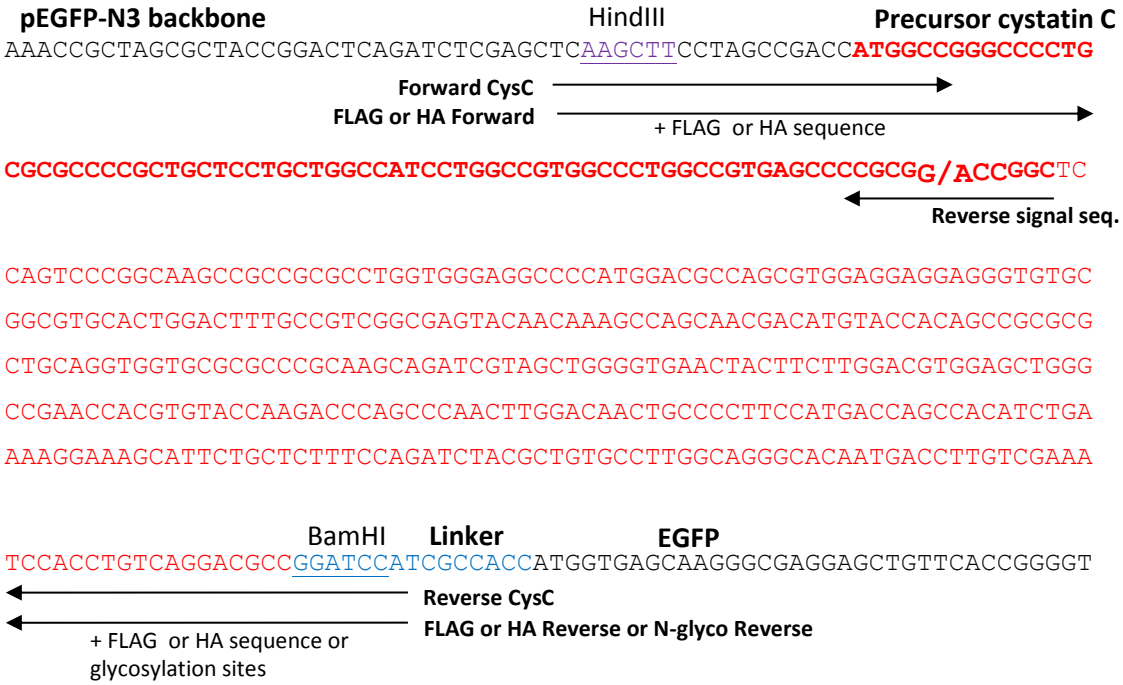

Figure 2.2 Sequence of the wild-type or variant cystatin C linked to EGFP in pCys-EGFP and Ala25Thr_pCys EGFP constructs respectively. The existing constructs expressing wild-type or variant B cystatin C linked to EGFP were used as template to generate the new recombinant plasmids. The arrows represent the sequences used for the forward and reverse primers, with the additional nucleotides to linking cystatin C sequence to a specific tag.

Table 1 - Sequences of forward and reverse primers used to generate the new constructs and for sequencing purposes. Primers included restriction site sequences for HindIII or BamHI in forward and reverse primers, respectively (in bold, black). Some primers contained a sequence encoding a tag, FLAG or HA (in bold, red) or for N-glycosylation sites (in blue). All primers are produced by Integrated DNA Technologies (IDT).

PRIMERS	SEQUENCE (5'-3')	Description	T annealing
Forward CysC	TC**AAGCTT**CCTAGCCGACCA TGGCC	Forward primer used to amplify insert from the N-terminus of full-length precursor cystatin C or leader sequence	61°C-65°C
Reverse CysC	AA**GGATCC**TTAGGCGTCCT GACAGGTGGA	Reverse primer to amplify from the C-terminus of cystatin C	61°C
Reverse signal seq.	WT: GG**GGATCC**GCCGGCCGCG VB: GG**GGATCC**GCCGGTCGCG	Reverse primers to amplify from the wild-type or variant B leader sequence of cystatin C	65°C
N-glyco reverse	AA**GGATCC**TTA**CTTGTCATC GTCGTCCTTGTAGTC**CATGG TGCTGTTACTGGTGCTGTTA CCGGCGTCCTGACAGGTGG A	Reverse primer to amplify from the C-terminus of cystatin C linked to two N-glycosylation sites and a FLAG tag	65°C
FLAG reverse	AA**GGATCC**TTA**CTTGTCTCG TCGTCCTTGTAGTC**GGCGTC CTGACAGGTGGA	Reverse primer to amplify from the C-terminus of cystatin C linked to a FLAG tag	61°C
HA reverse	AA**GGATCC**TTA**AGCGTAAT CTGGAACATCGTATGGGTA** GGCGTCCTGACAGGTGGA	Reverse primer to amplify from the C-terminus of cystatin C linked to HA tag	61°C
FLAG forward	AA**AAGCTT**GATTGCCGACC ATG**GACTACAAGGACGACG ATGACAAG**GCCGGGCCCCT GCGCGCCC	Forward primer to amplify from the N-terminus of cystatin C linked to a FLAG tag	61°C
HA forward	AA**AAGCTT**GATTGCCGACC ATG**TACCCATACGATGTTCC AGATTACGCT**GCCGGGCCC CTGCGGCCC	Forward primer to amplify from the N-terminus of cystatin C linked to a HA tag	61°C
E1-pEGFP	TATAAGCAGAGCTGGTTTA G	Forward primer for pEGFP-N3-based constructs sequencing	-
E2-pEGFP	CGTCGCCGTCCAGCTCGACC AG	Reverse primer for pEGFP-N3-based constructs sequencing	-

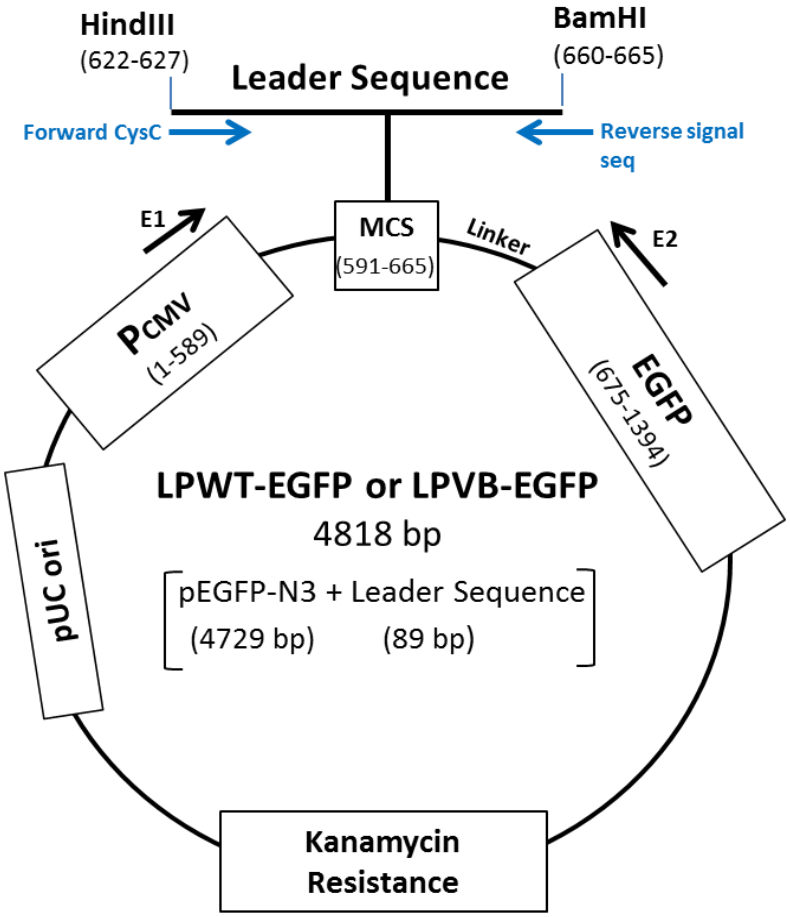

Figure 2.3 - Representation of LPWT-EGFP and LPVB-EGFP constructs. Sequence encoding the leader peptide of wild-type or variant cystatin C (89 bp including the Kozak sequence) was inserted into the multiple cloning site (MCS, restriction sites HindIII/BamHI) of a pEGFP-N3 vector (4729 bp). Leader Peptide-EGFP fusion proteins, including a 9 bp linker between their sequences, are expressed from a CMV promoter.

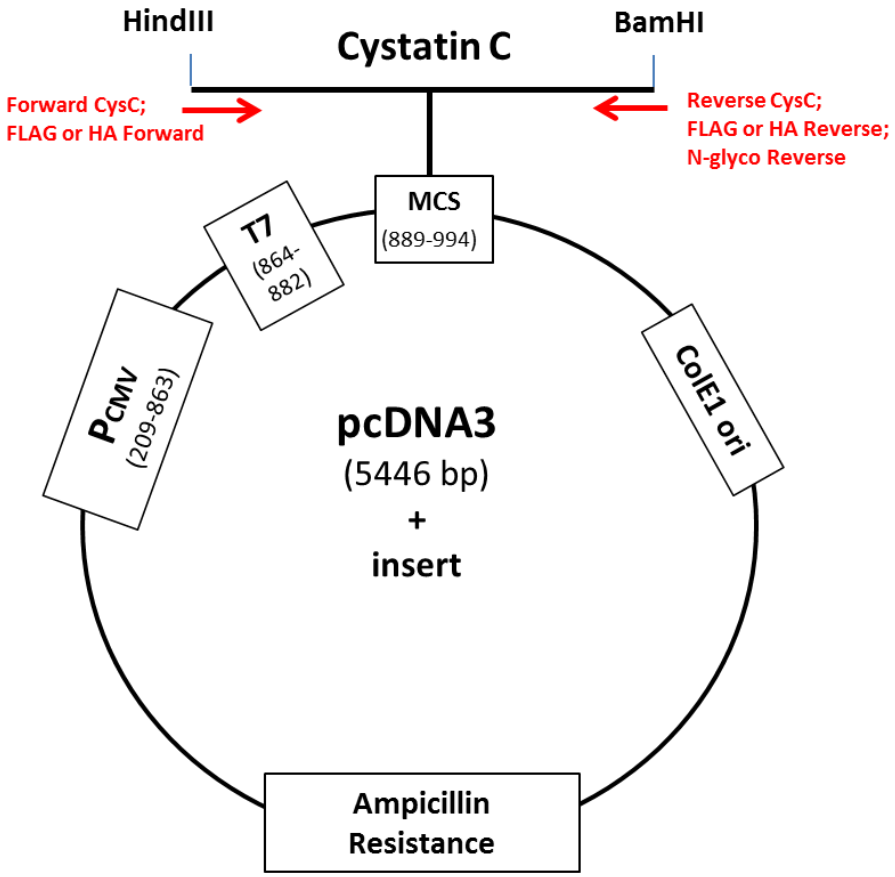

Figure 2.4 - Diagram of new pcDNA3-based constructs. Sequence encoding wild-type or variant cystatin C (449 bp) was inserted into the multiple cloning site (MCS) of a pcDNA3 vector (5.4kb) (Invitrogen) at HindIII/BamHI restrictions sites. Depending on the constructs, the sequence inserted into the vector includes also additional nucleotides to link cystatin C at either C- or N-terminal or both to small tags (FLAG or HA) or N-linked glycosylation sites.

Table 2 - Summary table of new constructs developed in this study. Names assigned to the new constructs, vectors used and size of the plasmid are reported in the table below. In the description, amino acid sequences of the tags used are also shown: N-glycosylation site in orange, FLAG in red and HA in blue.

CONSTRUCT	NAME	Description	Vector	Size
Leader peptide constructs	LPWT-EGFP and LPVB-EGFP	WT or VB Leader sequence of cystatin C linked to EGFP	pEGFP-N3	4729 + 89 = 4818 bp
Untagged cystatin C constructs	WT-Cystc and VB-CystC	WT or VB precursor cystatin C untagged	pcDNA3	5446 + 452 = 5898 bp
Cystatin C linked to N-glycosylation sites	WT Glyco and VB-Glyco	WT or VB precursor cystatin C linked at the C-terminal to two N-linked glycosylation sites and a FLAG tag: G-[NST]-S-[NST]-M-DYKDDDDK)	pcDNA3	5446 + 503 = 5949 bp
C-terminal FLAG-tagged cystatin C	WT-FLAG and VB-FLAg	FLAG tag (DYKDDDDK) at the C-terminal of precursor WT or VB cystatin C	pcDNA3	5446 + 476 = 5922 bp
C-terminal HA-tagged cystatin C	WT-HA and VB-HA	HA tag (YPYDVPDYA) at the C-terminal of precursor WT or VB cystatin C	pcDNA3	5446 + 479 = 5925 bp
N-terminal FLAG-tagged cystatin C	FLAG-WT and FLAG-VB	FLAG tag (DYKDDDDK) at the N-terminal of precursor WT or VB cystatin C	pcDNA3	5446 + 476 = 5922 bp
N-terminal HA-tagged cystatin C	HA-WT and HA-VB	HA tag (YPYDVPDYA) at the N-terminal of precursor WT or VB cystatin C	pcDNA3	5446 + 479 = 5925 bp
FLAG- and HA-tagged cystatin C constructs at both N- and C-terminus	HA-WT-FLAG, HA-VB-FLAG and FLAG-WT-HA, FLAG-VB-HA	FLAG and HA at either the N-terminal or C-terminal of precursor WT or VB cystatin C	pcDNA3	5446 + 503 = 5949 bp

2.2.2. Generation of new constructs

All the steps were performed according to manufacturer's guidelines.

Sequences of interest were generated by PCR using the existing EGFP-linked full-length cystatin C constructs as template and a thermostable proofreading DNA polymerase (Expand High Fidelity PCR Systems, Roche, 11 732 650 001). 100 ng of template DNA was mixed with 1µL of polymerase (3.5 U), 500 nM of primers and 200 µM of dNTPS and 5µL of Expand High Fidelity buffer in 50 µL of total volume.

The PCR parameters (shown in figure 2.5) used in a Peltier Thermal Cycler were optimised with annealing temperature as per Table 1.

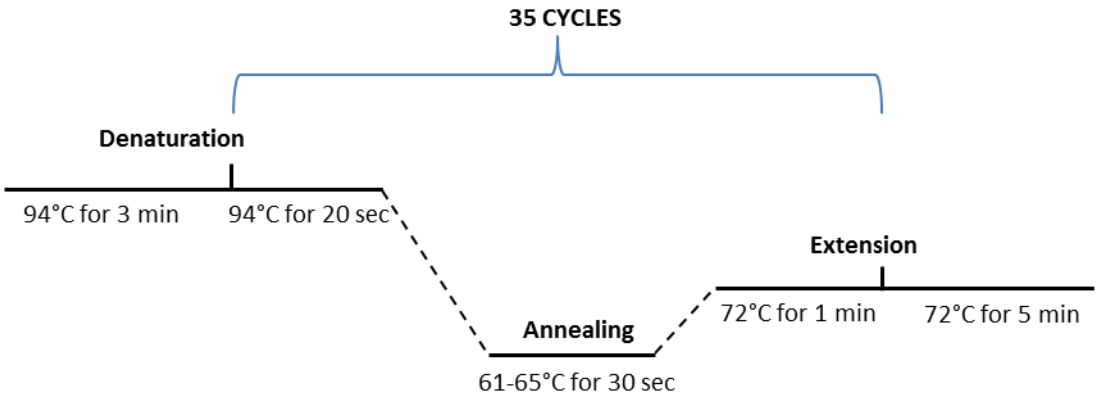

Figure 2.5 - PCR cycling conditions used for generation and amplification of new sequences of interest. After an initial denaturation step at 94°C for 3 min, 35 cycles of denaturation, annealing and extension were performed followed by a final extending step at 72°C for 5 min. Temperature of annealing differs for the different constructs depending on the primers used as described in Table 1.

PCR products were isolated by 1.5% agarose gel electrophoresis in the presence of ethidium bromide at 90V. DNA bands were visualised by use of a UV transilluminator and were then cut from the gel and purified using gel extraction kit (Qiagen). All the amplified sequences and the vectors (pEGFP-N3 or pcDNA3) were digested with BamHI and HindIII restriction endonucleases (FastDigest, Thermo Fisher Scientific, FD0054 and FD0504) by incubation at 37°C for 30 min. DNA was then purified using a QIAquick PCR purification kit (Qiagen).

Ligation was performed to insert PCR products into vectors, using Quick Ligation Kit (New England BioLabs, M2200S) followed by transformation using Subcloning Efficiency™ DH5α™ Competent Cells (Thermo Fisher, 18265-017), in order to either amplify the new constructs or for routine amplification of existing ones. Briefly, around 10 ng of DNA plasmids was used for each construct; cells were subject to heat-shock at 42°C and then grown in 1mL LB medium for 1 hour at 37°C. Different volumes of the initial 1mL culture were plated on either Kanamicyn (50 µg/mL) or Ampicillin (100 µg/mL) agar plates, depending on the vector used, in order to obtain well-defined colonies.

Transformed colonies were picked and cultured over/night in 5 ml LB broth with Kanamicyn or Ampicillin antibiotic in a shaking incubator at 250 rpm. Plasmid DNA was then purified using QIAprep Mini-Prep DNA isolation kit (Qiagen) following manufacturer's protocol. Plasmid DNA was resuspended in 50 µL of nuclease-free water and analysed by restriction digestion, using HindIII and BamHI enzymes, and gel electrophoresis as previously described. Positive clones were then further grown overnight in 100 mL LB broth with Kanamicyn or Ampicillin antibiotic and the final DNA plasmids purified using large scale QIAGEN Endo Free Plasmid DNA Purification Maxi-Prep kit (Qiagen) and checked by restriction analysis and DNA sequencing using primers shown in Table 1 (DNA Sequencing Facility, IMCB, A*STAR, Singapore). Quantification and quality control of DNA preparations were carried out by measuring absorbance using a Nanodrop spectrophotometer.

2.3. Gene expression analysis

2.3.1. RNA isolation

Total RNA was extracted from cells using TRIzol Reagent (Thermo fisher, 15596) following the standard protocol (as described in the manufacturer's guidelines). Briefly, ARPE19 cells seeded in 6-well plates were homogenised using 1mL of TRIzol, which extracts RNA, DNA and proteins. Subsequent phase separation was performed following addition of 0.2 mL of chloroform (Sigma) and the clear aqueous phase taken. RNA was precipitated by adding an equal volume of 100%

isopropanol (Sigma). RNA was pelleted by centrifugation at 14,000g and then washed with 1mL of 70% Ethanol. The RNA pellet was air dried and then dissolved in 50 µL of nuclease free water. RNA concentration and purity was measured using a Nanodrop spectrophotometer.

2.3.2. cDNA synthesis

RNA was reverse-transcripted into cDNA using M-MLV Reverse Transcriptase (RT) (Promega, M170), following the protocol described in the manufacturer's guidelines. Briefly, 1µg of RNA was incubated with 1µL of random primers (Promega, C1181) at 70 °C for 5 minutes to ensure proper denaturation of GC-rich RNA. Subsequently M-MLV 5X Reaction buffer, 2mM of dNTPs (Bioline, BIO-3944) and 200 U of M-MLVRT polymerase were added and the reaction mixture incubated at 37°C for 1 hour, to allow cDNA synthesis, and 95°C for 10 minutes to terminate the reaction.

2.3.3. Quantitative RT-PCR

qPCR was used in this study to quantify the mRNA level of cystatin C in response to treatment with proteasome-inhibitor MG132. This was performed by using GoTaq@qPCR Master Mix (Promega, A6002), which utilizes a proprietary double stranded DNA-binding dye, which works similarly to the widely used SYBR Green to allow quantification of PCR product (Zipper et al. 2004, Ponchel et al. 2003). Analysis was carried out using an Applied Biosystems 7300 instrument. The reaction mixture consi_sted of cystatin C or GAPDH primers at a final concentration of 300nM, 2X PCR Master Mix and cDNA generated as described in 2.3.2. Primers for both cystatin C and GAPDH (Eurogentec) are shown in table 3. Cystatin C primers were designed by using Primer Express Software.

Table 3 - Sequence information of cystatin C and GAPH primers used in qPCR experiments.

Gene	Strand	Sequence
Cystatin C	Forward	5'-CGT AGC TGG GGT GAA CTA CT-3'
	Reverse	5'-ATC TGG AAA GAG CAG AAT GC-3'
GAPDH	Forward	5'-ATG GGG AAG GTG AAG GTC G-3'
	Reverse	5'-TAA AAG CAG CCC TGG TGA CC-3'

Three independent experiments were performed. For each of them, three non-treated and three treated samples were analysed. Each of them was run in triplicate and analysed for both cystatin C and GAPDH. The relative mRNA levels were quantified using the ΔCt method (Rao et al. 2013), by using the Ct values generated by the qPCR software, using the formula:

$$2^{\wedge}(-\Delta Ct) = 2^{-(Ct\ CysC\ -\ Ct\ GAPDH)}$$

Values of relative mRNA abundance were obtained for both treated and not treated cells for comparison.

2.4. Protein analysis

2.4.1. Sample preparation

In many of the experiments performed in this study cell lysates and conditioned media were analysed. Cells used for protein analysis were usually seeded in 6 well-plates, grown in 2-3 mL of complete media. Conditioned media was collected from each well and subjected to centrifugation at 3000 g for 10 minutes at 4°C to remove cell debris. Cells were washed with PBS and collected in 200 µL of RIPA lysis buffer (appendix 1). Cells were then homogenised by sonication. 1X Laemmli buffer (appendix 1) was added to both cell lysate and media samples and heated to 95°C for 5 minutes to denature the proteins. Total protein concentration was calculated for the cell lysates using the Bradford assay (Bio-Rad Protein Assay Dye Reagent

Concentrate, 500-0006). This was performed to ensure equal loading on western blots.

Depending on the experiment, cell lysates samples were either normalised to their protein content (10-20 µg) or loaded at the same volumes (8-20 µL), which also correspond approximately to the same protein concentration. Conditioned media samples were loaded at the same volumes (20-40 µL).

2.4.2. Polyacrylamide gel electrophoresis (SDS-PAGE)

Cell lysates and conditioned media were loaded on polyacrylamide gels, using a Bio-Rad Electrophoresis System, to allow proteins to be separated based on size. Resolving gel (appendix 1) was typically prepared at concentration of 12 or 15%. The higher concentration was used to allow separation of proteins with similar molecular weight. The stacking gel (appendix 1) was always at 4% concentration. Gels were then assembled in the electrode module and tank, adequately filled with running buffer (Appendix 1).

Samples were loaded on the gels, together with a Prestained Protein Ladder (Thermo Fisher) used to indicate molecular weight. Gels were typically run at 110V for approximately 2 hours, until bands were adequately separated.

2.4.3. Western blotting

Proteins separated by SDS-PAGE were transfer onto a nitrocellulose membrane using electric current, and subsequently detected by specific antibodies. The transfer was typically conducted at 100V for 2 hours at 4°C. After the transfer was completed, the membrane was washed and stained with Ponceau S solution (Sigma) to verify that the transfer was successful. Subsequently, membranes were washed 0.1% Tween-20 in PBS, blocked for 1.5 hours in blocking buffer (0.1% Tween-20 in PBS, 5% dry milk or BSA) and incubated with primary antibodies diluted in blocking buffer over-night at 4°C. Membranes were then washed in 0.1%

Tween-20 in PBS and incubated with HRP-conjugated secondary antibodies diluted in blocking buffer for 1.5 hours at room temperature.

Primary and secondary antibodies used are described in Table 4 and 5.

Bands corresponding to the proteins of interest were visualised using the appropriate chemiluminescent substrate reagent (Pierce ECL Substrate, SuperSignal West Pico Chemiluminescent Substrate or SuperSignal West Femto Maximum Sensitivity Substrate (Thermo Fisher)) and imaged through either exposure to X-ray films or by using a Bio-Rad ChemiDoc imaging system. Densitometry analysis, when needed, was performed using either Image J analysis software (NIH) or Image Lab 5.0 (Bio-Rad) software.

Membranes were usually incubated with Restore™ Western Blot Stripping Buffer, (Thermo Fisher, 21059) to re-probe the membrane with a different antibody (e.g. anti-GAPDH).

Table 4 - Primary antibodies used for Western Blot and immunofluorescence

Antibody	Supplier catalogue number	Description	Concentration	
			WB	IF
EGFP	Clontech, 632381	Mouse monoclonal	1:1000	-
Cystatin C	Merk Millipore, ABC20	Rabbit polyclonal	1:2000	1:500
Cystatin C	Abcam, ab109508	Rabbit monoclonal	1:10000	-
GAPDH	Merk Millipore, MAB374	Mouse	1:40000	-
GAPDH	Abcam ab8245	Mouse monoclonal	1:30000	-
TOM20	Santa Cruz sc-11415	Rabbit polyclonal	1:2000	1:200
Mannosidase II	Abcam ab77353	Goat polyclonal	1:1000	-
FLAG (M2)	Sigma F3165	Mouse monoclonal	1:2000	1:300
FLAG	Abcam ab1162	Rabbit polyclonal	1:10000	-
HA	Roche 11867423001	Rat monoclonal	1:1000	1:200
Calreticulin	Thermo Fisher PA3-900	Rabbit polyclonal	-	1:500
GM130	BD Biosciences 610822	Mouse monoclonal	-	1:100

Table 5 - Secondary antibodies used in this study for Western Blot

Antibody	Supplier catalogue number	Description	Concentration
Anti-mouse	Bio-Rad 170-6516	Goat IgG, HRP-linked	1:5000
Anti-rabbit	Bio-Rad 170-6515	Goat IgG, HRP-linked	1:5000
Anti-goat	Santa Cruz SC-2350	Bovine IgG, HRP-linked	1:5000
Anti-rat	Jackson ImmunoResearch Laboratories 712-035-153	Donkey IgG, HRP-linked	1:5000

2.4.4. Deglycosylation

Cell lysates and conditioned media samples, collected as previously described, were subjected in some experiments to deglycosylation treatments, prior to SDS-PAGE.

Endo H, PNGase F and protein Deglycosylation Mix (New England BioLabs, P0702S, P0704S, P6039S) were used for this purpose, following manufacturer's guidelines.

Endo H removes N-glycans attached to proteins in the ER compartment, whereas PNGase F can also remove complex N-glycans that were further modified in the Golgi apparatus (Maley et al. 1989). Resistance or sensitivity to Endo H can therefore be used to monitor whether a glycosylated protein traffics through the Golgi.

Protein Deglycosylation Mix is composed of five different glycosidases: PNGase F, O-Glycosidase, Neuraminidase, β1-4 Galactosidase, β-N-Acetylglucosaminidase (as described in the manifacturer's datasheet). This mix therefore allows removal of all N-linked oligosaccharides and most of the common O-linked glycans from glycoproteins.

To perform deglycosylation, 10X denaturing buffer was added to 9 µL of cell lysate or 18 µL of conditioned media and heated at 100°C for 10 minutes. Subsequently, reaction buffer and H_2O were added to the sample together with the specific enzyme, EndoH (2 µL) or PNGaseF (1 µL) (in a total volume of 20 and 30 µL of reaction for cells and media respectively), and incubated for 1 hour at 37°C. Alternatively, samples were treated with Protein Deglycosylation Mix (3 µL) (in a total volume of 40 µL) and incubated for 5 hours at 37°C.

2.5. Protein pull-down

In this study, pull-down of cystatin C constructs was carried out for different experiments: to analysis the signal cleavage (chapter 4), the species secreted (chapter 5), the dimerization (chapter 6.3) and the interacting partners of cystatin C (chapter 6.5).

Depending on the experiment, immunoprecipitation (IP) was performed for CysC-FLAG or HA-Cys-FLAG constructs, by using the ANTI-FLAG M2 Affinity Gel (Sigma, A2220), following manufacturer's guidelines. This resin consists of Anti-FLAG M2 monoclonal antibodies attached to agarose beads, which permit pull-down of FLAG-tagged cystatin C constructs.

In general, RPE cells seeded in 6-well-plates were transfected and subjected to IP 24-hour post-transfection. Cell lysates were collected in RIPA buffer and homogenised, as described previously. Cells from three wells (2-4 mg) were combined and diluted to a final volume of 1mL in RIPA buffer. 40 µL of anti-FLAG beads, after being adequately washed in RIPA buffer, were added to the sample (~2-4 mg) followed by incubation over-night at 4°C with gentle shaking. The resin was then washed three times and collected by spinning at 8000g for 5 minutes at 4°C.

Elution of the FLAG-constructs was performed using the 3X FLAG Peptide (Sigma, F4799), following manufacture's protocols. 50-100 µL of 3X FLAG solution at a concentration of 250 ng/µL was added to each sample and incubated for 1 hour at 4°C with gentle shaking. Resin was then pelleted by centrifugation and the supernatant transferred to a fresh tube. Prior to Western Blotting analysis Laemmli buffer was added to the samples followed by denaturation, as described previously.

Also media samples were subjected to IP. Anti-FLAG beads were added to 1mL of conditioned media collected from cells in 6-well plates and immunoprecipitation and elution were performed, as described before.

Regarding samples subjected to IP, prior to mass spectrometry analysis, cells were seeded in 100mm dishes. Cell lysates and conditioned media derived from two dishes were combined and subjected to IP as described before. Conditioned media was first concentrated by spinning using Amicon Ultra-4 3K Centrifugal Filter Devices (Merk Millipore) to a final volume of approximately 1.5 mL. Both media samples and cell lysates (~10 mg) were subjected to IP using 50 µL of anti-FLAG beads and eluted in 30 µL of 3X FLAG peptide (2.5 µg/mL).

2.6. Mass spectrometry

Samples for mass spectrometry analysis were obtained after pull-down, as described above. 5µL of the 30 µL eluted sample (either from cell lysates or conditioned media), were subjected to Western blotting analysis and the other 25 µL sent to the Proteomics facility for analysis (IMCB, A*STAR, Singapore). Here the samples were processed through mass spectrometry and analysed. Essentially, samples were first separated by SDS-PAGE and proteins visualised by coomassie blue staining. For each sample, the bands of interest or the entire lanes of the gel, depending on the experiment (as shown in results chapter), were cut and subjected to in-gel digestion by trypsinization. The extracted peptides were then analysed using an Orbitrap mass spectrometer.

The proteins within each sample were identified using the Mascot search engine and analysed using the proteasome software Scaffold (Searle 2010). Each protein reports the UniProt code, the spectra counts and the percentage of coverage, as described in chapter 4. This peptide mapping analysis permits only a qualitative characterization of the proteins.

2.7. Mitochondria isolation

Mitochondria were isolated for subsequent protein localization analysis by immunoblotting. Two methods were used for this purpose: magnetic separation and differential centrifugation.

2.7.1. Magnetic separation (MACS)

Mitochondria were isolated by using the Human Mitochondrial Isolation Kit (Miltenyi Biotec, 130-094-532), according to manufacturer's guidelines. This method is based on MACS technology, consisting of magnetic separation of mitochondria. In general, cells collected from two 100mm dishes were resuspended in 1 mL of Lysis Buffer (provided in the kit) and homogenised by syringing with 26 G needle. Subsequently, the lysate was subjected to magnetic labelling by incubation with 50 µL of anti-TOM22 MicroBeads for 1 hour at 4°C with

gentle shaking. Antibody anti-TOM22 specifically binds mitochondrial outer membrane proteins (Pfanner, Craig & Hönlinger 1997). By using MACS separation columns, placed in the magnetic field of a QuadroMACS separator, the labelled mitochondrial are retained inside the column. Elution was carried out by removing the magnetic field after which the mitochondria were pelleted by centrifugation and resuspended in storage buffer.

2.7.2. Differential Centrifugation (DC)

This method allows cellular sub-fractionation in order to isolate the different cellular compartments.

Cells collected from two 100 mm dishes were resuspended in 2 mL of ice-cold Mitochondrial Isolation Buffer (MIB) (Appendix 1), described by Takeyama et. al (Takeyama et al. 2002). Cells were then lysed by syringing with 26 G needle and subjected to several step of centrifugation at different speed.

The first spin was carried out at 750g for 10 minutes at 4°C to pellet nuclei. This fraction contains also cell debris and whole cells escaped from homogenization. The pellet obtained was resuspended in 0.5 mL of MIB, further homogenised and spun again to improve the purity of the nuclear pellet (P1). The supernatants were combined and centrifuged at 13000g for 20 minutes at 4°C to pellet the mitochondria. The pellet was washed and spun again. The final mitochondria enriched pellet (P2) also contains lysosomes and peroxisomes. Golgi apparatus are also mainly present in this fraction. The supernatant (SF) contains the soluble fraction (cytosolic proteins) as well as ER and microsomes. The pellets P1 and P2 were finally resuspended in 0.5 mL of MIB.

Fractions obtained with both MACS and DC methods were analysed by Western blotting. Regarding the MACS fractions, 50 µg of each mitochondria fraction and 80 µg of each entire cell lysate were loaded on a polyacrylamide gel. For the DC fractions, 40 µg for each mitochondria fraction (P2) and 100 µg of each entire cell lysate were loaded on gel. Fraction P1 and SF were loaded at the same volume used for the P2.

2.8. Cell imaging

2.8.1. Live cell imaging

Cells were seeded on glass-bottom dishes 35 mm (Greiner Bio-One, 627861) at a density of 3-5 X 10^5 cells and transfected with EGFP-linked constructs as described previously.

Cells were imaged 24-hours post-transfection using a Zeiss Axio Observer-Apotome fluorescence microscope or Zeiss LSM700 Confocal microscope.

Prior to imaging, the cells were incubated for 30 minutes with either 250 nM Mitotracker Red FM (Thermo Fisher, M22425) or 5 µM BODIPY TR Ceramide complexed to BSA (Thermo Fisher, B-34400) diluted in media, as described in the manufacturer's guidelines. These dyes accumulate within the mitochondria and Golgi complex respectively (Chazotte 2011, Pagano et al. 1991), emitting red fluorescence at 644 and 617 nm. NucBlue Live ReadyProbes Reagent (Thermo Fisher, R37605), containing Hoechst 33342 dye, was used to stain nuclei, and emits blue fluorescence at 460 nm.

Fluorescence images were taken for green, red and blue channels. Co-localisation of the EGFP-tagged protein (in green) with mitochondria and Golgi (in red) was carried out based on overlap of the two different fluorescence patterns.

For EGFP-tagged cystatin C, twelve independent experiments were carried out in ARPE19 cells and representative results from one experiment are shown in the respective section. Two independent experiments were carried out in D4O7 and Hela and one in hTertRPE-1. For the Leader Peptide constructs, seven independent experiments were carried out in ARPE19 cells and representative results from one experiment are shown in the respective section.

2.8.2. Immunofluorescence

Cells were grown on sterile glass coverslips in 24-well plates (5 X10^4 - 1X10^5 cells/well). They were transfected with cystatin C constructs and fixed 24-hours post-transfection for subsequent immunostaining and analysis using an Olympus Fluoview upright confocal microscope.

Cells were washed with PBS and fixed for 30 minutes at room temperature (RT) with 4% paraformaldehyde (PFA) in PBS. The reaction was then quenched with 50mM NH_4Cl in PBS for 10 minutes at RT and cells were permeabilized with 0.2% Triton X-100 in PBS for 10 minutes at RT. Before immunostaining, cells were blocked for 1 hour at RT in blocking buffer (0.1% Triton X-100 in PBS, 1% BSA), followed by incubation with primary antibody diluted in blocking solution for 1.5 hour. The cells were washed with PBS and incubated for 1h with appropriate secondary antibodies conjugated to AlexaFluor 488 (green) and AlexaFluor 594 (red). Cells were stained with 10 mM DAPI (Thermo Fisher, D3571) in PBS for 10 minutes, washed and finally mounted onto glass slides using mounting solution (Clear Mount with Tris Buffer, Electron Microscopy Sciences 17985-15).

The primary and secondary antibodies used are shown in table 5 and 6. In some experiments mitochondria were stained by using Mitotracker Red CMXRos (Thermo Fisher, M7512), which emits red fluorescence at 599nm. As for Mitotracker Red FM used for live imaging, cells were incubated for 30 minutes at 37°C with 250nM of the dye, prior to cell fixation.

Table 6 - Secondary antibodies used for immunofluorescence.

Antibody	Supplier (catalogue number)	Description	Concentration
Anti-rabbit	Thermo Fisher (A11008)	Goat IgG, Alexa Fluor 488	1:1000
Anti-rabbit	Thermo Fisher (A21207)	Donkey IgG, Alexa Fluor 594	1:1000
Anti-mouse	Thermo Fisher (A21202)	Donkey IgG, Alexa Fluor 488	1:1000
Anti-mouse	Thermo Fisher (A21203)	Donkey IgG, Alexa Fluor 594	1:1000
Anti-rat	Thermo Fisher (A11006)	Goat IgG, Alexa Fluor 488	1:1000
Anti-rat	Thermo Fisher (A11007)	Goat IgG, Alexa Fluor 594	1:1000

For the EGFP-tagged cystatin C, three independent experiments were carried out in ARPE19 and D4O7 cells and representative results from one experiment are shown in the respective section. For the untagged and C-terminal FLAG- and HA-tagged cystatin C constructs, three independent experiments were carried out in ARPE19 cells and two independent experiments were carried out in D4O7 cells.

For the N-terminal constructs, two independent experiments were carried out in ARPE19 and D4O7 cells and representative results from one experiment are shown in the respective section.

2.9. Statistical analysis

Unpaired, paired, or one-sample t-test were used as statistical tests depending on the experiment, as specified in the respective results sections. The unpaired t-test is suitable for analysis of two independent samples, whereas the paired t-test is applied to a sample of matched pairs of data samples, and the one-sample t-test for comparing a data set against a single hypothetical value. The analyses were calculated using GraphPad Prism version 5.0 (GraphPad Software Inc.). P-values are reported for each experiment to quantify the statistical significance. In this study, analyses were typically carried out to compare wild-type versus variant B cystatin C proteins, or treated versus non-treated samples.

Pearson's chi-square (χ^2) test was also used for comparison of discreet categorical data (e.g. cell counts in the analysis of cystatin C distribution in section 3.2).

Chapter 3 - Analysis of intracellular localization, trafficking and secretion of cystatin C variant B

3.1. Introduction

Cystatin C is a secretory protein synthesised as a precursor containing a N-terminal signal peptide that leads the nascent protein to the ER. Here the mature form is generated by cleavage of the leader peptide, subsequently delivered to the Golgi apparatus and finally, through secretory vesicles, released into the extracellular matrix (Paraoan et al. 2001).

The Ala25Thr mutation in the leader peptide of cystatin C, which generates the haplotype B, has been reported to affect the intracellular trafficking of the protein both in vitro and in vivo. In particular a reduction in the level of secretion of the variant B has been described, possibly as a result of a decreased efficiency of the signal sequence in targeting or processing the precursor protein through the secretory pathway (Benussi et al. 2003, Paraoan et al. 2004). One of these studies has also reported that the variant B accumulates intracellularly, where it mislocalizes in the cytoplasm, nucleus and particularly in the mitochondria (Paraoan et al. 2004). The impairment in cystatin C secretion can be therefore a consequence of such intracellular mistrafficking. Both these events have been hypothesised to contribute to cellular dysfunction associated with AMD and AD pathologies, as a consequence of a proteolytic activity imbalance both inside and outside the cell as well as a disruption of mitochondria functionality (Benussi et al. 2003, Paraoan et al. 2004).

However, other studies found no difference in secretion between the wild-type and variant form of cystatin C (Nguyen, Hulleman 2016, Chuo et al. 2007) and, so far, no additional studies have reported the mitochondrial association detected for the variant B. Furthermore a number of groups have also debated about the involvement of the Cystatin C haplotype B in both AD and AMD development, as no association was identified in their studies (Roks et al. 2001, Maruyama et al. 2001, Monastero et al. 2005, Nacmias et al. 2006, Wang et al. 2008, Butler et al. 2015).

The aim of the first part of this study was therefore to further investigate the effect of the A25T mutation on the trafficking of the variant B cystatin C, in order to

identify whether there is any impairment in this process that helps us to understand how the protein is linked to disease development. For this purpose we analysed the intracellular localization of cystatin C, investigated whether the variant B protein accumulates intracellularly or follows the canonical ER-Golgi secretory pathway, evaluated the level of protein secretion in the conditioned media and finally we assessed the targeting properties of the signal sequence.

For these analyses different RPE cell lines were used. Most of the experiments were carried out in ARPE19 cells, which are the most representative cells to study RPE given their high morphological and functional similarities (Dunn et al. 1996). In addition, D4O7 cells were used in some experiments due to their higher transfectability and yield of protein expression, which was necessary for some of the experiments (Davis et al. 1995). Finally, hTert-RPE1 and the widely used cervical adenocarcinoma cell line HeLa were used as additional controls for imaging analysis to study the protein localization (Gong et al. 2014).

Different constructs were made in this study as described in materials and methods. The ones used for the analyses described in this chapter include C-terminal tagged cystatin C proteins with either an EGFP, FLAG or HA tag, untagged constructs, constructs with N-glycosylation sites. In addition, leader peptide constructs linked to the EGFP tag were used.

3.2. Analysis of protein localization

Analysis of intracellular localization of cystatin C was investigated by imaging and fractionation studies to determine whether the variant B deviates from the secretory pathway, thus mislocalizing in a different cellular compartment. As a foundation for the subsequent work and given the discrepancies in the literature (Nguyen, Hulleman 2016, Paraoan et al. 2004), it was important to confirm the reported localization of the variant B in mitochondria.

3.2.1. Both wild-type and variant B EGFP-tagged constructs show partial mitochondrial mislocalization

Via their fluorescent EGFP tag, cells transfected with full-length cystatin C-EGFP constructs were first analysed for their protein distribution by live cell imaging.

Figure 3.1 and 3.2 show representative images obtained by fluorescence microscopy of ARPE19 cells transfected with WT-EGFP and VB-EGFP constructs respectively. To assess their intracellular localization, mitochondria and Golgi apparatus were stained. An ER/Golgi localization of cystatin C, as indicated by its colocalization with BODIPY, and therefore consistent with the distribution of secretory proteins, was found for both wild-type and variant constructs. However, a significant fraction of cells also showed mitochondrial colocalization for both the wild-type and variant B proteins. A dual Golgi-mitochondria distribution was also sometimes observed. Percentages of cells showing mitochondrial and secretory pathway distributions were quantified as shown in figure 3.3. Twelve independent experiments were performed and a chi-square test was used to assess whether there was a significant difference between wild-type and variant B protein distribution. 56% and 46% of ARPE19 cells were found to display the unusual mitochondrial association for the WT-EGFP and VB-EGFP proteins respectively, and this difference was statistically significant. Percentages were calculated by considering the total number of cells, obtained combining all the individual experiments (Figure 3.3.). Analysis of mitochondrial distribution at the level of each individual replicate resulted in 51%±16 and 40%±15 (Mean±SD, N=12) for wild-type and variant B, respectively.

A)

WILD-TYPE CYSTATIN C

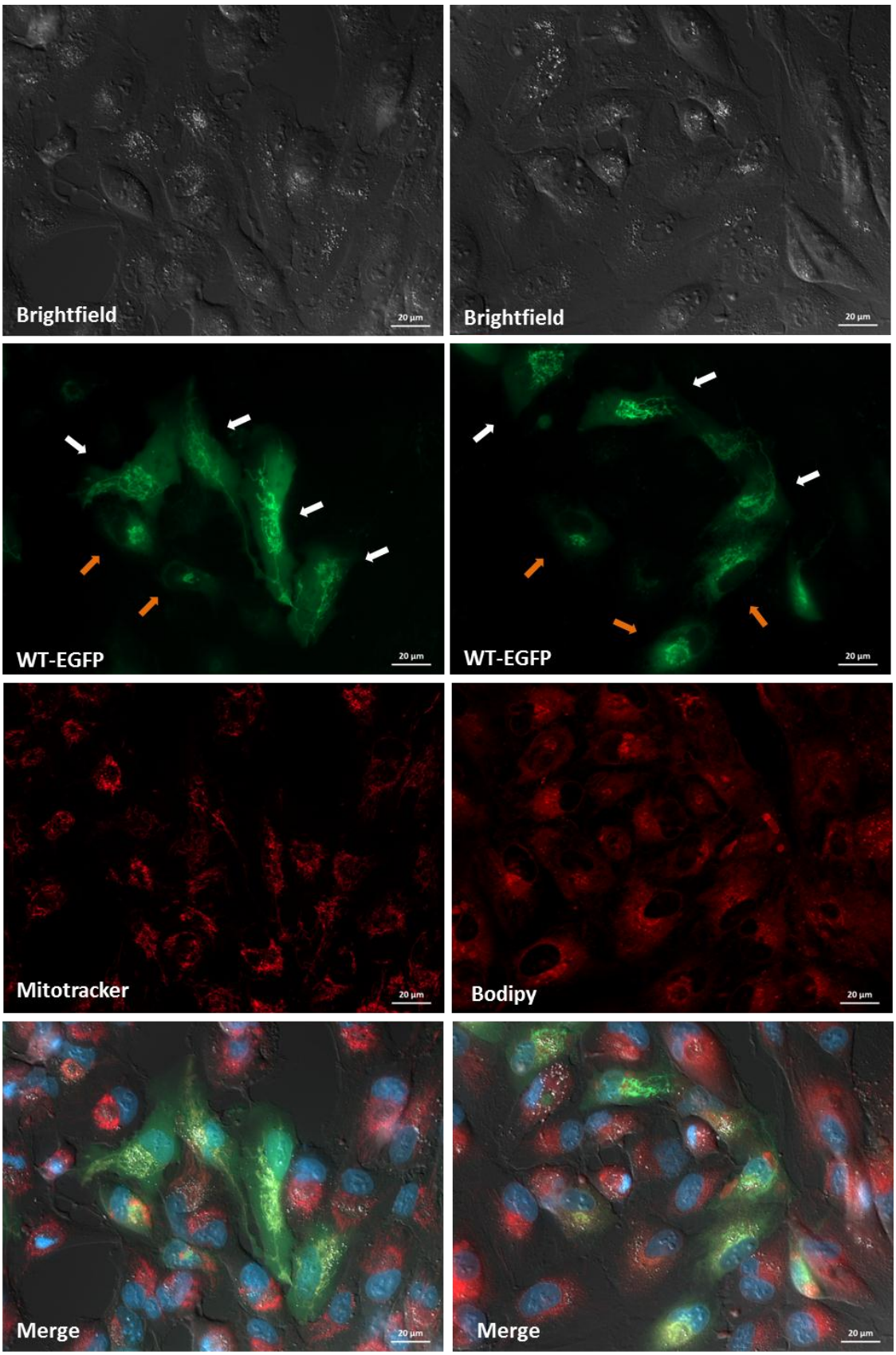

B)

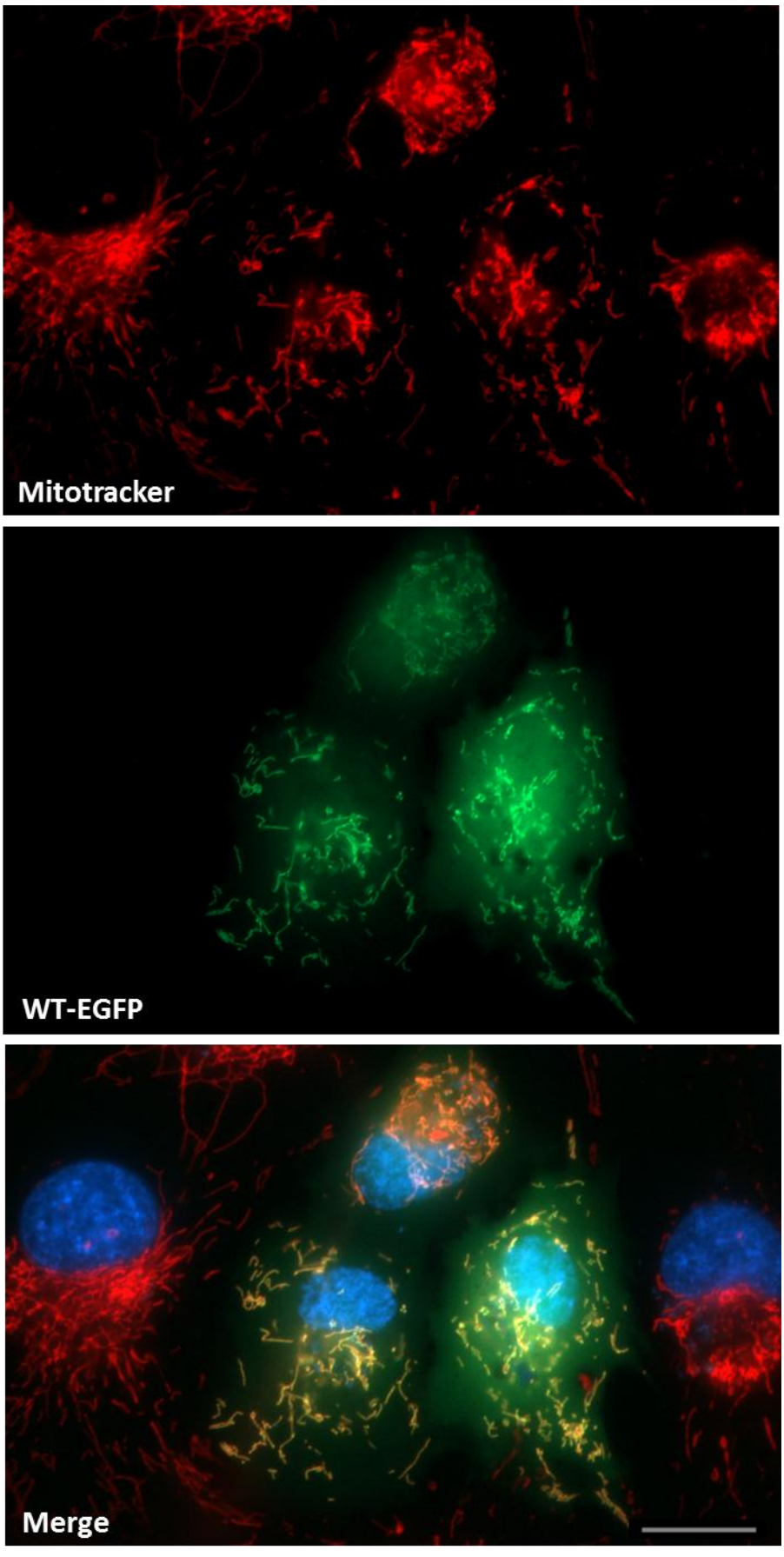

C)

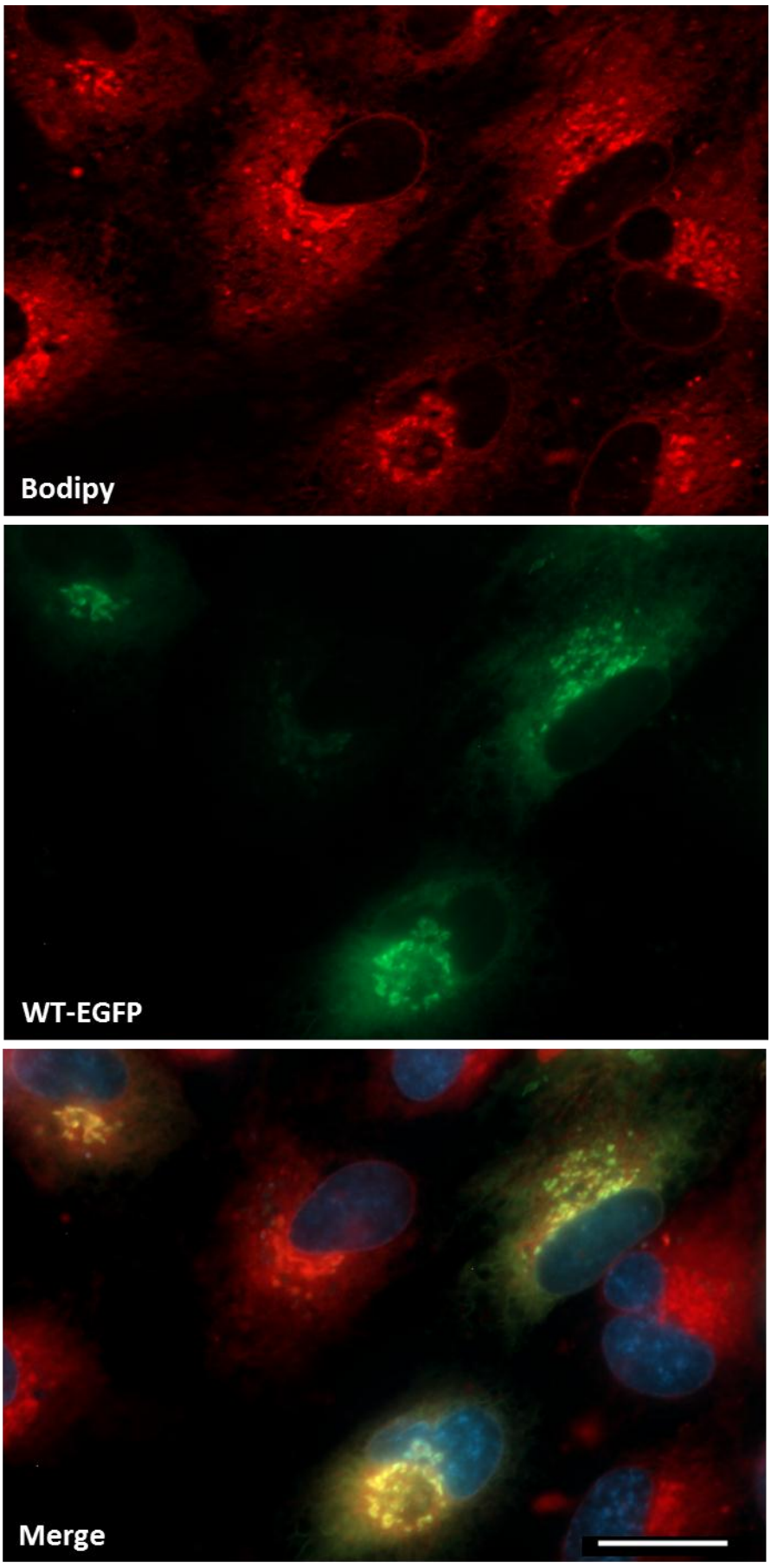

Figure 3.1 - Localization of EGFP-tagged wild-type cystatin C constructs (WT-EGFP). A) Living cultured human ARPE19 cells expressing wild-type cystatin C linked to eGFP were imaged 24 h post-transfection. The emission specific for eGFP constructs is shown in green. Mitotracker and Bodipy, which fluoresce red, were used to visualize mitochondria and Golgi complex, respectively. The blue fluorescent Hoechst 33342 probe was used to stain nuclei. For each field of cells imaged, green and red fluorescence were recorded as separate images and then merged, along with the blue signal and bright field, for assessing the overlap of the respective signals. Cells showing ER/Golgi or mitochondrial distribution are indicated by orange and white arrows, respectively. B) and C) show higher magnification of images of cells expressing wild-type constructs with Mitotracker (B) and Bodipy (C). Scale bars are 20 μM.

A)

VARIANT B CYSTATIN C

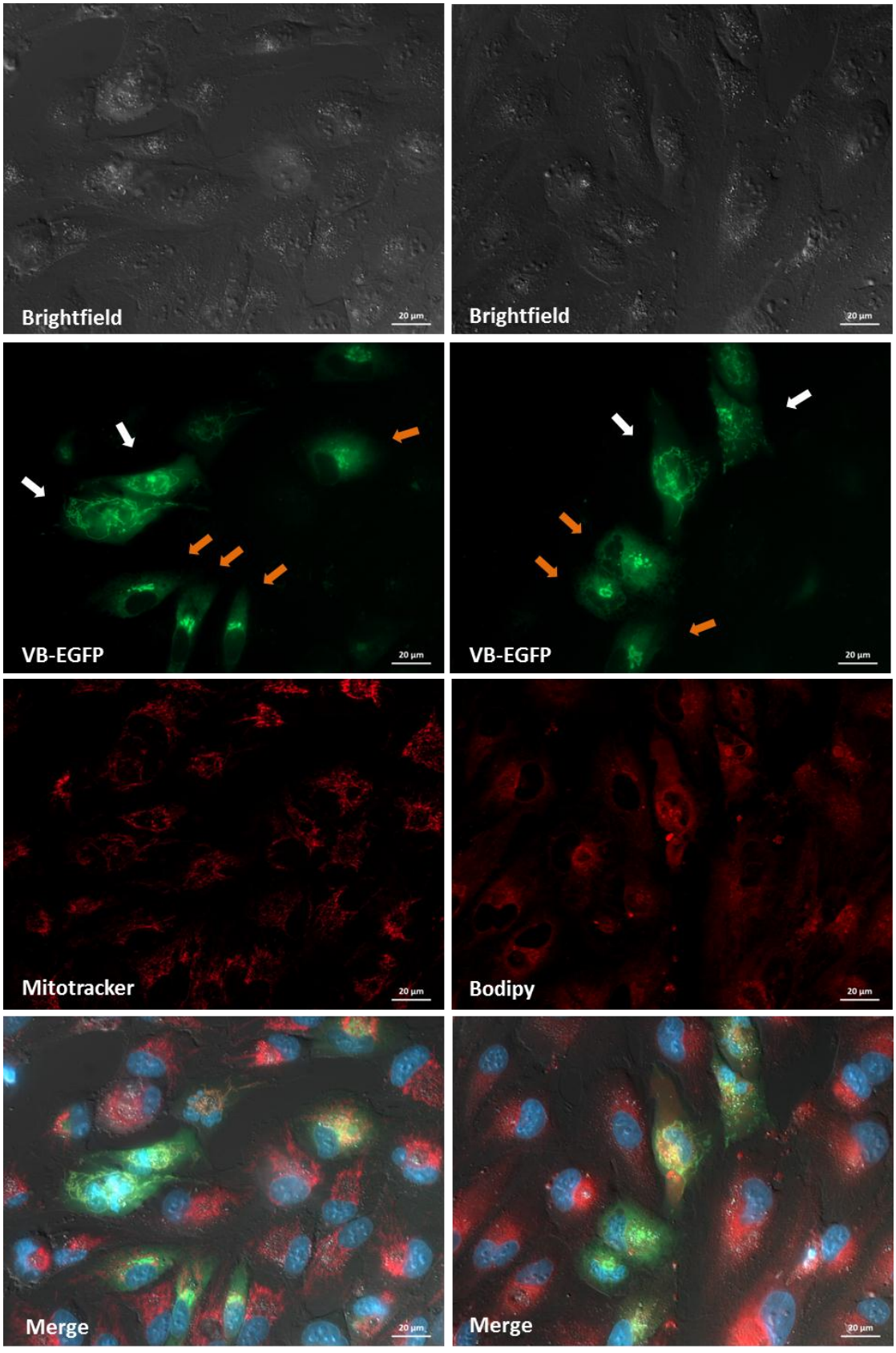

B)

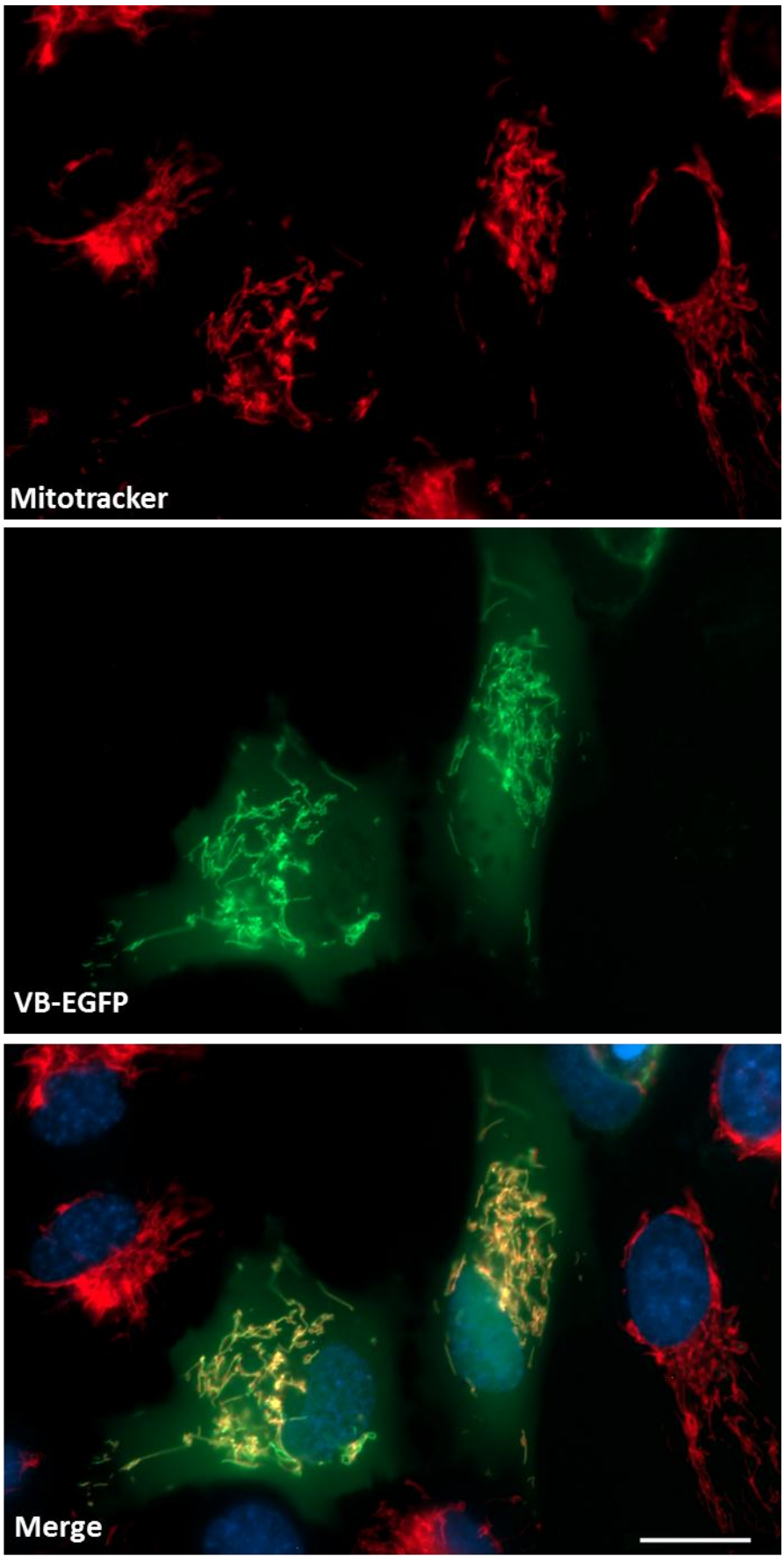

C)

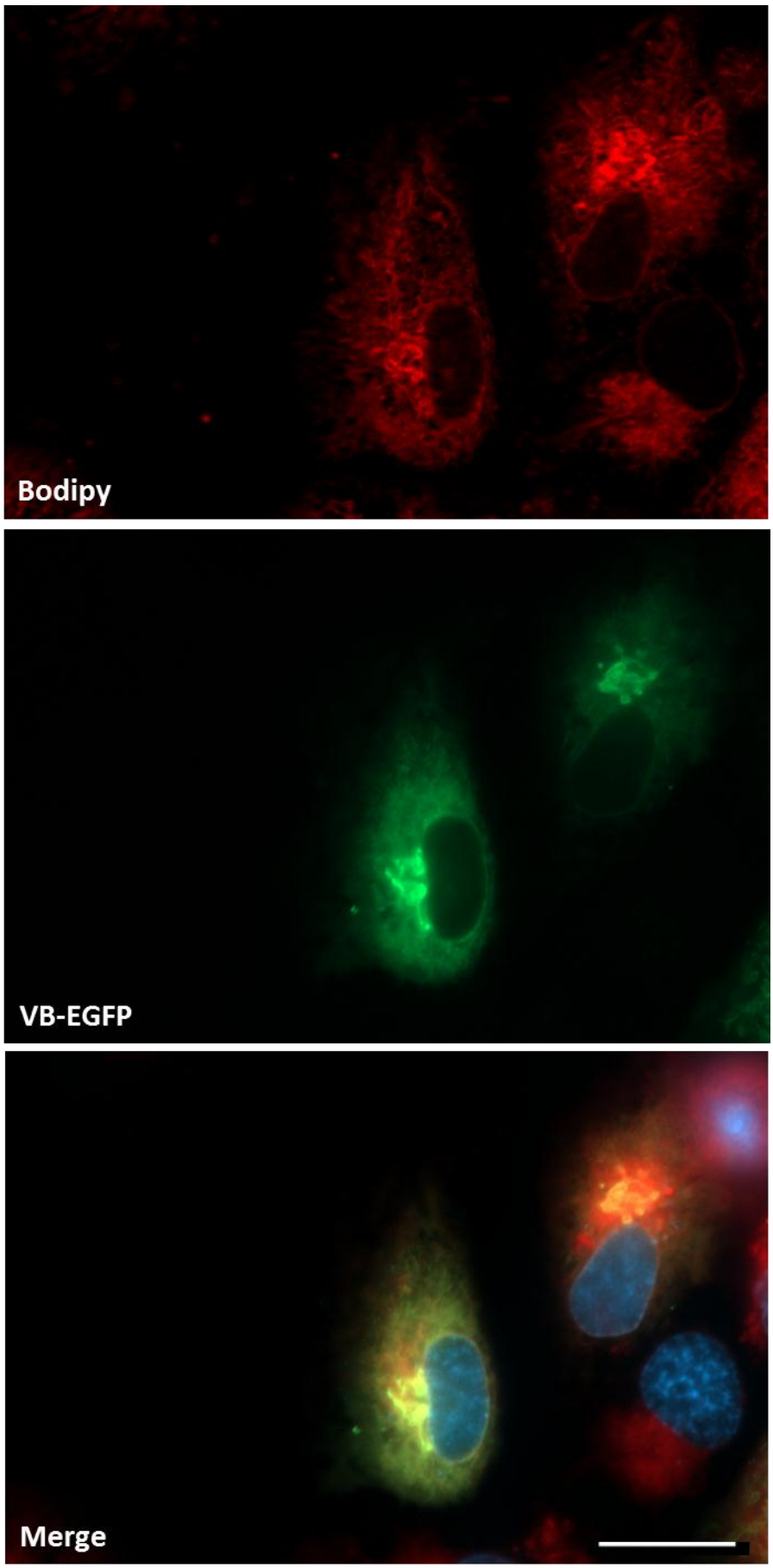

Figure 3.2 - Localization of EGFP-tagged variant B cystatin C constructs (VB-EGFP). Living cultured human ARPE19 cells expressing variant B cystatin C linked to eGFP were imaged 24 h post-transfection. The emission specific for eGFP constructs is shown in green. Mitotracker and Bodipy, which fluoresce red, were used to visualize mitochondria and Golgi complex respectively. The blue fluorescent Hoechst 33342 probe was used to stain nuclei. For each field of cells imaged, green and red fluorescence were recorded as separate images and then merged, along with the blue signal and bright field, for assessing the overlap of the respective signals. Cells showing ER/Golgi or mitochondrial distribution are indicated by orange and white arrows, respectively. B) and C) show higher magnification of images of cells expressing variant B constructs with Mitotracker (B) and Bodipy (C)**.** Scale bars are 20 μM.

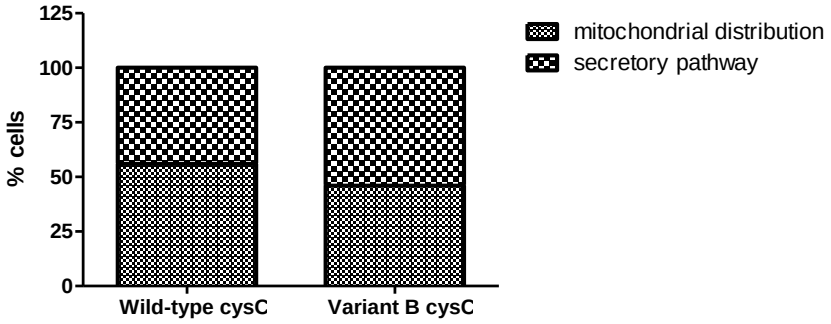

Figure 3.3 - Quantification of EGFP-tagged cystatin C distribution in live transfected ARPE19 cells. ARPE19 cells transfected with either WT or VB-EGFP constructs were quantified to compare secretory pathway distribution and mitochondrial localization of cystatin C. The fraction of cells showing mitochondrial association results 56% and 46% for the WT and VB-EGFP proteins respectively. Percentages are calculated by considering the total number of cells obtained combining all the individual experiments. Chi-square test (χ^2 =25.63), *p*-value <0.00001.

Analysis of intracellular localization in live cells for the EGFP-tagged cystatin C constructs was also performed in D4O7, hTert-RPE1 and HeLa cell lines as shown in Figure 3.4 a, b and c, respectively.

Mitochondrial association for both wild-type and variant B constructs was again observed in a significant number of cells, thus excluding an ARPE19 cell-related effect. In particular, for all cell lines analysed, cells with an ER/Golgi distribution, a mitochondrial association or a dual Golgi-mitochondria distribution were observed for both wild-type and mutant cystatin C.

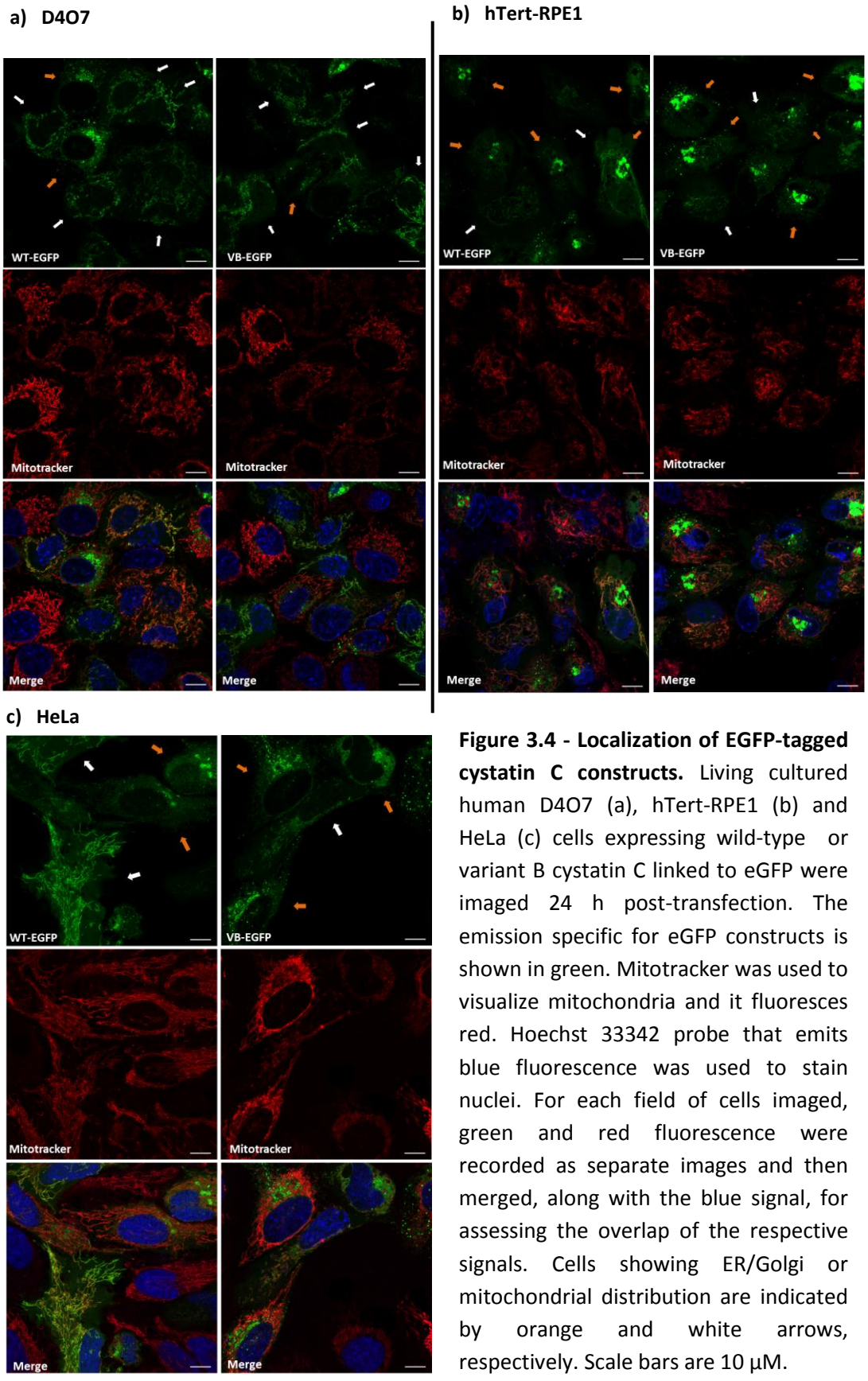

Figure 3.4 - Localization of EGFP-tagged cystatin C constructs. Living cultured human D4O7 (a), hTert-RPE1 (b) and HeLa (c) cells expressing wild-type or variant B cystatin C linked to eGFP were imaged 24 h post-transfection. The emission specific for eGFP constructs is shown in green. Mitotracker was used to visualize mitochondria and it fluoresces red. Hoechst 33342 probe that emits blue fluorescence was used to stain nuclei. For each field of cells imaged, green and red fluorescence were recorded as separate images and then merged, along with the blue signal, for assessing the overlap of the respective signals. Cells showing ER/Golgi or mitochondrial distribution are indicated by orange and white arrows, respectively. Scale bars are 10 µM.

3.2.2. EGFP-tagged constructs mislocalise unlike untagged, FLAG- and HA-tagged constructs which localise in the ER/Golgi compartments

To confirm the results obtained by life cell imaging, analysis of intracellular localization was also performed by immunofluorescence (IF) on PFA-fixed cells. In addition to the EGFP-tagged constructs, untagged, FLAG- or HA-tagged constructs were analysed. Since the latter do not emit fluorescence, immunostaining was needed for protein visualization. Figure 3.5 shows ARPE19, D4O7, hTert-RPE1 and HeLa cells (a, b, c and d, respectively) transfected with WT-EGFP or VB-EGFP cDNAs. Mitotracker was used to stain mitochondria. As observed for live cell imaging, cells displayed either a secretory distribution or a mitochondrial association for both wild-type and variant B constructs. Percentages were calculated by considering the total number of cells, obtained combining all the individual experiments Quantification shown in figure 3.6 for the ARPE19 cells resulted in 32% and 30% of the cells expressing wild-type and variant B, respectively, showing mitochondrial localization, with no significant difference observed between them. Analysis of mitochondrial distribution at the level of each individual replicate resulted in 32%±10 and 31%±6 (Mean±SD, N=3) of the cells expressing wild-type and variant B, respectively, showing mitochondrial localization.

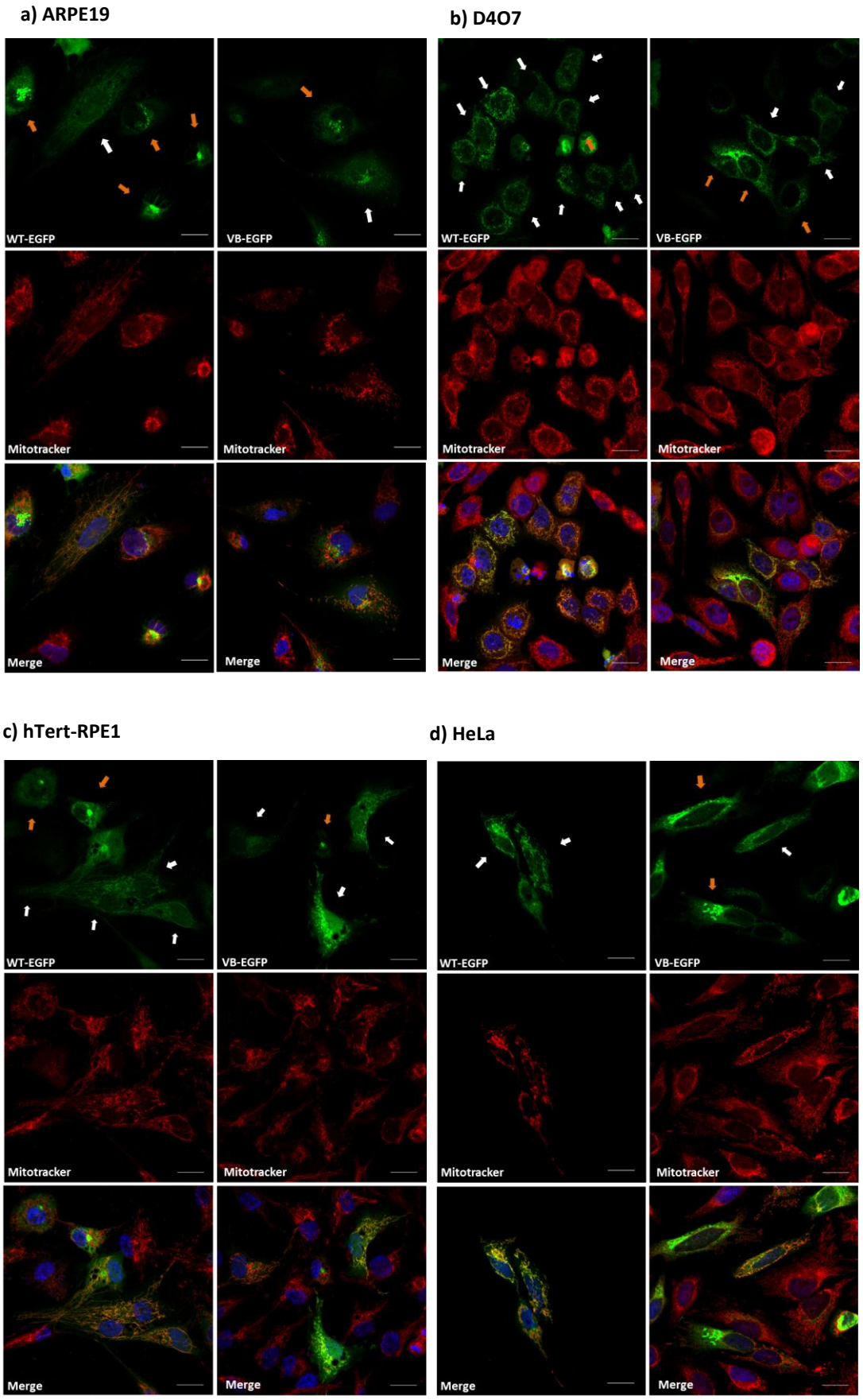

Figure 3.5 - Localization of EGFP-tagged cystatin C constructs. Cultured human ARPE19 (a) D4O7 (b), hTert-RPE1 (c) and HeLa (d) cells expressing wild-type or variant B cystatin C

linked to EGFP were PFA-fixed 24 h post-transfection and subsequently imaged. The emission specific for EGFP constructs is shown in green. Mitotracker, which fluoresces red, was used to visualize mitochondria. The blue fluorescent DAPI was used to stain nuclei. For each field of cells imaged, green and red fluorescence were recorded as separate images and then merged, along with the blue signal, for assessing the overlap of the respective signals. Cells showing ER/Golgi or mitochondrial distribution are indicated by orange and white arrows, respectively. Scale bars are 20 μM.

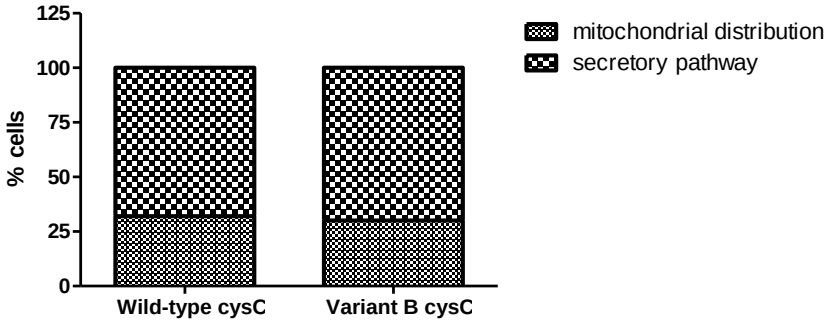

Figure 3.6 - Quantification of EGFP-tagged cystatin C distribution in fixed transfected ARPE19 cells. ARPE19 cells transfected with either WT or VB-EGFP constructs were quantified to compare secretory pathway distribution and mitochondrial localization of cystatin C. Percentages are calculated by considering the total number of cells obtained combining all the individual experiments. The fraction of cells showing mitochondrial association results 32% and 30% for the WT and VB-EGFP proteins respectively. Chi-square test (χ^2 =0.19), *p*-value =0.66.

Subsequently, IF was performed on cells transfected with the untagged constructs or constructs tagged with the small FLAG or HA tags to further investigate the protein distribution. Antibodies against cystatin C, or FLAG or HA tag were used to detect the untagged or the fusion proteins. DAPI, mitotracker and anti-calreticulin and anti-GM130 antibodies were used to stain nuclei, mitochondria, ER and Golgi, respectively.

Figure 3.7 shows ARPE19 cells transfected with the untagged cystatin C cDNAs and immunostained with anti-cystatin C, mitotracker and anti-GM130. Surprisingly, and in contrast to the results obtained for the EGFP-tagged constructs, neither the variant or wild-type proteins showed mitochondrial localisation. Colocalisation with

the Golgi apparatus was instead observed, suggesting that both WT-CysC and VB-CysC localise in the secretory pathway. Figure 3.8 shows the same analysis performed on D4O7 cells. Again, no colocalization with mitotracker was found for either the untagged wild-type or variant B cystatin C. Also in D407 cells, although no other organelles were stained, anti-cystatin C antibody gave us a typical reticular and perinuclear staining, consistent with the ER/Golgi.

The same results were obtained by using wild-type and variant B cystatin C constructs tagged with FLAG- or HA-tags in both ARPE19 and D4O7 cells (ARPE19 in figure 3.9 and 3.10 and D4O7 in figure 3.11 and 3.12), where cystatin C was again found to be distributed in the ER/Golgi with no mitochondria localization detected.

Untagged cystatin C constructs

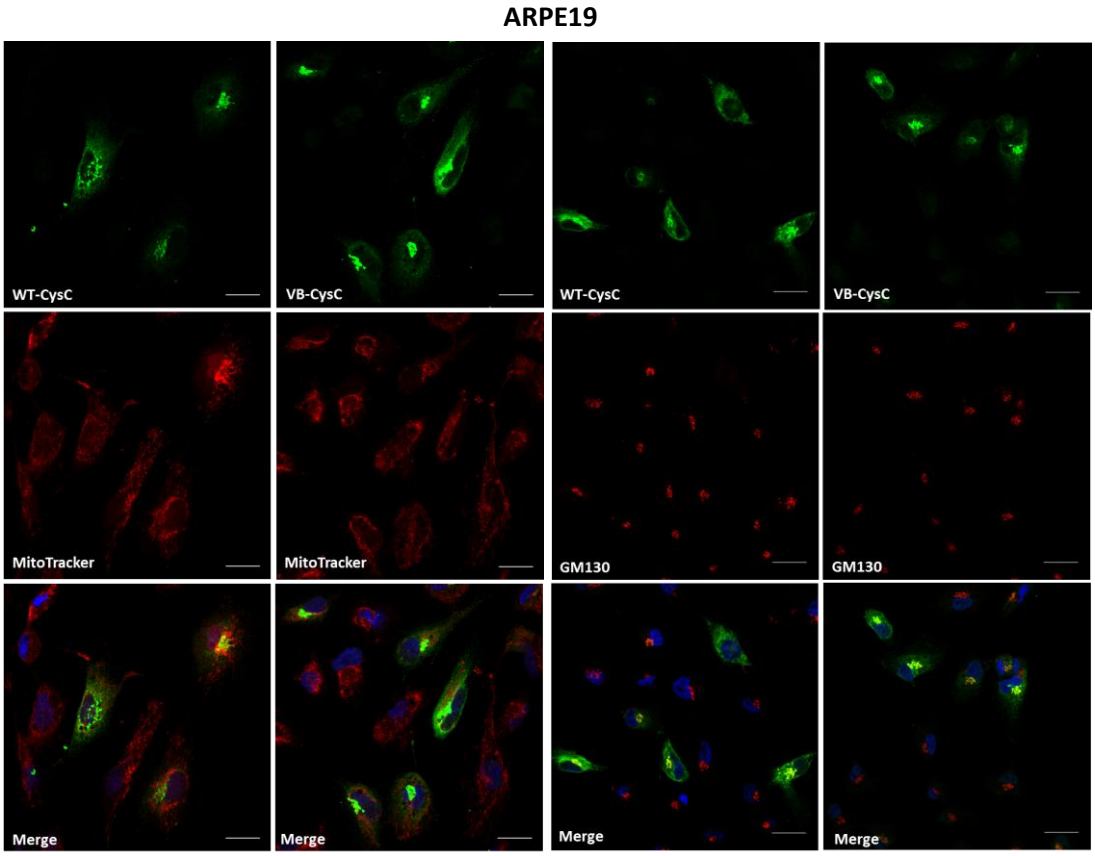

Figure 3.7 - Localization of untagged cystatin C constructs. Human ARPE19 cells expressing wild-type or variant B cystatin C were PFA-fixed 24 h post-transfection, immunostained with anti-cystatin C antibody and subsequently imaged. The emission specific for cystatin C constructs is shown in green. Mitotracker and anti-GM130 antibody, which fluoresce red, were used to visualize mitochondria and Golgi complex, respectively. The blue fluorescent DAPI was used to stain nuclei. For each field of cells imaged, green and red fluorescence

were recorded as separate images and then merged, along with the blue signal, for assessing the overlap of the respective signals. Scale bars are 20 µM.

D4O7

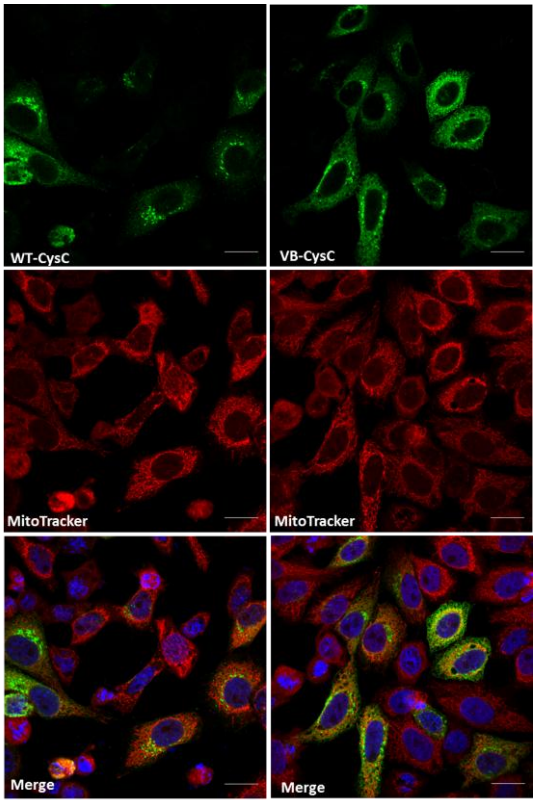

Figure 3.8 - Localization of untagged cystatin C constructs. Human D4O7 cells expressing wild-type or variant B cystatin C were PFA-fixed 24 h post-transfection, immunostained with anti-cystatin C antibody and subsequently imaged. The emission specific for cystatin C constructs is shown in green. Mitotracker, which fluoresces red, was used to visualize mitochondria. The blue fluorescent DAPI was used to stain nuclei. For each field of cells imaged, green and red fluorescence were recorded as separate images and then merged, along with the blue signal, for assessing the overlap of the respective signals. Scale bars are 20 µM.

FLAG-tagged cystatin C constructs

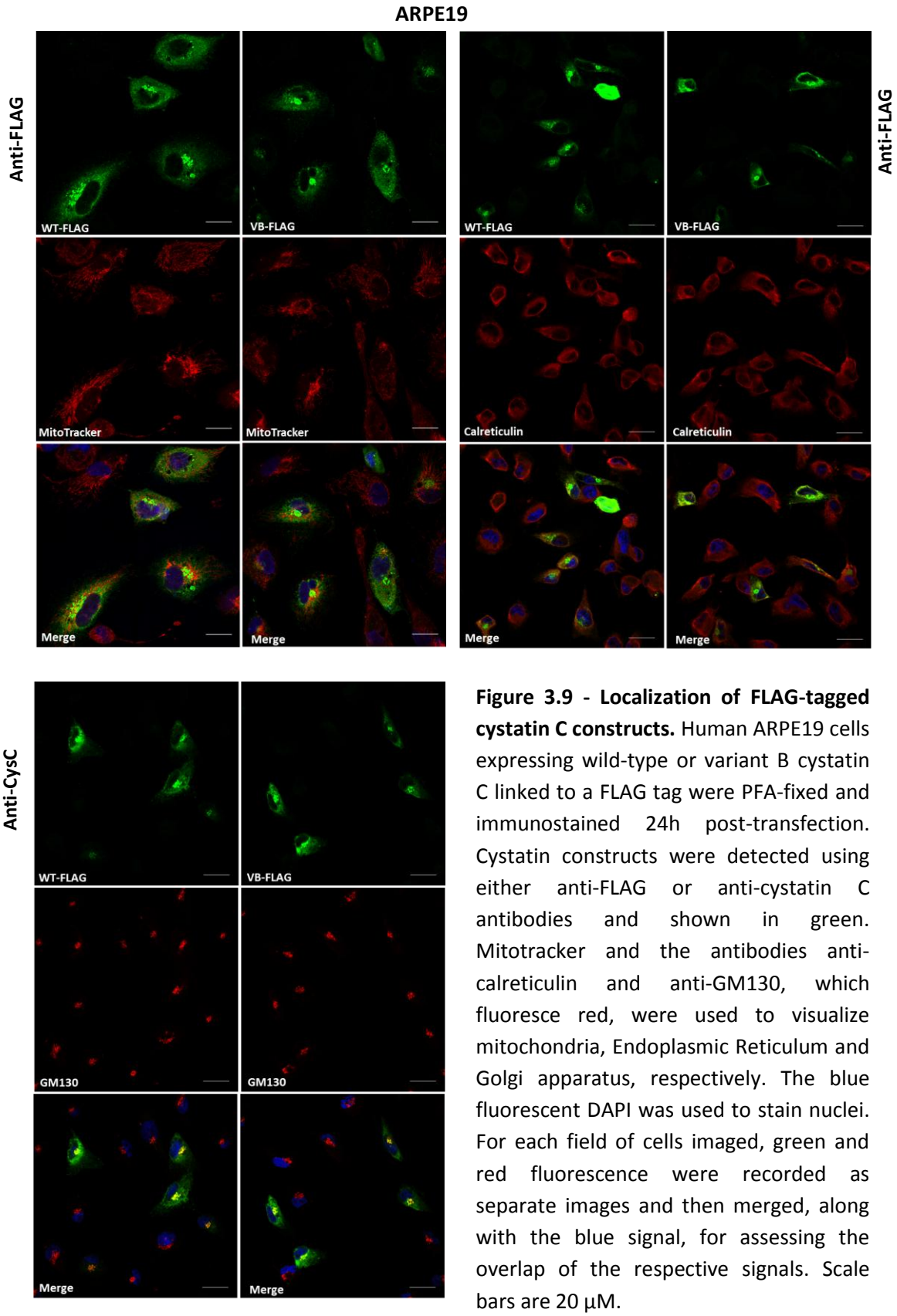

Figure 3.9 - Localization of FLAG-tagged cystatin C constructs. Human ARPE19 cells expressing wild-type or variant B cystatin C linked to a FLAG tag were PFA-fixed and immunostained 24h post-transfection. Cystatin constructs were detected using either anti-FLAG or anti-cystatin C antibodies and shown in green. Mitotracker and the antibodies anti-calreticulin and anti-GM130, which fluoresce red, were used to visualize mitochondria, Endoplasmic Reticulum and Golgi apparatus, respectively. The blue fluorescent DAPI was used to stain nuclei. For each field of cells imaged, green and red fluorescence were recorded as separate images and then merged, along with the blue signal, for assessing the overlap of the respective signals. Scale bars are 20 µM.

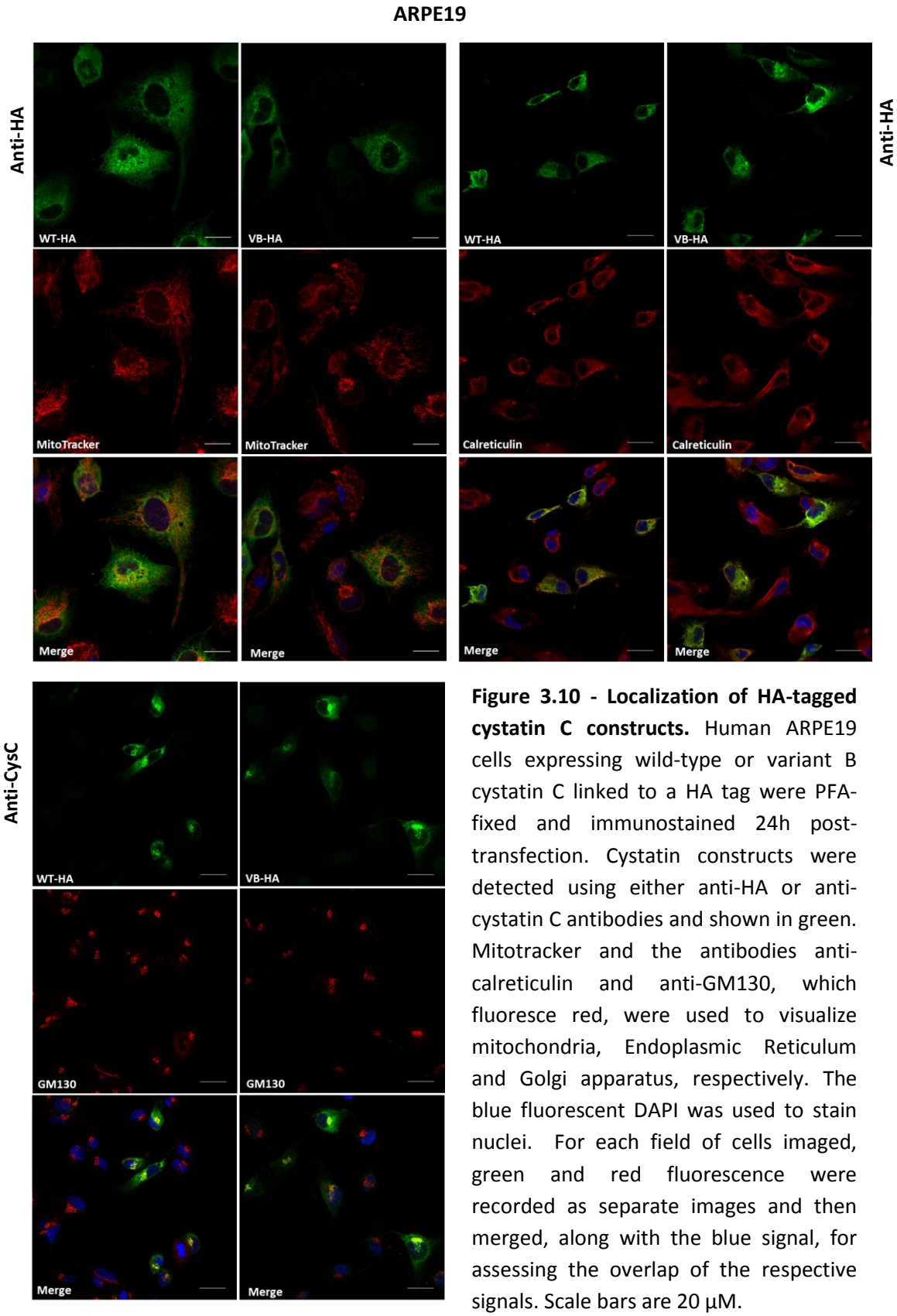

Figure 3.10 - Localization of HA-tagged cystatin C constructs. Human ARPE19 cells expressing wild-type or variant B cystatin C linked to a HA tag were PFA-fixed and immunostained 24h post-transfection. Cystatin constructs were detected using either anti-HA or anti-cystatin C antibodies and shown in green. Mitotracker and the antibodies anti-calreticulin and anti-GM130, which fluoresce red, were used to visualize mitochondria, Endoplasmic Reticulum and Golgi apparatus, respectively. The blue fluorescent DAPI was used to stain nuclei. For each field of cells imaged, green and red fluorescence were recorded as separate images and then merged, along with the blue signal, for assessing the overlap of the respective signals. Scale bars are 20 µM.

D4O7

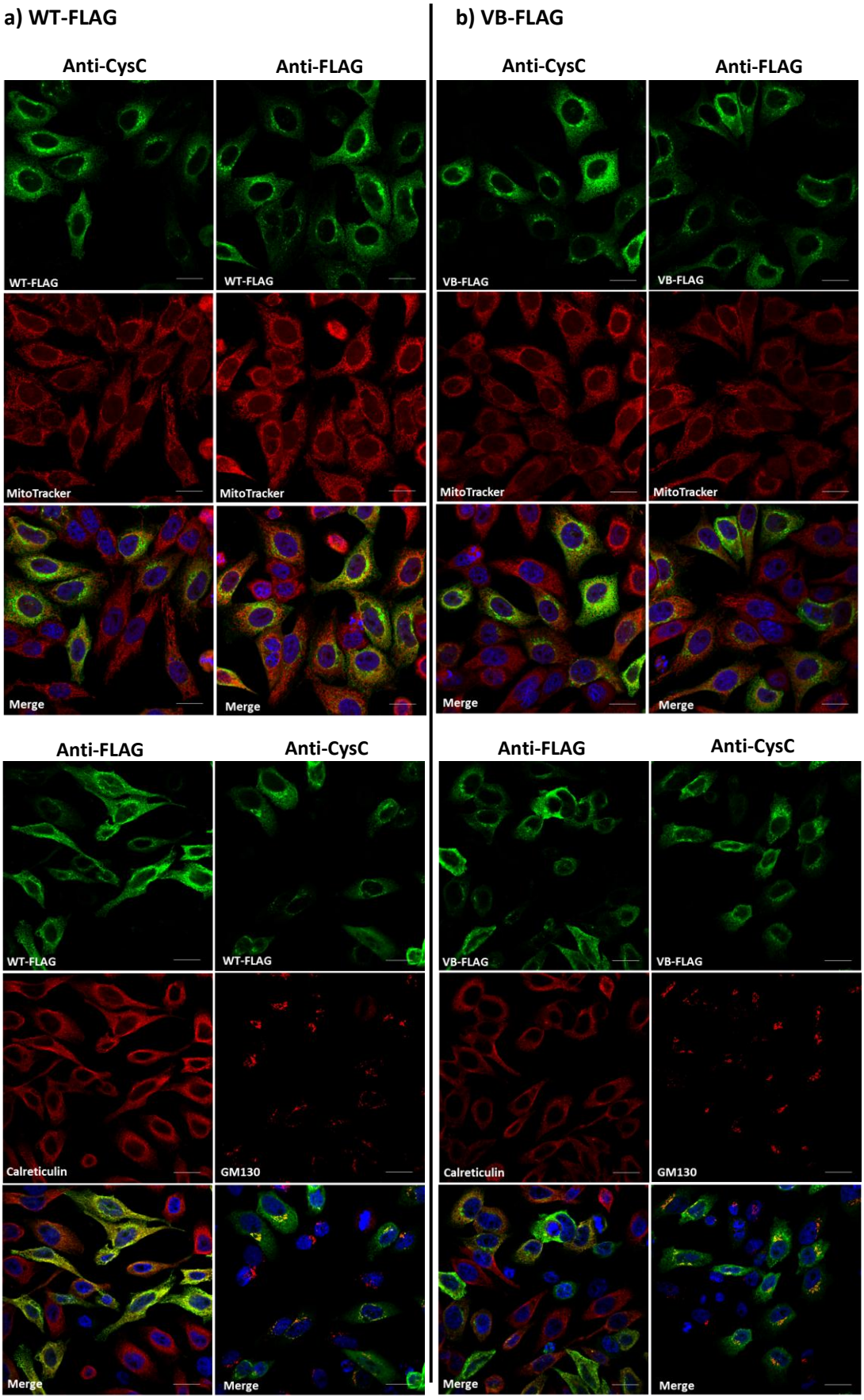
a) WT-FLAG
b) VB-FLAG
Anti-CysC
Anti-FLAG
Anti-CysC
Anti-FLAG
WT-FLAG
WT-FLAG
VB-FLAG
VB-FLAG
MitoTracker
MitoTracker
MitoTracker
MitoTracker
Merge
Merge
Merge
Merge
Anti-FLAG
Anti-CysC
Anti-FLAG
Anti-CysC
WT-FLAG
WT-FLAG
VB-FLAG
VB-FLAG
Calreticulin
GM130
Calreticulin
GM130
Merge
Merge
Merge
Merge

Figure 3.11 - Localization of FLAG-tagged cystatin C constructs. Human D4O7 cells expressing wild-type (a) or variant B (b) cystatin C linked to a FLAG tag were PFA-fixed and immunostained 24h post-transfection. Cystatin constructs were detected using either anti-FLAG or anti-cystatin C antibodies and shown in green. Mitotracker and the antibodies anti-calreticulin and anti-GM130, which fluoresce red, were used to visualize mitochondria, Endoplasmic Reticulum and Golgi apparatus, respectively. The blue fluorescent DAPI was used to stain nuclei. For each field of cells imaged, green and red fluorescence were recorded as separate images and then merged, along with the blue signal, for assessing the overlap of the respective signals. Scale bars are 20 µM.

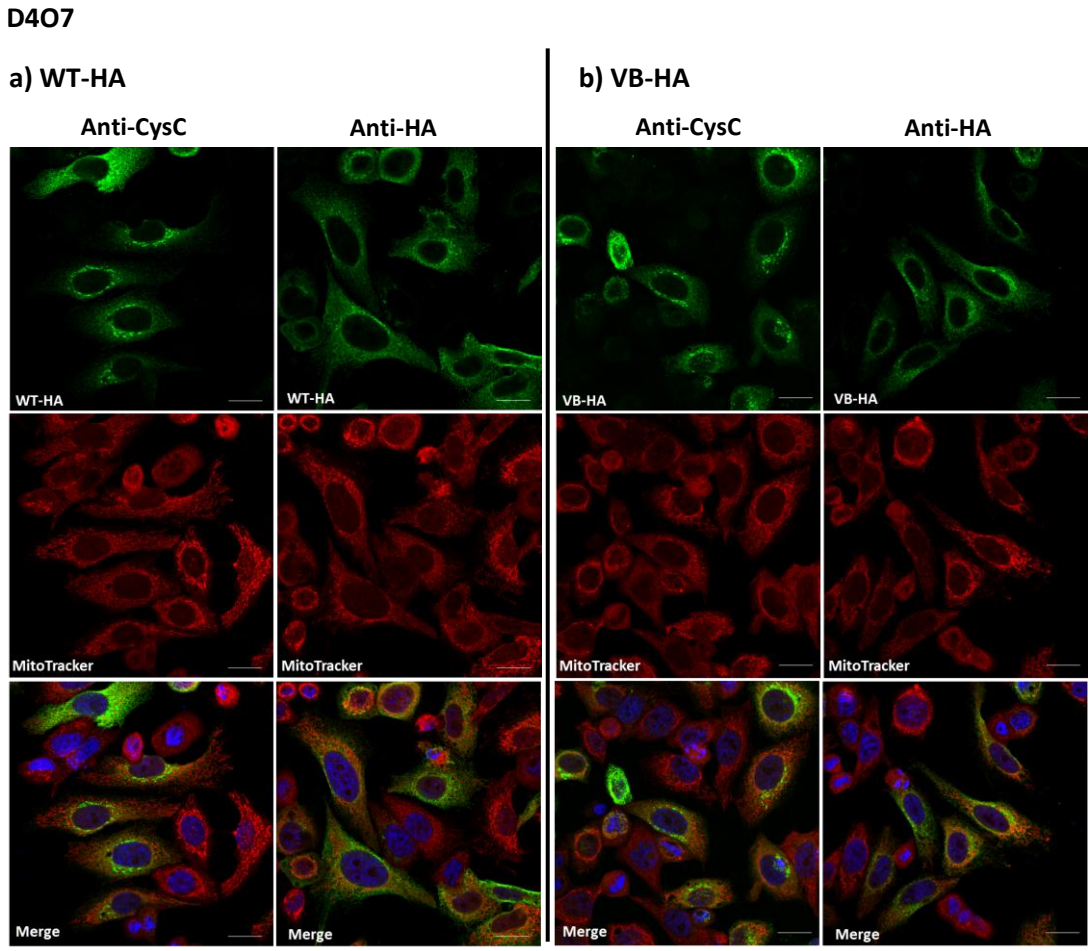

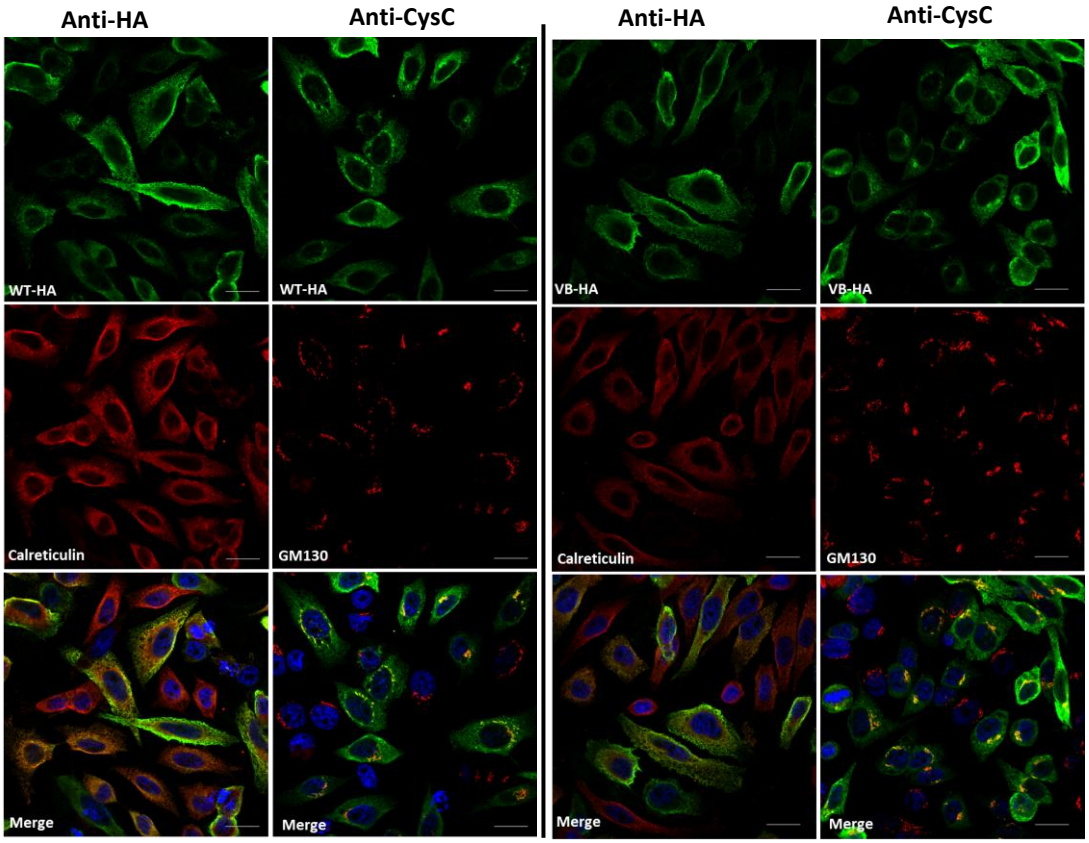

Figure 3.12 - Localization of HA-tagged cystatin C constructs. Human D4O7 cells expressing wild-type (a) or variant B (b) cystatin C linked to a HA tag were PFA-fixed and immunostained 24h post-transfection. Cystatin constructs were detected using either anti-HA or anti-cystatin C antibodies and shown in green. Mitotracker and the antibodies anti-calreticulin and anti-GM130, which fluoresce red, were used to visualize mitochondria, Endoplasmic Reticulum and Golgi apparatus, respectively. The blue fluorescent DAPI was used to stain nuclei. For each field of cells imaged, green and red fluorescence were recorded as separate images and then merged, along with the blue signal, for assessing the overlap of the respective signals. Scale bars are 20 µM.

3.2.3. Wild-type and variant B EGFP-tagged constructs are similarly present in the mitochondria fraction and both differ from the endogenous cystatin C distribution

Analysis of intracellular localization of cystatin C was also performed by cell fractionation and subsequent immunoblotting of cellular organelle fractions, in particular to determine whether the variant B cystatin C is present in the mitochondrial fraction.

For this purpose, mitochondria were enriched from D4O7 cells transfected with the EGFP-linked wild-type or variant B cystatin C constructs by using an antibody-based magnetic separation (MACS) protocol or, alternatively, they were enriched along with nuclear and ER/cytosolic fractions by a differential centrifugation method (DC).

Data from 4 independent transfection experiments were analysed for each method (MACS and DC). The entire cell lysate and the different cellular fractions were analysed by probing with either anti-cystatin C or anti-EGFP antibodies to detect the level of fusion protein in each fraction. Golgi and Mitochondria markers (anti-Mannosidase II and anti-TOM20 antibodies, respectively (Pfanner, Craig & Hönlinger 1997, Shah, Kuntz & Rose 2008)) were used to assess organelles cross-contamination and evaluate the purity of each fraction.

Representative immunoblots of cellular fractions obtained by DC or MACS are shown in figure 3.13 and 3.14, respectively. Neither of these separation techniques allowed me to get pure mitochondria fractions, as shown by the presence of Golgi marker (Mannosidase II) as well as endogenous cystatin C in such cellular fraction. In the same way the mitochondrial marker Tom20 was also found in the nuclei and ER/Cytosol fractions. For this reason, the presence of both wild-type and variant proteins in the enriched mitochondrial samples may be due to such organelles cross-contamination and this limitation did not allow a proper unequivocal analysis. Nevertheless, the levels of the two constructs in the mitochondrial fraction were compared to identify whether there was a significant difference between them that may be attributed to the actual presence of cystatin C in the mitochondria. To

compare their levels in the mitochondria fractions, the expression level of the two constructs in the respective cell lysates was taken into account as well as the amount of mitochondria and Golgi organelles present in the isolated mitochondrial fractions. Considering similar levels of mitochondria and Golgi contamination, results seem to indicate no difference in the level of EGFP wild-type or variant cystatin C fusion protein found in the mitochondrial fractions obtained from either MACS or DC techniques. However, regarding the analysis of the DC fractions a remarkable difference in the distribution of the endogenous cystatin C compared to the transfected EGFP fusion proteins was observed (figure 3.13 a). While the former was mainly present in the soluble fraction (SF) that includes ER and cytosol, the EGFP-linked proteins were predominantly in the Golgi/Mitochondria fraction (P2). As a control, the distribution of EGFP on its own was also analysed, and was found to be mainly in the cytosolic fraction as expected (figure 3.13 b).

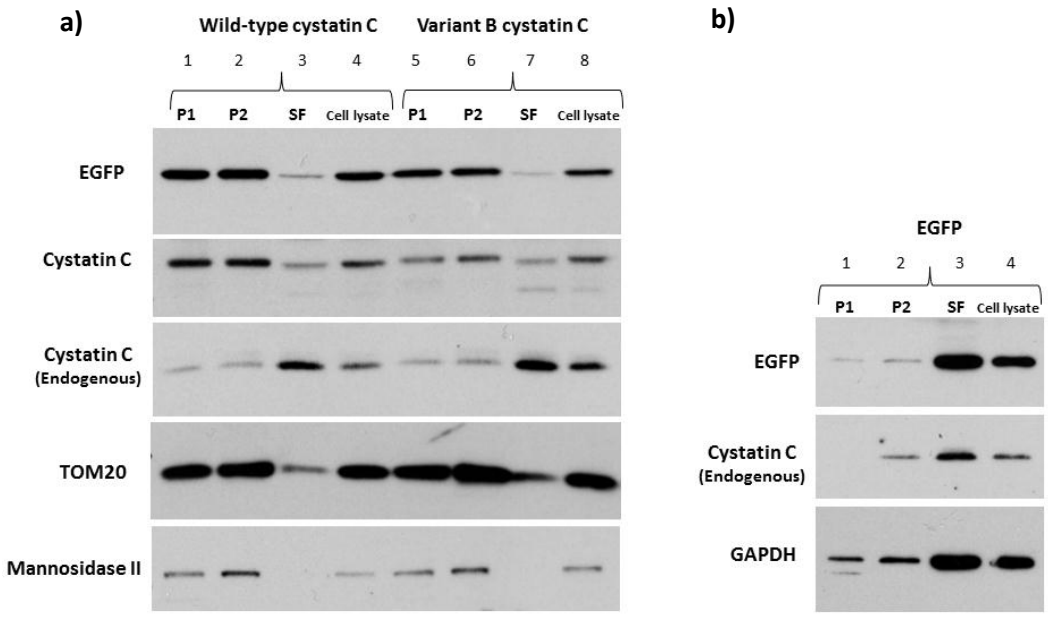

Figure 3.13 - Subcellular fractionation by differential centrifugation. P1, P2 and SF are respectively the nuclear fraction, mitochondria/Golgi fraction and the ER/cytosolic fraction. The entire cell lysate prior to fractionation was also loaded. In figure a) samples 1 to 4 are from D4O7 cells transfected with EGFP-tagged wild-type cystatin c and samples 5 to 8 are from cells transfected with EGFP-tagged Variant B cystatin C. Protein of interest was detected using either anti-EGFP or anti-cystatin C antibodies. Anti-Mannosidase II and anti-Tom20 are used as Golgi and mitochondria marker respectively. In figure b) subcellular fractions from cells transfected with EGFP alone we analysed.

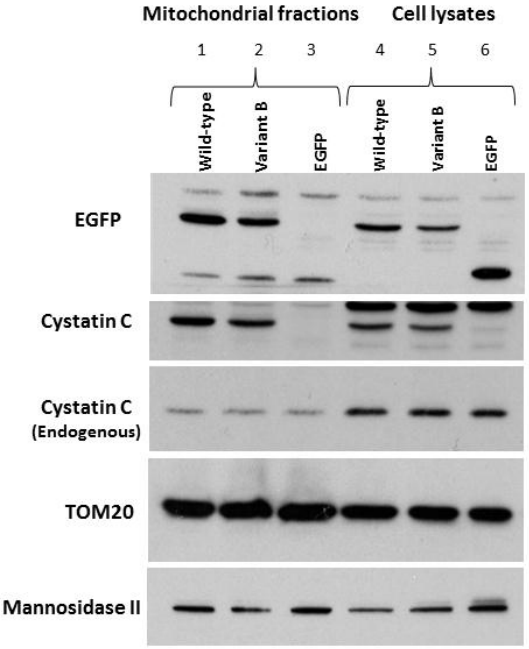

Figure 3.14 - Mitochondria isolation by magnetic separation (MACS). Lanes 1, 2, 3 are mitochondrial fractions isolated from cell transfected respectively with EGFP-tagged cystatin C wild-type, variant B and only EGFP. Lanes 4, 5, 6 are the respective entire cell lysates transfected with wild-type, variant B and only EGFP.

Overall, a partial localization of the EGFP tagged wild-type and variant cystatin C constructs into the mitochondria was observed by both imaging and fractionation analyses. In contrast, mitochondrial localization was not apparent for the cystatin C-constructs carrying FLAG or HA tags, or for endogenous or overexpressed untagged cystatin C. These data suggest that the EGFP tag mediates mitochondrial mislocalization of both the wild-type and variant B cystatin C constructs, whereas the other constructs a delivered to the ER-Golgi secretory pathway.

3.3. Analysis of intracellular accumulation

Variant B cystatin C has been previously reported to accumulate intracellularly (Paraoan et al. 2004). As a consequence a reduction of its secretion in the cultured media was also observed (Paraoan et al. 2004). This situation has been suggested to generate an unbalance in the proteolytic activity both inside and outside the cell,

thus affecting RPE functionality (Paraoan et al. 2004). Moreover, given the amyloidogenic properties of cystatin C, intracellular accumulation of the protein may lead to formation of intracellular aggregates (Tsiolaki et al. 2015). Previously, a mitochondrial association of the variant B using the EGFP-linked constructs was reported (Paraoan et al. 2004). As we observed that this occurs for both wild-type and variant B, and only when cystatin C is linked to the EGFP tag, we further investigated and compared the intracellular amounts of wild-type and variant B for the EGFP- as well as the FLAG- or HA-tagged cystatin C constructs.

For this purpose, inhibition of protein synthesis by cycloheximide was carried out in transfected ARPE19 cells and levels of intracellular and secreted cystatin C were analysed at different time points. After inhibition of protein synthesis a progressive reduction in the levels of intracellular cystatin C is expected, as the protein is gradually secreted into the extracellular environment.

3.3.1. EGFP-tagged constructs are partially retained intracellularly compared to the HA- or FLAG-constructs which are entirely secreted

Immunoblotting in figure 3.15 shows cell lysates and media of treated and non-treated ARPE19 cells transfected with Cys-HA (a) Cys-FLAG (b), Cys-EGFP (c) or only EGFP (d) after 2h (a) and 7h (b, c, and d).

After 2h of cycloheximide treatment (a) a difference in the intracellular level of cystatin C can be already observed compared to the untreated samples. No difference occured between WT and VB constructs where levels of protein expression decrease at similar rate if compared to the respective levels in non-treated cells. GAPDH immunodetection was also used as a loading control. After 7h of treatment the reduction of the intracellular levels increases for both EGFP- (c) and FLAG-tagged (b) constructs, unlike EGFP alone (d) that only slightly decreases, consistent with it not undergoing secretion but remaining intracellularly (Tsien 1998). This indicates that all the cystatin C constructs are progressively released

extracellularly and again no difference between wild-type and variant B is observed. However, at equal levels of expression in the non-treated samples can be observed that the reduction of the cysC-FLAG constructs in the intracellular fraction (Fig. 3.15 b) is notably higher than the one of the cysC-EGFP constructs (c). To be able to detect Cys-FLAG proteins intracellularly after 7h of cycloheximide treatment a higher exposure needed to be carried out. This suggests that the EGFP constructs, either wild-type or variant B, may be partially retained intracellularly or be secreted with significantly slower kinetics.

To investigate this aspect further, an overnight treatment with cycloheximide was performed to give sufficient time to let all the proteins be secreted into the conditioned media. Figure 3.16 (a) shows ARPE19 transfected with Cys-FLAG constructs and treated overnight with cycloheximide. No bands were detected for either wild-type or variant B in the cell lysates, even at higher exposure. Only in the conditioned media was it possible to detect cystatin C proteins. This indicated that all the proteins were eventually secreted and no accumulation had occurred. On the contrary, cells transfected with CysC-EGFP constructs, shown in figure 3.16 (b) still revealed the presence of cystatin C constructs inside the cells even after overnight cycloheximide treatment, suggesting that CysC-EGFP constructs are partially retained intracellularly.

Furthermore, live imaging of ARPE19 cells transfected with EGFP-linked cystatin C constructs were performed prior to the immunoblotting analysis to confirm the intracellular presence of the EGFP-tagged proteins through emission of green fluorescence. As can be observed in Figure 3.17 Cys-EGFP proteins were still detected in a fraction of cells after overnight treatment, therefore confirming immunoblotting results and indicating a tendency of EGFP-linked constructs to accumulate intracellularly. Furthermore, in these cells, the fluorescence was emitted from what appeared to be mitochondria and diffused in the cytosol. This is consistent with proteins being entirely secreted from those cells where proteins localised in the ER/Golgi, therefore not fluorescing after cycloheximide treatment.

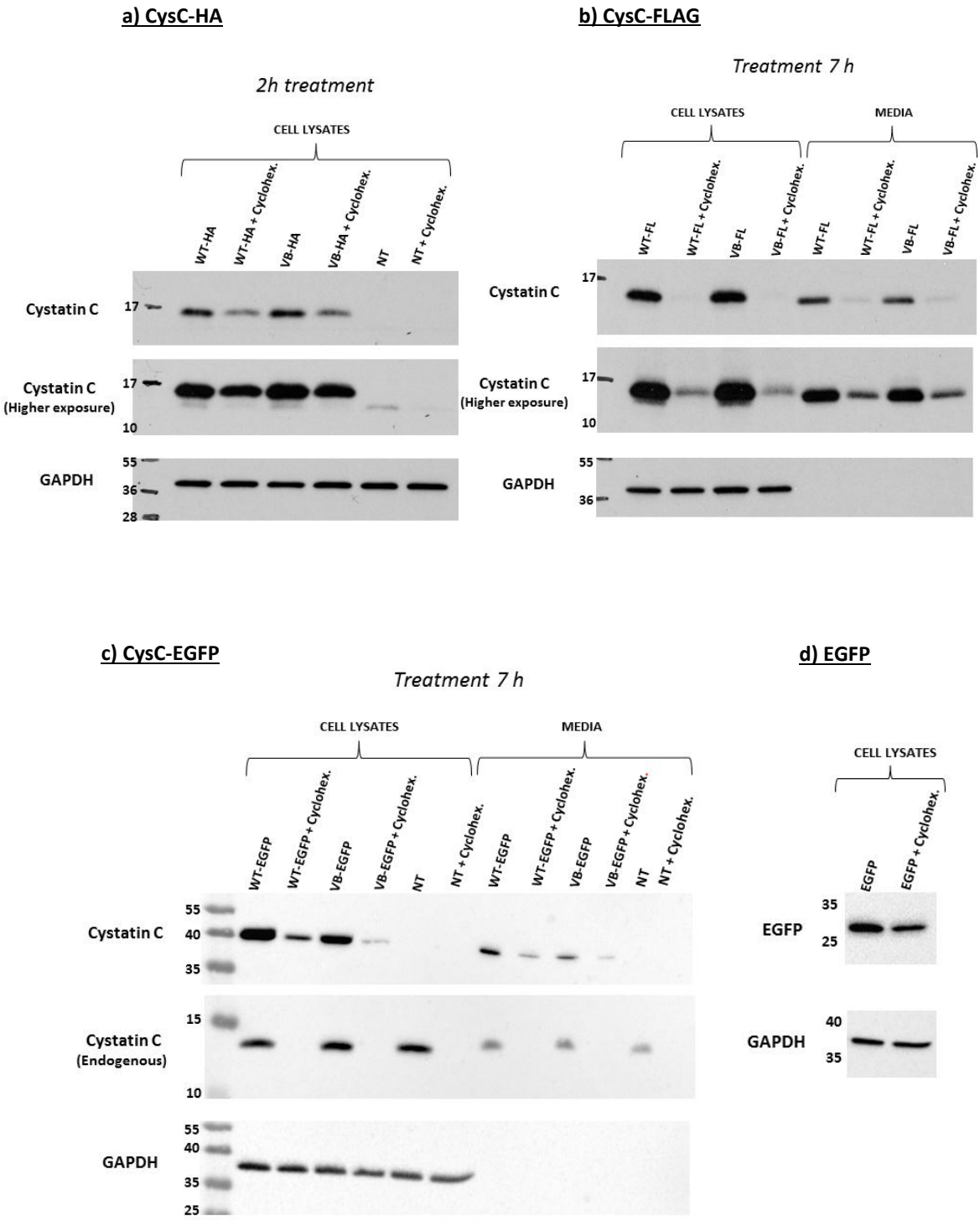

Figure 3.15 - Immunodetection of cystatin C upon inhibition of protein synthesis. ARPE19 cells transfected with Cys-HA (a), Cys-FLAG (b), Cys-EGFP (c) or only EGFP (d) were treated with cycloheximide 200 uM for 2h (a) or 7h (b, c and d) in order to inhibit synthesis of new proteins. Cells treated or non-treated were then immunoblotted with anti-cystatin C to assess whether the protein is secreted or tends to accumulate intracellularly. GAPDH immunoblotting detection was used as a loading control. In figure b) and c) also media samples from treated or non-treated cells were loaded together with the respective cell lysates. The amount of cell lysate loaded was 7X more than the media (cell lysate 20µL/250 µL, media 30µL/2.5mL).

a) CysC-FLAG

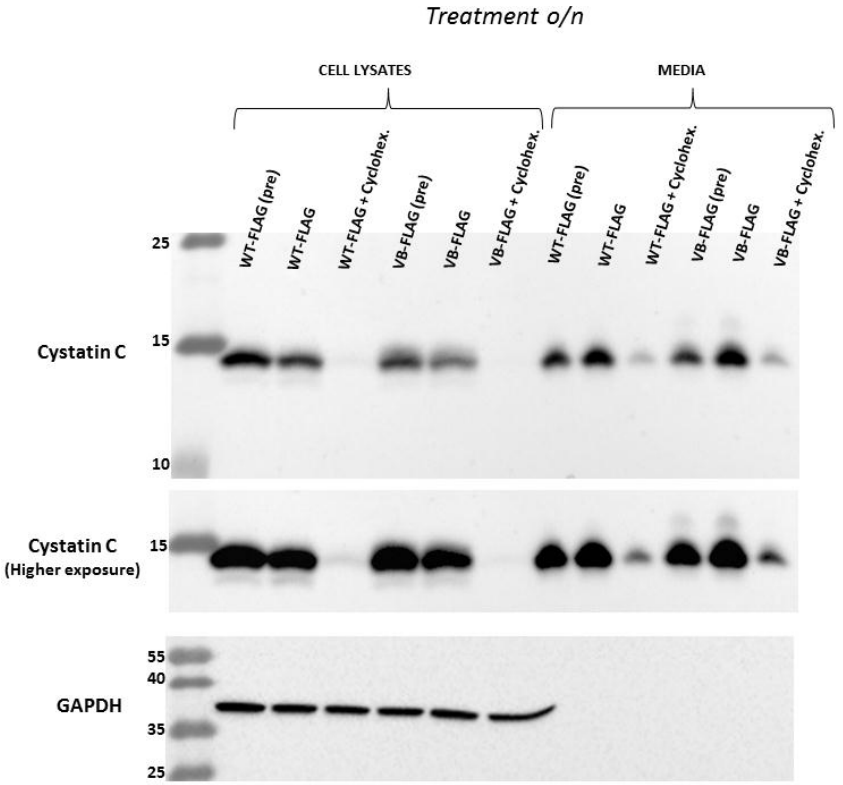

b) CysC-EGFP

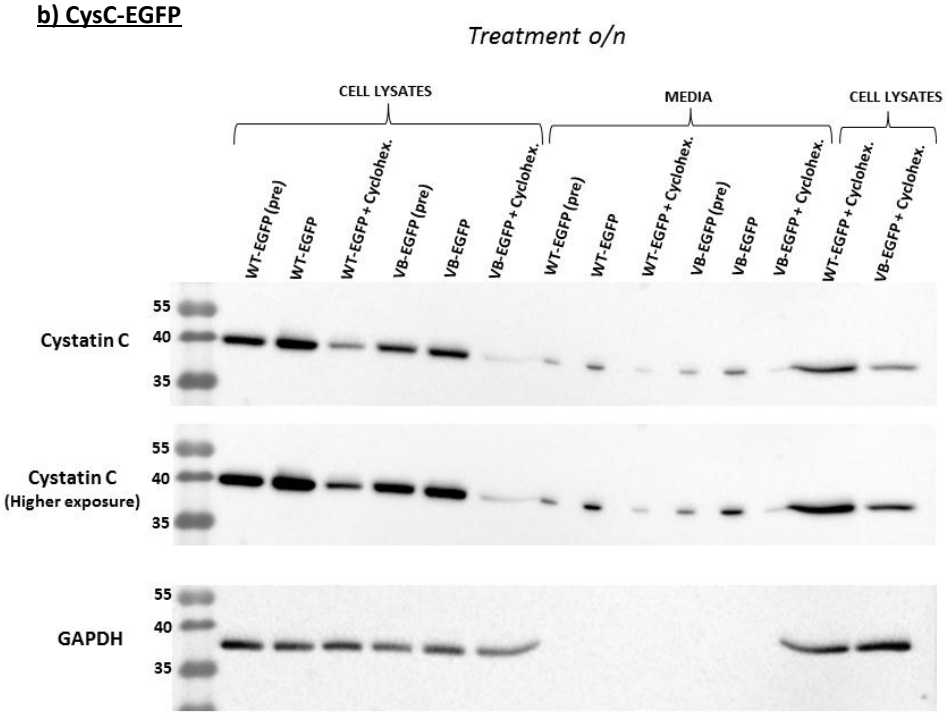

Figure 3.16 - Immunodetection of cystatin C upon inhibition of protein synthesis. ARPE19 cells transfected with Cys-FLAG (a) or Cys-EGFP (b) were treated o/n with cycloheximide 200 µM in order to inhibit synthesis of new proteins. Cells treated or not treated were then

immunoblotted with anti-cystatin C to assess whether the protein is secreted or tend to accumulate intracellularly. GAPDH immunoblotting detection was used as a loading control. In figure b) and c) also media samples were loaded together with the cell lysates. Samples were also collected before the treatment with cycloheximide, indicated with (pre) in the blots, to evaluate level of protein inside and outside the cells at the time of the treatment. The amount of cell lysate loaded was 7X more than the media (cell lysate 20µL/250 µL, media 30µL/2.5mL).

Wild-type CysC-EGFP + Cycloheximide (200uM) overnight

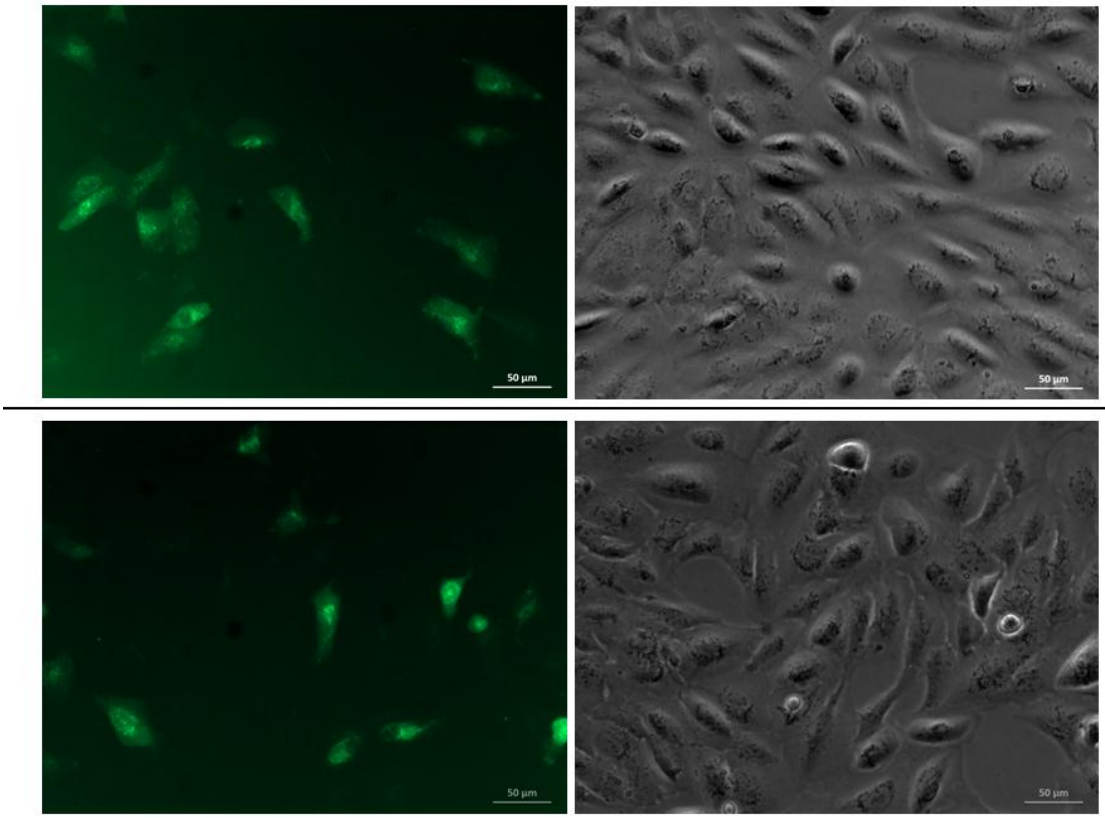

Figure 3.17 - Live cell imaging of ARPE19 cells transfected with WT-EGFP and treated o/n with cycloheximide. Cells treated with cycloheximide 200 µM were imaged before being analysed by immunoblotting in figure 3.2.2 (b) to evaluate cell viability and double check the intracellular presence of proteins thanks to the presence of EGFP linked to cystatin C. Scale bars are 50 µm.

Overall, these results show again a different behaviour between the cysC-EGFP constructs, which seem to be partially retained intracellularly, and the FLAG-tagged cystatin C, which completes its passage along the secretory pathway and is consequently released from the cells, equally for wild-type and variant B.

3.4. Analysis of secretion

Cystatin C variant B has been reported to show impaired secretion, likely due to a reduced efficiency in the cleavage of the signal sequence or in the translocation through the ER membrane as a consequence of the change in hydrophobicity caused by the Ala to Thr substitution in the leader peptide (Benussi et al. 2003, Paraoan et al. 2004). Paraoan et al. (2004) also attributed the reduced secretion of the variant cystatin C to a mistargeting that leads to the unusual mitochondrial association. However, another study failed to report such difference in secretion between wild-type and variant B (Nguyen, Hulleman 2016).

As described in the previous sections, neither mitochondrial localization nor intracellular accumulation was observed for the variant B, which followed the secretory pathway similarly to the wild-type form of cystatin C, eventually being secreted into the culture media. On the contrary, intracellular retention and mistrafficking of cystatin C was observed to occur only in the presence of EGFP, affecting similarly wild-type and variant B proteins.

Even though cystatin C variant B seems to normally undertake the secretory pathway, a difference in the extent of secretion might occur due to reduced efficiency of targeting/processing of the precursor protein for secretion, as suggested by different groups (Benussi et al. 2003, Paraoan et al. 2004). As contrasting data on this aspect have been reported in literature, I decided to further investigate whether the level of secreted cystatin C differs between wild-type and variant proteins by using EGFP-, FLAG-, HA-tagged or untagged cystatin C constructs in ARPE19 and D4O7 cells.

3.4.1. Wild-type and variant B EGFP-, FLAG- and HA-tagged and untagged cystatin C are similarly secreted by RPE

Culture media from cells transfected with the different constructs were subjected to SDS-PAGE electrophoresis, together with the respective cell lysates, and immunodetected by using anti-cystatin C and the specific anti-tag antibodies (EGFP,

FLAG or HA) depending on the construct used. Cell lysate and culture medium from untransfected cells were sometimes used as controls.

For each construct, the level of secretion was analysed 24h after transfection. Same volume of cell lysates, also corresponding to same protein content, was loaded onto the gel, as well as the same volume of media samples. The fraction of secreted cystatin C was assessed by calculating the total protein secreted and normalising this value to the total cystatin C protein, combining the total secreted and the total intracellular cystatin C levels. This method of normalization removes variability due to difference in number of cells or transfection efficiency, as it just calculates the percentage of protein secreted out of the total after a certain period of time.

Immunoblots and analysis of secreted fractions in ARPE 19 cells are shown in figure 3.18, 3.19, 3.20 and 3.21 for Cys-EGFP, untagged Cys, Cys-FLAG and Cys-HA, respectively. The wild-type and variant B proteins were secreted with similar efficiencies, irrespective of whether an anti-EGFP, an anti-cystatin C, an anti-FLAG or anti-HA antibody, depending on the construct used, was used for detection.

a) CysC-EGFP

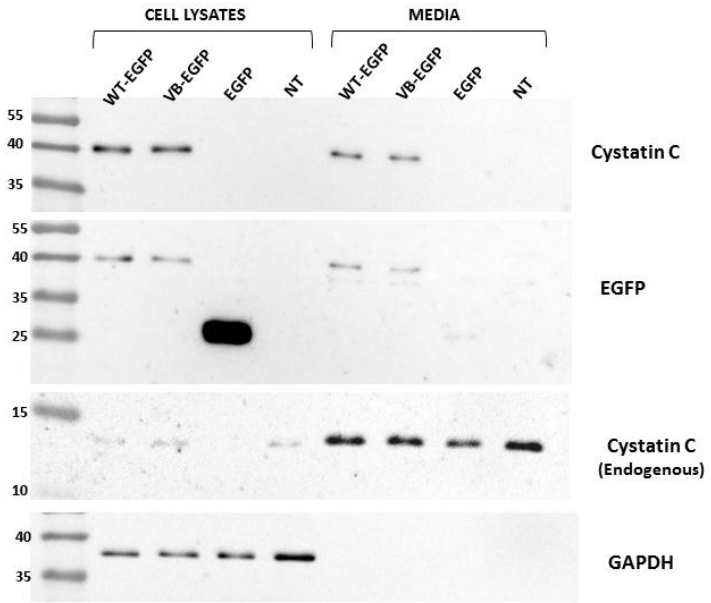

b) Anti-EGFP **c) Anti-cystatin C**

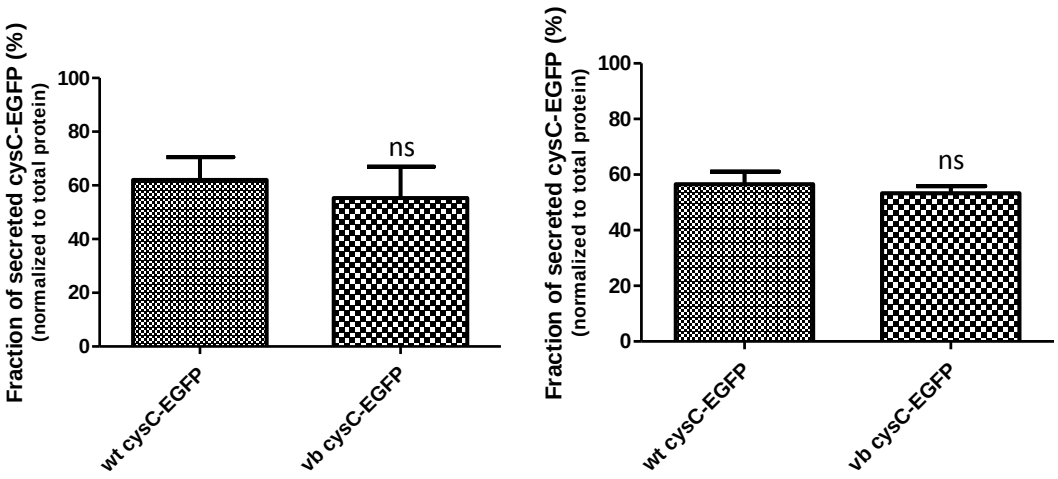

Figure 3.18 - Analysis of secretion of cystatin C wild-type or variant B linked to EGFP in ARPE19. (a) Immunoblot of cell lysates and conditioned media collected from cells expressing respectively wild-type Cys-EGFP, variant B Cys-EGFP, only EGFP and untransfected cells not expressing any of these proteins. Western blots were probed with anti-cystatin C antibody, which detected the cystatin C-EGFP fusion protein, consisting of a band of approximately 40KDa, and the endogenous cystatin C of 13KDa, and with anti-EGFP antibody, which also identified the fusion proteins and EGFP on its own (27KDa). Anti-GAPDH antibody was also used as loading control for cell lysates, whereas endogenous cystatin C in the media can be used as loading control for the media samples. The amount of cell lysate loaded was 4X more than the media (cell lysate 8µL/250 µL, media 20µL/2.5mL). Level of secreted cysC-EGFP fusion proteins in the conditioned medium of cells transfected with wild-type or mutant constructs were evaluated by densitometry of western blots probed with anti-EGFP (b) or anti-cystatin C (c) and the total cystatin C secreted was calculated and normalized to total cystatin C protein (total intracellular + total secreted). Using anti-EGFP antibody the fractions of secreted proteins result to be 0.62 ± 0.09 (SD) for wild-type and 0.55 ± 0.12 (SD) for variant B. *Unpaired t test (N=4) two-tailed*, p=0.39. Using anti-cystatin C antibody the fractions of secreted proteins result to be 0.56 ± 0.05 (SD) for wild-type and 0.53 ± 0.03 (SD) for variant B. *Unpaired t test (N=4) two-tailed,* p=0.26. Results are presented as percentages. ns=non-significant.

a) CysC untagged

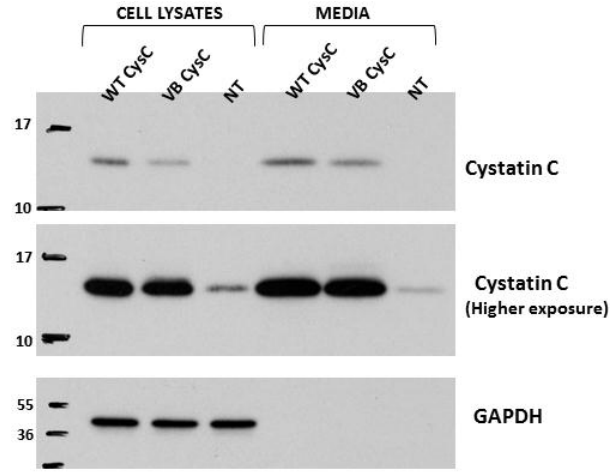

b) Anti-cystatin C

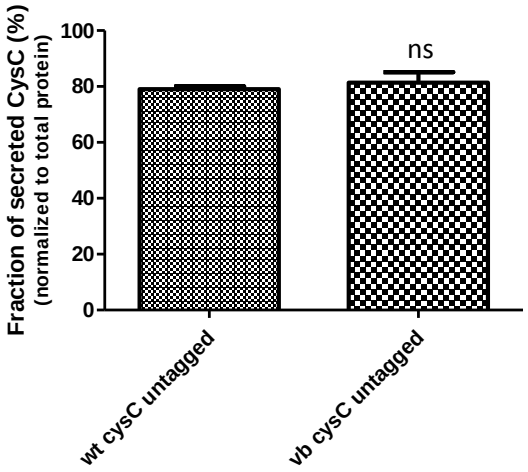

Figure 3.19 - Analysis of secretion of untagged cystatin C wild-type or variant B in ARPE19. (a) Immunoblot of cell lysates and conditioned media collected from cells expressing respectively wild-type CysC, variant B CysC and untransfected cells. Western blots were probed with anti-cystatin C antibody, which detected the transfected untagged cystatin C protein, consisting of a band of approximately 13KDa, and the endogenous cystatin C that can be also detected at higher exposure. Anti-GAPDH antibody was also used as loading control for cell lysates. The amount of cell lysate loaded was 5X more than the media (cell lysate 10µL/250 µL, media 30µL/3.75mL). Level of secreted cysC proteins in the conditioned medium of cells transfected with wild-type or mutant constructs were evaluated by densitometry of western blots probed with anti-cystatin C (b) and the total cystatin secreted was calculated and normalized to total cystatin C protein (total intracellular + total secreted). The fractions of secreted proteins result to be 0.79 ±0.01 (SD) for wild-type and 0.81 ±0.04 (SD) for variant B. *Unpaired t test (N=3) two-tailed*, p=0.36. Results are presented as percentages. ns=non-significant.

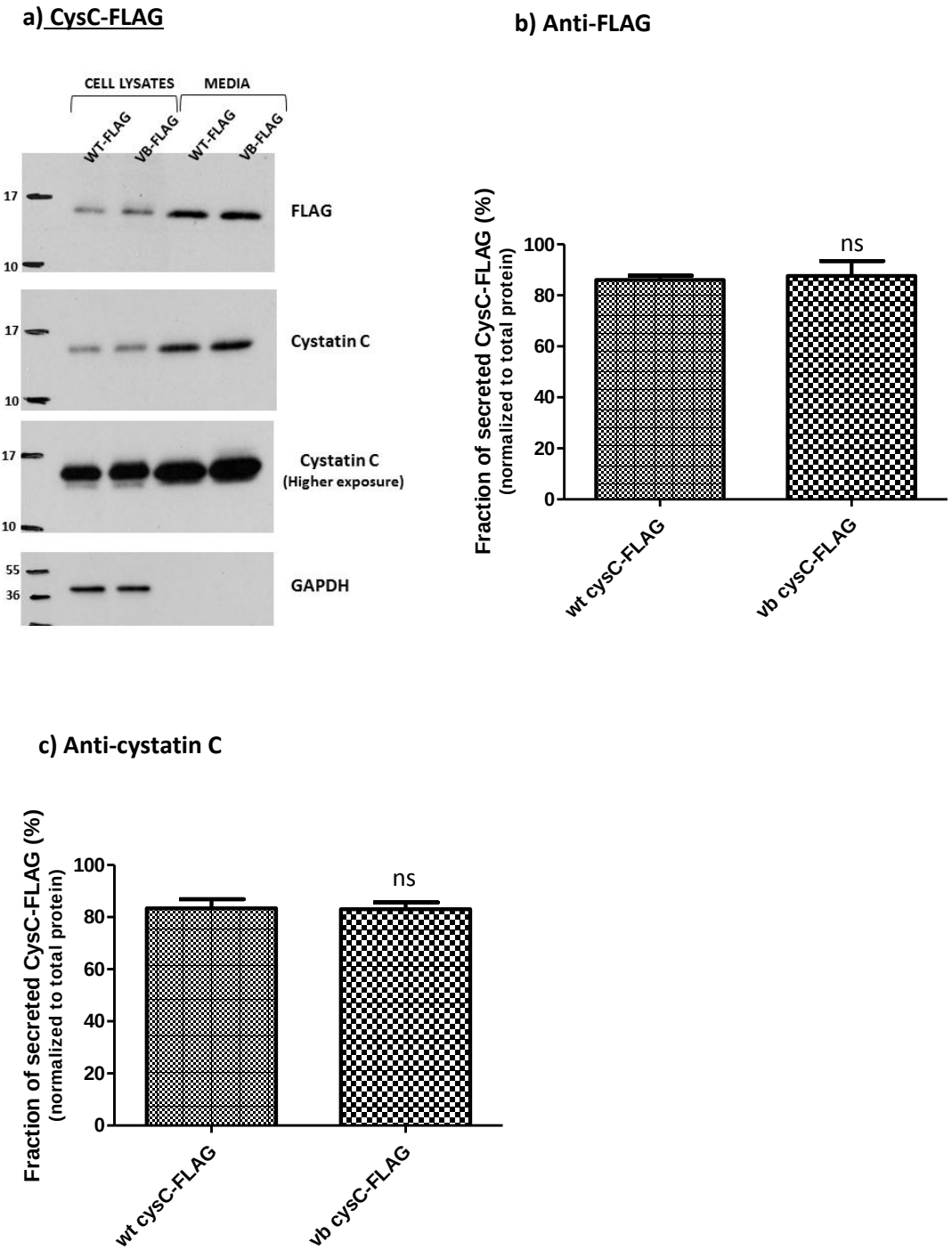

Figure 3.20 - Analysis of secretion of cystatin C wild-type or variant B linked to FLAG in ARPE19. (a) Immunoblot of cell lysates and conditioned media collected from cell expressing respectively wild-type Cys-FLAG and variant B Cys-FLAG. Western blots were probed with anti-cystatin C antibody, which detected the cystatin C-FLAG fusion protein, consisting of a band of approximately 14KDa, and the endogenous cystatin C of 13KDa that can be detected at higher exposure, and with anti-FLAG antibody, which also identified the cystatin C fusion proteins. Anti-GAPDH antibody was used as loading control for cell lysates. The amount of cell lysate loaded was 5X more than the media (cell lysate 10µL/250 µL, media 30µL/3.75mL). Level of secreted cysC-FLAG fusion proteins in the conditioned medium of cells transfected with wild-type or mutant constructs were evaluated by

densitometry of western blots probed with anti-FLAG (b) or anti-cystatin C (c) and the total cystatin secreted was calculated and normalized to total cystatin C protein (total intracellular + total secreted). Using anti-FLAG antibody the fractions of secreted proteins result to be 0.86 ± 0.02 (SD) for wild-type and 0.88 ± 0.06 (SD) for variant B. *Unpaired t test (N=3) two-tailed*, p=0.66. Using anti-cystatin C antibody the fractions of secreted proteins result to be 0.83 ± 0.04 (SD) for wild-type and 0.83 ± 0.03 (SD) for variant B. *Unpaired t test (N=3) two-tailed,* p=0.90. Results are presented as percentages. ns=non-significant.

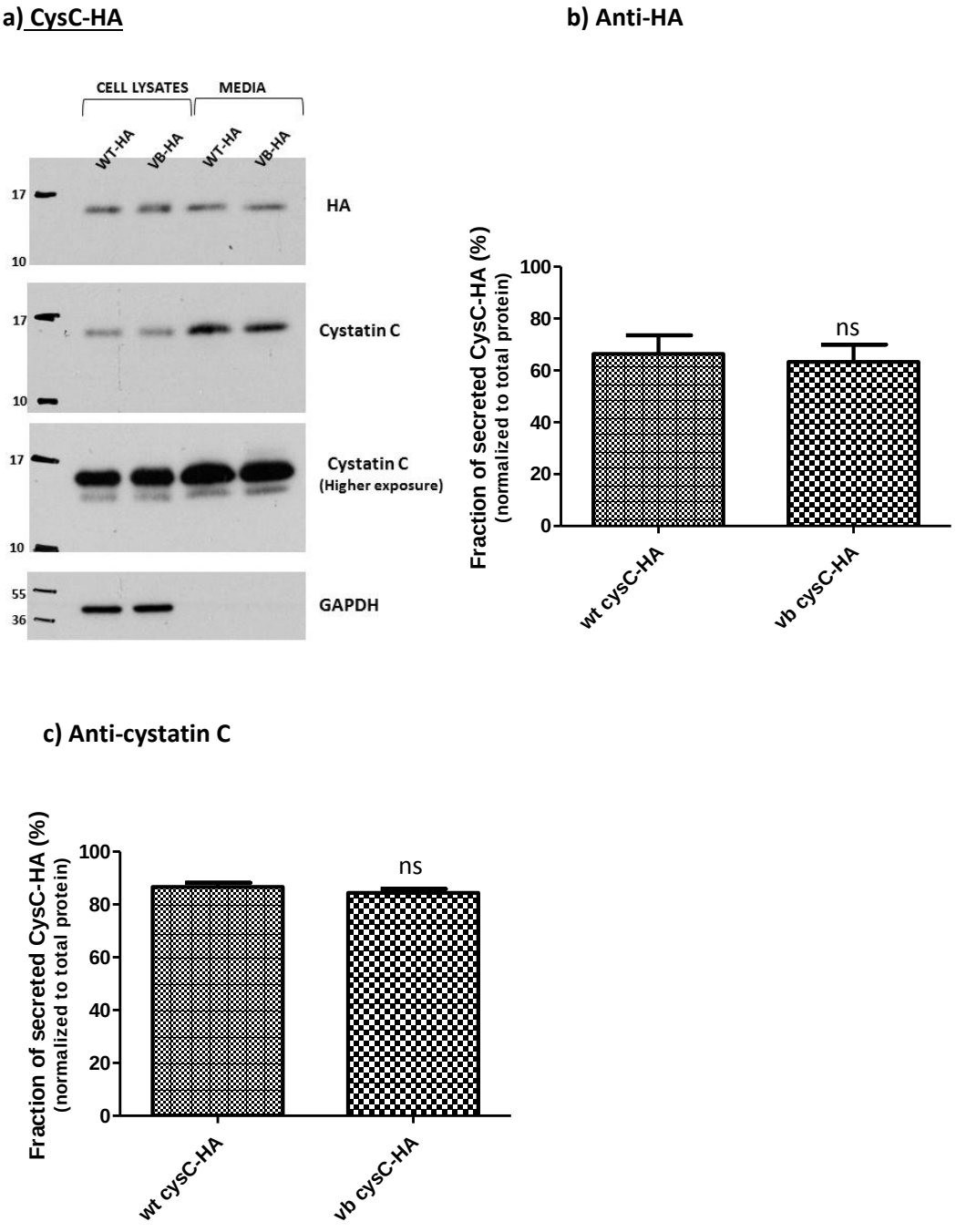

Figure 3.21 - Analysis of secretion of cystatin C wild-type or variant B linked to HA in ARPE19. (a) Immunoblot of cell lysates and conditioned media collected from cell expressing respectively wild-type Cys-HA and variant B Cys-HA. Western blots were probed

with anti-cystatin C antibody, which detected the cystatin C-HA fusion protein, consisting of a band of approximately 14.1KDa, and the endogenous cystatin C of 13KDa that can be detected at higher exposure, and with anti-HA antibody, which also identified the cystatin C fusion proteins. Anti-GAPDH antibody was used as loading control for cell lysates. The amount of cell lysate loaded was 5X more than the media (cell lysate 10µL/250 µL, media 30µL/3.75mL). Level of secreted cysC-HA fusion proteins in the conditioned medium of cells transfected with wild-type or mutant constructs were evaluated by densitometry of western blots probed with anti-HA (b) or anti-cystatin C (c) and the total cystatin secreted was calculated and normalized to total cystatin C protein (total intracellular + total secreted). Using anti-HA antibody the fractions of secreted proteins result to be 0.66 ± 0.07 (SD) for wild-type and 0.63 ± 0.07 (SD) for variant B. *Unpaired t test (N=3) two-tailed*, p=0.63. Using anti-cystatin C antibody the fractions of secreted proteins result to be 0.87±0.02 (SD) for wild-type and 0.84±0.02 (SD) for variant B. *Unpaired t test (N=3) two-tailed,* p=0.14. Results are presented as percentages. ns=non-significant.

The same analysis was also performed in D4O7 cells to control for cell line specificity. Immunoblots and analyses of secretion are shown in figure 3.22, 3.23 and 3.24 for untagged CysC, Cys-FLAG and Cys-HA constructs, respectively. Again, wild-type and variant B proteins are secreted similarly apart from a subtle, statistically significant decrease for variant B found for the untagged constructs.

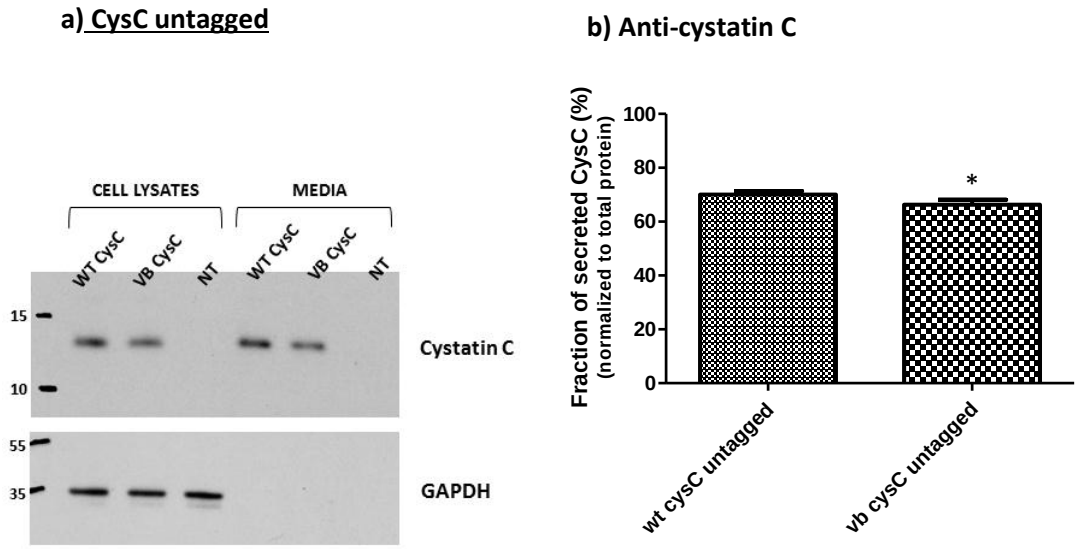

Figure 3.22 - Analysis of secretion of untagged cystatin C wild-type or variant B in D4O7. (a) Immunoblot of cell lysates and conditioned media collected from cell expressing respectively wild-type CysC, variant B CysC and untransfected cells. Western blots were probed with anti-cystatin C antibody, which detected the transfected untagged cystatin C protein, consisting of a band of approximately 13KDa. Anti-GAPDH antibody was used as loading control for cell lysates. The amount of cell lysate loaded was 6X more than the

media (cell lysate 8µL/250 µL, media 20µL/3.75mL). Level of secreted cysC proteins in the conditioned medium of cells transfected with wild-type or mutant constructs were evaluated by densitometry of western blots probed with anti-cystatin C (b) and the total cystatin secreted was calculated and normalized to total cystatin C protein (total intracellular + total secreted). The fractions of secreted proteins result to be 0.70±0.01 (SD) for wild-type and 0.66±0.02 (SD) for variant B. *Unpaired t test (N=4) two-tailed*, p=0.02 (*). Results are presented as percentages.

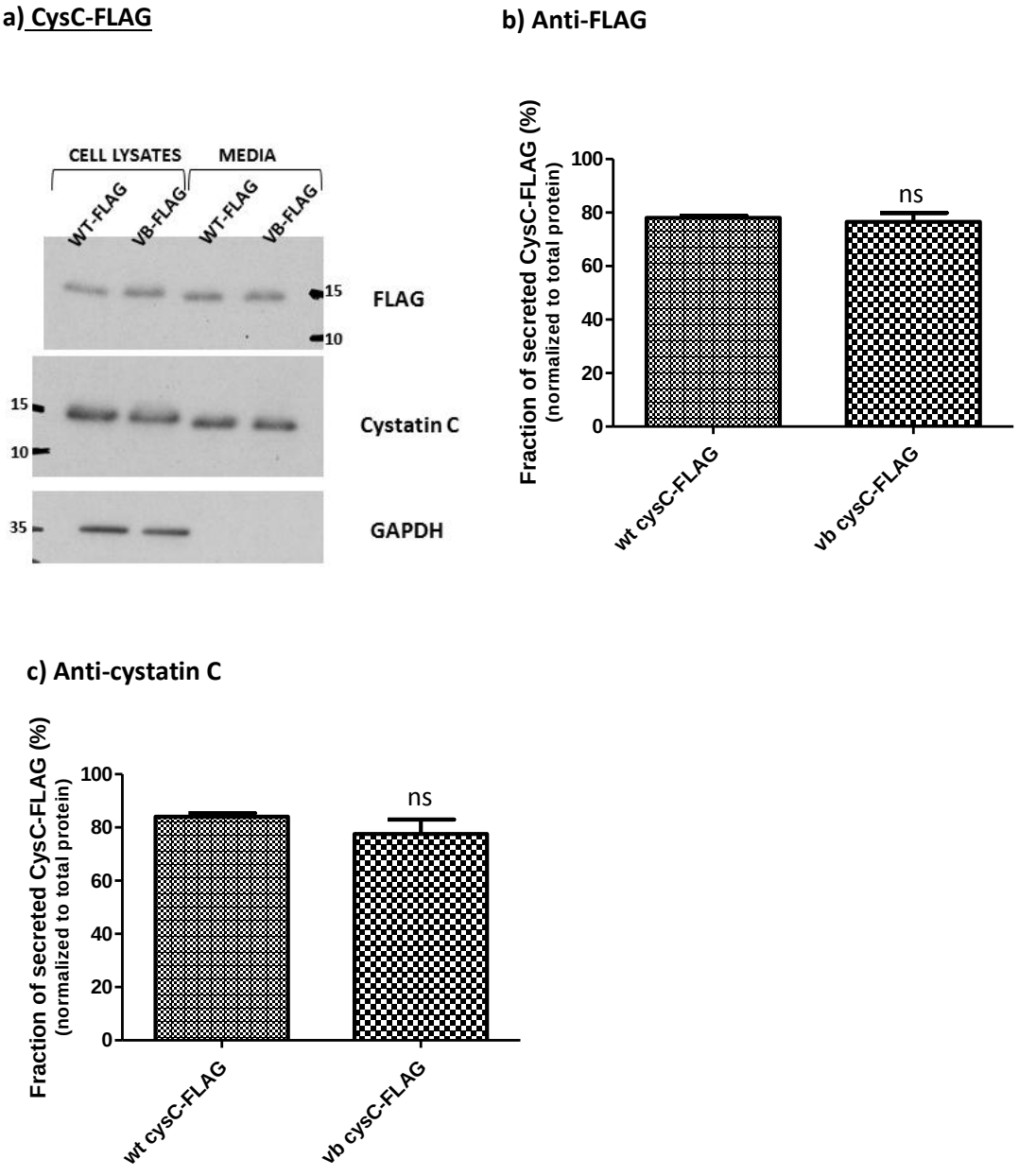

Figure 3.23 - Analysis of secretion of cystatin C wild-type or variant B linked to FLAG in D4O7. (a) Immunoblot of cell lysates and conditioned media collected from cell expressing respectively wild-type Cys-FLAG and variant B Cys-FLAG. Western blots were probed with anti-cystatin C antibody, which detected the cystatin C-FLAG fusion protein, consisting of a band of approximately 14KDa, and with anti-FLAG antibody, which also identified the cystatin C fusion proteins. Anti-GAPDH antibody was used as loading control for cell

lysates. The amount of cell lysate loaded was 6X more than the media (cell lysate 8µL/250 µL, media 20µL/3.75mL). Level of secreted cysC-FLAG fusion proteins in the conditioned medium of cells transfected with wild-type or mutant constructs were evaluated by densitometry of western blots probed with anti-FLAG (b) or anti-cystatin C (c) and the total cystatin secreted was calculated and normalized to total cystatin C protein (total intracellular + total secreted). Using anti-FLAG antibody the fractions of secreted proteins result to be 0.78±0.01 (SD) for wild-type and 0.76±0.03 (SD) for variant B. *Unpaired t test (N=4) two-tailed*, p=0.43. Using anti-cystatin C antibody the fractions of secreted proteins result to be 0.84±0.01 (SD) for wild-type and 0.77±0.05 (SD) for variant B. *Unpaired t test (N=4) two-tailed,* p=0.06. Results are presented as percentages. ns=non-significant.

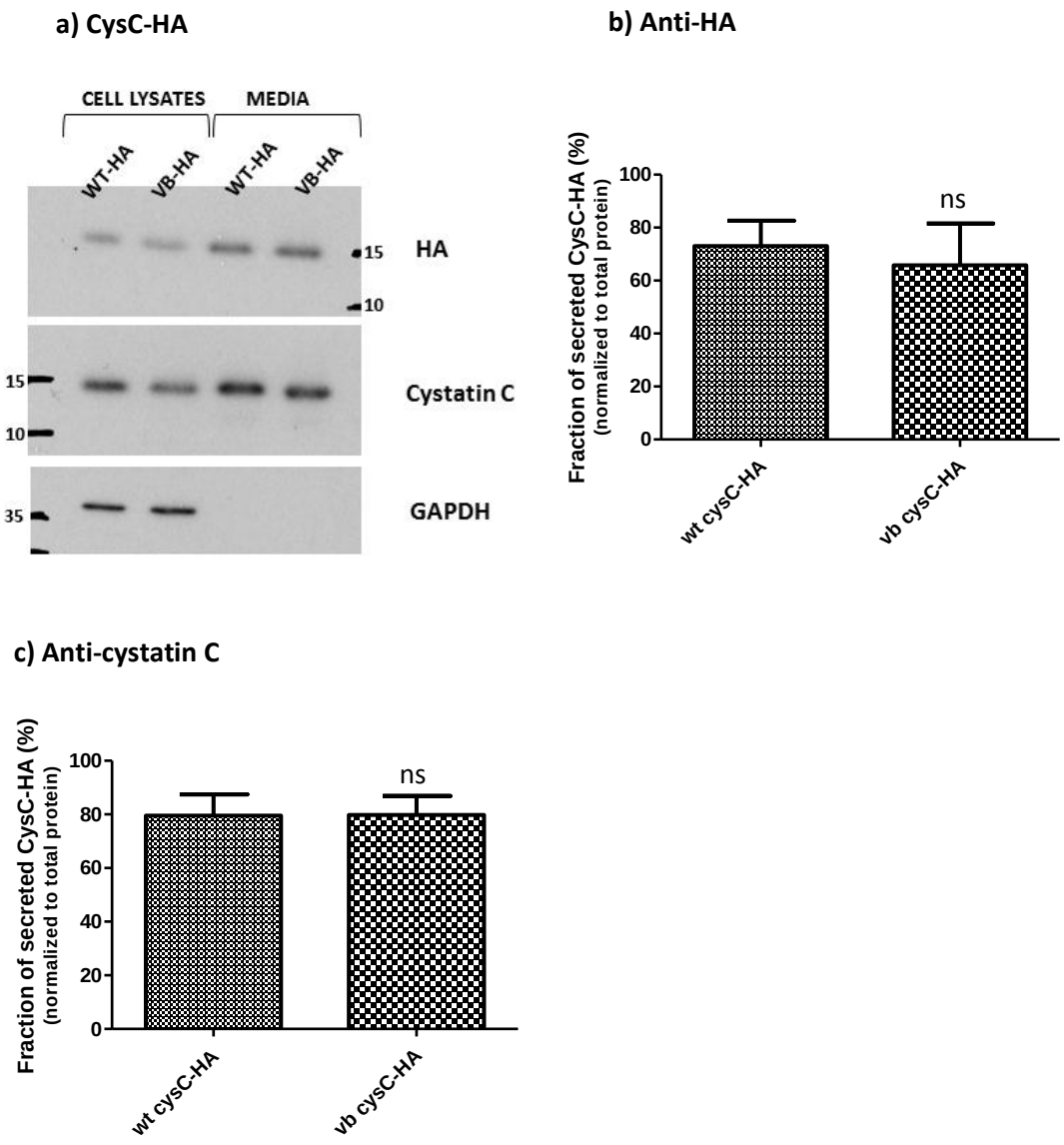

Figure 3.24 - Analysis of secretion of cystatin C wild-type or variant B linked to HA in D4O7. (a) Immunoblot of cell lysates and conditioned media collected from cell expressing respectively wild-type Cys-HA and variant B Cys-HA. Western blots were probed with anti-cystatin C antibody, which detected the cystatin C-HA fusion protein, consisting of a band

of approximately 14.1KDa, and with anti-HA antibody, which also identified the cystatin C fusion proteins. Anti-GAPDH antibody was used as loading control for cell lysates. The amount of cell lysate loaded was 6X more than the media (cell lysate 8µL/250 µL, media 20µL/3.75mL). Level of secreted cysC-HA fusion proteins in the conditioned medium of cells transfected with wild-type or mutant constructs were evaluated by densitometry of western blots probed with anti-HA (b) or anti-cystatin C (c) and the total cystatin secreted was calculated and normalized to total cystatin C protein (total intracellular + total secreted). Using anti-HA antibody the fractions of secreted proteins result to be 0.73±0.10 (SD) for wild-type and 0.66±0.16 (SD) for variant B. *Unpaired t test (N=4) two-tailed*, p=0.96. Using anti-cystatin C antibody the fractions of secreted proteins result to be 0.79±0.08 (SD) for wild-type and 0.80±0.07 (SD) for variant B. *Unpaired t test (N=4) two-tailed,* p=0.46. Results are presented as percentages. ns=non-significant.

3.4.2. Secreted levels of EGFP constructs are significantly lower compared to the untagged, FLAG- or HA-tagged constructs and to the endogenous cystatin C

Looking at the analyses of secretion described in the previous section for the different constructs, a difference in the fraction of cystatin C secreted can be observed between EGFP-linked constructs and the other three constructs (untagged, FLAG- and HA-tagged). To exclude a possible variability due to the use of different antibodies, I considered the values obtained using the anti-cystatin C antibody, which can detect all the four different constructs, for the comparison. In table 7 all of the fractions of secreted proteins calculated previously are reported for each construct. It is clear that the fraction of secreted protein is lower for the EGFP-constructs in comparision to the FLAG or HA tagged constructs, being around 50% of the total, compared to the about 80% for the other constructs or untagged cystatin C.

Table 7 - Fraction of secreted cystatin C from ARPE19 cells transfected with Cys-EGFP, Cys-FLAG, Cys-HA or untagged CysC constructs. Values obtained by densitometry of western blots probed with anti-cystatin C were normalized as described in section 3.3.1. and the resulting fractions of secreted Cystatin C calculated for each construct.

FRACTION OF SECRETED CYSTATIN C		
CONSTRUCT:	Wild-type	Variant B
Cys-EGFP	0.56 ± 0.05	0.53 ± 0.03
Cys-FLAG	0.83 ± 0.04	0.83 ± 0.03
Cys-HA	0.87 ± 0.02	0.84 ± 0.02
CysC untagged	0.79 ± 0.01	0.81 ± 0.04

Moreover, ARPE19 cells cultured in the same conditions and transfected with the different constructs were analysed by western blotting, loading same volume of cell lysate and medium for all the constructs. Blots were probed with anti-cystatin C antibody so that all the different constructs could be detected at the same time, minimizing the variability caused by using different antibodies and allowing comparison among the different constructs (figure 3.25). The level of secreted cystatin C was significantly lower in the case of the Cys-EGFP constructs when compared to the other three constructs. Indeed, an increase in exposure time was needed to be able to detect cystatin C in the conditioned media samples for the Cys-EGFP construct. At higher exposure it was also possible to detect the endogenous cystatin C in the cell and media samples from both transfected and untransfected ARPE19 cells. Interestingly, the proportion of endogenous cystatin C inside and outside the cells differed from the EGFP constructs but was similar to that observed for the Cys-FLAG, Cys-HA and untagged CysC constructs. These results suggest that these three constructs are properly secreted from the cells with similar rates as the endogenous protein. In contrast, the EGFP-constructs show a reduced level of secretion and higher intracellular levels, consistent with their tendency to accumulate intracellularly and mislocalize. This can be easily

assessed by comparing the level of secreted and cell associated protein in figure 3.25.

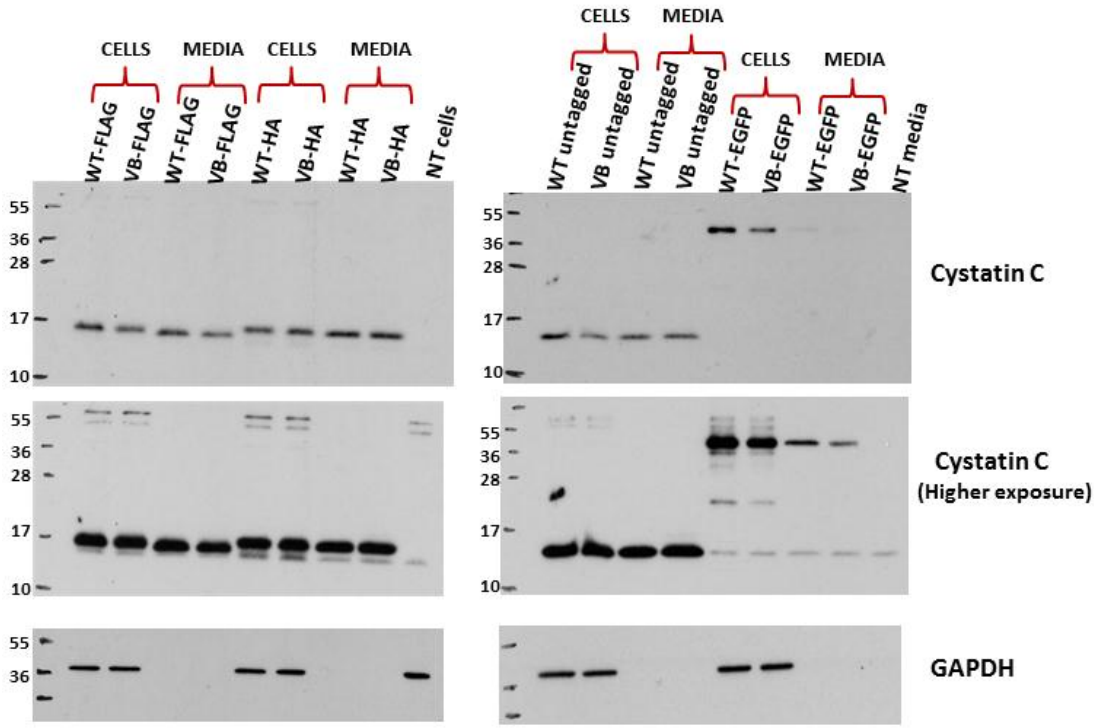

Figure 3.25 - Immunodetection of cystatin C in cell lysate and culture media samples from ARPE19 cells transfected with Cys-FLAG, Cys-HA, Cys untagged and Cys-EGFP constructs. Same volumes of cell lysates and same volumes of media samples were loaded on gels for all the constructs in order to directly compare the level of proteins inside and outside the cells. The amount of cell lysate loaded was 5X more than the media (cell lysate 10µL/250 µL, media 30µL/3.75mL). Anti-cystatin C antibody was used to detect bands of interest and anti-GAPDH as additional control. Cys-FLAG, Cys-HA, untagged CysC and Cys-EGFP are detected at approximately 14KDa, 14.1KDa, 13KDa and 40KDa, respectively. At higher exposure endogenous cystatin C is also detected for all the constructs except the untagged ones being of the same size.

Overall, these results indicate that there is no major difference in secretion between wild-type and variant B. Furthermore, they are consistent with the hypothesis that EGFP likely affects the trafficking of cystatin C, causing intracellular accumulation with mitochondrial association of the protein and consequently a reduction in its level of secretion.

3.5. Analysis of secretory trafficking

In addition to the canonical ER/Golgi secretory pathway, other unconventional pathways have been described to target proteins for secretion. For instance, ER- and/or Golgi-independent secretion, lysosomal exocytosis and exosomes pathway have been reported, as described in section 1.5.2. Moreover, cystatin C itself has been also shown to be secreted by exosomes under certain circumstances (described in section 1.2.2) (Ghidoni et al. 2011b).

For this reason, even though the rate of secretion was similar between wild-type and variant B in our analysis, I investigated whether the variant B is secreted by pathways other than the conventional one, which may shed light onto its postulated link to disease. Inhibition of the classical pathway was therefore carried out to assess whether the protein was still secreted.

3.5.1. Variant B cystatin C is targeted to the conventional secretory pathway

ARPE19 cells transfected with wild-type or variant Cys-FLAG constructs were treated with either Brefeldin A (BFA) or Monensin for 7h. BFA inhibits transport of proteins from ER to Golgi (Klausner, Donaldson & Lippincott-Schwartz 1992), thus causing protein accumulation in the ER. Monensin blocks protein transport through the Golgi stack (Mollenhauer, Morré & Rowe 1990), resulting in retention of proteins in the Golgi apparatus. In both cases, protein secretion is prevented. By inhibiting the conventional secretory pathway by two different means and analysing the secretion of cystatin C, it is possible to exclude the involvement of other ER/Golgi-independent secretory pathways.

Immunoblot in figure 3.26 shows the levels of FLAG-tagged cystatin C fusion proteins after treatment with either BFA or Monensin in both the cell and media samples. Untreated samples were used as control. Higher levels of cystatin C proteins in the cell lysates were observed for both the wild-type and variant B proteins after treatment with either BFA or Monensin, consistent with the

accumulation of proteins in the ER and Golgi, respectively. Concurrently, a significant decrease in the levels of secreted proteins in the culture media is observed in both cases. Only at higher exposures it is possible to detect cystatin C in the media after Monensin treatment, probably reflecting that Monensin does not completely block the secretory pathway at the concentration used. Interestingly, no difference between wild-type and variant B was observed, as their levels equally increased intracellularly and decreased in the media. This is consistent with the notion that cystatin C followed the same canonical ER-Golgi secretory pathway and no alternative pathways are involved.

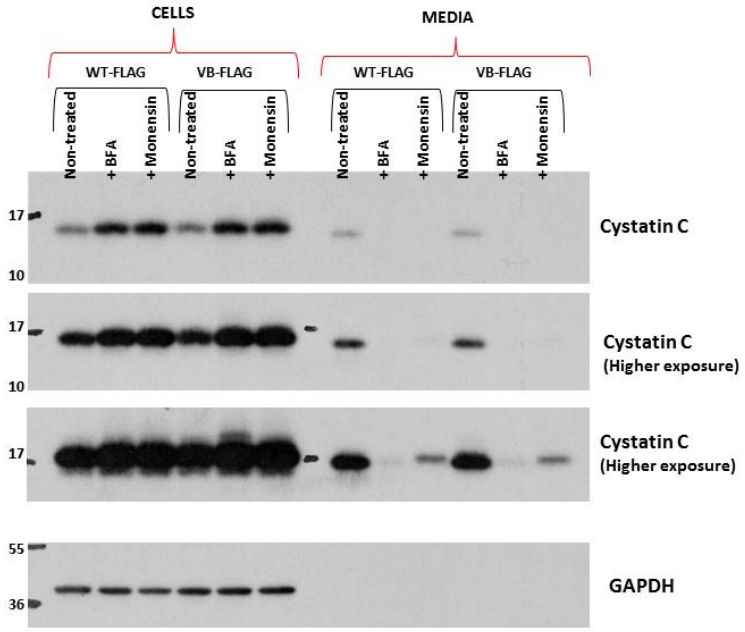

Figure 3.26 - Immunodetection of cystatin C in cell lysates and conditioned media of ARPE19 cells transfected with wild-type and variant B cys-FLAG constructs after treatment with BFA or Monensin. Samples collected from RPE cells transfected with either wild-type or variant B constructs and subjected to inhibition of secretory pathway by using BFA 5 µg/mL or Monensin 5µM for 7h were analysed by immunoblotting with anti-cystatin C antibody, shown at different time exposure to allow detection of proteins present in small amounts. Anti-GAPDH antibody was used as loading control for cell lysates. The amount of cell lysate loaded was 10X more than the media (cell lysate 20µL/250µL, media 20µL/2.5mL).

ARPE19 cells transfected with Cys-FLAG constructs and treated with either BFA or Monensin were also imaged by IF/ICC. Figure 3.27 shows images of PFA-fixed cells

immunostained with anti-FLAG or anti-cystatin C antibodies to detect the fusion protein and with anti-calreticulin or anti-GM130 to detect ER and Golgi, respectively. After 7-hour treatment with BFA (Figure 3.2 a), cystatin C is localized within the ER but not within the Golgi apparatus. The Golgi apparatus appeared to be disrupted as GM130 shows a diffuse distribution. This is consistent with the block of the transport of all the proteins from the ER to Golgi. In contrast, after 7-hour treatment with Monensin (Figure 3.27 b), the structure of the Golgi apparatus was maintained, with GM130 staining concentrated to a specific perinuclear region, characteristic of the Golgi. Cystatin C was distributed to both the ER and Golgi, colocalizing with both organelles markers. No difference between wild-type and variant B proteins was observed.

These results strongly indicate that both cystatin C proteins follow the classical ER-Golgi secretory pathway, further excluding mislocalization of the variant B.

a) Treatment with BFA

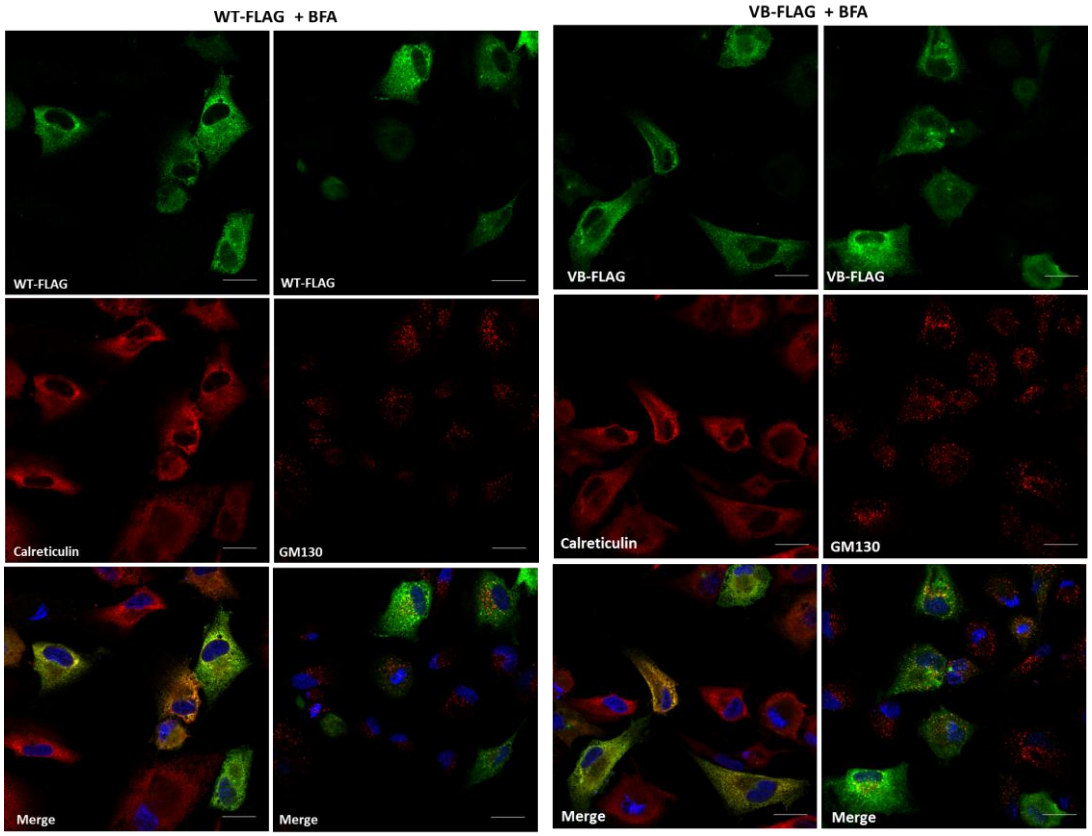

b) Treatment with Monensin

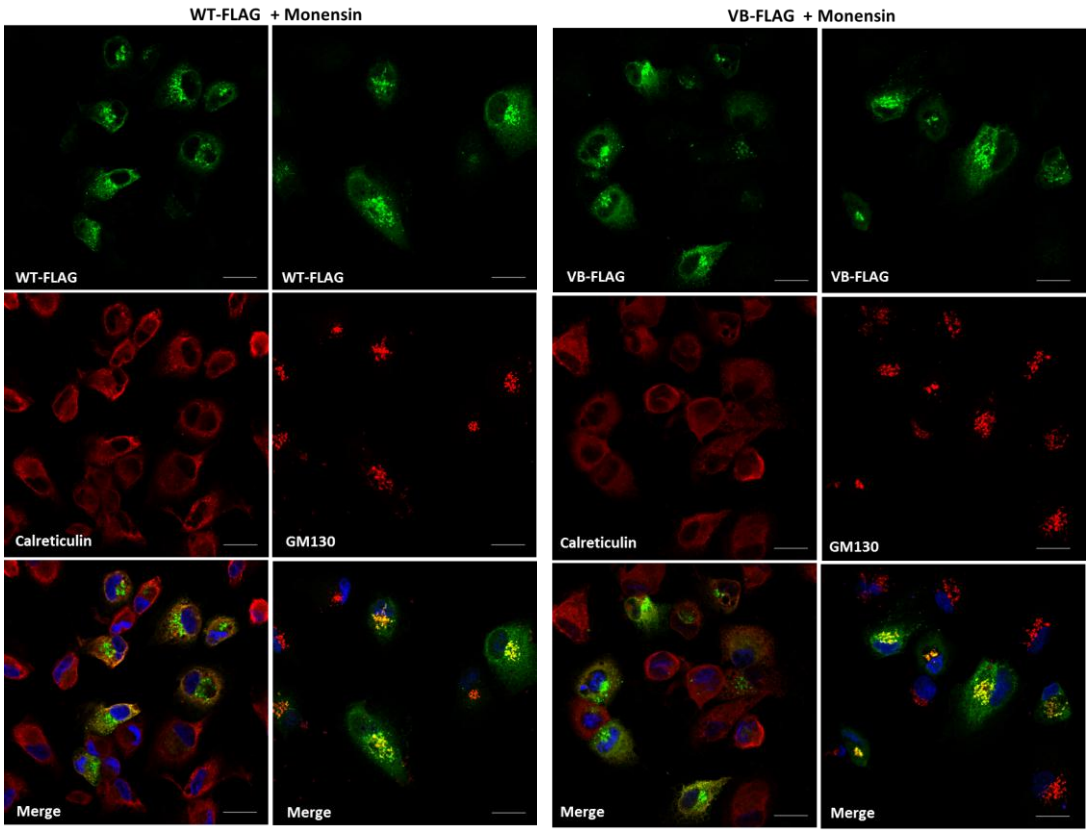

Figure 3.27 - Localization of FLAG-tagged cystatin C constructs in ARPE19 cells after treatment with BFA or Monensin. Living cultured human ARPE19 cells expressing wild-type or variant B cystatin C linked to a FLAG tag were PFA-fixed and immunostained after treatment with BFA (a) or Monensin (b) for 7h. Cystatin C constructs were detected using either anti-FLAG or anti-cystatin C antibodies and shown in green. Anti-calreticulin and anti-GM130 antibodies, which fluoresces red, were used to visualize Endoplasmic Reticulum and Golgi apparatus, respectively. The blue fluorescent DAPI was used to stain nuclei. For each field of cells imaged, green and red fluorescence were recorded as separate images and then merged, along with the blue signal, for assessing the overlap of the respective signals. Scale bars are 20 µM.

3.5.2. Wild-type and variant B are processed through the secretory pathway with the same efficiency

Analysis of secretory trafficking undertaken by variant B cystatin C was further investigated by using the Glyco-Cys constructs, encoding for cystatin C encoding two N-linked glycosylation sites and a FLAG tag at the C-terminus, as described in materials and methods.

N-linked glycosylation site, consisting in the consensus amino acid sequence Asn-X-Ser/Thr, is a specific site that undergoes glycosylation in the lumen of the ER by the action of an oligosaccharyltransferase (OST), as described in section 1.5.1. The glycan attached to the protein can subsequently be modified in the Golgi apparatus through removal or addition of sugar residues (Stanley 2011). This post-translational modification is important for the correct folding and function of several eukaryotic proteins (Stanley 2011).

Addition of glycans on cystatin C, which normally does not undergo such modification in humans (Paraoan, Grierson 2007), may therefore affect its structure and activity. However, for the purpose of this study, it is only important that the trafficking is not affected. If so, then the addition of glycosylation sites allows the analysis of cystatin C trafficking because glycoslylation of the recombinant protein can be monitored. If the protein is translocated into the ER, it will be modified by addition of a sugar molecule. Should it then proceed to the Golgi apparatus, it is likely that the glycan structure will undergo further modification. Analysis of this glycosylation will therefore provide further evidence to determine whether wild-type and variant B are secreted through the ER-Golgi pathway.

a) Western blot analysis:

Protein expression of the Glyco-constructs was analysed by immunoblotting. Both cell lysate and media samples of D407 RPE cells were analysed 24h post-transfection. Analysis of the conditioned media was carried out to evaluate whether cystatin C proteins are still normally processed for secretion.

Immunoblots in figure 3.28 shows cell lysates (a) and media samples (b) from RPE transfected with wild-type or variant B Glyco-Cys constructs. Anti-cystatin C revealed two main bands at approximately 18KDa and 15KDa in both cell and media samples, likely corresponding to a glycosylated form and a non-glycosylated form, respectively, the latter suggesting incomplete glycosylation. The size of the fusion protein without glycosylation is indeed expected to be about 15KDa. This form is present in lower amount compared to the glycosylated one. At higher

exposures the endogenous cystatin C (13KDa) is also detected in both cell lysates and conditioned media.

These results indicate that the presence of two glycosylation sites and a FLAG tag at the C-terminal of cystatin C does not prevent the protein to be secreted. Moreover, the event of N-linked glycosylation seems to occur similarly for both wild-type and variant B, consistent with both entering the secretory pathway.

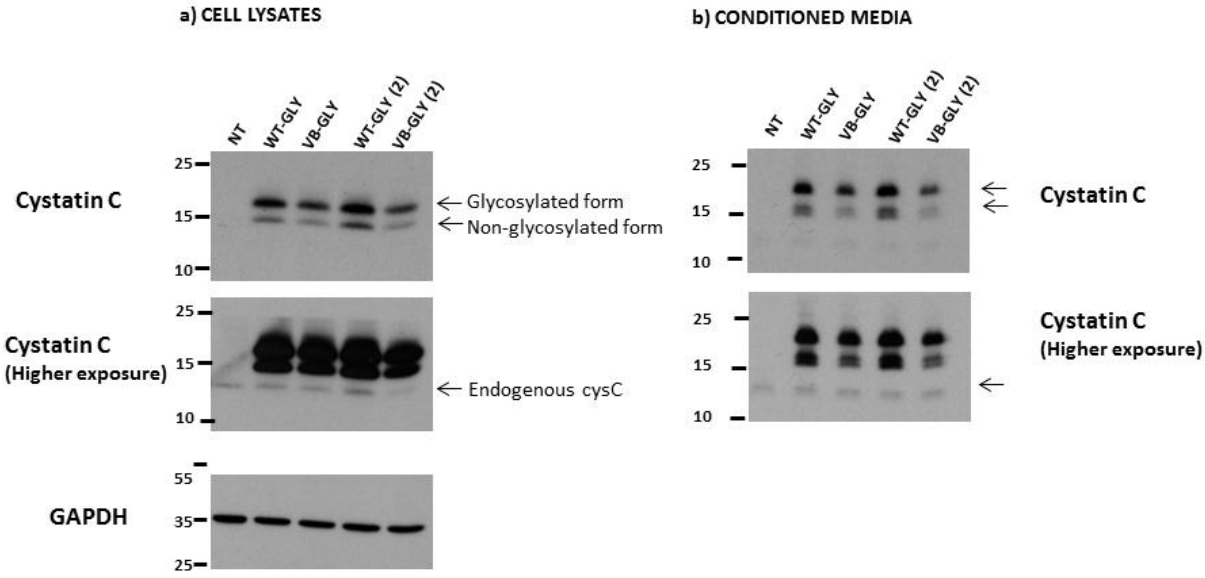

Figure 3.28 - Immunodetection of cystatin C in cell lysates and conditioned media of D4O7 cells transfected with Glyco-cysC constructs. Cell lysate (a) and conditioned media (b) samples collected from RPE cells transfected with either wild-type or variant B constructs were analysed by immunoblotting with anti-cystatin C antibody, shown at two different exposure times. Three bands were detected at approximately 18, 15 and 13KDa and corresponding to glycosylated cystatin C, non-glycosylated cystatin C and endogenous cystatin C, respectively. Anti-GAPDH antibody was used as loading control for cell lysates. Two independent samples were loaded for each construct.

b) Immunofluorescence analysis

RPE cells transfected with Glyco-constructs were also imaged by IF/ICC using anti-FLAG antibodies to analyse the distribution of recombinant cystatin C, which appears not to be affected by its linkage, as shown in Figure 3.29.

a) WT-GLYCO **b) VB-GLYCO**

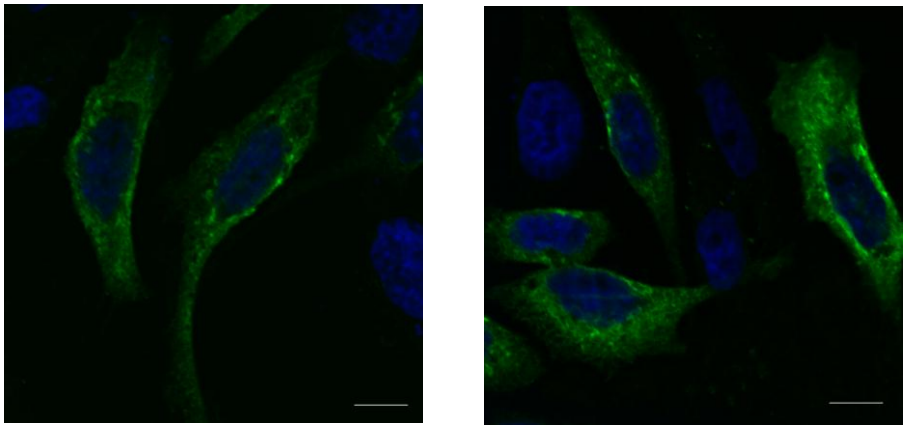

Figure 3.29 - Localization of Glyco-cystatin C constructs in D4O7 cell. Cultured human D4O7 cells expressing wild-type (a) or variant B (b) cystatin C linked to two N-linked glycosylation sites and a FLAG were PFA-fixed and immunostained 24h post-transfection. Cystatin C fusion proteins were detected using anti-FLAG antibody, shown in green. The blue fluorescent DAPI was used to stain nuclei. Scale bars are 10 µM.

c) Deglycosylation experiments

To investigate whether the bands detected actually correspond to the glycosylated and non-glycosylated forms of the protein, cell lysates and media samples were subjected to deglycosylation with either Endoglycosydase H or PNGaseF enzymes. EndoH is able to remove the glycan added in the ER lumen prior to any further modification in the Golgi. PNGase F can remove any sugar molecules prior or after modification in the Golgi apparatus (Maley et al. 1989).

As shown in figure 3.30 (a), treatment of cell lysates with EndoH resulted in a decrease of the 18KDa band and a simultaneous increase of the 15KDa band, thus indicating, as hypothesized, that the larger band represents the glycosylated form and the smaller one the non-glycosylated. At higher exposures it was still possible to detect a fraction of glycosylated cystatin C.

PNGaseF treatment also determines the removal of the glycosylated band and increase of the 15KDa protein. In this case the 18KDa band disappeared completely after treatment. This likely indicates that EndoH removes only the glycan added in the ER and not yet modified in the Golgi, unlike the PNGase F, which removes any sugar molecules from cystatin C. This is therefore consistent with the protein

moving through both the ER and Golgi apparatus, confirming cystatin C trafficking along the canonical secretory pathway.

Analysis in the conditioned media (figure 3.30. b) confirms this, as EndoH was no longer able to act on the glycosylated form, unlike PNGaseF, which completely converted the 18KDa band into the 15kDA species. This is consistent with the secreted protein, after going through the Golgi apparatus, having acquired a mature glycan structure which is no longer a substrate for the EndoH enzyme.

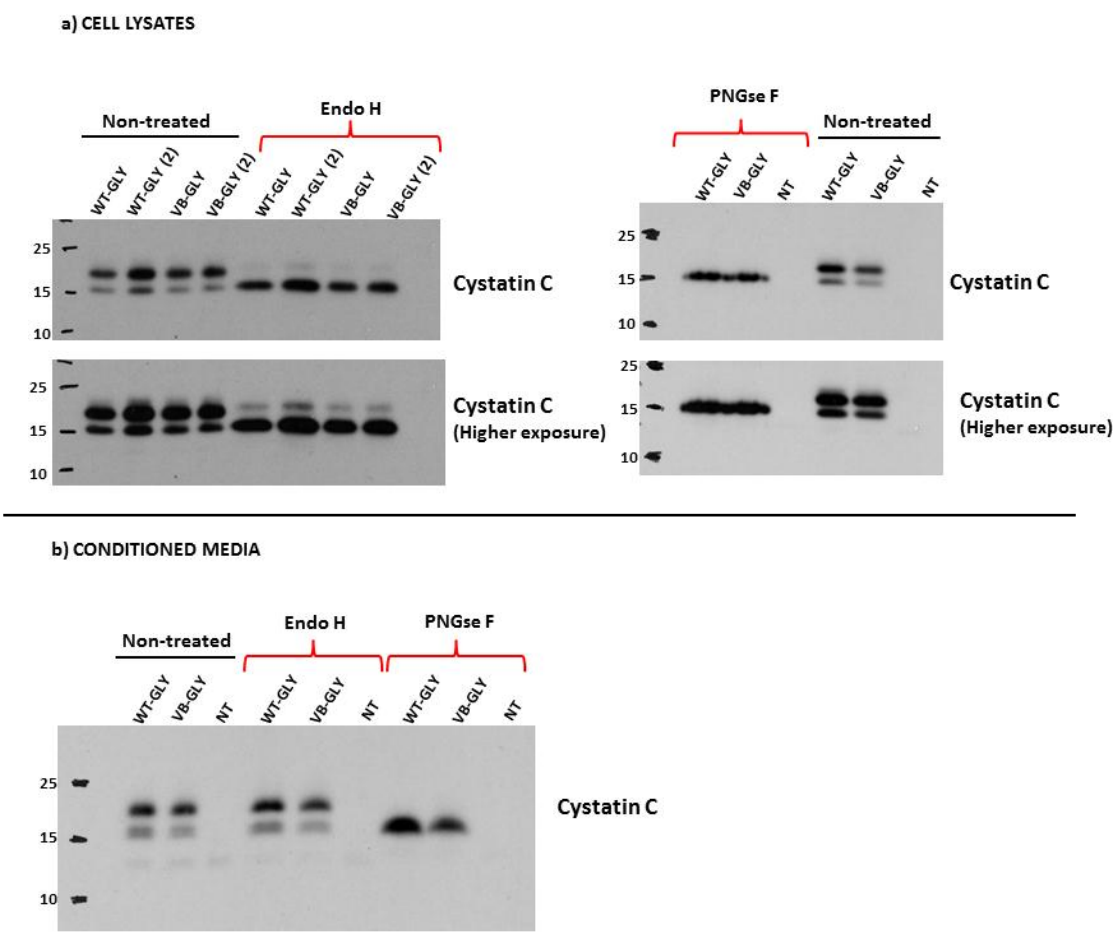

Figure 3.30 - Immunodetection of cystatin C in cell lysates and conditioned media of D4O7 cells transfected with Glyco-cysC constructs and subjected to deglycosylation treatment. Cell lysate (a) and conditioned media (b) samples collected from RPE cells transfected with either wild-type or variant B constructs were subjected to deglycosylation with either EndoH or PNGaseF and subsequently analysed by immunoblotting with anti-cystatin C antibody. Two bands were detected at approximately 18 and 15KDa and corresponding to glycosylated and non-glycosylated form of cystatin C.

d) Inhibition of secretion

Since the 15kDa form that is not glycosylated is still secreted into the culture media, inhibition of secretion with either BFA, Monensin or Nocodazole was performed to verify whether it also goes through the ER-Golgi secretory pathway. After treatment for 3h with any of these compounds, conditioned media from WT- or VB-Glyco transfected cells were analysed (figure 3.31). A reduction of both glycosylated and non-glycosylated forms occurs, thus indicating that both forms follow the ER-Golgi secretory pathway and involvement of a non-classical secretory pathway for the 15kDa fraction can be excluded.

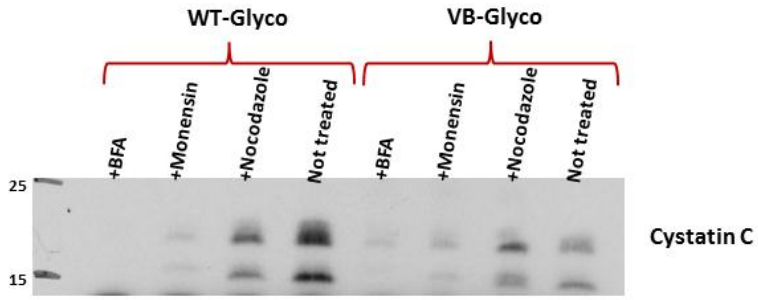

Figure 3.31 - Immunodetection of cystatin C in conditioned media of D4O7 cells transfected with Glyco-cysC constructs and subjected to inhibition of secretion. Conditioned media collected from RPE cells transfected with either wild-type or variant B constructs and treated with either BFA (5 µg/mL), Monensin (5 µM) or Nocodazole (10 µg/mL) for 3h, was probed with anti-cystatin C antibody. Two bands were detected at approximately 18 and 15KDa and corresponding to glycosylated and non-glycosylated form of cystatin C.

Overall, the results obtained in this section further support the notion that both wild-type and variant proteins pass similarly through the conventional ER/Golgi secretory pathway.

3.6. Analysis of targeting properties of the cystatin C signal sequence

Since the A25T mutation occurs in the leader sequence, it has been proposed that the mutation affects the targeting of cystatin C into the secretory pathway.

However, our results so far indicate that the variant B is still properly targeted for secretion; no differences in localization, trafficking and secretion were observed. To further investigate whether the mutation affects the ER targeting properties of the signal sequence, constructs encoding the leader peptide from wild-type or variant B cystatin C linked to EGFP were made and expressed in RPE cells and the distribution and secretion conferred to EGFP was then analysed.

3.6.1. Both wild-type and variant B leader sequences are functional in targeting the EGFP to the secretory pathway

Protein distribution of the leader peptide constructs was analysed in living ARPE19 cells. Figure 3.32 shows representative images obtained by fluorescence microscopy of ARPE19 cells transfected with wild-type or variant Leader constructs or EGFP alone (a, b and c, respectively). In order to evaluate whether EGFP is targeted to the ER/Golgi pathway, the Golgi complex was also stained with the specific dye BODIPY.

As shown in figure 3.32 (a) and (b), an ER/Golgi localization of EGFP, indicated by colocalization with BODIPY, was found in ARPE19 cells for both wild-type and variant leader peptide constructs. However, a significant fraction of cells also showed a diffuse distribution in cytosol and nuclei for both wild-type and variant B leader constructs, similar to the distribution of the EGFP on its own (c).

The presence of EGFP in the ER/Golgi secretory pathway suggests that the wild-type and mutated leader peptides are still able to target the proteins linked to it for secretion. On the other hand the diffuse distribution observed for both constructs indicates that in a fraction of cells EGFP is not properly targeted. Quantification of cells showing either an ER/Golgi distribution or a diffuse distribution for both wild-type or mutated leader peptide constructs is shown in figure 3.33. Results show that 45% and 46% of ARPE19 cells were found to display the diffuse distribution for the LPWT-EGFP and LPVB-EGFP proteins respectively, with no significant difference between the two constructs. Percentages were calculated by considering the total number of cells obtained combining all the individual experiments (Figure 3.33).

Analysis of diffuse distribution at the level of the individual replicates results in 42%±12 and 44%±13 (Mean±SD, N=7) for wild-type and variant B Leader constructs, respectively.

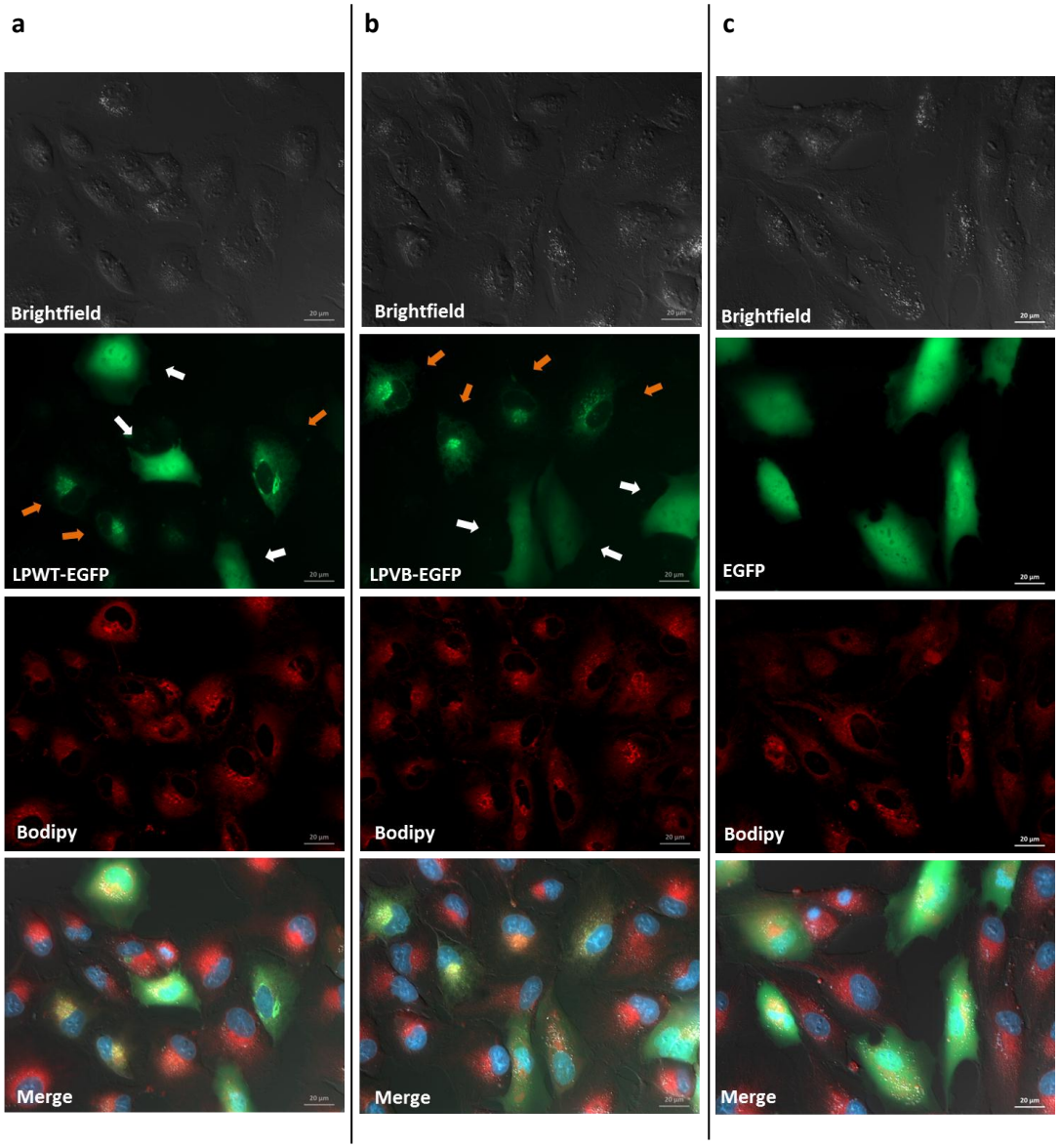

Figure 3.32 - Localization of cystatin C leader sequence constructs. Living cultured human ARPE19 cells expressing the leader peptide from wild-type (LPWT-EGP) or variant B (LPVB-EGFP) cystatin C linked to EGFP (a and b respectively) and EGFP on its own (c) were imaged 24 h post-transfection. The emission specific for eGFP constructs is shown in green. Bodipy, which fluoresces in red, was used to visualize Golgi complex. The blue fluorescent Hoechst 33342 probe was used to stain nuclei. For each field of cells imaged, green and red fluorescence were recorded as separate images and then merged, along with the blue signal and brightfield, for assessing the overlap of the respective signals.

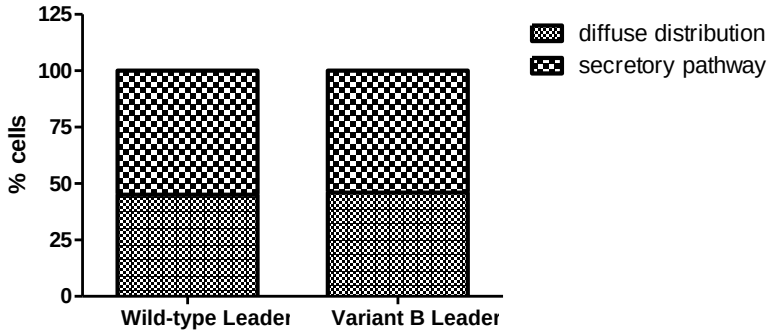

Figure 3.33 - Quantification of Leader sequence constructs distribution in live transfected ARPE19 cells. ARPE19 cells transfected with either wild-type or variant B leader peptide constructs were quantified to compare secretory pathway distribution and diffuse distribution of EGFP. Percentages are calculated by considering the total number of cells obtained combining all the individual experiments. The fraction of cells showing diffuse distribution results 45% and 46% for the WT and VB Leader constructs respectively.
No difference in distribution was found between LPWT and LPVB. Chi-square test (χ^2 =0.20), *p*-value=0.65.

3.6.2. Wild-type and variant B leader peptides direct EGFP similarly for secretion

Secretion of EGFP linked to wild-type or variant B leader peptide was also analysed to further investigate whether the signal sequence targets proteins for secretion and whether there is a difference between the two constructs.

Culture media and respective cell lysates from ARPE 19 cells transfected with wild-type or variant B leader construct, EGFP on its own and from non-transfected cells were subjected to SDS-PAGE electrophoresis and probed with an anti-EGFP antibody (figure 3.34 a). A band of 27KDa corresponding to EGFP protein was detected in both cell and media samples for both LPWT and LPVB transfected cells. Anti-cystatin C and anti-GAPDH antibodies were used as loading controls.

The bands detected for both the leader peptide constructs show the same electrophoretic mobility as EGFP alone, indicating that the proteins entered the ER, where the signal sequence was cleaved. The presence of EGFP fusion proteins in the conditioned media further indicates that the proteins are secreted, thus confirming the imaging results. In contrast, EGFP on its own was present only in the intracellular fraction and, as expected, was not secreted.

The fraction of secreted EGFP fusion proteins from both LPWT and LPVB transfected cells was assessed by calculating the total protein secreted and normalising this value to the total fusion protein, combining the total secreted with the total cell associated, as described previously for the full-length cystatin C constructs. Results shown as percentages are plotted in figure 3.34 b. No significant differences were observed in the level of secretion of EGFP fusion proteins between the wild-type and variant B leader constructs.

a)

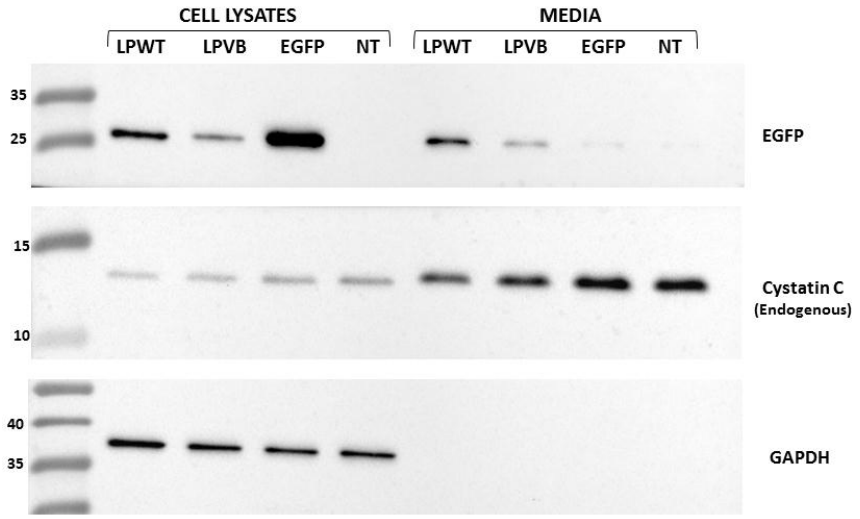

b)

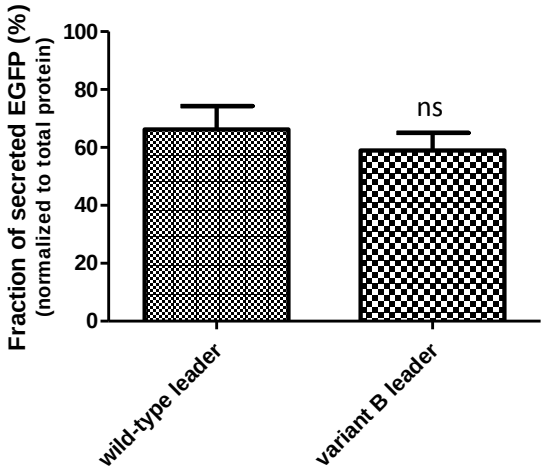

Figure 3.34 - Analysis of secretion of wild-type or variant B Leader Sequence constructs in ARPE19. (a) Immunoblot of cell lysates and conditioned media collected from cells expressing respectively wild-type and variant B Leader peptide-EGFP constructs, only EGFP and untransfected cells not expressing any of these proteins. Western blots were probed

with anti-EGFP antibody, which detected the LP-EGFP proteins and EGFP on its own, both consisting of a band of approximately 27KDa. Anti-cystatin C and anti-GAPDH antibodies were used as loading control for media and cell lysates, respectively. The amount of cell lysate loaded was 4X more than the media (cell lysate 8µL/250 µL, media 20µL/2.5mL). b) Level of secreted EGFP in the conditioned medium of cells transfected with wild-type or mutant leader constructs were evaluated by densitometry of western blots and the total secreted protein was calculated and normalized to the total EGFP protein (total intracellular + total secreted). Using anti-EGFP antibody the fractions of secreted proteins result to be 0.66 ± 0.08 (SD) for wild-type and 0.59 ± 0.06 (SD) for variant B. *Unpaired t test (N=8) two-tailed*, p=0.06. Results are presented as percentages. ns=non-significant.

Overall, imaging and secretion analyses show that both wild-type and variant B signal sequences of cystatin C when fused to EGFP direct EGFP similarly to the secretory pathway, in contrast to the leaderless EGFP. This indicates that the mutated leader peptide has a similar capacity to target proteins to the ER, and subsequently for secretion, as the wild-type leader sequence.

3.7. Discussion

Cystatin C targeting and trafficking were previously reported to be impaired in the case of the variant B. In particular a mislocalization in the mitochondria (Paraoan et al. 2004) and a decreased secretion were found to characterise this mutated form of cystatin C (Benussi et al. 2003, Paraoan et al. 2004). However, another study, published while my work was in progress, reported no difference in trafficking and secretion (Nguyen, Hulleman 2016), and even the association of variant B with AMD and AD diseases remains controversial.

This study therefore aimed to further investigate whether or not the A25T mutation in the precursor cystatin C variant B affects its intracellular trafficking, which might explain its possible link to disease.

Results obtained in this study revealed no difference in protein localization, trafficking and secretion between wild-type and variant B proteins. However, contrasting results depending on the construct used were observed. By using constructs encoding cystatin C tagged to small FLAG or HA tags, or untagged, both wild-type and variant B proteins localize in the ER/Golgi complex and no mitochondrial localization was observed for any of these constructs. Accordingly, no intracellular accumulation and normal levels of secretion were observed with these constructs.

On the contrary, using EGFP-tagged cystatin C constructs, both wild-type and variant B proteins resulted in partial mitochondrial localization in a significant fraction of cells. Analysis of subcellular fractions also indicates that this abnormal mitochondrial association occurs with both EGFP-tagged proteins, as they appear to be present in the mitochondria/Golgi fraction in similar amount. Consistently, they were both observed to be partially retained intracellularly and, as a result, a smaller fraction of the total synthesised EGFP-linked wild-type and variant B proteins is secreted as compared to the FLAG-, HA- tagged or untagged proteins as well as the endogenous cystatin C. Taken together, these results indicates an impairment in the trafficking of the EGFP-tagged constructs, resulting in

intracellular mislocalization and consequent reduction in the levels of secreted cystatin C, for both wild-type and variant B proteins. In living cells, the Chi-square test also reported a significant difference between them, i.e. the unusual localization occurs with a higher frequency for the wild-type cystatin C. However, looking at the individual experiments, this frequency seems to vary considerably, suggesting that the extent of mitochondrial association is subject to considerable experimental variation and hence, likely not biologically significant. Moreover, this difference was not found to be significant when analyzed by IF analysis. Furthermore, since untagged cystatin C and constructs with a small tag were never found in mitochondria, the main conclusion from these results is that EGFP appears to mediate the mitochondrial mislocalization of cystatin C, either wild-type or mutated, in a significant fraction of cells.

In the analysis of subcellular fractionation, it was not possible to obtain pure mitochondria fraction because of both technical and biological limitations. Mitochondria are indeed in contact with other organelles, such as ER (Kornmann et al. 2009, Phillips, Voeltz 2015), hindering their isolation from these other cellular compartments and meaning that both DC and MACS methods only permitted an enrichment of mitochondria. Therefore, because of these limitations and the consequent significant organelle cross-contamination, it was not possible to properly quantify the protein levels in each fraction. However, to further minimize the possibility that the presence of either wild-type and variant B proteins in the mitochondrial fraction was not simply due to organelles cross-contamination, their distribution was compared to that of endogenous cystatin C, which was mainly present in the ER/cytosolic fraction, thus indicating the EGFP-linked cystatin C constructs behave differently from the endogenous protein. This difference suggests that the cystatin C fusion proteins either accumulate in the Golgi apparatus, or are actually present in the mitochondria. In both cases, however, the results indicate that trafficking of both wild-type and variant proteins is influenced by the presence of EGFP tag. Taking into account the results obtained by imaging, however, it is likely that proteins are present in this fraction as a result of their mislocalization in the mitochondria, as opposed to being retained in the Golgi

complex. Furthermore, the notable reduction in their level of protein secretion is also consistent with the larger intracellular pool of the EGFP-constructs.

The fact that the protein accumulates intracellularly could consequently determine the uncommon mitochondria association. Alternatively, the improper mitochondrial targeting itself may be the reason of the intracellular retention and impaired secretion observed for both wild-type and variant B proteins linked to EGFP (as discussed later in this section).

Conversely, results obtained using the constructs untagged or carrying a short FLAG or HA tag, showed that these cystatin C constructs do not mislocalize intracellularly and are efficiently secreted from RPE cells, similarly to the endogenous protein. Thus, unlike the EGFP-tagged constructs, neither their overexpression nor the presence of the tag seem to affect trafficking of these constructs, showing their suitability for these studies.

Specifically regarding the variant B cystatin C, the results obtained with short tagged or untagged constructs showed that, in contrast with a previous report (Paraoan et al. 2004), the variant B is not retained intracellularly, is still targeted to the secretory pathway and does not differ in its level of secretion compared to the wild-type protein. An exception to this was the untagged cystatin C constructs in D4O7 cells, where a small but statistically significant difference was observed in the protein secretion. Whether this reflects the particular cell type is unclear, but probably lacks biological significance.

The correct targeting of the variant B cystatin C to the secretory pathway is further confirmed by the results obtained by suppression of the conventional secretory pathway and by monitoring the N-glycosylation of the Cys-Glyco proteins. With these experiments, the presence of cystatin C in both ER and Golgi apparatus, before being secreted, was specifically demonstrated. This also excludes the possibility of major contributions of alternative secretory pathways for the release of the variant B.

Moreover, the N-linked glycosylation event appeared not to differ between wild-type and variant B proteins, indicating that their maturation occurred similarly in acquiring glycosylation in the ER and subsequent modification in the Golgi apparatus. Besides confirming the intracellular trafficking, this also suggests that wild-type and variant B proteins are targeted to the secretory pathway with similar efficiencies. In this analysis an additional 15kDa species was also detected, present at lower amount compared to the glycosylated protein, and likely representing the non-glycosylated protein. However, this fraction was also observed to pass through the ER and Golgi apparatus before being secreted, thus excluding again a major involvement of an alternative pathway also for this fraction. The presence of this non-glycosylated form in the secreted pool, observed for both wild-type and variant, may reflect partial inaccessibility of the glycosylation site during biosynthesis, or saturation of the glycosylation machinery due to the overexpression of the recombinant proteins (as suggested by a number of groups (Massotte 2003, Dalton, Barton 2014, Cottet, Corthésy 1997)), or a combination of both. In any case, these results confirm that both the wild-type and variant B proteins follow similarly the conventional secretory pathway, excluding the possibility that the variant B undertakes a different secretory pathway or mislocalizes to a different intracellular compartment. This further supports our finding that the variant B is not mistargeted to mitochondria.

Finally, the similar ER/Golgi distribution and secretion of EGFP proteins, determined by the wild-type and variant B leader peptides, indicates that the mutated signal sequence is still functional in targeting the protein to the secretory pathway, with similar efficiency. No mitochondria association was observed for these constructs. However, not all the cells displayed the proper targeting of the protein, showing a distribution comparable to that of unmodified EGFP, i.e. diffused throughout the cytosol and nuclei, in a fraction of the cells. This occurs similarly for the wt and variant leader, suggesting that the signal sequence is not 100% efficient in targeting EGFP for secretion (discussed below). No significant difference was also observed in the level of secretion of EGFP between the wild-

type and variant B leader constructs. Because of the mistrafficking observed in a large fraction of cells, these constructs are probably unsuitable for a proper quantification of the secreted fractions.

The main reason why the trafficking of the leader sequence constructs was analysed was to characterise the role of the A25T mutation within the signal sequence, to determine whether the leader peptide alone is sufficient to affect the trafficking/processing of the protein linked to it. Despite the limitations of these constructs due to the mislocalization observed, results obtained suggest that the variant B leader constructs did not lose its targeting properties and the signal sequence alone was not sufficient to determine any significant change that may explain cystatin C variant B association with diseases. Therefore, the consequences of the A25T mutation, if present, must involve the entire cystatin C protein.

Overall, these results show that the EGFP tag affects the trafficking of cystatin C, independently of whether it is fused to the wild-type or variant form of the protein. Other constructs with short tags were distributed and secreted in RPE cells in a manner similar to untagged overexpressed or the endogenous cystatin C.

Mislocalization in the mitochondria was previously reported by Paraoan et al. (Paraoan et al. 2004). That study used EGFP-linked cystatin C constructs. Because the current study does not demonstrate similar findings when cystatin C is untagged or linked to a different smaller tag, it seems likely that mitochondria association of cysC is actually an artefact caused by the EGFP tag and that variant B does not actually show any difference in its intracellular pathway compared to the wild-type.

It is noteworthy that a partial mistrafficking occurs for both the EGFP-linked constructs, either fused to the full-length cystatin C or only to the signal sequence, although being different for each constructs, i.e. mainly associated with mitochondria and diffused throughout the cell, respectively. This strongly indicates that in both cases, proteins are not properly targeted to the secretory pathway.

Protein labelling with a fluorescent tag has been shown to influence folding, function and localization of the host protein, especially in case of small proteins (Tsien 1998). In particular, other cases of protein mislocalization due to fluorescent proteins have also been reported, most commonly in nuclei and cytoplasm (Zhu et al. 2013, Seibel et al. 2007).

The green fluorescent protein (GFP) and other fluorescent tags, such as EGFP or YFP, are widely used in real-time imaging to determine the subcellular localization of proteins in living cells, thus representing one of the most valuable tools in cell biology. However, several disadvantages and limitations need to be considered (Tsien 1998, Giepmans et al. 2006, Miyawaki, Sawano & Kogure 2003, Zhang et al. 2002, Andresen, Schmitz-Salue & Jakobs 2004).

One main limitation is that all the currently used fluorescent proteins are relatively large in size, being all approximately 25-30kDa. Therefore the tag is often similar in size or larger than the protein fused to it. This could potentially interfere with the folding of the host protein, affect its stability and consequently its abundance (Arluison, Taghbalout 2015). An increased protein degradation has been for example observed for some fusion proteins (Lisenbee, Karnik & Trelease 2003). Furthermore, change in the protein folding can also alter the function of the protein as well as its targeting/trafficking (Andresen, Schmitz-Salue & Jakobs 2004). It is therefore important to confirm that the recombinant protein maintains the normal function and localization of the host protein, in order to avoid misinterpretations due to artefactual results. Fusion to a fluorescent protein was indeed shown not to be always successful (Tsien 1998), even though only few cases are reported in literature, probably due to the fact that the unsuccessful fusions are unlikely to be published.

In certain cases, the use of small tags with less steric bulk is therefore recommended as they are less likely to interfere with the localization or function of the proteins (Andresen, Schmitz-Salue & Jakobs 2004, Arluison, Taghbalout 2015), thus in contrast to the large fluorescent labels. Examples are the FLAG and HA tags, which consist of only 8 and 9 amino acids respectively (~1kDa). Their disadvantage is the lack of fluorescence and for this reason they cannot be used in live cell

imaging. Nevertheless, in our study both tags were found to not affect cystatin C trafficking since the respective recombinant proteins, either wild-type or variant, followed the ER-Golgi secretory pathway, in the same way as the untagged cysC constructs.

Few examples of abnormal cellular localization due to the linkage of proteins with fluorescent tags have been reported. A YFP-labelled small protein has been shown to mislocalize in Escherichia coli probably due to misfolding or aggregation of the fusion proteins (Arluison, Taghbalout 2015). Interestingly, labelling the same protein of interest with other large fluorescent tags caused the same aberrant localization. In contrast, when the protein was fused to a short tag, such as FLAG or HA, it resulted to be normally localised. These results indicate that only large tags interfered with the targeting of the host protein, causing artefactual localization. This is a similar difference as observed in our study.

Other cases of mislocalization of the fusion protein have been described. For instance, the use of EGFP tags has been reported not to be particularly appropriate to study nuclear import of small proteins (Zhu et al. 2013, Seibel et al. 2007). EGFP alone normally diffuses throughout the cytosol as well as into the nucleus by passive diffusion through the nuclear pores due to its relatively small size. However, when in fusion to a protein particularly small in size, the resulting recombinant protein might still passively translocate to the nucleus, thus generating misleading results (Zhu et al. 2013). This may explain why in our study the leader constructs are partially distributed in the nucleus as well as a fraction of the EGFP-cystatin C constructs, as reported by Paraoan et al. (Paraoan et al. 2004), considering the low molecular weight of cystatin C.

Distribution of EGFP in form of monomers and tetramers has been also reported. Interestingly the monomers were found to be mainly concentrated in the nucleus, while the oligomers were located especially in the cytosol (Seibel et al. 2007). This results suggest that the size of the protein plays an important role in the protein trafficking and might explain in our study why the leader constructs localize in the

nucleus while the full-length cystatin C constructs, which have a larger molecular weight compared to the leader constructs, tend mainly to localize and accumulate in the cytosol. This intra-cytoplasmic accumulation may consequently lead to a mitochondria association, as described below.

Mistargeting to other cellular compartments, including mitochondria, has also been reported due to the GFP tag (Lisenbee, Karnik & Trelease 2003, Bejarano, Gonzalez 1999, González, Bejarano 2000). Several reasons of such mistrafficking have been suggested. It might occur because of unspecific interactions with proteins located in different organelles, or it may be due to protein aggregation, or to the activation of cryptic targeting signals. In particular, the cryptic signals consist of potential targeting signal sequences. They are normally inactive because located within the folded protein and therefore not accessible, or because a dominant signal sequence is present, which leads the protein to a different cellular organelle. However, the fusion with a tag protein can cause activation of these signals as a consequence of a change in the protein conformation, which will therefore expose such signal sequences (González, Bejarano 2000). For example, these silent signals have been identified as short open reading frame (ORF), found at very high abundance in the genomic DNA of Drosophila by analysing distribution of random genomic DNA sequences fused to GFP in transfected human cells. Interestingly, 15% of the clones generated showed localization of these fusion proteins in the mitochondria, even though they were not mitochondrial proteins (Bejarano, Gonzalez 1999), thus indicating a frequent presence of cryptic signals for mitochondrial targeting. This might explain the mislocalization of cystatin C, whose folding is likely affected by the large EGFP tag protein linked to it, and as a consequence it may expose a cryptic signal sequence for mitochondrial targeting.

In addition to the size of the fluorescent proteins, there are other limitations that can also interfere with the intrinsic properties of the host protein, causing its abnormal localization. One of them consists in the tendency of large fluorescent proteins to form dimers/oligomers. Formation of protein aggregates can consequently alter the protein function as well as the protein localization (Miyawaki, Sawano & Kogure 2003, Lisenbee, Karnik & Trelease 2003).

Another main disadvantage is the overexpression of the fusion protein, which can determine accumulation of the protein in one of the cellular compartment prior to its final target organelle or can completely alter the protein localization (Arluison, Taghbalout 2015, Bejarano, Gonzalez 1999). This may also be one of the reasons for the improper accumulation in the mitochondria/Golgi fraction observed for the cysC-EGFP constructs during the fractionation analysis. In addition, overexpression can also lead to accumulation of unfolded proteins, when the protein folding machinery is overwhelmed, and to generation of aggregates (Bejarano, Gonzalez 1999). Indeed, proteins are more inclined to undergo dimerization/oligomerization when present at high concentrations. This propensity of overexpressed GFP fusion proteins to form dimers might consequently also lead to organelle aggregation, thus causing aberrant protein localization (Lisenbee, Karnik & Trelease 2003). This situation can be consistent with the high level of fusion proteins that occurs intracellularly for the EGFP-cystatin C proteins in our investigation. For instance, one study has shown that cells overexpressing a GFP-fusion protein, which is normally targeted to peroxisomes, contained aggregated peroxisomes, mitochondria and plastids. Interestingly, proteins were normally distributed in peroxisomes after 5h post-transfection and somehow were mislocalized to mitochondria and plastids only when highly overexpressed for 20-24h (Lisenbee, Karnik & Trelease 2003), suggesting that the mitochondrial compartment is a common target for overexpressed proteins.

Overall, this suggests that, in the case of cystatin C, EGFP is not a suitable tag for studying the intracellular localization and trafficking of the protein. Because of the size of EGFP, which is twice bigger than that of cystatin C, it is likely to interfere with its folding/targeting. As a consequence the fusion protein is not properly directed to the secretory pathway and, conversely, tends to accumulate intracellularly. Regarding the unusual mitochondrial localization, the accumulated overexpressed fusion proteins in the cytoplasm and/or the presence of cryptic signal sequences might consequently determine such artefactual localization.

Regarding the leader constructs, in addition to the role of EGFP that can itself determine their impaired distribution, another reason could be the fact that the signal sequence in study is specific for cystatin C, and is not made to target EGFP or any other proteins. Indeed, all the secretory proteins possess unique signal sequences, which share similar physical-chemical properties but differ in the amino acid sequences (as described in section 1.5.1). Therefore it is likely that the leader peptide, which is very efficient to target cystatin C, is simply less efficient for the EGFP protein. That may also explain why they partially diffuse throughout the cytosol and nuclei as normally occurs for EGFP on its own. These constructs can therefore be used to confirm the targeting properties of the signal peptide but, like the cysC-EGFP constructs, they are not probably suitable to properly quantify protein secretion and analyse its intracellular localization.

On the other hand, results obtained by using the more suitable untagged and FLAG- or HA-tagged cystatin C constructs indicate that trafficking and localization of cystatin C variant B is not affected by the A25T mutation. Both wild-type and variant are normally distributed in the ER/Golgi, they follow the conventional secretory pathway and they are efficiently secreted by RPE cells, comparable to endogenous cystatin C. Protein mistargeting appears therefore not to be one of the consequences caused by the variant B polymorphism, thus excluding a protein mislocalization as a possible cause of an increased risk of developing AMD or AD diseases.

Moreover, in our analysis the level of secretion seems not to be affected in the case of cystatin C haplotype B. Our findings therefore contrast with earlier reports (Paraoan et al. 2004, Benussi et al. 2003), which indicated a decrease in secretion in the case of the variant B, but are in agreement with another study (Nguyen, Hulleman 2016), where also no difference was observed. *In vivo* studies have also reported decreased levels of cystatin C in CSF or plasma in presence of the variant B in several pathological conditions (Noto et al. 2005, Maetzler et al. 2010, Yamamoto-Watanabe et al. 2010, Åkerblom et al. 2014). However, Chuo et. al,

although reporting association of the variant B specifically with AD, showed no difference in its plasma level compared to wild-type cystatin C (Chuo et al. 2007).

It is important to consider that the experimental conditions used in our study might influence the outcome and that the possible effect on secretion may not be detectable under certain circumstances. For example, the cellular systems used in this study consisted of immortalized cell cultures, which are transiently transfected and characterized by overexpression of the protein in study. The experiments carried out by Benussi et al (2003) used human primary fibroblasts cultures carrying the wild-type or variant B genotype. However, similar to this study, transiently transfected primary or immortalized cell lines, characterised by overexpression of the protein of interest, were also used in other studies (Paraoan et al. 2004, Nguyen, Hulleman 2016). Interestingly, these two groups have reported contrasting findings, showing (Paraoan et al. 2004) or not (Nguyen, Hulleman 2016) a difference in the secretion between wild-type and variant B. It is noteworthy that in the first case only an EGFP-tagged cystatin C construct was used, which has been also observed to localize into mitochondria, and, in the second case, like in my work, different tagged and untagged constructs were used.

Moreover, since exogenous proteins are analysed in our system, another factor that could influence the results is the time of the analysis that in our investigation was performed 24-hours post-transfection. It is possible, for example, that the difference in secretion is too small to be detectable after only 24-hours and may accumulate over time and become significant only after a longer period. If this is the case, such a time-dependent cumulative effect could be consistent with the contribution of variant B to age-related diseases, such AMD and AD, where its contribution would occur progressively with ageing.

As suggested in earlier reports, a decreased efficiency in one of the steps of protein maturation may occur in the case of the variant B, such as the signal sequence interaction with the SRP, the protein translocation across the ER membrane or the signal sequence cleavage by the SPC. Therefore, in the case of a subtle reduction in the efficiency of protein processing, it might be possible to affect the level of secretion only over a long period of time, which may not be detected at 24-hours.

Moreover, should this be the case, over-expression of transfected proteins is also probably not appropriate to evaluate small differences in protein secretion.

To further investigate whether there is any change in the efficiency of the protein maturation, the signal sequence cleavage was analysed in the next chapter.

Chapter 4 - Analysis of signal sequence cleavage and fate of the variant B precursor protein

4.1. Introduction

Cystatin C variant B is characterized by a point mutation in its signal peptide, an Ala to Thr substitution at the -2 position, which alters the hydrophobic properties of the sequence and, in particular, of its C-terminal region. The hydrophobicity profile of the signal peptide is known to be essential for its functionality as well as the integrity of the C-terminal-region (Nilsson et al. 2015, Auclair, Bhanu & Kendall 2012), as described in section 1.5.1. This mutation might therefore affect one of the steps essential for the precursor protein processing, such as the signal-recognition process by SRP, the translocation across the ER membrane or the cleavage of the signal sequence itself, therefore preventing the correct maturation of the precursor protein. Moreover, since the mutation is present in the precursor protein, its effect is expected to be exerted at the maturation stage as once the signal sequence has been cleaved, the mature protein would not differ from the wild-type form of cystatin C.

Different hypotheses have been suggested in earlier reports. One study suggested that the A25T mutation prevents the precursor cystatin C undergoing efficient cleavage by the signal peptidase complex (SPC) (Paraoan et al. 2004). As a consequence, the resulting unprocessed fraction was proposed to divert from the ER pathway and accumulates intracellularly (Paraoan et al. 2004). Benussi et al. similarly suggested impairment in the protein maturation due to a reduced efficiency in the cleavage of the precursor protein, ultimately causing the lower levels of protein secretion reported in their study (Benussi et al. 2003). Alternatively, it has been suggested that the cleavage of the precursor protein still occurs but at a different location (Nguyen, Hulleman 2016, Nilsson et al. 2009). An additional cleavage site for cystatin C has been predicted and suggested to be utilized under certain circumstances, particularly in the case of the variant B (Nguyen, Hulleman 2016, Nilsson et al. 2009). This differently processed protein could possibly assume a different conformation and/or undergo different post-translational modifications, which in both cases may affect its function and/or stability.

The aim of the work presented in this chapter was to investigate whether the cleavage of the signal sequence is affected in the case of the precursor variant B. For this purpose the processing of the precursor was analysed biochemically by using N-terminal tagged precursor constructs to determine if the levels of precursor/mature proteins differs between wild-type and variant B. Immunofluorescence imaging was performed to analyse the fate of the signal sequence and, if not cleaved, determine the intracellular localization of the precursor proteins.

4.2. Analysis of uncleaved precursor cystatin C

The level of uncleaved precursor fraction was monitored by using N-terminal tagged cystatin C, with either FLAG or HA, and N- and C-terminal tagged constructs, described in the materials and methods, section (2.2). The addition of a tag at the N-terminal end of the leader peptide should readily allow the identification of the precursor form of cystatin C and comparison of wild-type and variant B protein levels by Western blotting and immunoprecipitation.

4.2.1. N-terminal tag does not affect cystatin C trafficking and levels of precursor fraction appear to be higher in the variant B cystatin C

Labelling cystatin C at the N-terminus of the signal sequence may potentially affect the processing/cleavage of the precursor protein. Therefore, correct maturation of the protein needed to be confirmed before proceeding with the analysis.

Cell lysates and cultured media from transfected D4O7 cells expressing the N-terminal cystatin C constructs were analysed by immunoblotting. Blots were probed with an anti-cystatin C antibody, which can detect mature and precursor forms, or with anti-FLAG or anti-HA antibodies that, depending on the construct used, allowed visualisation specifically of the unprocessed cystatin C.

For both the FLAG and HA N-terminal tagged constructs, the expected size of the precursor cystatin C is approximately 16.5 kDa (untagged cystatin C precursor of 15.5 kDa + tag of ~1 kDa), whereas for the mature form should be the same mass as wild-type cystatin C (13 kDa) since the tagged leader peptide is removed.

As expected, bands at 13kDa were detected in both the cell lysate and media samples (Figure 4.1.), indicating that the precursor cystatin C was properly processed in the ER. Moreover, the presence of the mature form in the conditioned media further confirmed that the constructs were normally targeted to the secretory pathway. This indicates that the FLAG or HA tags on the signal sequence do not affect the ER targeting, translocation and processing of the tagged cystatin C, thus establishing their suitability for studying cystatin C processing and trafficking.

Anti-cystatin C antibody also detected a band at around 16.5kDa, which corresponds to the precursor form of cystatin C. This band was better visible with increased exposure time. This was confirmed by using anti-FLAG or anti-HA antibodies, depending on the constructs used, (in figure 4.1. a and b, respectively), to detect the N-terminal tag on the signal sequence and which recognized a band at the same mass. This 16.5kDa band was not detected in the media, further indicating that it corresponds to the unprocessed precursor form of cystatin C. The use of N-terminal tagged constructs therefore permitted clear visualisation of the uncleaved fraction of cystatin C, allowing their levels to be compared between wild-type and variant B proteins. By using either FLAG or HA-tagged constructs, the levels of the immature uncleaved cystatin C were found to be noticeably higher for the variant B (in figure 4.1 a and b respectively). These levels have been qualitatively compared taken in consideration the levels of mature proteins for wild-type and variant B. GAPDH was also used as loading control. However, this difference observed by using anti-FLAG or anti-HA antibodies was less evident when comparing the level of the same precursor fractions visualized with the anti-cystatin C antibody, especially for the HA-CysC constructs (figure 4.1).

The immunoblots in figure 4.2 show the same analysis performed in D4O7 cells expressing the constructs tagged at both the N- and C-terminus with each combination of FLAG and HA tags. Again, both constructs are efficiently processed and secreted in the conditioned media, as previously observed for the other constructs. Antibody against the tag located at the C-terminal (HA in fig. 4.2 a, and FLAG in 4.2 b) allows detection of both the mature and precursor forms of cystatin C, whereas probing with the antibody against the tag at the N-terminus (FLAG in fig. 4.2 a, and HA in 4.2 b) permits visualization of only the unprocessed fraction. For each construct, the mass expected for mature and precursor proteins are approximately 14kDa and 17.5kDa, respectively. Evaluation of the level of non-mature cystatin C indicates, also with these constructs, a difference between wild-type and variant B, especially by probing with antibodies against the N-terminal tags, with a higher level of unprocessed protein in the case of the variant B.

In ARPE19 cells, bands representing the precursor proteins were not detected (data not shown). This is probably due to the lower protein expression in these cells, meaning that the sensitivity of the assay was not high enough to identify the precursor fraction, which is present at considerably lower levels than the mature one.

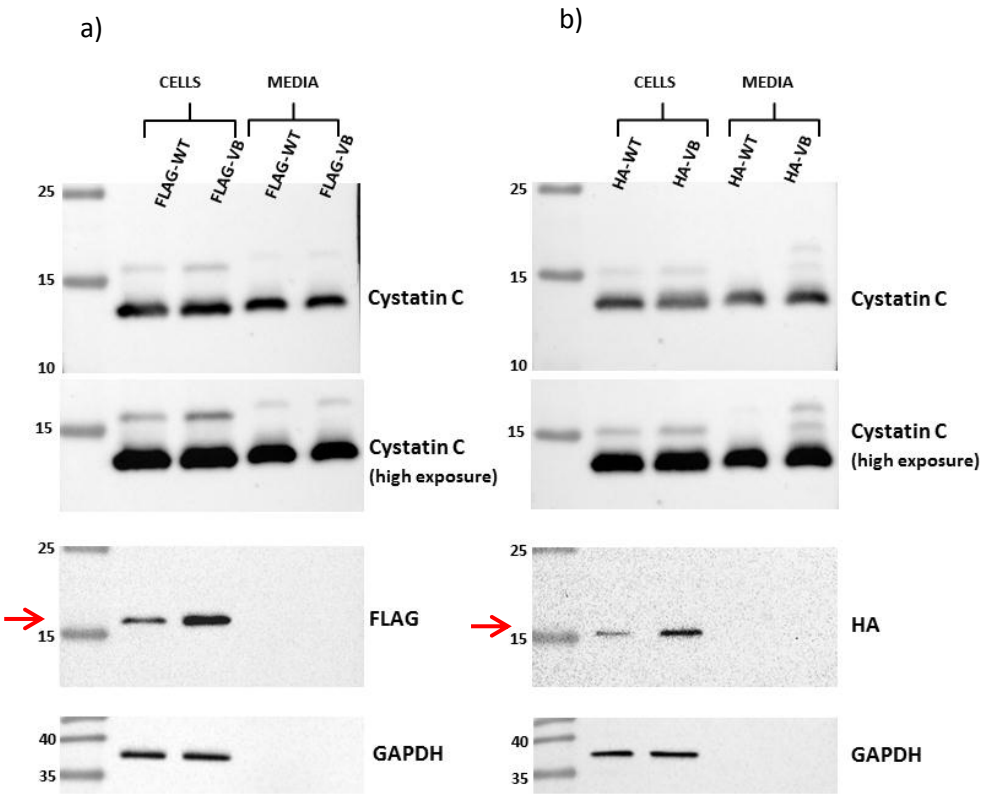

Figure 4.1 - Immunodetection of N-terminal tagged cystatin C constructs in D4O7 cells. Immunoblots of cell lysates and conditioned media collected from cell expressing N-terminal FLAG- (a) or HA- (b) tagged wild-type or variant B cystatin C 24h post-transfection. Blots were probed with anti-cystatin C antibody, which detected both precursor and mature forms of cystatin C, corresponding to bands of approximately 16.5kDa and 13kDa respectively, and with anti-FLAG or anti-HA antibody, depending on the construct used, which identified only the uncleaved precursor cystatin C protein (indicated by the arrow). Anti-GAPDH antibody was used as loading control for cell lysates.

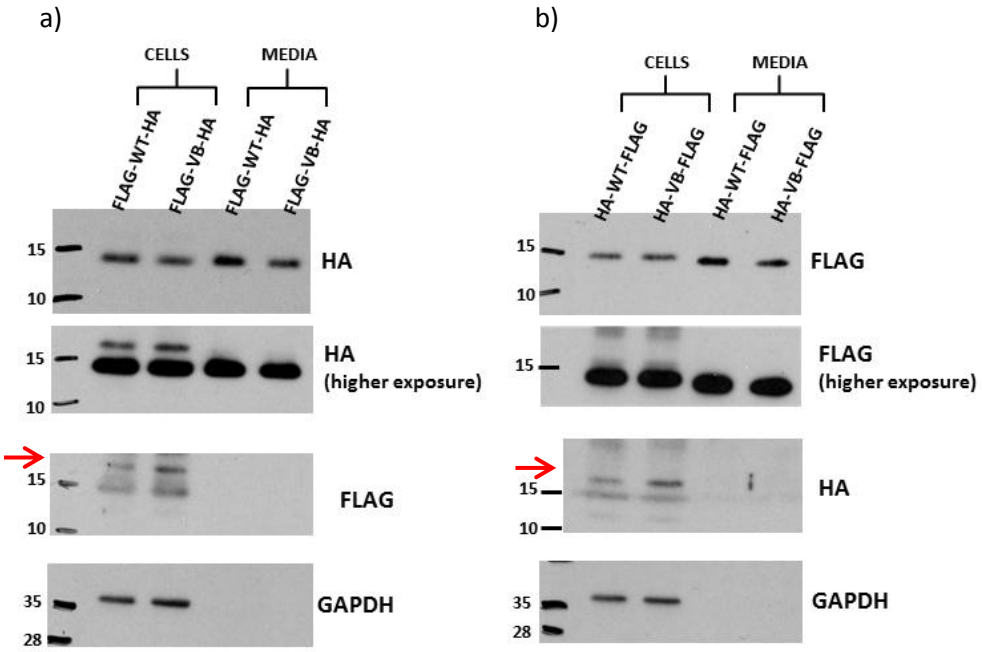

Figure 4.2 - Immunodetection of N- and C-terminal tagged cystatin C constructs on D4O7 cells. Immunoblots of cell lysates and conditioned media collected from cell expressing N-terminal FLAG-tagged and C-terminal HA-tagged (a) or, vice versa, N-terminal HA-tagged and C-terminal FLAG-tagged (b) wild-type or variant B cystatin C. In blot (a) anti-HA antibody was used to visualize both the precursor and the mature forms of cystatin C, consisting of bands of approximately 17.5kDa and 14kDa respectively, and anti-FLAG antibody to detect only the uncleaved precursor cystatin C protein (indicated by the arrow). Conversely, in blot (b) anti-FLAG antibody was used to visualize both precursor and mature forms of cystatin C protein, consisting of bands of 17.5kDa and 14kDa respectively, and anti-HA antibody to detect only the uncleaved precursor cystatin C protein (indicated by the arrow). Both blots were probed with anti-GAPDH antibody used as loading control.

4.2.2. Comparison of the level of variant B precursor fraction to wild-type cystatin C

The Western blot analysis described in the previous section revealed that the level of unprocessed cystatin C is very low if compared to the mature form. It was possible to detect the corresponding band only at very long exposure in the D4O7 cell line and could not be detected in ARPE19 cells. A pull-down of the transfected protein was therefore performed to increase the concentration of the uncleaved fraction of cystatin C, so that immunoblotting analysis would be able to more accurately evaluate possible differences between the level of unprocessed wild-type and variant B proteins.

For this experiment, constructs encoding cystatin C tagged to HA at the N-terminus and to FLAG at the C-terminus were used. Immunoprecipitation of the wild-type and variant proteins was performed by using anti-FLAG beads, as described in section 2.5 of Materials and Methods, so that both precursor and mature forms were isolated. The IP samples obtained were analysed by immunoblotting together with the respective cell lysates collected prior to the pull-down. Anti-HA antibody was used to detect the unprocessed form of cystatin C and anti-FLAG antibody to visualize both the unprocessed and mature proteins.

Cell lysates were loaded as an additional control to ensure that a similar protein expression/transfection efficiency was obtained for both wild-type and variant constructs. This showed that the yield of protein obtained after immunoprecipitation was similar. The bands obtained in the cell lysates, in figure 4.4, were also quantified.

Figure 4.3 shows immunoblots of samples obtained from D4O7 (A) and ARPE19 (B) cell lines. Figure 4.3 A shows a representative blot obtained in D4O7 cells. Bands of 17.5kDa size, corresponding to the uncleaved precursor cystatin C, were detected in the IP samples when probing with anti-HA antibody. At longer exposure time, bands of the same mass could also be detected in the cell lysates. Considering the similar level of mature protein in wild-type and variant B IP samples, detected with anti-FLAG antibody, the level of precursor cystatin C for the variant B appeared to be noticeably higher than the wild-type. It was not possible to replicate this finding using the ARPE19 cell line, where levels of variant precursor were inconsistent and either higher 4.3 B (a) or lower 4.3 B (b) compared to the wild-type. This is likely due to the extremely small amount of precursor detected in this cell line. Indeed, very long exposure times were required to detect bands corresponding to unprocessed proteins in the IP samples and no bands for the precursor were detected in the cell lysates.

In this analysis, levels of precursor protein were qualitatively compared between wild-type and variant B by taking in consideration the level of mature proteins. Quantification of the precursor cystatin C, in D4O7 cells, was also performed by densitometry of the bands visualized by using anti-HA antibody (figure 4.3 C).

However, normalization of the precursors to the mature proteins was not possible for this first set of experiments as the bands corresponding to the mature proteins were saturated. Comparison of the precursor levels is therefore performed assuming that the levels of mature proteins were approximately the same. Results confirm a higher level of precursor in the case of the variant B (figure 4.3 C). However, to properly quantify the precursor fraction, a new set of three independent experiments was performed again for the D4O7 cells and the respective immunoblots are shown in figure 4.4. Levels of precursor proteins obtained in either IP or cell lysate samples were evaluated by densitometry and normalised to the level of mature proteins. The level of unprocessed protein was calculated from the bands obtained with either anti-HA or anti-FLAG antibodies, and in both cases they were normalized to the mature form obtained by probing with anti-FLAG antibody. Surprisingly, in this experiment the difference observed between wild-type and variant precursor was inconsistent. Levels of uncleaved precursor in IP samples were higher for the variant B in blots (a) and (c) but not in blot (b). Quantification of the blots in figures 4.4 is shown in figure 4.5 and 4.6. These show levels of wild-type and variant B precursor in IP samples and cell lysates, respectively. Level of wild-type precursor was set to 1.

Results obtained using either cell lysate or IP samples, analysing the fraction of precursor proteins detected with either anti-FLAG or anti-HA, showed no statistically significant difference between wild-type and variant B. However, a trend corresponding to higher levels of variant B precursor is observed. Taken together with the results obtained in the first set of experiments, shown in figure 4.3 A (plotted in 4.3 C), it may indicate a difference, albeit small in comparison to the mature proteins, in the level of precursor proteins between wild-type and variant B.

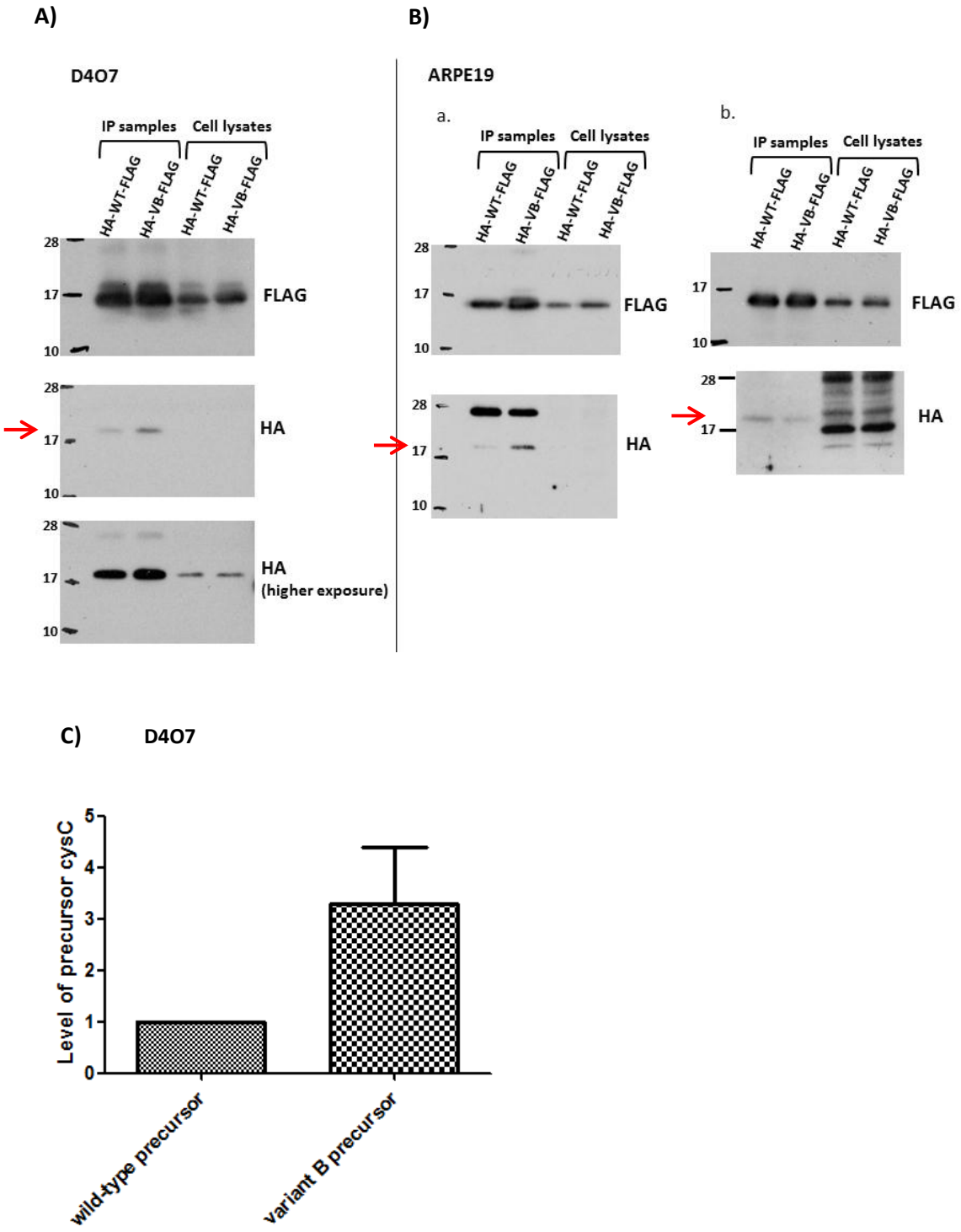

Figure 4.3 - Immunodetection of pulled-down N- and C-terminal tagged cystatin C constructs from transfected D4O7 and ARPE19 cells. D4O7 (A) and ARPE19 (B) cells transfected with wild-type or variant HA-CysC-FLAG constructs were subjected to immunopecipitation with anti-FLAG beads in order to pull down the total cystatin C protein, including both the precursor and mature forms. IP samples were then analysed by western blotting, together with the respective cell lysates, by probing with anti-FLAG and with anti-HA antibodies to detect the total cystatin C and only the precursor fraction (indicated by the arrow), respectively. Bands of mature and precursor correspond to 14kDa and 17.5kDa, respectively. (C) Levels of wild-type and variant B precursor protein obtained

by immunoprecipitation from transfected D4O7 cells were evaluated by densitometry. The level of wild-type precursor was set to 1 and level of variant B precursor resulted to be 3.28 ± 1.11 (N=3). Standard deviation is indicated in the graph.

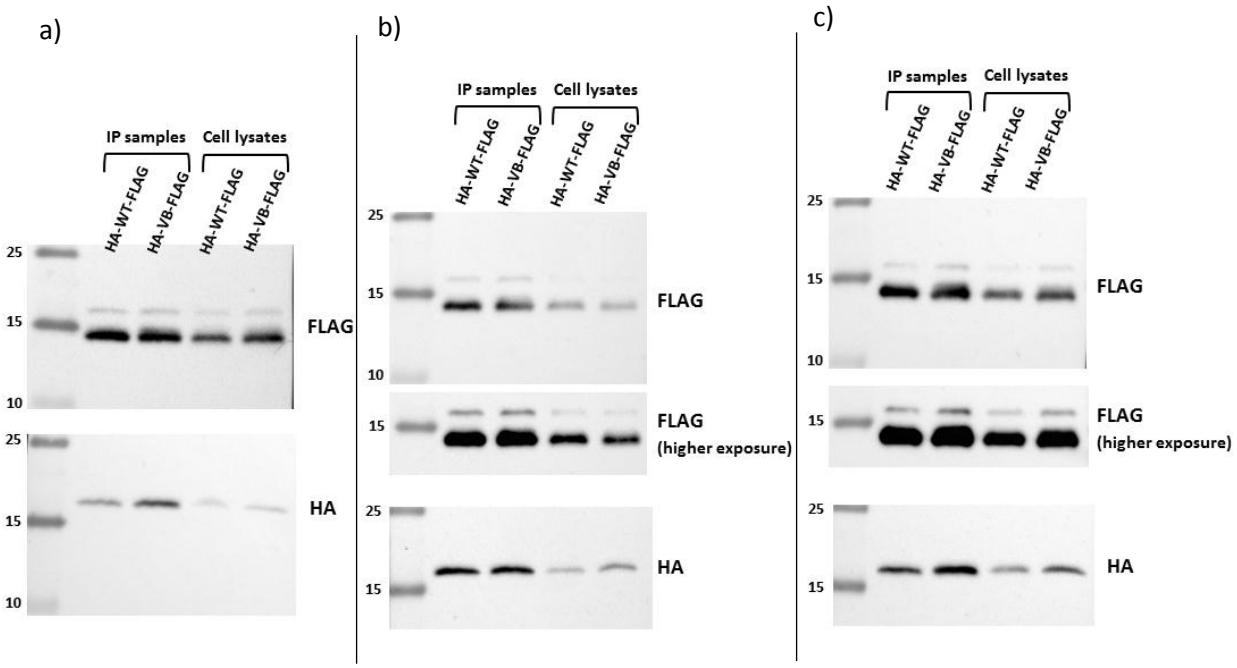

Figure 4.4 - Immunodetection of pulled-down N- and C-terminal tagged cystatin C constructs from transfected D4O7 cells. D4O7 cells transfected with wild-type or variant HA-CysC-FLAG constructs were subjected to immunopecipitation with anti-FLAG beads in order to pull down the total cystatin C protein, including both the precursor and mature forms. IP samples were then analysed by western blotting, together with the respective cell lysates, by probing with anti-FLAG and with anti-HA antibodies to detect the total cystatin C and only the precursor fraction, respectively. Bands of mature and precursor correspond to 14kDa and 17.5kDa, respectively.

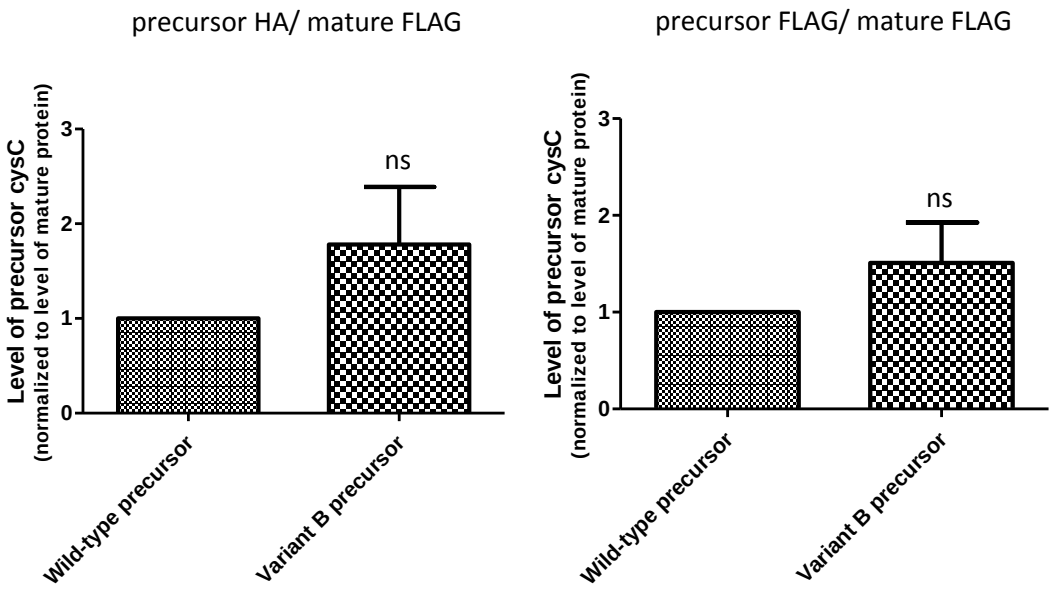

Figure 4.5 - Quantification of unprocessed precursor cystatin C after pull-down of HA-CysC-FLAG constructs. Level of precursor wild-type or variant B FLAG-cysC-HA obtained by immunoprecipitation from transfected D4O7 cells were evaluated by densitometry of western blots and normalized to the level of mature protein. In figure a) level of precursor obtained with anti-HA antibody was normalised to level of mature protein obtained with anti-FLAG antibody. In figure b) level of precursor was calculated from the band obtained with anti-FLAG antibody and normalised to the mature protein obtained with anti-FLAG antibody. In both cases, level of wild-type precursor was set to 1 and level of variant B precursor resulted to be 1.78 ± 0.61 (a) and 1.51 ± 0.42. One sample t test (N=3) (two-tailed) p= 0.16 and 0.17, respectively. Standard deviations are indicated in the graph.

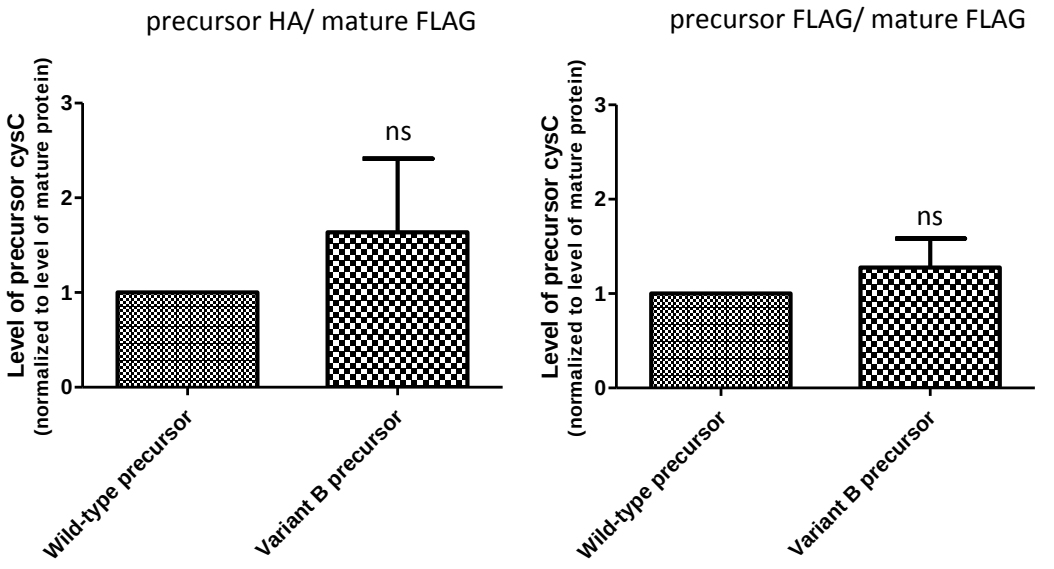

Figure 4.6 - Quantification of unprocessed precursor FLAG-CysC-HA constructs in D4O7 cell lysates. Level of precursor wild-type or variant B FLAG-cysC-HA in transfected D4O7 cells were evaluated by densitometry of western blots and normalized to the level of mature protein. In figure a) level of precursor obtained with anti-HA antibody was

normalised to level of mature protein obtained with anti-FLAG antibody. In figure b) level of precursor was calculated from the band obtained with anti-FLAG antibody and normalised to the mature protein obtained with anti-FLAG antibody. In both cases, level of wild-type precursor was set to 1 and level of variant B precursor resulted to be 1.64 ± 0.78 (a) and 1.28 ± 0.31. One sample t test (N=3) (two-tailed) p= 0.29 and 0.26, respectively. Standard deviations are indicated in the graph. (ns=non-significant)

4.3. Variant B and wild-type precursor cystatin C both localize to the ER

The precursor cystatin C has been suggested to partially divert from the secretory pathway leading the unprocessed protein, with the intact leader peptide, to accumulate intracellularly and associate with mitochondria (Paraoan et al. 2004). Considering the results obtained in the previous section, the unprocessed precursor cystatin C was analysed by IF to further assess whether a difference in its level occurs between wild-type and variant B. Although in the previous chapter no mislocalization was observed for the variant B, its low abundance might have required such a long exposure that it would have been masked by the resulting overexposure of the fluorescence from the mature protein. Therefore, the localization specifically of the precursor was this time analysed to identify whether it partially mislocalizes intracellularly, as hypothesised by Paraoan et al. (2004). For this reason, N-terminal tagged cystatin C constructs, with either FLAG or HA tags, were used to visualize the precursor protein and determine the fate of the signal sequence.

D4O7 cells were transfected and analysed after fixation by IF using anti-cystatin C antibody to detect the mature protein and anti-FLAG or anti-HA antibodies, for the N-terminal FLAG- or HA- tagged constructs respectively, to detect the unprocessed cystatin C. IF microscopy analysis, shown in figure 4.7, revealed that the precursor protein was not easily detected compared to the mature form. This was the case for both FLAG- (a) and HA-tagged (b) proteins. It was detected only at very long exposure times and did not appear in all the transfected cells. This is consistent with the extremely low amount of precursor observed by immunoblotting, suggesting that the proteins are rapidly processed to their mature form.

The distribution of antibody staining was assessed to determine whether the proteins mislocalize, particularly in the mitochondria as hypothesised earlier. D4O7 cells transfected with FLAG- or HA-tagged constructs were analysed with anti-cystatin C (figure 4.8) to detect the mature cystatin C, and with anti-FLAG or anti-HA, depending on the construct (figure 4.9) to detect the unprocessed proteins. Mitotracker was used to visualize mitochondria in both figures 4.8 and 4.9 (a). For the precursor fraction, the ER compartment was also visualized with anti-calreticulin antibody in figure 4.9 (b).

Results showed no mitochondrial distribution for either the mature or precursor cystatin C proteins. Mature cystatin C appeared to be present in the ER-Golgi complex, thus further indicating a normal localization for variant B protein and confirming that a tag at the N-terminal does not affect protein trafficking. The non-processed precursor was shown to localize in the ER compartment in both wild-type and variant proteins, thus indicating that it also does not mislocalize.

The same analysis was performed in ARPE19 for both FLAG- and HA-tagged constructs (in figures 4.10 and 4.11, respectively). Again the mature protein showed an ER/Golgi distribution, whereas the precursor was found to be distributed throughout the ER and no association with mitochondria was observed.

In some images the precursor appeared to show granule-like structures, which may likely represent protein aggregates destined for degradation, but which did not colocalize with mitotracker.

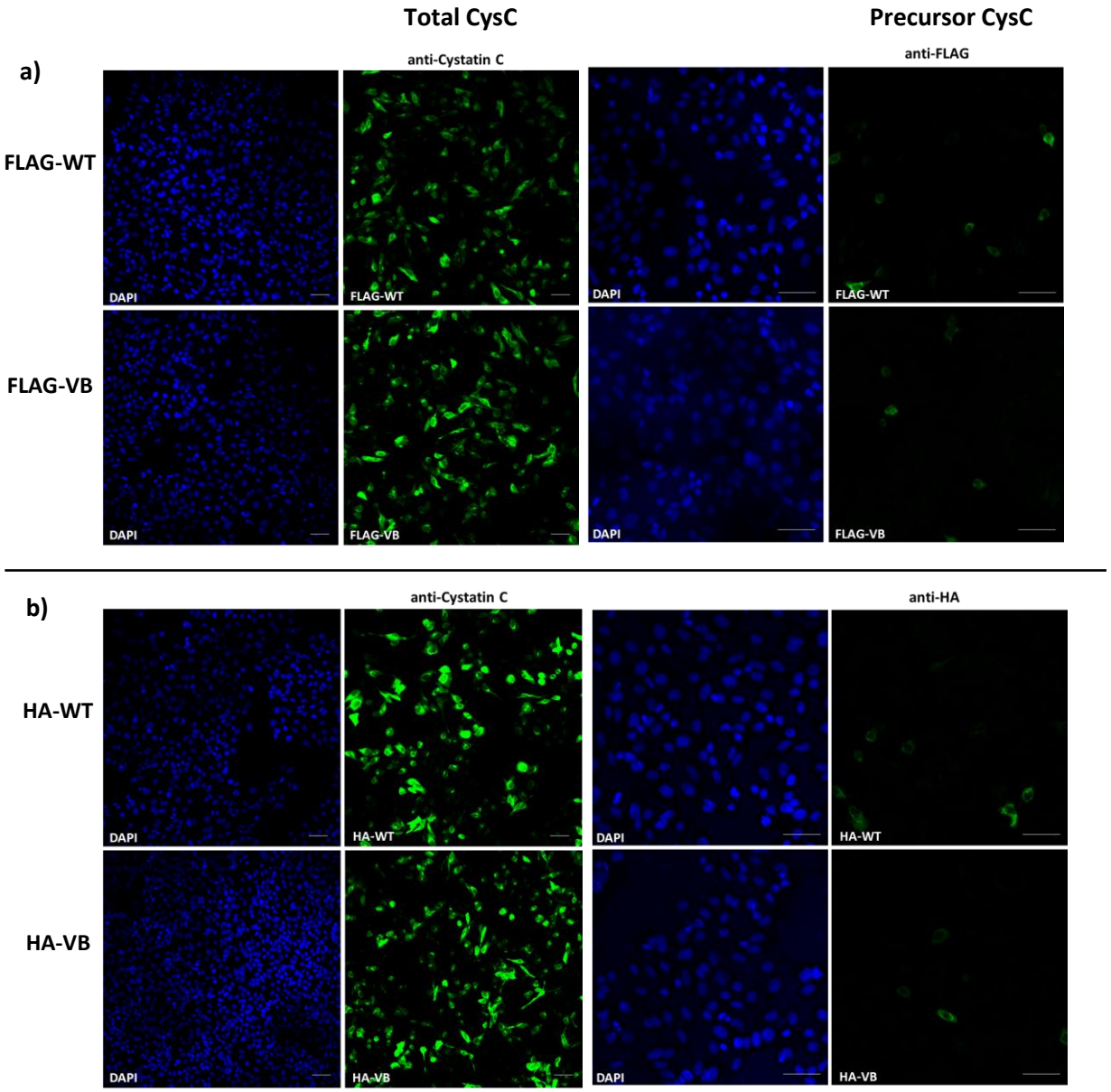

Figure 4.7 - Comparison between total and precursor fraction of cystatin C by using the N-terminal FLAG- or HA-tagged constructs in D4O7 cells. D4O7 cells expressing wild-type or variant B cystatin C linked to either FLAG (a) or HA (b) at the N-terminus were PFA-fixed and immunostained 24h post-transfection. Anti-cystatin C antibody was used to detect the total transfected cystatin C, precursor and mature forms, and anti-FLAG or anti-HA, depending on the constructs used, were used to detect only the unprocessed precursor, which all fluoresce in green. The blue fluorescent DAPI was used to stain nuclei. Scale bars are 50 µM.

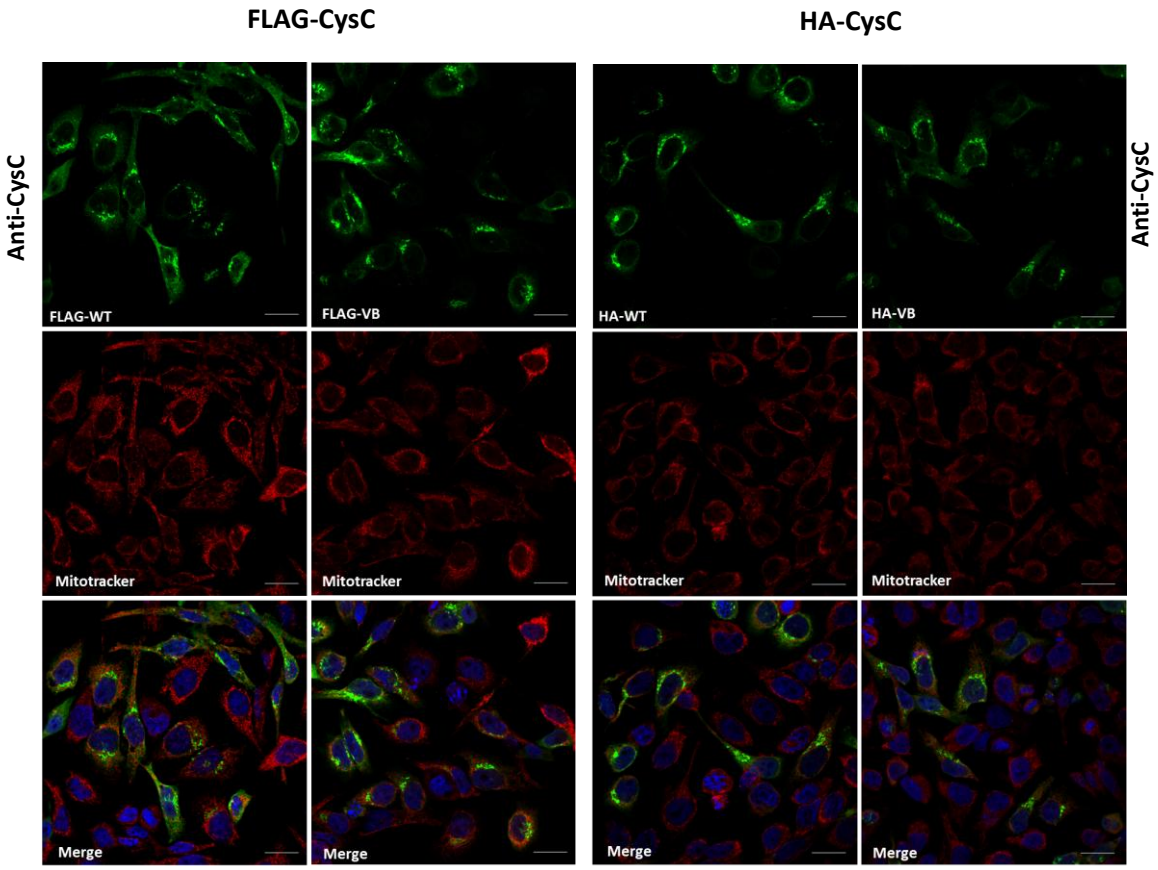

Figure 4.8 - Localization of mature cystatin C by using N-terminal FLAG- or HA-tagged constructs in D4O7 cells. D4O7 cells expressing wild-type or variant B cystatin C linked to either FLAG or HA at the N-terminus were PFA-fixed and immunostained 24h post-transfection. Anti-cystatin C antibody was used to detect the total transfected cystatin C, precursor and mature, which fluoresces in green. Mitotracker, which fluoresce red, was used to visualize mitochondria. The blue fluorescent DAPI was used to stain nuclei. For each field of cells imaged, green and red fluorescence were recorded as separate images and then merged, for assessing the overlap of the respective signals. Scale bars are 20 µM.

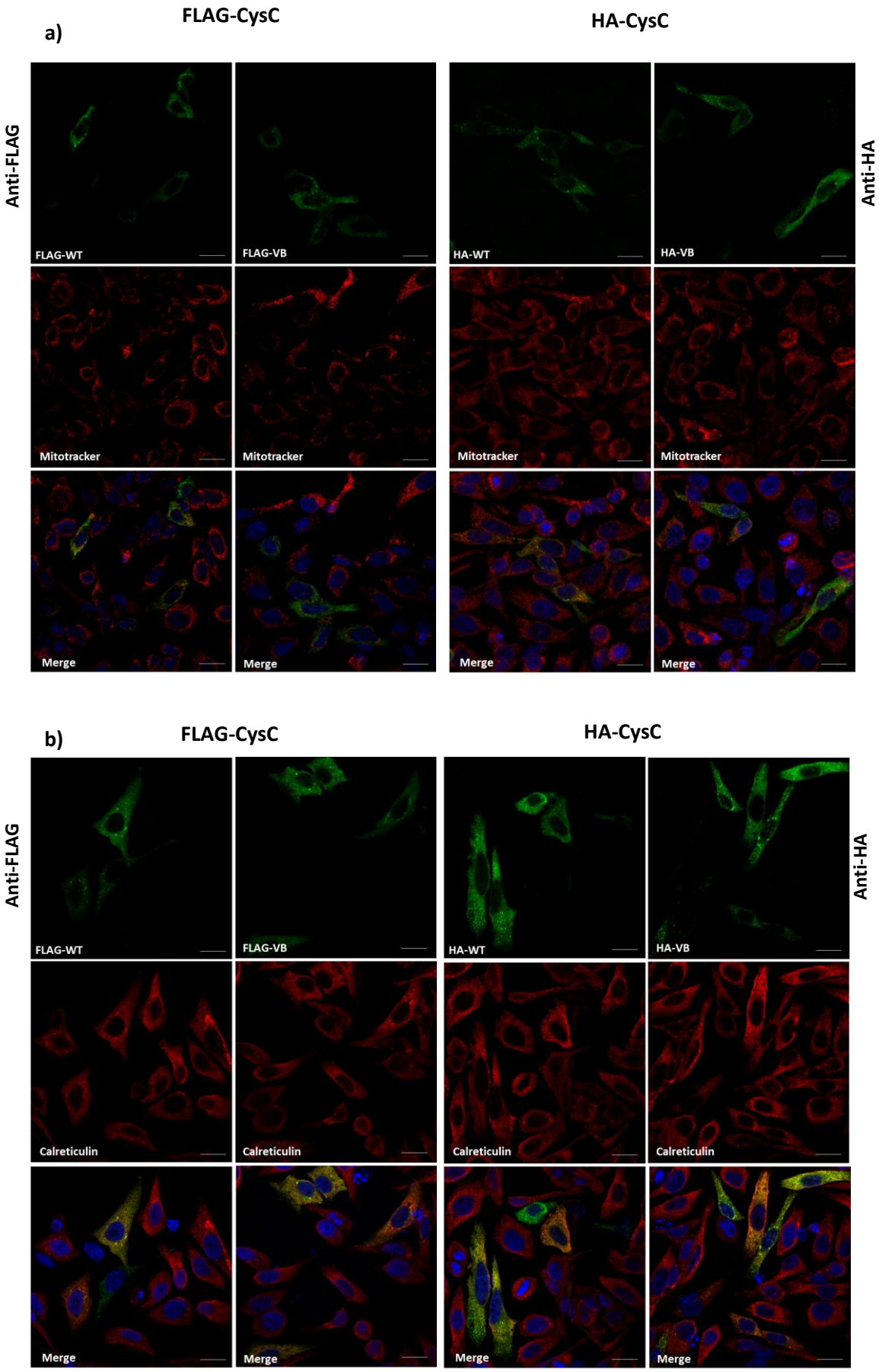

Figure 4.9 - Localization of precursor cystatin C by using N-terminal FLAG- or HA-tagged constructs in D4O7 cells. D4O7 cells expressing wild-type or variant B cystatin C linked to

either FLAG or HA at the N-terminus were PFA-fixed and immunostained 24h post-transfection. Anti-FLAG or anti-HA antibodies, depending on the construct used, were used to detect the unprocessed precursor cystatin C, which fluoresces in green. Mitotracker (a) or the antibody anti-calreticulin (b), which fluoresce red, were used to visualize mitochondria and ER, respectively. The blue fluorescent DAPI was used to stain nuclei. For each field of cells imaged, green and red fluorescence were recorded as separate images and then merged, for assessing the overlap of the respective signals. Scale bars are 20 µM

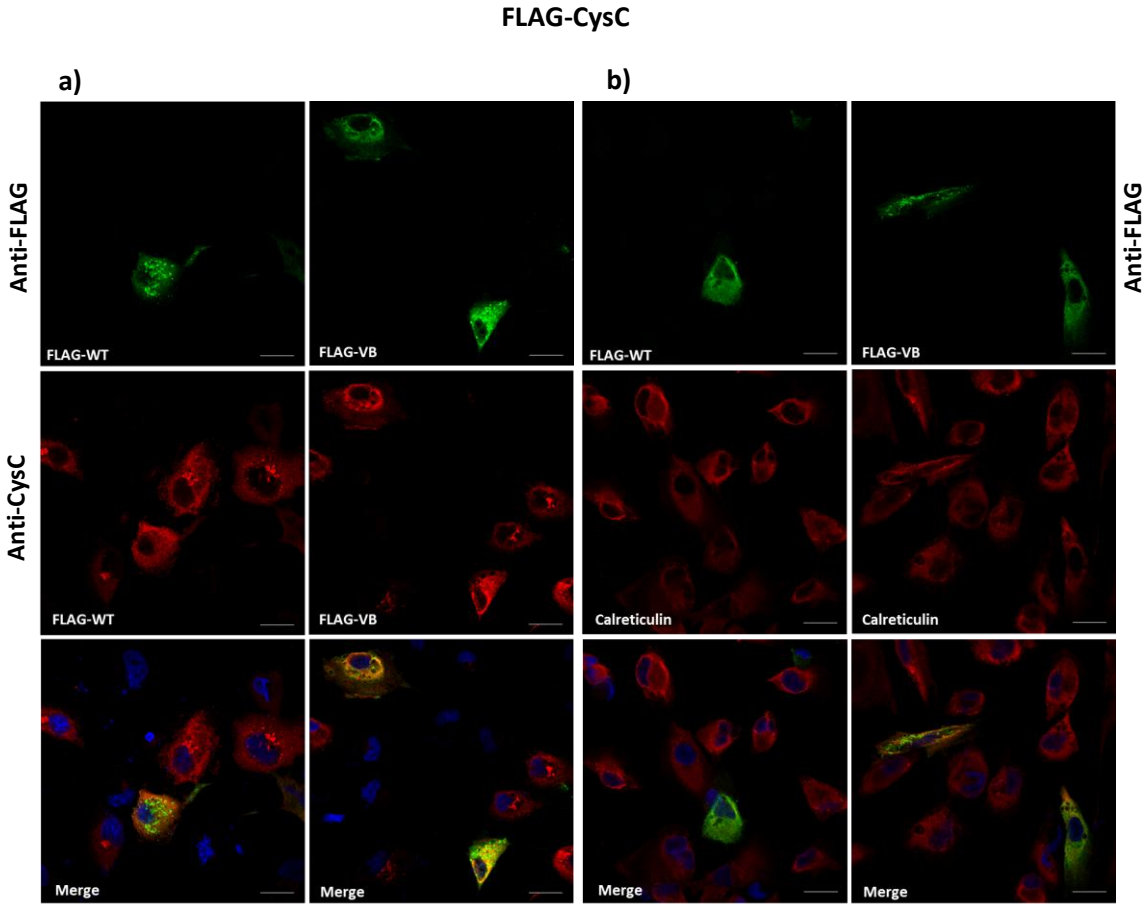

Figure 4.10 - Localization of N-terminal FLAG- tagged cystatin C constructs in ARPE19 cells. ARPE19 cells expressing wild-type or variant B cystatin C linked to FLAG at the N-terminus were PFA-fixed and immunostained 24h post-transfection. Anti-FLAG antibody was used to detect the unprocessed precursor cystatin C, which fluoresces in green. Anti-cystatin C and anti-calreticulin, which fluoresce red, were used to visualize the total cystatin C and the ER, respectively. The blue fluorescent DAPI was used to stain nuclei. For each field of cells imaged, green and red fluorescence were recorded as separate images and then merged, for assessing the overlap of the respective signals. Scale bars are 20 µM.

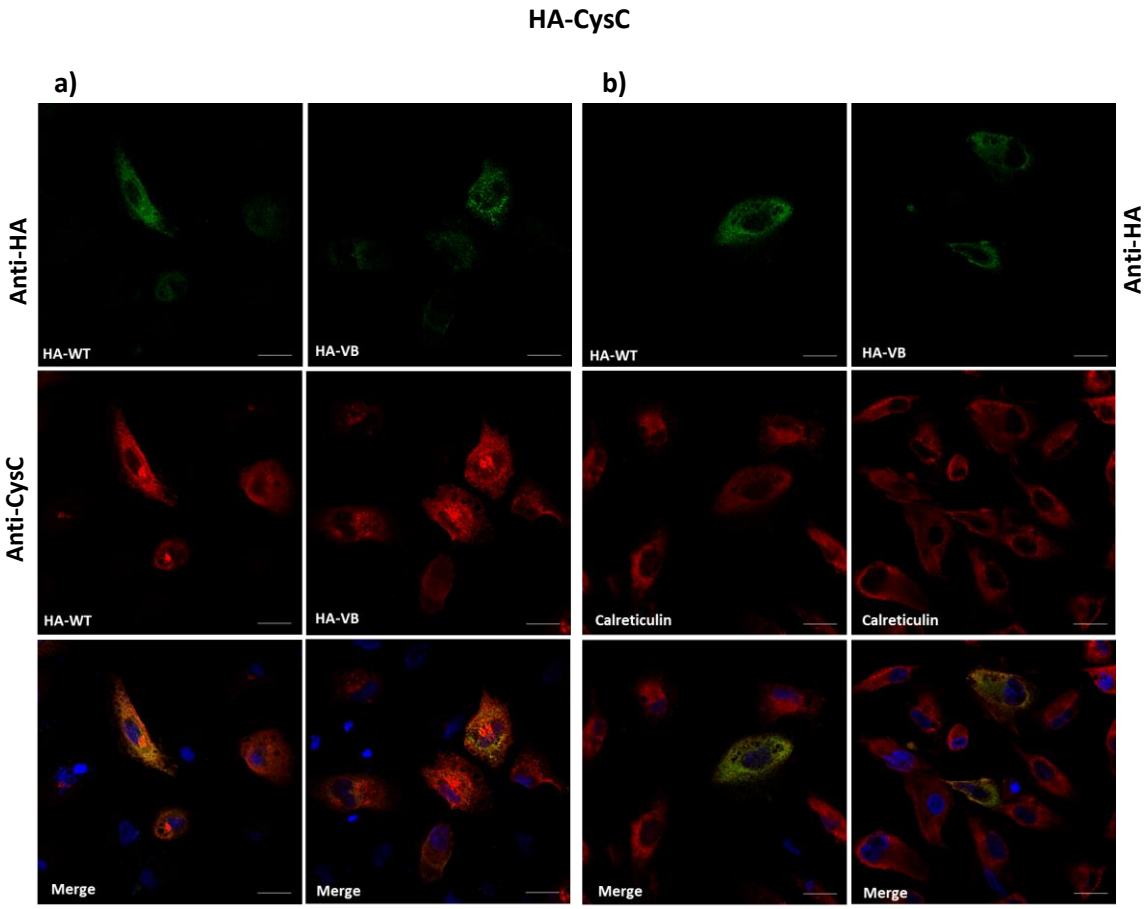

Figure 4.11 - Localization of N-terminal HA-tagged cystatin C constructs in ARPE19 cells. ARPE19 cells expressing wild-type or variant B cystatin C linked to HA at the N-terminus were PFA-fixed and immunostained 24h post-transfection. Anti-HA antibody was used to detect the unprocessed precursor cystatin C, which fluoresces in green. Anti-cystatin C and anti-calreticulin, which fluoresce red, were used to visualize the total cystatin C and the ER, respectively. The blue fluorescent DAPI was used to stain nuclei. For each field of cells imaged, green and red fluorescence were recorded as separate images and then merged, for assessing the overlap of the respective signals. Scale bars are 20 µM.

4.4. Discussion

Secretory proteins are synthesized as precursors with an N-terminal signal sequence that is usually cleaved during the co-translational translocation of the nascent polypeptide chain into the lumen of the ER. As described in section 1.5.1, signal sequences are essential to direct proteins to the secretory pathway as they mediate their targeting to ER, translocation across the membrane and cleavage by signal peptide complex (SPC) (Hegde, Bernstein 2006).

Targeting of the nascent chain-ribosome complex to the ER occurs by binding of the signal peptide to the SRP, which then associates with its receptor at the ER membrane (Halic et al. 2004). Subsequently, the signal peptide interacts with the Sec61 translocon, promoting the opening of the conducting channel and the consequent initiation of translocation (Rutkowski et al. 2003). Properties of the signal peptide also determine its orientation across the ER membrane (Kocik, Junne & Spiess 2012). Once it emerges into the ER lumen the signal peptide is removed by the SPC (Meyer, Hartmann 1997). The cleaved signal peptide is then further processed and degraded (Lyko et al. 1995), while the mature protein is released into the lumen once its translocation is completed. Therefore, mutations within the signal peptide could affect any of these steps, resulting in inefficient/improper protein maturation, as reported for several human proteins (Jarjanazi et al. 2008). However, in some case mutations have been shown not to have any measurable effect (Jarjanazi et al. 2008).

Substitution of the hydrophobic alanine residue in the penultimate position -2 of the signal sequence of cystatin C with a more polar threonine amino acid alters the hydrophobicity of the signal sequence, thus possibly affecting its functionality. In earlier studies, the variant B was processed less efficiently, thus eventually leading to a decreased protein secretion (Benussi et al. 2003). Furthermore, the precursor was suggested to only be partially cleaved, or cleaved at a different site (Paraoan et al. 2004, Nilsson et al. 2009, Nguyen, Hulleman 2016), thus generating a misfolded protein that could accumulate and/or mislocalise intracellularly. If the variant B

protein is associated with increased risk of disease development, impairment in the variant B protein maturation can be expected as, otherwise, the resulting mature form would not differ from wild-type cystatin C. The aim of this chapter was therefore to investigate whether the variant B polymorphism affects the maturation of cystatin C, which could consequently explain its association with diseases.

By using constructs encoding precursor cystatin C linked to a tag at the N-terminus it was possible to detect the unprocessed precursor fraction individually from the mature cystatin C protein. All N-terminal tagged constructs (either wild-type or variant B) used in this study resulted to be normally targeted for secretion thus confirming their suitability for these studies and also confirming the results on the protein trafficking obtained in the previous chapter with the C-terminal tagged and untagged constructs.

The main results obtained in this study revealed a possible difference between the levels of wild-type and variant B precursor proteins in D4O7 cells. This fraction appears to be higher in the case of the variant B, thus suggesting a less efficient processing of the variant precursor. This difference, however, was not obtained in ARPE19, likely due to the very low level of precursor present. Indeed, in ARPE19 cells, where the yield of protein expression is much lower compared to D4O7, it was not even possible to detect the precursor fraction in the cell lysates by immunoblotting, and it was detected only at very high exposure after selective pull-down. Consistent with these results, the unprocessed cystatin C could be detected in very few ARPE19 cells by IF analysis.

Regarding the results obtained in D4O7, a trend consisting in an increased level of precursor protein in the case of the variant B seems to constantly occur, although this difference resulted not to be statistically significant. This non-significance is likely due to the very small amount of proteins that are considered in this analysis, which is expected to be more susceptible to experimental variation. In addition, the analysis was performed 24 hours after transfection, a time that may not allow

sufficient accumulation of the precursors to detect a possible significant difference. If, as suggested by the results, subtle differences in the efficiency of cleavage of the variant B signal peptide indeed exist, over time they may become statistically and biologically significant. As a consequence, depending on the turnover of the secreted protein it could lead to a long-term reduction in the levels of the secreted protein. Therefore, although no difference in the fraction of secreted proteins was found between wild-type and variant B (as described in section 3.4), small differences in how the variant B precursor is processed could accumulate over time. This may explain an association of the variant B with aging related diseases. An alternative possibility, however, is that the detection of the precursors in the first place was only due to the overexpression of the cystatin C constructs (see below).

Cell imaging was then carried out to analyse the destiny of the variant B precursor. Results revealed that the mature form is normally distributed in the ER/Golgi, whereas the precursor cystatin C appears to localize in the ER, as it is expected for a precursor protein. No localization in the Golgi apparatus and no mislocalization in other cellular compartment such as mitochondria were observed for the uncleaved precursor, suggesting that this fraction, even when increased due to a less efficient maturation, is then either removed by degradation or processed, thus generating a normal mature protein that will be eventually secreted. If this is the case, the only direct consequence would be a gradual decreased in protein secretion. Overall, these results further confirm that no mislocalization into the mitochondria occurs for the variant B cystatin C, either as mature form or as uncleaved precursor, as the latter was instead suggested by Paraoan et al. 2004. It is not clear, though, why the precursor fraction was not detected in all the transfected cells. It may probably depend on the different efficiency of processing occurring in the different cells. However, this occurs similarly for the wild-type and variant B constructs.

The reason of the significant lower level of precursor protein compared to that of the mature protein, observed in both immunoblotting and imaging, is probably due to the fact that precursor proteins are processed as soon as the signal peptide cleavage site is exposed in the lumenal side, while protein translation is still occurring (Antonin, Meyer & Hartmann 2000). The full-lenght 146 amino acids precursor protein is therefore probably not normally present in the cells and it can be observed in this analysis because of the overexpression of the protein that may determine a saturation of the translocation/cleavage machinery, as suggested by a number of other groups (Cottet, Corthésy 1997, Massotte 2003, Dalton, Barton 2014). Its presence is indeed revealed particularly in D4O7 cells due to their higher protein expression. Moreover, after the precursor processing, the cleaved signal peptide is then rapidly processed/degraded by SPP (as described in section 1.5.1.1). For this reason, either the precursor protein or simply the cleaved signal peptide cannot be easily detected during imaging analysis by probing with antibodies against the N-terminal tags, as they are rapidly processed and degraded, respectively. This further indicates that, in such conditions of protein overexpression, the fact that the precursor/signal sequence is differently detected among the transfected cells may depend on the different efficiencies of cleavage and degradation in place for each cell.

The different levels observed between wild-type and variant B can still suggest a reduction in the efficiency of the variant B maturation. However, because of the considerable difference between the level of precursor and mature fractions and the very small difference identified between wild-type and variant B precursor, it appears unlikely that this inefficiency of cleavage is sufficient to significantly impair the trafficking and secretion of cystatin C, as indeed observed and reported in chapter 3, or at least not after 24 hours of analysis.

Considering the different functions of the signal peptide in the protein translocation and maturation, the mutation in study may affect one of the steps involved in this process. As described in detail in section 1.5.1.2, the signal sequences usually share the same tripartite structure, consisting of a positively

charged N-terminus, a hydrophobic core and a polar C-terminal domain, also termed respectively n-, h- and c-region (Nilsson et al. 2015). Each of these domains plays a specific role in the protein maturation. The n- and h-region mediate the SRP recognition process and the translocation across the membrane. The hydrophobicity profile of the h-region has been reported to be the main criterion for targeting the nascent protein to the SRP-dependent co-translational pathway (Hatsuzawa, Tagaya & Mizushima 1997), while the n-region contributes to modulate the affinity of the SRP-signal peptide association (Nilsson et al. 2015). The basic residues in the n-region and the hydrophobic core of the signal sequence are also responsible for the correct orientation of the signal sequence during the translocation, by interacting with the translocon components (Kocik, Junne & Spiess 2012, Nilsson et al. 2015). The integrity of the c-region is instead crucial for the cleavage of the signal sequence by the SPC. Based on the (-3, -1) rule, the amino acid residues at -1 and -3 positions have been described to be the most critical to establish the site of cleavage by determining the correct interaction with the active site of signal peptidase. These positions are usually occupied by small and neutral amino acids (Nothwehr, Gordon 1990, Auclair, Bhanu & Kendall 2012).

Several diseases caused by mutations within the signal sequence of secretory proteins have been reported, where protein function or localization were dramatically disrupted (Jarjanazi et al. 2008). Depending on the domain of the signal peptide in which the mutation occurs, different effects on protein maturation have been observed. For instance, mutation in the h-region of the signal sequence of the preproparathyroid hormone was suggested to impair the protein targeting or translocation of the protein. The consequent inhibition of protein secretion has been linked to a form of hypoparathyroidism (Arnold et al. 1990). Whereas mutations in the c-region, and in particular involving residues at -1 and -3 positions, were shown to mainly affect the cleavage process. For instance, amino acid substitution at -3 position of the signal peptide have been observed to cause either a failure in the cleavage, as in the case of the coagulation Factor X, or cleavage at an alternative site, as in the case of the anti-thrombin (Racchi et al.

1993). In the first case, the uncleaved precursor of factor X is retained intracellularly, where it is slowly degraded and the failed secretion causes a severe deficiency in the patients. In the case of the anti-thrombin, the cleavage occurs to a different site, two amino acids toward the C-terminus. Nevertheless, the resulting two residues shorter processed protein was reported to be normally secreted and to maintain its function. Indeed, no pathological condition results from this mutation. Another mutation at the -1 position, consisting in a Thr to Ala substitution, in the signal peptide of Vasopressin, has been shown to impact the efficiency of cleavage, generating a prevalent uncleaved and abnormally glycosylated product, which may accumulate intracellularly thus causing cell toxicity (Ito et al. 1993, Ito, Yu & Jameson 1999). This mutated vasopressin precursor protein has been associated with a form of Diabetes insipidus characterised by neuronal cell degeneration (Ito, Yu & Jameson 1999).

The mutation characterizing the variant B cystatin C occurs at the -2 position, within the c-region of the signal sequence. It is therefore likely that targeting and translocation of the nascent variant B protein are not affected. However, the amino acid substitution in position -2 may have an effect on the orientation of the C-terminal domain of the peptide, resulting in an unfavourable interaction between the cleavage site and the active site of the peptidase. A less efficient processing may result in the generation of protein that is uncleaved or cleaved at an alternative site, as suggested in earlier reports (Nguyen, Hulleman 2016, Paraoan et al. 2004). The resulting uncleaved or miscleaved fraction may undergo improper folding and accumulate intracellularly, as described for the above-mentioned Factor X and vasopressin proteins.

Furthermore, as suggested for vasopressin, the abnormal uncleaved precursor variant B might be retained within the ER, because of the signal peptide anchored to the ER membrane and/or due to the status of the precursor proteins most likely unfolded or misfolded. Misfolded proteins are indeed generally retained in the ER and then targeted for degradation through the ER-associated degradation (ERAD) system (Ito et al. 1993, Ito, Yu & Jameson 1999). ERAD is a specific mechanism

responsible for removal of ER-retained misfolded and damaged proteins. It includes several steps consisting of the recognition and targeting of the misfolded protein to the dislocation-machinery located on the ER membrane and its subsequent translocation to the cytosol for degradation by the proteasome (Schrul et al. 2010, Hegde, Ploegh 2010). However, as for vasopressin, the misfolded precursor protein may not entirely undergo degradation, thus accumulating in the ER and eventually forming aggregates, which impair cell functionality (Birk et al. 2009, Ito, Yu & Jameson 1999). Interestingly, a study has also reported that proteins appear to be less stable when the signal peptide is not cleaved, thus resulting in incorrect folding and increased propensity to aggregate (Singh et al. 2013).

A similar case has been also reported for the precursor form of insulin (Liu et al. 2012) where an Ala to Asp substitution at position -1 of the signal sequence was indeed reported to cause an inefficient cleavage of the protein, resulting in the formation of two alternatively processed molecules, either uncleaved or incorrectly cleaved at a different cleavage site. Both forms were suggested to be misfolded and therefore retained in the ER and targeted to ERAD. Again, they may escape ERAD, accumulating within the ER and ultimately leading to generation of protein aggregates. In addition, this condition has been also found to interfere with the trafficking of other proteins, precluding their exit from the ER and activating an ER stress response. Interestingly, in the same study they showed that a mutation at -2 position of the insulin precursor, consisting in an Ala to Ser substitution, therefore similar to cystatin C mutation, was not able to affect protein cleavage (Liu et al. 2012). The presence of favourable residues at the -1 and -3 positions seem to be particularly crucial for establishing the correct interaction with the signal peptidase, thus permitting an effective cleavage (Auclair, Bhanu & Kendall 2012). However, not all the mutations compromise the protein maturation. Only a small percentage of the mutations identified in the signal sequence was reported to affect the function of the signal peptide, which results in clinical conditions (Jarjanazi et al. 2008). Therefore, it is also possible that the mutation characterising the variant B protein, which does not reside in one of the critical residues of the c-region, may not have any significant effect on the protein processing.

However, in our study, the higher transfection rate and protein expression that characterise the D4O7 cells might have revealed a possible accumulation of the variant B precursor that normally may only occur over time, when the level of ER-retained precursor proteins is sufficiently significant. If this is the case, this time-dependent effect may occur with aging, thus being consistent with the progression/development of age-related diseases. As a result, even small difference in the cleavage might become significant in the long-term, thus causing, for instance, a reduction in secretion and/or an intracellular protein accumulation/aggregation of the uncleaved precursor. Interestingly, it has been recently reported that the uncleaved precursor cystatin C is highly amyloidogenic (Sant'Anna et al. 2016). Mature cystatin C is, per se, an aggregation-prone protein (Tsiolaki et al. 2015). By using validated bioinformatics programs that predict the aggregation propensity of proteins, Sant'Anna et al. (2016) have reported that the leader peptide of cystatin C contains a highly aggregation-prone sequence (Sant'Anna et al. 2016). As a consequence, the unprocessed precursor of cystatin C is even more amyloidogenic than the corresponding mature protein (Sant'Anna et al. 2016). Consistent with this prediction, the precursor cystatin C has been shown to form toxic aggregates and amyloid fibrils *in vitro* (Sant'Anna et al. 2016). This higher amyloidogenic propensity of the precursor, characterising wild-type and variant B equally, may be relevant in the case of an inefficient cleavage of the precursor, as hypothesised for the variant B. Therefore, the suggested impaired protein maturation may result in the intracellular retention of a highly amyloidogenic protein. Over time, accumulation of the precursor protein may lead to formation of aggregates and toxic fibrils.

In conclusion, the A25T mutation might impair the cleavage of the signal peptide, resulting in an uncleaved fraction, which is misfolded and retained within the ER. This mutant precursor protein will be normally degraded by ERAD. However, if this fraction is not rapidly or efficiently degraded it may accumulate over time. This could, for instance, occur in aging and contribute to age-related diseases, where

decreased activity/dysfunction of the proteolytic system has been extensively reported (Vilchez, Saez & Dillin 2014, Hipp, Park & Hartl 2014). As the uncleaved precursor accumulates within the ER, it could consequently interfere with normal synthesis and trafficking of other proteins, inducing ER stress and leading ultimately to cell dysfunction. Furthermore, as the cystatin C precursor is highly amyloidogenic its accumulation in the ER may lead to formation of aggregates over time, eventually affecting cellular function and leading to cell degeneration. Interestingly, ER stress has been suggested to play an important role in AMD pathogenesis (Salminen et al. 2010). However, the variant B was recently shown to be unable to activate, 48-hours post-transfection, the unfolded protein response (UPR), which is the classical ER stress response (Nguyen, Hulleman 2016). This is probably due to the very small amount of proteins retained and accumulated after only 48-hours.

Consistent with the hypothesis of an intracellular retention/accumulation of the unprocessed variant B, the precursor proteins, either wild-type or variant B, were sometimes observed in the IF analysis to be distributed in granules or dot-like structures, possibly representing protein aggregates. This may be due to the protein overexpression that exceeds the capacity of either the ER machinery to process the precursor proteins or the ERAD system to remove the excessive misfolded uncleaved ones. In either case, since the precursor cystatin C is highly amyloidogenic (Sant'Anna et al. 2016), even small amounts may lead to aggregate formation, as observed in IF imaging. Although in my analysis this was detected for both wild-type and variant B proteins, if the latter is less efficiently cleaved, variant B aggregates may over time accumulate and contribute to age-related disease conditions.

Further studies are needed to confirm the inefficient processing of the variant B precursor. As mentioned before, analysis at longer time periods may be appropriate in this case, especially considering the very low levels of precursor protein in study. Anyway, if the lower efficiency of cleavage is confirmed, it could determine on one side a decrease in cystatin C secretion, thus leading to a

dysregulation of the proteolytic activity in the extracellular matrix, or more likely, the induction of ER stress due to protein aggregation, eventually leading to cell death. Both effects, if confirmed, could support and explain an enhanced AD and AMD risk in the case of the variant B.

Chapter 5 - Characterization of cystatin C species secreted

5.1. Introduction

During analysis of secretion performed in section 3.4 the presence of two additional, slightly slower migrating bands, was consistently observed in the conditioned media of D4O7 cells transfected with variant B cystatin C, either untagged or tagged to FLAG or HA, after longer exposures. In this chapter, I describe the characterization of these bands in particular to determine whether these bands also represent the cystatin C protein and, if so, what causes their slower migration in SDS-PAGE. As an alternative cleavage site and consequent O-glycosylation have been previously suggested to occur for the variant B cystatin C (Nilsson et al. 2009, Nguyen, Hulleman 2016), analysis of such a post-translational modification was explored. This could explain the change in molecular weight of the protein and may correlate variant B to disease development.

5.2. Additional secreted forms of cystatin C are produced in RPE cells expressing variant B proteins.

The two extra-bands were observed by Western blotting in the cultured media of D4O7 cells expressing the variant B cystatin C, either untagged or tagged to FLAG or HA, as shown in Figure 5.1 a, b and c, respectively, and by probing with either anti-cystatin C, anti-FLAG or anti-HA antibodies, depending on the constructs. The extra-bands were visualized only after a relatively long exposure, thus indicating that these species are present at very low levels compared to the bulk of the presumably correctly processed cystatin C. The fact that the bands were detected with all the constructs and with different antibodies suggests that they represent a form of the cystatin C protein. However, in ARPE19 cells, only one additional band was detected in the conditioned media for the variant B, which was of similar size to the intermediate band detected in D4O7 cells (Fig. 5.2). This difference is probably due to the different protein expression levels in the two cell tpyes, as discussed earlier in chapter 3 and 4, or differences in the cellular mechanisms leading to the formation of these alternate forms of variant B between the two cell lines. Only analysis in D4O7 cells was carried out in this study.

To further investigate whether cystatin C is the protein corresponding to these bands, a cystatin C pull-down was performed from the media samples in order to reveal if the two bands are still present. Immunoprecipitation (IP) was carried out for the C-terminal FLAG-tagged constructs, using the anti-FLAG beads. Figure 5.3 shows immunoblots of media samples collected from D4O7 cells expressing wild-type or variant B cystatin C, prior to and after the protein pull-down. In addition to the main band, the two minor and slower migrating bands were also visualized after cystatin C pull-down, probing with either anti-cystatin C or anti-FLAG antibodies. This further substantiates that the two bands correspond to alternative forms of cystatin C.

Identification of the proteins in these bands was further characterised by mass spectrometry analysis of cystatin C pull-down samples from the conditioned media. Immunoprecipitates obtained from conditioned media of cells transfected with FLAG-tagged wild-type or variant B cystatin C or non-transfected cells (used as negative control), were subjected to SDS-PAGE and visualized by coomassie blue staining (Figure 5.4.), where it was also possible to visualize the two slightly slower migrating extra-bands. These bands, along with the major 13 kDa band corresponding to cystatin C, were isolated for all three samples (E1-E9 fractions as shown in figure 5.4.) and qualitatively analysed by mass spectrometry. Table 8 shows the proteins identified for each sample using the Mascot search engine and subsequent analysis using the proteasome software Scaffold. For each protein identified in each band, the exclusive unique spectra count and the percentage of coverage are reported in the first and second line, respectively. The number of unique spectra represents the number of distinct spectra associated only with the protein identified. Therefore it gives indication of the proteins detected in the sample and a rough estimate of their amount present. However, as discussed in material and methods, the peptide mapping analysis utilised here does not provide accurate protein quantification, so it was mainly used for protein identification. The percentage coverage is the percentage of all the amino acids in the protein

sequence that were detected in each sample, which gives an indication of the confidence that the identification assigned to each protein is correct.

Results show that cystatin C is the most abundant protein identified in all the fractions isolated from the transfected cells, E1-E3 for the wild-type and E4-E6 for the variant B, which correspond to the major correct sized band of cystatin C and to the size of the two extra-bands observed in the media sample of the variant B. As expected, cystatin C was found in lower abundance in the untransfected cells (E7-E9). Surprisingly, the cystatin C protein was identified within the two additional bands in both wild-type and variant B samples (E1/E2 and E4/E5 respectively). Percentage coverage gives us a high confidence that the protein identified is correct. For the other proteins detected, a very small number of unique spectra have been found, indicating that they are present at very low amounts. Moreover, the percentage coverage is also very small, thus not giving a high confidence of their presence. As the mass of proteins expected to be found at those sized bands analysed is in the range of 13-20kDa, all the larger molecular weight proteins revealed are likely contaminants. Furthermore, they are often present in the negative control. Regarding the protein within the right range, such as Protein IGKV2D-29 (Fragment), Calmodulin, Cofilin-1 and Peptidyl-prolyl cis-trans isomerase A, they are intracellular proteins that are therefore most likely contaminants present in small amount, as they show a very low number of unique spectra as well as of percentage coverage. And they are also often present in the untransfected control. Overall, this data indicates that the two extra bands most likely correspond to cystatin C proteins.

a) Untagged CysC constructs

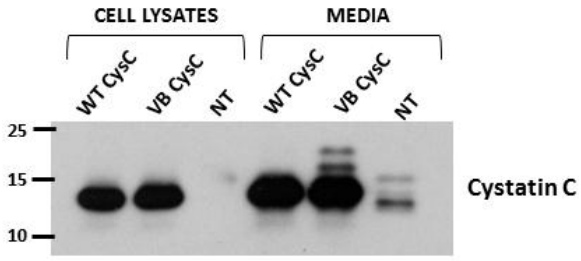

b) FLAG-tagged CysC constructs

c) HA-tagged CysC constructs

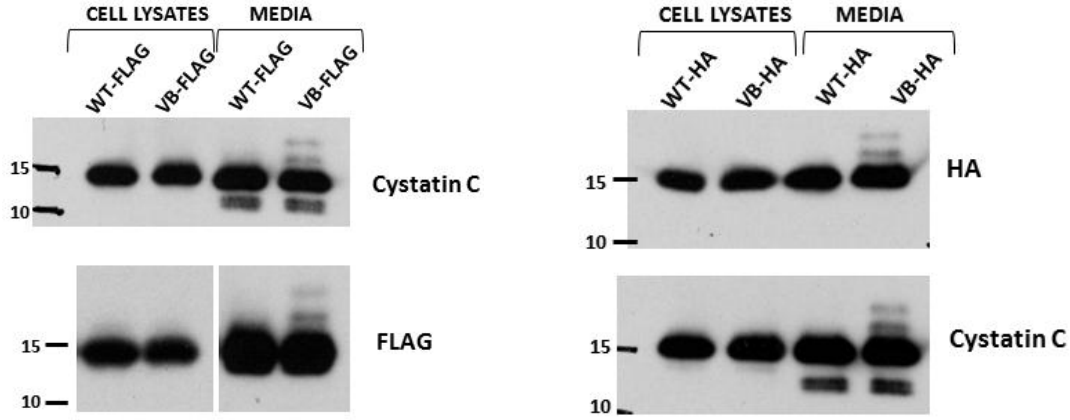

Figure 5.1 - Immunodetection of untagged and C-terminal tagged cystatin C constructs in D4O7 cells. Immunoblots of cell lysates and conditioned media collected from cells expressing respectively wild-type or variant B cystatin C untagged (a) or tagged to FLAG (b) or HA (c). Western blots were probed with anti-cystatin C antibody, which detected all the cystatin C constructs, anti-FLAG or anti-HA antibodies for FLAG- and HA-tagged constructs, respectively in figure b) and c).

a) Untagged CysC

b) HA-tagged CysC

c) FLAG-tagged CysC

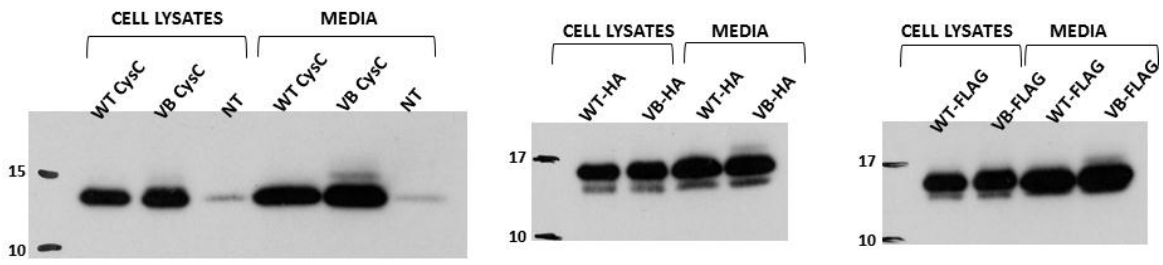

Figure 5.2 - Immunodetection of untagged and C-terminal tagged cystatin C constructs in ARPE19 cells. Immunoblots of cell lysates and conditioned media collected from cells expressing respectively wild-type or variant B cystatin C untagged (a) or tagged to HA (b) or FLAG (c). Western blots were probed with anti-cystatin C antibody, which detected all the cystatin C constructs, and the endogenous cystatin C.

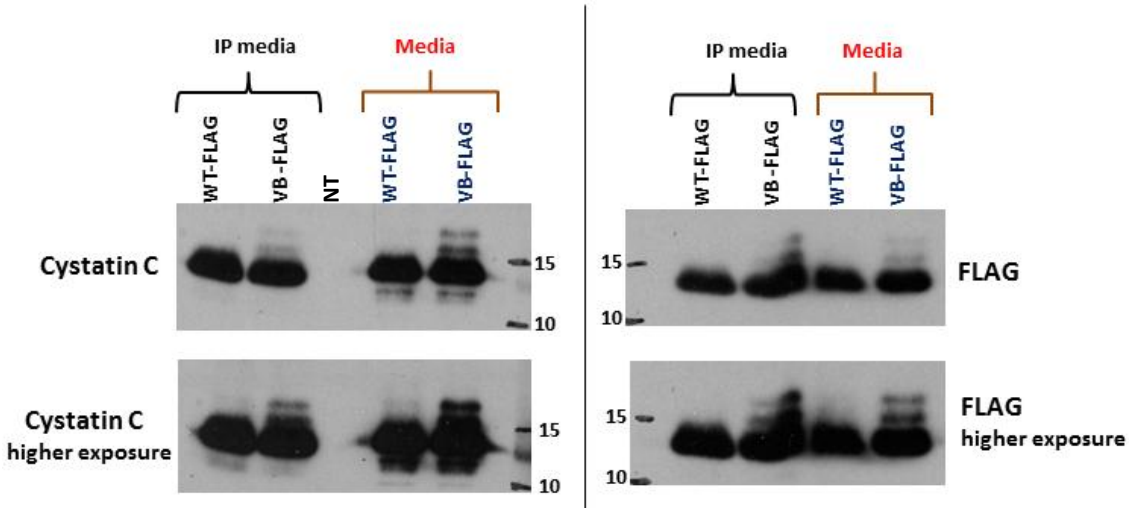

Figure 5.3 - Immunodetection of FLAG-tagged cystatin C constructs after protein pull-down from conditioned media of D4O7 cells. Immunoblots of conditioned media collected from cells expressing FLAG-tagged wild-type or variant B cystatin C or non-trasfected (NT), probed with anti-cystatin C or anti-FLAG antibodies. Conditioned media prior to immunoprecipitation was also loaded.

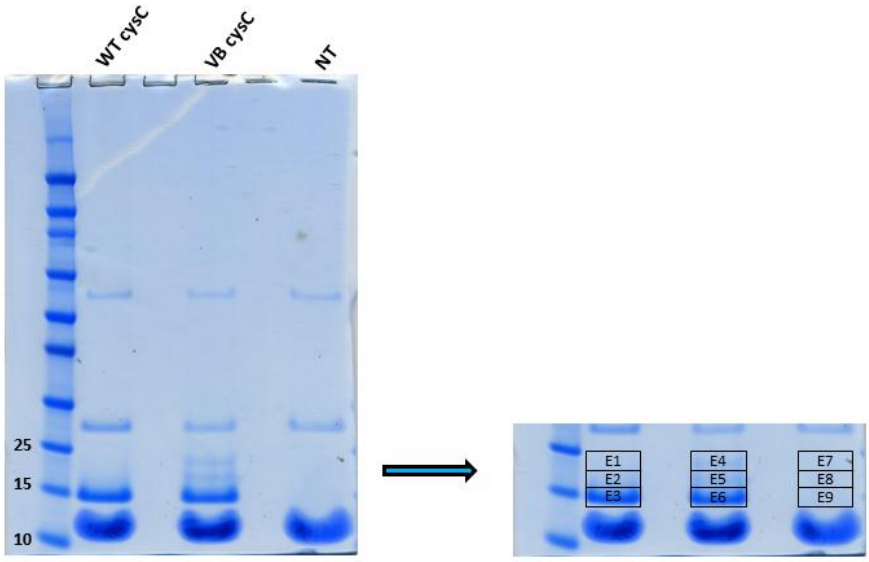

Figure 5.4 - Coomassie blue staining of FLAG-tagged cystatin C after protein pull-down from conditioned media of D4O7 cells. Conditioned media collected from cells expressing FLAG-tagged wild-type or variant B cystatin C or non-transfected (NT) cells were loaded on gel after immunoprecipitation and visualized by coomassie blue staining, prior to mass spectrometry analysis. Fractions E1-E9, corresponding to the main cystatin C band and the two additional bands, were cut from the gel for subsequent analysis.

Table 8 - Mass spectrometry analysis. Bands were extracted from the gel in figure 5.4., subjected to in-gel digestion using trypsin and analysed by mass spectrometry. Proteins identified in each fraction (E1-E9) by using Mascott are reported in the table below, showing, for each of them, number of exclusive unique spectra in the first line and percentage coverage in the second line.

#	Identified Proteins	Molecular Weight	E1	E2	E3	E4	E5	E6	E7	E8	E9
1	**Cystatin C**	**16 kDa**	**22**	**33**	**20**	**30**	**31**	**38**	**8**	**3**	**0**
			64%	**68%**	**57%**	**68%**	**68%**	**68%**	**45%**	**19%**	**0**
2	Desmoplakin	332 kDa	9	1	14	4	0	0	2	0	0
			3.0%	0.24%	4.7%	1.3%			0.84%		
3	Isoform of P02768, Serum albumin	69 kDa	5	4	4	4	3	0	2	4	4
			9.4%	7.8%	9.9%	8.1%	6.5%		3.3%	7.8%	7.8%
4	Protein IGKV2D-29 (Fragment)	13 kDa	2	2	2	2	2	0	1	2	2
			17%	17%	17%	17%	17%	0.00	11%	17%	17%
5	Calmodulin	17 kDa	3	3	4	2	4	0	0	0	0
			20%	24%	27%	10%	22%		0.00		
6	Hornerin	282 kDa	6	0	10	6	0	0	5	0	0
			4.0%		6.4%	3.8%	0.00		2.7%		
7	Cofilin-1	19 kDa	4	0	7	5	0	0	1	0	0
			34%		54%	41%			6.6%		
8	Junction plakoglobin	82 kDa	3	1	1	2	0	0	2	0	0
			6.3%	1.3%	1.6%	4.0%			4.7%		
9	Desmoglein-1	114 kDa	2	0	3	2	0	0	2	0	0
			3.1%		4.7%	2.9%			3.3%		
10	Peptidyl-prolyl cis-trans isomerase A	18 kDa	2	0	2	4	0	0	0	0	0
			12%	0.00	12%	25%	0.00		0.00		
11	Filaggrin-2	248 kDa	3	0	3	2	0	0	1	0	0
			1.4%		1.7%	0.96%			0.50%		
12	Isoform of P04406, Glyceraldehyde-3-phosphate dehydrogenase	28 kDa	1	0	2	1	0	0	1	0	3
			5.4%		12%	5.4%			5.4%		13%

5.3. O-glycosylation events appear to characterise an alternative form of variant B cystatin C

Results obtained in the previous section indicate that the two additional bands detected in the secretion media represent cystatin C proteins. The two bands show slightly slower migration by SDS-PAGE than the usual form of cystatin C. These shifts in molecular mass may be due to the presence of post-translational modifications. Cystatin C is thought to be a non-glycosylated member of the cystatin family (Paraoan, Grierson 2007). However, Nilsson et al. have reported that the variant B undergoes an O-glycosylation event, as a result of an alternative cleavage of the precursor (Nilsson et al. 2009). For this reason, glycosylation modification was analysed in this section.

Both N-linked and O-linked glycosylation were analysed. N-linked glycosylation occurs in the ER compartment, during the protein's co-translational translocation, as soon as the acceptor site is exposed to OST in the lumen of the ER (Chavan, Yan & Lennarz 2005). Subsequently, the attached glycan can be further modified in the Golgi apparatus (Stanley 2011). O-linked glycosylation can occur only after protein translation, in either the ER or the cis-Golgi, on Serine or Threonine residues within the protein (Stanley 2011). Then, it can be also subsequently modified in the other Golgi compartments. For this analysis, untagged cystatin C constructs were used.

Analysis of N-linked glycosylation was performed by EndoH and PNGaseF treatment of media samples from transfected D4O7 cells, which can cleave only N-glycans, added in the ER, and complex/hybrid glycans generated in the Golgi apparatus, respectively, as described previously. Figure 5.5 shows an immunoblot of conditioned media from D4O7 cells transfected with wild-type or variant B cystatin C or non-transfected cells, either treated or not with EndoH or PNGaseF. The two extra-bands are not removed after either treatment, indicating that the increased mass of cystatin C is not due to an N-linked glycosylation. The functionality of these

enzymes was confirmed earlier with the Glyco-cysC constructs as positive controls (section 3.5.2).

Analysis of O-linked glycosylation was carried out by using a deglycosylation enzyme mix, consisting of five different glycosidases able to remove both N- and O-linked glycans (see section 2.4.4). Figure 5.6 (a) shows an immunoblot of conditioned media from D4O7 cells transfected with variant B cystatin C treated or not with the deglycosylation mix. Both bands seem to disappear after treatment. However, after prolonged exposure, the intermediate band appeared to be still present. Because of the components present in the enzyme mix (e.g. glycerol), the bands were noticeably distorted. To exclude the possibility that the extra-bands are not visible because of the distorted migration, the enzyme mix was added to samples and then either incubated at 37°C or left on ice for 5-hours to allow or not the enzymes to act. Figure 5.6 (b) shows the immunoblot of these samples treated with (+) or without (-) incubation. Although the intensity and shape of the bands are affected by the mix, at longer exposure times it is still possible to detect the largest band in the treated samples without incubation. In contrast, in the incubated samples the slowest migrating band had disappeared. The intermediate band, on the contrary, seemed still to be present in both samples. A positive control was used to ensure that the enzyme mix worked (Figure 5.6 (c)). These results suggest that the shift in apparent molecular mass of at least one of the alternative forms of cystatin C, detected for the variant B, is likely due to an event of O-glycosylation. However, the intermediate band was not affected by the treatment, thus indicating that its different molecular weight may not be due to O-glycosylation events.

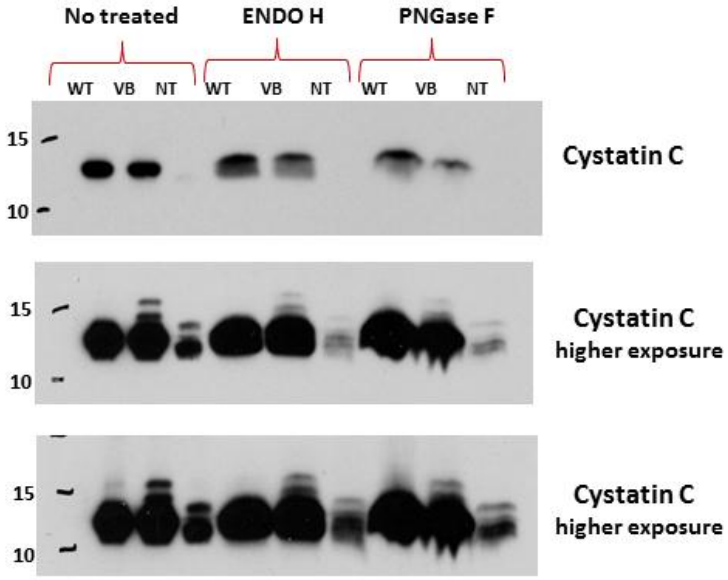

Figure 5.5 - Immunodetection of untagged cystatin C in conditioned media of D4O7 cells subjected to N-linked deglycosylation treatment. Conditioned media collected from D4O7 cells transfected with untagged wild-type or variant B cystatin C or non-transfected, were treated with EndoH or PNGaseF glycosidases and subsequently analysed by immunoblotting probing with anti-cystatin C antibody. Non-treated samples were also loaded as control.

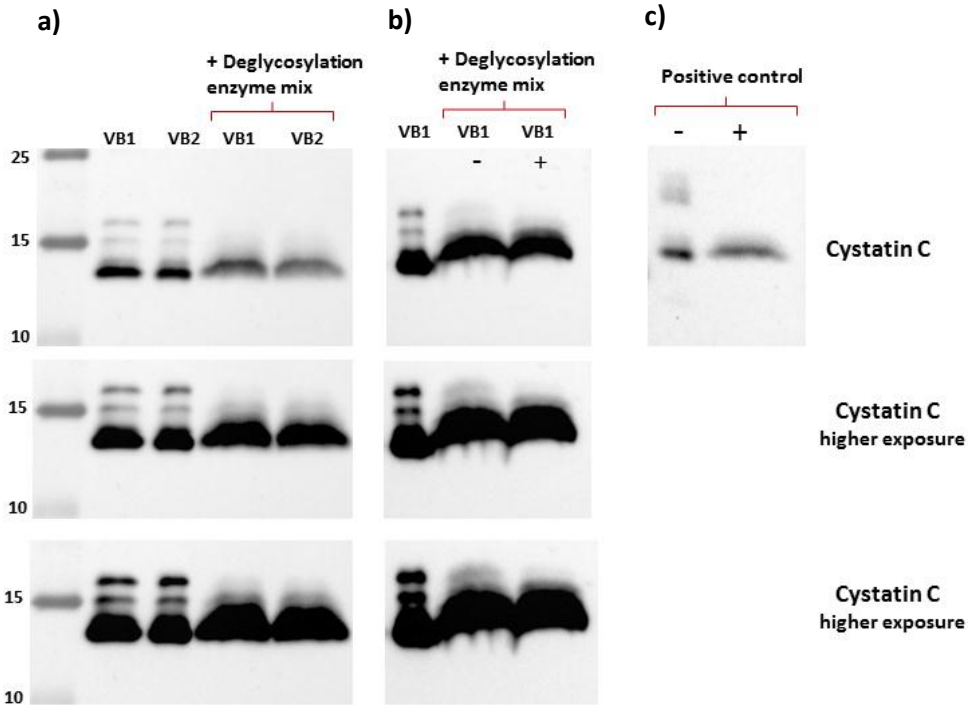

Figure 5.6 - Immunodetection of untagged cystatin C in conditioned media of D4O7 cells subjected to deglycosylation treatment. Conditioned media collected from D4O7 cells transfected with untagged variant B cystatin C constructs were treated with

Deglycosylation enzyme mix and subsequently analysed by immunoblotting with anti-cystatin C antibody. a) Immunoblot showing two media samples treated or not with the deglycosylation enzyme mix. b) Immunoblot showing media samples non-treated (first line) and treated with the mix and either incubated (+) or not (-) for 4 hours (second and third line respectively), to evaluate the effect of the mix on the shape of the bands. c) Positive control, consisting of Glyco-cystatin C constructs treated or not with the enzyme mix.

5.4. Discussion

The signal sequence of cystatin C consists of 26 amino acids located at the N-terminus of the mature protein (Figure 5.7). Mutations within this sequence, at the penultimate residue, generates the variant B cystatin C, which has been found, in human cerebrospinal fluid, to be alternatively cleaved between the residues Ala-20 and Val-21 of the signal peptide (Nilsson et al. 2009). This results in a six residues longer mature protein, which still carries the A25T mutation. Furthermore, an O-linked glycosylation was found to be present in this alternative processed variant B form, which is suggested to be on Ser27 or Ser28 residues, near the traditional Gly-26 cleavage site, or on the mutated Thr25 residue, still present in the mature form (Nilsson et al. 2009). Furthermore, prediction software for signal sequence, such as SignalP, has also confirmed the presence of a second potential cleavage site for the precursor Cystatin C (Nguyen, Hulleman 2016), either wild-type or variant B, with similar propensity compared to the conventional cleavage site at Gly-26. This alternative site is predicted to occur at the same Ala-20 position, reported by Nilsson et al. (2009) for the variant B.

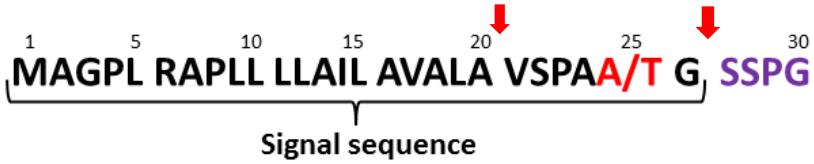

Figure 5.7 - Signal sequence of cystatin C. Amino acid sequence of the wild-type or variant signal peptide, residues 1 to 26, plus the first 4 amino acids of the mature protein. An alternative cleavage may occur at position Ala20-Val21.

The presence of secreted mature proteins larger than the expected sized cystatin C, observed in this study, can be therefore due to the alternative cleavage that generates a longer processed protein and, most likely, to the presence of a post-translational modification, such as O-glycosylation. The addition of these six amino acids would increase the molecular weight of the mature protein by approximately 530 Da, while the attached glycan would result in a further increase in molecular weight dependent upon its structure and composition.

Since these alternative forms are detected in the conditioned media, it is unlikely that they represent the unprocessed precursor protein as it would not go through the secretory pathway. These processed/secreted forms are therefore more likely to be generated by an alternative form of protein processing.

The aim of the work presented in this chapter was to identify the nature of the two bands, whether they correspond to alternative forms of cystatin C and, if this is the case, investigate the cause that determines these partial shifts in the size of the protein. The presence of alternative forms generated only in the case of the variant B may explain its link to diseases.

Results obtained in section 5.2 strongly indicate that the two bands observed in the media from D4O7 cells expressing the variant B correspond to cystatin C proteins. They have been indeed revealed by immunoblotting using different constructs and probing with different antibodies, thus excluding unspecificity of the antibody used. Furthermore, the two bands were also detected after cystatin C pull-down, also probing with different antibodies, which confirms the nature of the two larger proteins. Finally, in agreement with immunoblotting and IP results, the extra bands for variant B were identified as cystatin C also by mass spectrometry analysis. Interestingly, cystatin C protein was detected at the size of the two extra bands also in the wild-type sample. This is likely due to the higher sensitivity of mass spectrometry, compared to coomassie staining and immunostaining, that is able to detect the alternative forms of cystatin C for the wild-type, even though there were no visible bands on the gel/blot, meaning that they are present in very small amount. In only one of the blots shown (figure 5.5), it was actually possible to detect these extra bands also for the wild-type cystatin C, even though in lower levels compared to the variant B, as well as for the endogenous protein.

The peptide mapping analysis performed by mass spectrometry in this study only permits a qualitative characterization of the proteins. The in-gel-digestion approach used prior to the analysis, does not give accurate protein quantification due to variability in the gel cutting and protein extraction efficiency from the gel. The

intensity of protein bands, observed on both gels and blots, therefore provides a more reliable relative quantification information than mass spectrometry, thus indicating that the amount of these alternative forms of cystatin C is higher in the case of the variant B. Other proteins revealed in this analysis are most probably contaminants. They are present at lower level compared to cystatin C, the confidence of their identification is low and they are often detected in the negative controls. Moreover, alternative forms of cystatin C were revealed also for the wild-type (E1 and E2), with a number of unique spectra comparable to those seen for variant B, despite no visible bands on the blot/gel. This further suggests that proteins detected with spectra counts much lower than the cystatin C in E1 and E2 fractions, must be present at insignificant levels.

The shifts in molecular mass identified by immunoblotting suggested that there might be a post-translational modification and/or a shift in signal sequence cleavage. Based on mass spectrometry results, it suggested that this phenomenon can also occur for the wild-type cystatin C, but at a lower frequency. The A25T mutation seems therefore to increase the frequency with which the alternative cleavage normally occurs, as observed earlier by Nguyen and Hulleman (2016). However, that study showed that the higher propensity to undergo cleavage at Ala-21 in the case of the variant B occurred only under certain experimental conditions. These consisted of introducing modifications, by addition or substitution of amino acid residues, in the region close to the Gly-26 site of cleavage. In the presence of these modifications, all the variant B proteins produced and secreted corresponded to the alternative cleaved form, suggesting that these modifications exacerbated the effect of the variant B mutation. In our study, where no additional modifications were introduced, these alternative forms are only present at very low levels, compared to the normal sized protein. Nilsson et al (2009) have revealed the presence of the miscleaved variant B, carrying O-glycans, by studying the glycoproteome in the CSF of human donors, therefore only analysing proteins carrying sugar molecules. Hence, in the CSF samples analysed in their study it

cannot be excluded the presence, along with this alternative form, of canonically cleaved, non-glycosylated variant B proteins.

After having identified the nature of the proteins corresponding to the two extra bands, the cause of their shifts in size was investigated in section 5.3. In particular, glycosylation events were analysed. Results indicate that no N-linked glycosylation occurs, consistent with the lack of N-glycosylation acceptor sites within the sequence of cystatin C, whereas an O-linked glycosylation appears to characterise the largest band present in the conditioned media, thus confirming results obtained by Nilsson et al. (2009). Nguyen et al. also have reported, by using O-glycosylation prediction software, that the Variant B cystatin C has a higher probability to undergo O-glycosylation compared to the wild-type protein (Nguyen, Hulleman 2016). Therefore, the amino acid substitution at the position -2 may determine the conditions that facilitate the occurring of the alternative cleavage at Ala-21, generating a form of cystatin C that is more inclined to O-glycosylation. However, the intermediate band, also observed in this study, appears not to be affected by the deglycosylation treatment. It may therefore represent the non-glycosylated form of the alternative cleaved cystatin C. Another possibility is the presence of a third alternatively cleaved form of cystatin C, at the Ala-13 residue, reported by Nguyen et al. (2016), resulting in a 13 residue longer protein, whose size is consistent with the intermediate band detected in our study (Nguyen, Hulleman 2016).

In ARPE19 cells only one additional minor band was detected in the conditioned media by immunoblotting, also at higher molecular weight, in the case of the variant B, but no further characterization was carried out. However, it also indicates that there might be a difference in the processing of the variant B, resulting in an alternative form of cystatin C.

The second cleavage site at Ala-21, observed by Nilsson et al. (2009) and predicted by the use of specific software by Nguyen et al. (2016) is supported by the

presence, in the signal sequence of cystatin C, of another Ala-X-Ala motif, which often characterises the -1 and -3 residues of a signal peptide (Auclair, Bhanu & Kendall 2012), as described in section 1.5.1.2. Residues at these positions, usually consisting of small and neutral amino acids, are critical for the signal peptidase interaction and therefore for specifying the site of cleavage (Nothwehr, Gordon 1990, Auclair, Bhanu & Kendall 2012). Cleavage at the site between residues 21 and 22 of the precursor cystatin C is therefore also predicted by the (-1,-3) rule, as alanine residues occupy positions 18 and 20 (figure 5.7).

The presence of Thr instead of Ala at -2 position may have an effect on the orientation of the c-region of the signal peptide at the active site of the signal peptidase, resulting in a less favourable interaction between the usual cleavage site (Gly-26) and the enzyme. Conversely, it may facilitate at the same time SPC interaction with the alternative site at Ala-21, which has probably become more accessible to signal peptidase. However, the effect of the A25T mutation on the position of the signal sequence is probably subtle, as the conventional mature protein is still obtained with much higher frequency compared to the alternative one, even in the case of the Variant B, where it represents only a partial minor fraction of the total processed protein. However, the higher presence of these alternatively glycosylated proteins may have an effect over time if they accumulate in the extracellular matrix.

Alteration of the cleavage position modifies the amino acid composition of the mature protein, resulting in additional residues at its N-terminal. This may affect the protein folding, which, in turn, could allow specific acceptor amino acids to be conformationally accessible for O-glycosylation, and ultimately influence function and stability of cystatin C. O-glycosylation can affect many aspects of a protein, as folding, function and stability (Steen et al. 1998), which could influence the proteolytic regulation of cystatin C in the extracellular matrix. It is therefore important to understand how this alternative form can affect cystatin C properties.

Glycosylation represents one of the main post-translational modifications, which has been shown to play a role in many biological processes (Steen et al. 1998). O-glycans have been found to monitor the status of the protein folding and to ensure their proper sorting to specific cellular compartment. They can modulate protein expression, their proteolytic processing, influence their structure and solubility, and consequently affecting their stability and half-life (Steen et al. 1998, Bektas, Rubenstein 2011). For instance, some oligosaccharides have been shown to increase protein stability, conferring protease-resistance (Steen et al. 1998). Conversely, glycans have also been found to increase protein ubiquitination, thus promoting proteasomal degradation (Steen et al. 1998). In addition, they can also influence the quaternary structure, promoting protein aggregation (Steen et al. 1998). Furthermore, by affecting the conformation and stability of a protein, O-glycans could influence a protein biological activity (Steen et al. 1998). O-glycans have been described to be critical for some protein-ligand interactions, mediating their binding and/or the signal transduction (Steen et al. 1998, Bektas, Rubenstein 2011). Some O-glycans, in particular, can function as sensors in certain stress conditions, such as cell starvation and oxidative stress, promoting cell adaptation and survival by regulating gene expression and activity of signalling molecules, enzymes, structural proteins and transcription factors (Steen et al. 1998, Bektas, Rubenstein 2011). Improper glycosylation of these proteins has been shown to play a role in human diseases (Bektas, Rubenstein 2011). Interestingly, defects in glycosylation have been observed in several proteins involved in AD pathogenesis and neuronal function (Schedin-Weiss, Winblad & Tjernberg 2014). This indicates that O-glycosylation modification plays an important role in protein biogenesis.

As mentioned above, the alternative processed form of cystatin C would have six additional amino acids at the N-terminus and an O-glycosylation likely residing in this region. Importantly, the N-terminal region of the mature cystatin C is critical for functional and regulatory mechanisms of the protein. The N-terminal segment, particularly the residues at positions 8-11 (Arg-Leu-Val-Gly), is essential for the protease inhibition function of cystatin C (Abrahamson et al. 1991). This region

ensures the optimal interaction with the target peptidase and is responsible for the initial binding to its target cathepsins (Abrahamson et al. 1991, Nycander et al. 1998). Cystatin C inactivation and regulation also depends on the N-terminal regions. Its proteolytic degradation occurs through its N-terminal truncation by different types of proteases, as described in section 1.2.2, so that its inhibitory capacity is removed (Abrahamson et al. 1991, Popovič et al. 1999). Furthermore, it has also been found that cystatin C uptake is dependent on the integrity of the N-terminal segment; cleavage or amino acid substitution within this region has been shown to affect internalization of the protein (Wallin, Abrahamson & Ekstrom 2013). Finally, during the process of dimerization it has been found that the inhibitory regions of cystatin C, including the N-terminal chains, are buried within the dimer interface, so that its activity is inhibited (Ekiel, Abrahamson 1996) and N-truncated forms of cystatin C have been reported to be more prone to dimerization and aggregation (Janowski et al. 2004). Structural integrity of the N-terminal region of cystatin C is therefore crucial for its correct functionality and regulation.

The presence of additional residues and the O-glycosylation in this region may therefore affect cystatin C inhibitory function, its inactivation, internalization or the dimerization process. As a consequence, in the first two cases, there would be an increase or decrease of cathepsin activity resulting in an imbalance of proteolytic activity in the extracellular matrix. If the uptake is prevented, there would be a dysregulation of proteolysis both intracellularly, in the lysosome, and extracellularly. Proteolytic dysfunction, both inside and outside the cell, can be linked to AMD and AD. A similar effect would occur in case the dimerization mechanism is disrupted, increasing or reducing the level of active protease inhibitor. Increased tendency for dimer formation could lead to generation of protein aggregates which may affect cystatin C functionality and sequester functional wild-type proteins reducing inhibitory function. Presence of the aggregates themselves can also be disruptive for proper cell function. Interestingly, cystatin C has been detected in β-amyloid plaques, even though its role is still controversial (section 1.3.3), as it has been reported to either inhibit or contribute to their formation (Kaur, Levy 2012). It is possible that cystatin C has a different

effect on the β-amyloid plaques depending on its status, and thus contributes to plaque formation when present as alternative glycosylated form. If this is the case, the presence of these alternative forms, at higher abundance in the case of the variant B may explain its link to AD. Furthermore, β-amyloid peptides have been also described in the drusen deposits (Zhao et al. 2015, Feng, Wang 2016), suggesting a possible role of cystatin C also in AMD pathogenesis.

O-glycans can modify protein stability, making cystatin C more resistant or susceptible to degradation. In the first case, the presence of this fraction may become significant in the long-term. That would be even more relevant in condition of decreased activity of the cellular proteolytic system, as occurs in aging and age-related diseases (Vilchez, Saez & Dillin 2014, Hipp, Park & Hartl 2014). If this fraction is not rapidly degraded, it might result in its accumulation over time, and especially for the variant B where this alternative form occurs at higher frequency. The gradual higher presence of this alternatively processed, secreted form may affect the proteolytic regulation in the extracellular matrix, depending on its effect on the protein (as discussed above). Another possibility is that the glycosylation occurring on alternatively cleaved cystatin C may, for example, act as a signal to convey to the cell the miscleavage and so send it for degradation or could target the protein to a different cellular compartment.

Some members of the secretory type 2 family of cystatins (e.g. cystatin E/M, F) have been reported to carry glycosylation and differ in function and substrate selectivity compared to cystatin C (Ni et al. 1998, Soh et al. 2016, Hamilton et al. 2008). Glycosylation may therefore influence the target selectivity of the protease inhibitor. Furthermore, N-glycans could be responsible for targeting cystatin F to endosomal-lysosome pathway, likely upon internalization of secreted proteins (Cappello et al. 2004), thus playing a role in the protein targeting. On the contrary, Cystatin C was always believed not to carry any glycosylation. Nilsson et al. (2009) for the first time have shown that glycosylation can also occur on cystatin C, even

though this was observed only for the variant B protein. Interestingly, several N- and O-linked glycoforms of the rat homologue of cystatin C have been found to be produced and secreted in adult rat hippocampal derived stem/progenitor cells (Dahl et al. 2004). N-glycans were described to be essential for bioactivity of cystatin C and contribute to stimulate neurogenesis in rat hippocampus, for the proliferation of adult neuronal stem cells (Dahl et al. 2004). Moreover, rat glycosylated form of cystatin C was also shown to induce proliferation of neural progenitor cells derived from human brains, thus suggesting a role of glycoforms in human cells (Dahl et al. 2004). Several O-glycosylated forms of cystatin C have been also shown to be secreted in mouse primary neurons in association with exosomes, a mechanism that seems to be involved in both AD and AMD pathogenesis (Wang et al. 2009, Tong et al. 2016, Vella et al. 2008, Ghidoni et al. 2011b).

Overall, this suggests that glycosylation may also occur for the human cystatin C protein, although to a minor extent, and this could affect its function, stability and targeting. Glycosylation appears to occur especially in the case of the variant B, thus suggesting a possible link of the protein with the increased risk of disease development.

Further analysis of the mechanisms of cystatin C regulation was carried out and is discussed in the next chapter.

Chapter 6 - Analysis of cystatin C protein regulation

6.1. Introduction

Intracellular processing and trafficking of the variant B cystatin C have been mainly investigated in earlier reports. Since the A25T mutation occurs in the leader sequence, it was expected to have an effect on these cellular mechanisms, thus affecting localization and secretion of the protein.

Based on the results obtained in this study and presented in the previous chapters, trafficking and secretion of variant B was shown not to significantly differ from that of wild-type cystatin C (chapter 3). Regarding the cleavage of the signal peptide, results suggested a less efficient processing for the variant B precursor, generating an uncleaved or alternatively cleaved product (chapter 4 and 5). However, no direct consequences in the short-term, such as mislocalization of the precursor protein or substantial change in the level of secreted proteins were identified.

The aim of the work presented in this chapter was to further investigate possible differences between the two forms of cystatin C that could explain the link of the variant B with the increased risk of developing AD and AMD conditions. For this purpose, several aspects of protein regulation were explored, such as degradation, as well as mechanisms of regulation typical of cystatin C protein, such as dimerization and internalization. These aspects were evaluated within the wild-type and variant proteins. Furthermore, preliminary identification of proteins that may differentially interact with the two forms of cystatin C, was carried out to identify possible differences between wild-type and variant B.

6.2. Analysis of degradation pathways

Degradation pathways were examined to analyse the protein stability of variant B cystatin C, which could affect the cellular concentration of the protein and consequently its protease inhibition activity in the cell.

The two main proteolytic mechanisms include the ubiquitin-proteasome system (UPS) and the autophagy-lysosome pathway (ALP), both essential for the maintenance of cell homeostasis (described in section 1.2.3.1). The UPS is mainly

involved in degradation of misfolded proteins, which, if not removed, can cause ER stress and aggregation of damaged proteins in the cytosol (Amm, Sommer & Wolf 2014). The ALP is involved in the removal of extracellular and membrane proteins as well as cytosolic large protein aggregates and damaged organelles (García-Arencibia et al. 2010, Chang et al. 2015). They are therefore both fundamental components of quality control to guarantee protein turnover, regulate protein concentration and remove toxic, damaged cellular components (Hipp, Park & Hartl 2014, Vilchez, Saez & Dillin 2014). Impairment in both degradative systems has been reported to occur in aging and be involved in several degenerative conditions, including AMD and AD (Cheung, Ip 2011, Nedelsky, Todd & Taylor 2008, Hipp, Park & Hartl 2014, Vilchez, Saez & Dillin 2014).

Cystatin C inactivation occurs by proteolytic cleavage both in the extracellular environment and in the intracellular lysosomal compartment by the action of various proteases, such as cathepsin D and L, elastase and MMP2 (Abrahamson et al. 1991, Lenarčič et al. 1991, Dean et al. 2007, Laurent-Matha et al. 2012). Removal of the intracellular cystatin C occurs in the lysosomes. However, if proteins are not properly folded they could be delivered, through the ERAD pathway, for proteosomal degradation. Variant B cystatin C has been hypothesised to be partially uncleaved or differently cleaved (as described in chapter 4 and 5). These alternative forms can result in misfolded and/or amyloidogenic proteins, with impaired function or stability, which could accumulate intra- and extra-cellularly. If misfolded proteins are not removed by the proteasome system, they can lead to formation of large protein aggregates, which then can be removed by autophagy and degraded in the lysosome (Buchberger, Bukau & Sommer 2010).

Therefore, both UPS and ALP pathways were analysed to investigate whether they are activated in the case of the variant B, to determine whether there is any impairment associated with this form of cystatin C. Analysis was carried out by evaluating the level of cystatin C following inhibition of either the UPS or ALP pathways using the inhibitors MG132 and Chloroquine (CQ), respectively. MG132 blocks the proteolytic activity of the 26S proteasome complex (Han et al. 2009, Zhan et al. 2016), whereas Chloroquine (CQ) inhibits lysosomal enzyme activity by

altering the intra-lysosomal pH, and prevents fusion of autophagosomes and endosomes with lysosomes (Solomon, Lee 2009). Cystatin C constructs tagged to FLAG or HA at the C-terminus were used in this analysis.

6.2.1. Inhibition of degradative systems affects equally wild-type and variant B cystatin C

ARPE19 cells transfected with HA-tagged wild-type or variant B cystatin C constructs were treated over-night with MG132 or CQ. Cell lysates and conditioned media were then collected and analysed by immunoblotting using anti-cystatin C antibody, which detects transfected and endogenous cystatin C. Non-transfected cells were also analysed as a control. Immunoblots using anti-GAPDH antibody were used as loading control.

Results obtained after MG132 treatment showed a reduction in the levels of both wild-type and variant B cystatin C constructs as well as of the endogenous cystatin C detected after higher exposure (Figure 6.1). However, no difference was apparent between wild-type and variant B levels after proteasome inhibition. A reduction of secreted proteins could be also observed in the conditioned media, probably as a consequence of the decreased intracellular level. Interestingly, in figure 6.1, the bands likely corresponding to the uncleaved precursor were enhanced after proteasome inhibition in both wild-type and variant B proteins.

Results obtained after CQ treatment displayed an increase in the levels of both wild-type and variant B cystatin C constructs as well as of the endogenous protein in ARPE19 cells, as compared to the non-treated controls (Figure 6.2). Also in the conditioned media an increase of secreted proteins could be observed.

The same analysis was performed in ARPE19 cells transfected with FLAG-tagged cystatin C constructs, shown in figure 6.3. Cell lysate and media were collected after over-night treatment with either MG132 or CQ and analysed by immunoblotting. Results obtained after proteasome inhibition showed again a reduction in the levels of cystatin C at a similar extent for both wild-type, variant B,

and endogenous cystatin C. However, results obtained after CQ treatment do not show the same extent of protein increase observed with HA tagged constructs.

Overall, there is no evidence for a difference in the effect of either ALP or UPS on cystatin C levels between wild-type and variant B proteins. However, a general effect on cystatin C protein, endogenous and transfected, consisting in a decrease or increase, seems to occur after UPS and ALP inhibition, respectively.

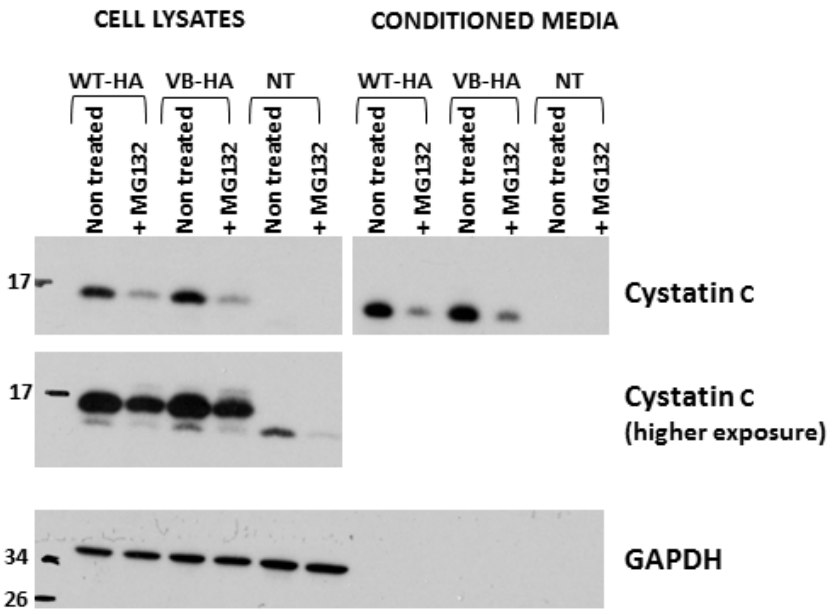

Figure 6.1 - Immunodetection of cystatin C in ARPE19 cells transfected with HA-tagged constructs after treatment with proteasome inhibitor MG132. Cell lysate and conditioned media samples collected from ARPE19 cells transfected with either wild-type or variant B constructs and subjected to UPS inhibition using MG132 (5µM) over-night were analysed by immunoblotting. Anti-cystatin C antibody was used to detect the transfected cystatin C constructs as well as the endogenous cystatin C visible at higher exposure. Anti-GAPDH antibody was used as loading control for cell lysates. Non-transfected cells were also analysed.

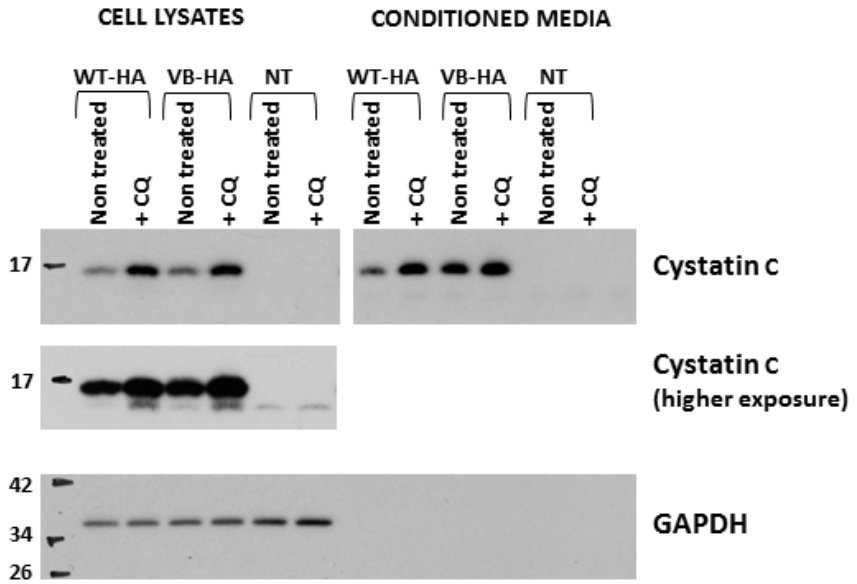

Figure 6.2 - Immunodetection of cystatin C in ARPE19 cells transfected with HA-tagged constructs after treatment with ALP-inhibitor chloroquine (CQ). Cell lysate and conditioned media samples collected from ARPE19 cells non-transfected and transfected with either wild-type or variant B constructs and subjected to ALP inhibition using CQ (25µM) over-night were analysed by immunoblotting. Anti-cystatin C antibody was used to detect the transfected cystatin C constructs as well as the endogenous cystatin C visible at higher exposure. Anti-GAPDH antibody was used as loading control for cell lysates. Non-transfected cells were also analysed.

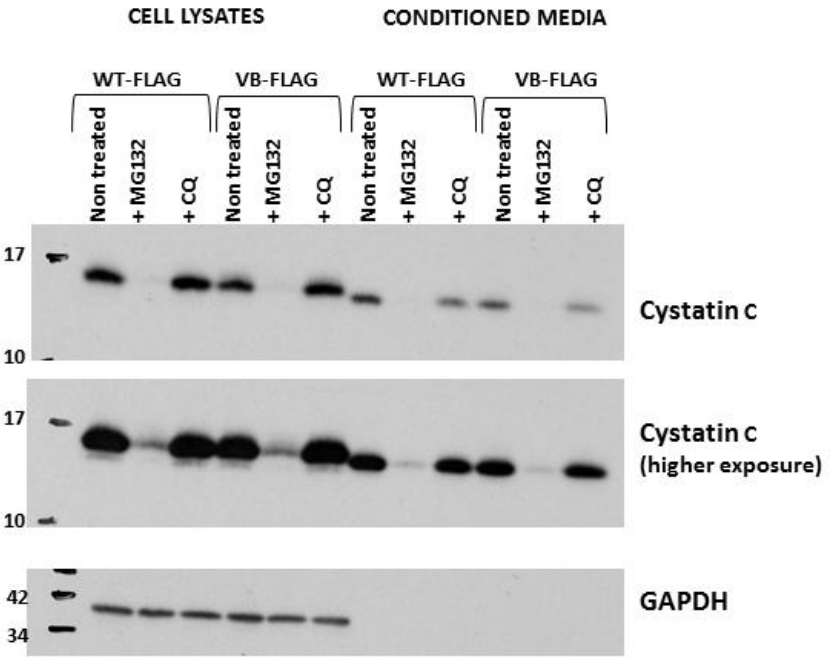

Figure 6.3 - Immunodetection of cystatin C in ARPE19 cells transfected with FLAG-tagged constructs after treatment with MG132 or Chloroquine (CQ). Cell lysate and conditioned

media samples collected from ARPE19 cells non-transfected and transfected with either wild-type or variant B constructs and subjected to MG132 (5μM) or CQ (25μM) over-night were analysed by immunoblotting. Anti-cystatin C antibody was used to detect the transfected cystatin C constructs as well as the endogenous cystatin C visible at higher exposure. Anti-GAPDH antibody was used as loading control for cell lysates.

6.2.2. Cystatin C expression increases after ALP inhibition and decreases after UPS inhibition

Since no difference was identified between wild-type and variant B levels and the same effect was obtained for both the transfected proteins and the endogenous cystatin C, the level of the endogenous protein only was further analysed in non-transfected ARPE19 cells. Immunoblotting analysis (figure 6.4 a) shows results obtained after CQ treatment over-night. The levels of endogenous cystatin C were quantified and normalised to the level of GAPDH. Quantification is reported in the graph in figure 6.4 b, with the level of cystatin C in the non-treated sample set to 1. Results showed a significant increase in cystatin C levels compared to the non-treated control, thus confirming the observation in figure 6.2.

The same analysis on endogenous cystatin C levels was performed on cells treated over-night with proteasome inhibitor MG132 (figure 6.5 a). Levels of cystatin C were quantified and normalised to the levels of GAPDH and results plotted in graph 6.5 b. Results showed a significant decrease in the level of endogenous cystatin C compared to the non-treated control. Proteasome inhibition seems therefore to have a particularly important effect on cystatin C levels. Such an effect could be due to an indirect regulation operating at the translational or transcriptional level.

To further investigate this aspect, the levels of mRNA expression of endogenous cystatin C were analysed by quantitative RT-PCR after over-night treatment with MG132. mRNA levels of cystatin C were normalised to levels of GAPDH and Ct values were measured in treated and not treated cells for comparison (figure 6.6 a). ΔCt values were plotted using a column bar graph (figure 6.6 b). No significant differences between cystatin C mRNA levels in MG132-treated and non-treated samples were found by using two different statistical tests.

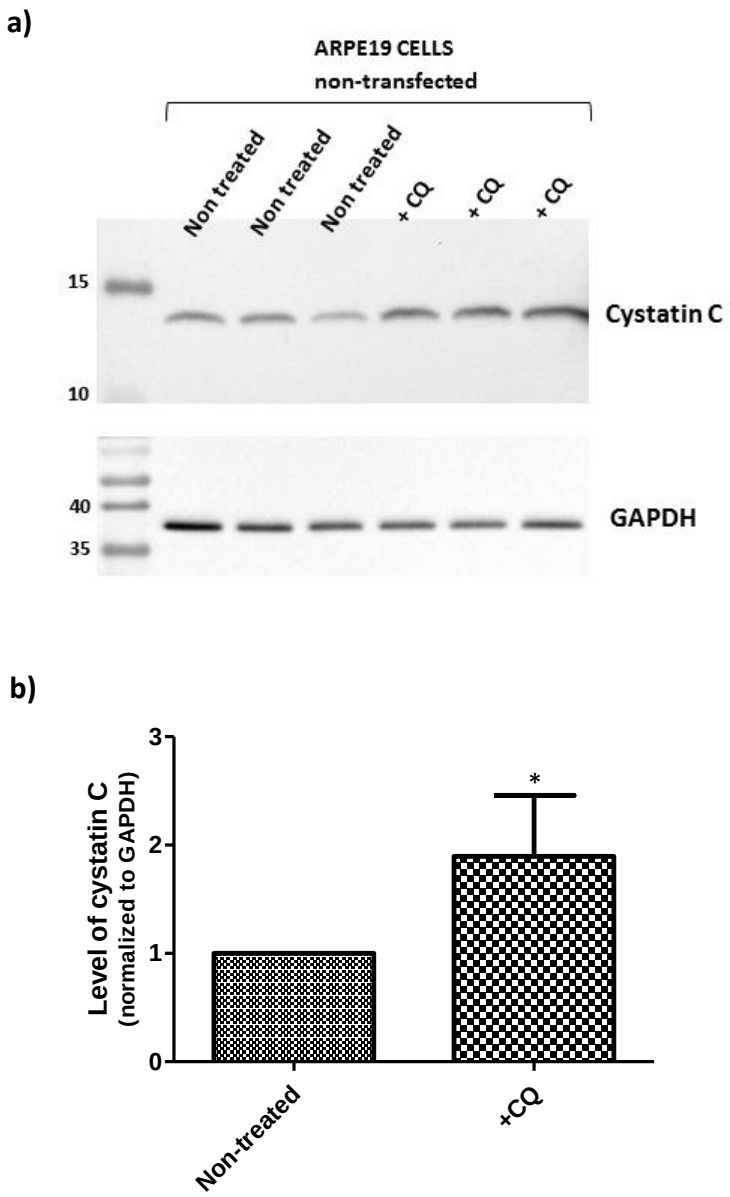

Figure 6.4 - Immunodetection of endogenous cystatin C in ARPE19 cells after treatment with Chloroquine (CQ). a) Cell lysates collected from ARPE19 cells subjected to CQ (25µM) treatment over-night were analysed by immunoblotting with anti-cystatin C antibody. Anti-GAPDH antibody was used as loading control for cell lysates. b) Levels of cystatin C were quantified by densitometry and normalized to level of GAPDH. Level of cystatin C in non-treated cells was set to 1. Level after treatment results 1.90 ± 0.56. Standard deviation is shown in the graph. One-sample t test (N=3), p=0.03 (*p<0.05)

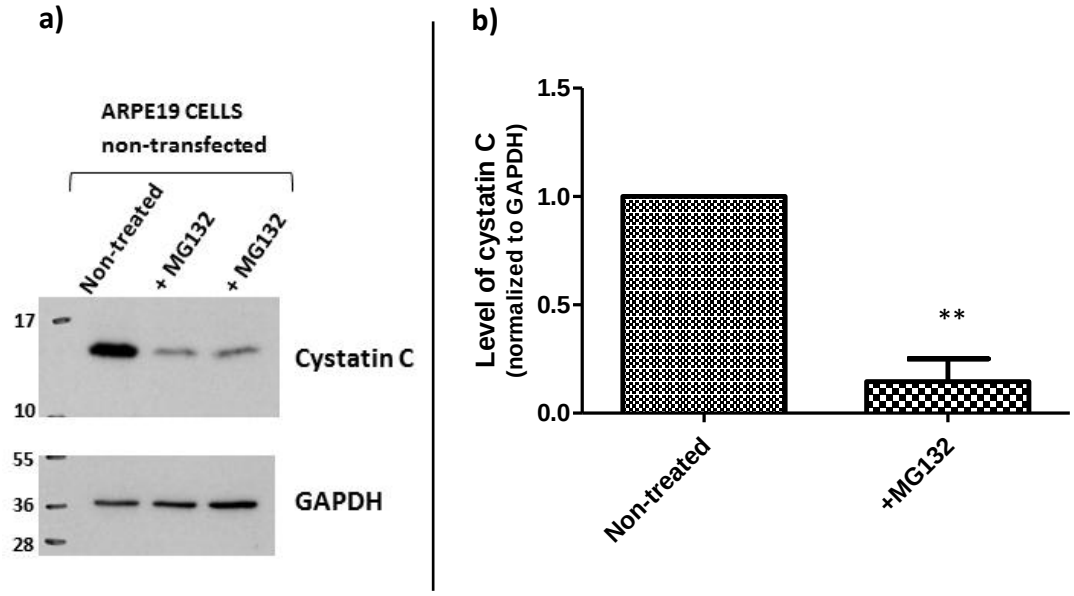

Figure 6.5 - Immunodetection of endogenous cystatin C in ARPE19 cells after treatment with MG132. a) Cell lysates collected from ARPE19 cells subjected to MG132 (5µM) treatment over-night were analysed by immunoblotting with anti-cystatin C antibody. Anti-GAPDH antibody was used as loading control for cell lysates. b) Levels of cystatin C were quantified by densitometry and normalized to level of GAPDH. Level of cystatin C in non-treated cells was set to 1. Level after treatment results 0.15±0.11. Standard deviation is shown in the graph. One-sample t test (two-tailed, N=3), p=0.005 (** p≤0.005)

a)

Exp1	**Non-treated**	**+MG132**
Average	0.275	0.227
StDev	0.037	0.012
Exp2		
Average	0.200	0.184
StDev	0.006	0.005
Exp3		
Average	0.230	0.229
StDev	0.018	0.009

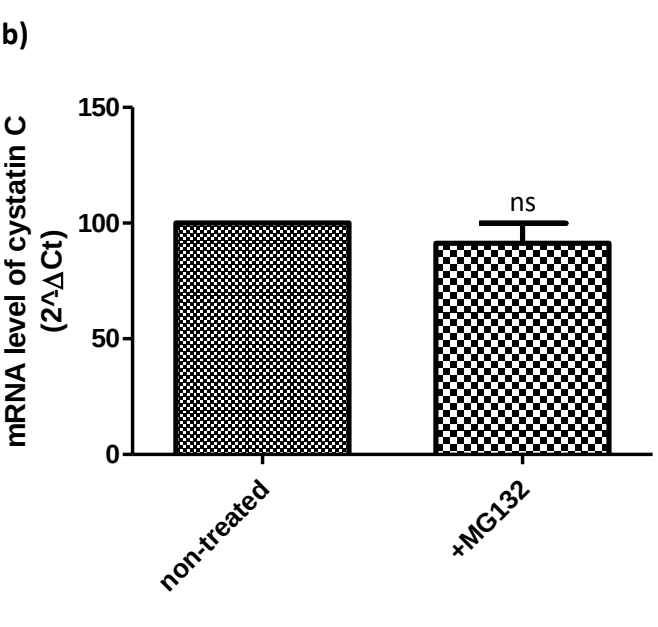

Figure 6.6 - Relative quantification of cystatin C mRNA in ARPE19 cells after proteasome inhibition. RNA was isolated from ARPE19 cells treated and non-treated with MG132 (5µM) over-night. cDNA was subsequently generated and analysed by qPCR. Comparative Ct method (ΔCt) was used for relative quantification. Data were normalized using human GAPDH and ΔCt values obtained in treated cells were compared to non-treated. 2^-ΔCt was calculated to assess whether there is a change of cystatin C mRNA expression. a)

Values of calculated 2^-ΔCt are reported in the table for three independent experiments. Paired t test (N=3), p=0.26 b) Data were plotted in bar graph with standard deviation shown. mRNA level of non-treated was set to 100% and level after MG132 treatment results 91.33% ± 8.56%. One-sample t-test (N=3), p=0.22, ns=non-significant.

6.3. Analysis of cystatin C dimerization shows no difference between wild-type and variant B

Protein dimerization is a mechanism that has been suggested to regulate level of active cystatin C in the cell, as in this conformation its activity is inhibited. This mechanism has been hypothesized to be involved in different cellular processes (described in section 1.2.2) and its impairment can lead to a proteolytic dysregulation and, more importantly, to protein aggregation (Janowski et al. 2001). Dimerization was particularly promoted in the case of the L68Q variant cystatin C that causes a severe form of amyloidosis (Wei et al. 1998, Rodziewicz-Motowidlo et al. 2006). The aim of the work presented in this section was to investigate whether a difference in the tendency of dimerization occurs between wild-type and variant B cystatin C proteins. If this is the case, a proteolytic imbalance or aggregation-related conditions may occur affecting cell functionality.

In order to analyse dimerization of intracellular cystatin C, RPE cells were co-transfected with both the FLAG-tagged and the HA-tagged cystatin C constructs, either wild-type or variant B. Cell lysates where then subjected to immunoprecipitation by using anti-FLAG beads to pull down only the FLAG-tagged constructs. Subsequent immunoblotting, by probing with either anti-FLAG or anti-HA, was performed to assess whether HA-tagged cystatin C constructs were also pulled down, which would indicate that they were in a dimer/multimer with the FLAG constructs. Levels of HA-tagged constructs were compared between wild-type and variant B proteins to estimate a difference in their dimerization.

In figure 6.7, immunoblotting results obtained in both ARPE19 (a) and D4O7 (b) cells show that HA-linked constructs are also detected in the pull-down samples (IP), and, taking in consideration the level of FLAG-tagged constructs isolated, their

level appears to be similar in both wild-type and variant B. For the D4O7 cells, non-transfected cells were also analysed as control. Cell lysates, prior to protein pull-down, were also displayed on the gel, showing that cells have similar levels of wild-type and variant protein expression, for both HA and FLAG constructs used. However, cystatin C-HA was only detected in the IP samples at very high exposure, indicating that dimerization did not occur extensively.

Analysis of dimerization was subsequently performed also for the extracellular cystatin C. Immunoprecipitation was carried out on the conditioned media samples collected from co-transfected D4O7 cells. This time, to ensure that the presence of the HA-constructs was not due to unspecific binding/pull-down but was actually due to its dimerization with the FLAG-constructs, samples from cells transfected with only the FLAG constructs or the HA constructs were analysed in parallel.

In figure 6.8 immunoblotting analysis was performed on media samples subjected to immunoprecipitation (a), media samples prior to pull-down (b) and respective cell lysates (c). For each of them, samples co-transfected with both constructs or transfected with only one construct, are shown. Cell lysates and media samples prior the pull-down were used to show the level of expression of the various constructs. For each construct, both wild-type and variant B showed a similar level of expression and secretion. In the blot in figure 6.8 a, the presence of HA-tagged cystatin C can be observed in the pull-down samples, meaning that dimers are also formed in the extracellular environment. At higher exposure it is possible to see bands corresponding to the HA-tagged constructs also in the samples deriving from cells transfected only with those constructs, which should not be present in the IP samples. This indicates that there is a fraction of protein that is non-specifically pulled down during the immunoprecipitation. However, when compared to the level detected in the co-transfected samples, it is much lower, especially considering their higher levels in the media (prior to pull-down) compared to the one of the co-transfected sample. Therefore, the bands detected in the co-transfected immunoprecipitated samples, using anti-HA antibody, mainly correspond to HA-tagged proteins that were in association with the FLAG-tagged cystatin C, even though they probably contain some non-specific pulled down

proteins. Overall, no differences were found in the level of protein dimerization for both intracellular and extracellular cystatin C between the wild-type and variant B proteins.

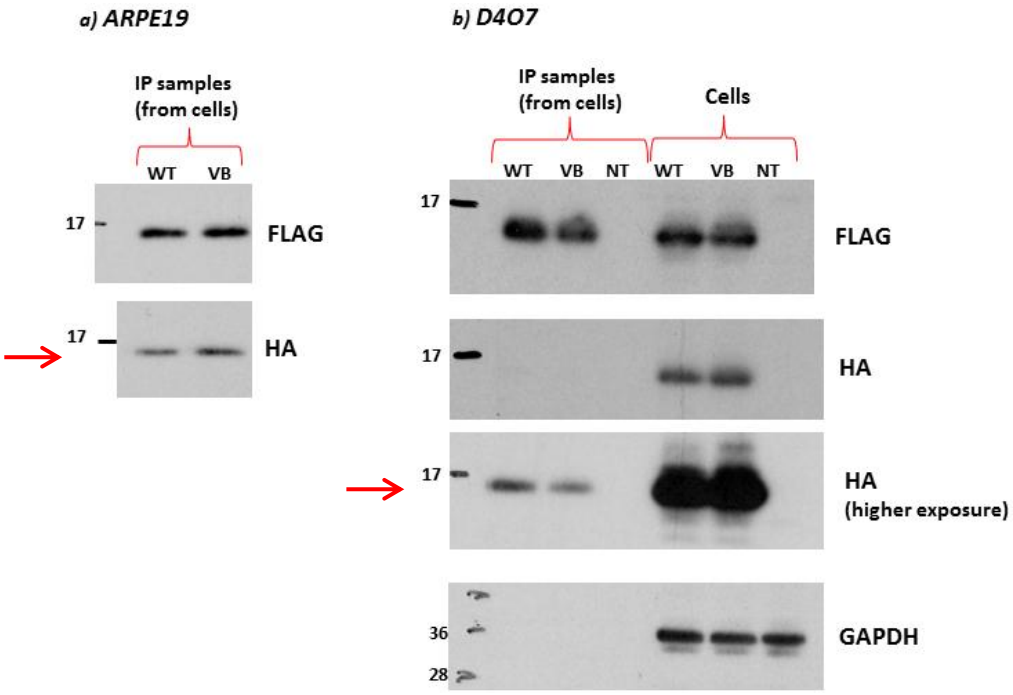

Figure 6.7 - Dimerization analysis in RPE cells co-transfected with FLAG- and HA-tagged constructs after immunoprecipitation from cell lysates. Cell lysates collected from ARPE19 (a) or D4O7 (b) cell line co-transfected with both FLAG- and HA-tagged constructs were subjected to immunoprecipitation to pull down the FLAG-tagged constructs and subsequently analysed by immunoblotting to assess level of HA-tagged constructs. For the D4O7 cells (b), cell lysate samples, prior the pull-down, were also analysed. Non-transfected cells (NT) were used as control. Anti-FLAG and anti-HA antibodies were used to detect FLAG-tagged and HA-tagged constructs respectively. Level of GAPDH in the cell lysates was also shown.

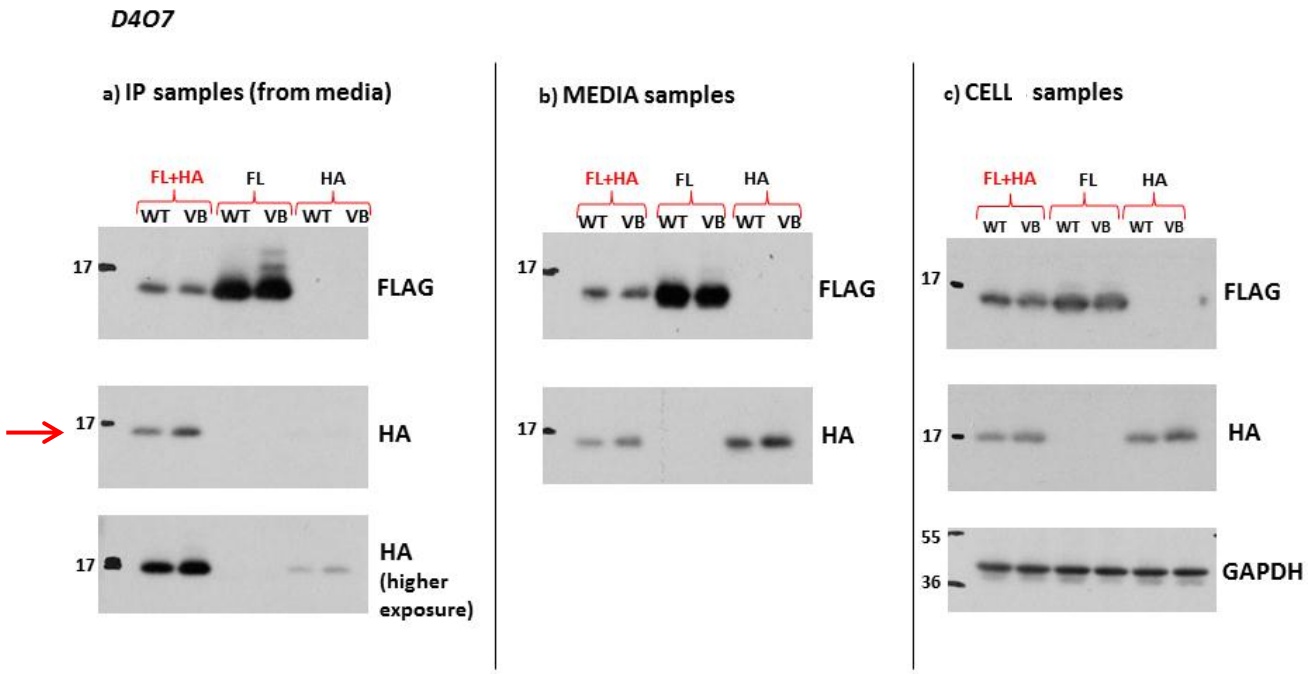

Figure 6.8 - Dimerization analysis in D4O7 cells co-transfected with FLAG- and HA-tagged constructs after immunoprecipitation from conditioned media. a) Conditioned media collected from D4O7 cell line co-transfected with both FLAG- and HA-tagged constructs or only with FLAG or HA-tagged cystatin C were subjected to immunoprecipitation to pull down the FLAG-tagged constructs and subsequently analysed by immunoblotting to assess level of HA-tagged constructs. Media samples (b), prior to pull-down, and cell lysates (c) of the respective transfected cell lines were also shown. Anti-FLAG and anti-HA antibodies were used to detect FLAG-tagged and HA-tagged constructs respectively. Level of GAPDH was shown for the cell lysates. Samples from cells transfected with only one construct, either FLAG- or HA-tagged, were used as control.

6.4. Analysis of cystatin C internalization shows no difference between wild-type and variant B

Cystatin C re-uptake from the extracellular matrix is a clathrin-mediated endocytosis mechanism essential to ensure the presence of cystatin C in the intracellular endosomal-lysosome compartment, where it is crucial for the regulation of the lysosomal cathepsin activity (Wallin, Abrahamson & Ekstrom 2013). This mechanism has been also suggested to regulate the level of cystatin C both intracellularly and extracellularly (Wallin, Abrahamson & Ekstrom 2013, Wallin et al. 2010). Impairment of cystatin C uptake can therefore result in imbalance of proteolytic activity in both lysosomes and the ECM.

Analysis of protein uptake was therefore investigated to see whether any difference occurs between wild-type and variant B protein. Both FLAG-tagged and HA-tagged constructs were used for this analysis.

Conditioned media from RPE cells transfected with wild-type and variant B constructs were collected 24-hour post-transfection and used to culture non-transfected RPE cells. After 24 hours these cells were collected and analysed for their internalization by immunoblotting using anti-cystatin C antibody (figure 6.9). A main band corresponding to the endogenous cystatin C was detected in these cell lysates. In D4O7 cells it is also detected a slower migrating band that corresponds to the exogenous cystatin C construct that has been internalized by endocytosis. Using either FLAG- or HA- tagged constructs, no difference was observed between wild-type and variant B cystatin C, indicating no modification to the internalization process in the case of the variant B protein. However, after 24 hours it was not possible to detect internalised proteins in ARPE19 cells. Probably the time is not sufficient to permit a substantial uptake of cystatin C in this cell line.

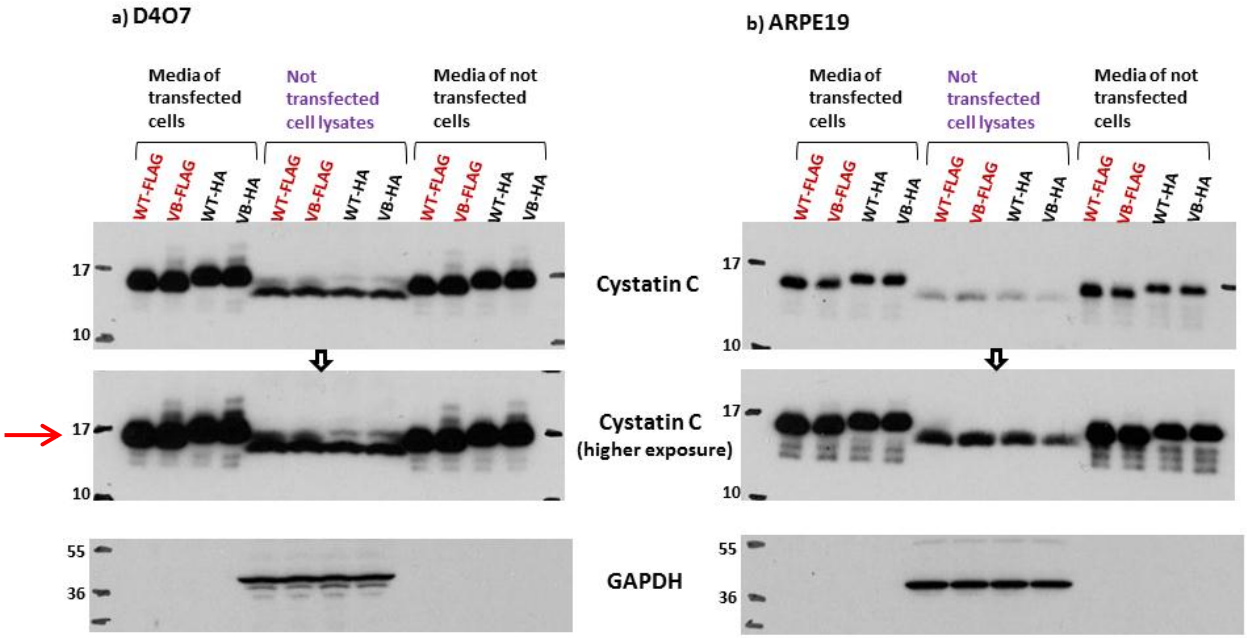

Figure 6.9 - Immunodetection of cystatin C in RPE cells for internalization analysis. D4O7 (a) or ARPE19 (b) cells were cultured in conditioned media collected from cells transfected with wild-type or variant B cystatin C constructs linked to either FLAG or HA tag at the C-terminal. Media was collected 24 hours after transfection (shown in the first four lanes of each blot) and cells and media from the non-transfected collected after another 24 hours. GAPDH levels were also detected as loading control for the cell lysates.

6.5. Analysis of cystatin C interacting proteins shows no difference between wild-type and variant B

To further investigate possible differences between wild-type and variant B cystatin C proteins, analysis of the proteins interacting with cystatin C form was performed.

D4O7 cells transfected with FLAG-tagged wild-type and variant B cystatin C were subjected to immunoprecipitation by using anti-FLAG beads in order to pull down the FLAG-tagged proteins. These samples were then analysed by mass spectrometry to reveal the proteins pulled-down together with cystatin C, which represent potential binding partners. The blot in figure 6.10 a) shows pull-down samples immunodetected with anti-FLAG antibody to ensure that the immunoprecipitation of the protein of interest was successful before proceeding with the mass spectrometry. Cell lysates prior the pull down were also loaded to ensure that the transfection worked comparably for both constructs. Subsequently, the pull-down samples were loaded onto a gel and detected by coomassie blue staining (figure 6.10 b). For each sample the entire lanes were cut from the gel and subjected to mass spectrometry analysis to identify the proteins pulled down together with the protein of interest, in order to analyse whether the variant B interacts with different proteins compared to the wild-type. As discussed for the previous mass spectrometry analysis (chapter 5), the approach as used does not allow a proper quantification of the proteins, so it can be used only as a qualitative analysis.

Table 9 shows the proteins identified for each sample, in two independent experiments, where the exclusive unique spectra count is shown. Proteins selected and displayed in the table 9 are only those that were not present or present in a much lower level in the negative control compared to the FLAG-tagged constructs pull-down samples. The negative control was non-transfected cells also subjected to anti-FLAG beads precipitation, representing proteins that bind non-specifically to the beads. Proteins with less than five spectra counts were not considered and shown in the table.

The first four samples (highlighted in bold) listed in table 9 confirm the effectiveness of the analysis, as cystatin C is one the most abundant proteins present in the cystatin C pull-down samples compared to the negative control. The other three proteins listed were also expected as they are known binding proteins of cystatin C. Cathepsins B, L and C are targets for inhibition by cystatin C (Turk, Bode 1991). Their presence suggests the effective pull-down of cystatin C interacting proteins, thus giving credibility to the analysis. The other proteins identified may therefore likely represent other potential binding proteins of cystatin C. Furthermore, the presence of cathepsins also indicates that the cystatin C constructs effectively bind their normal targets and confirming that the protein functionality is likely not affected by the tag. More importantly, their presence also in the variant B protein indicates that the protein may still fulfil its activity similar as the wild-type cystatin C.

Among the proteins identified, some of them are worth brief description (Table 10). Most are chaperones and enzymes present in the ER/Golgi secretory pathway thus likely representing cystatin C interacting proteins. The Uniprot accession number for each protein identified was provided with the analysis. Information reported was also obtained from the Uniprot database.

Other proteins identified correspond to structural proteins probably non-specifically pulled down and some others proteins detected (not listed in table 9) have a very small spectra count that renders their presence unreliable. Overall, no difference between wild-type and variant B cystatin C samples was identified. However, some potential intracellular binding partners for cystatin C may be of interest for further investigation to determine the significance of this interaction.

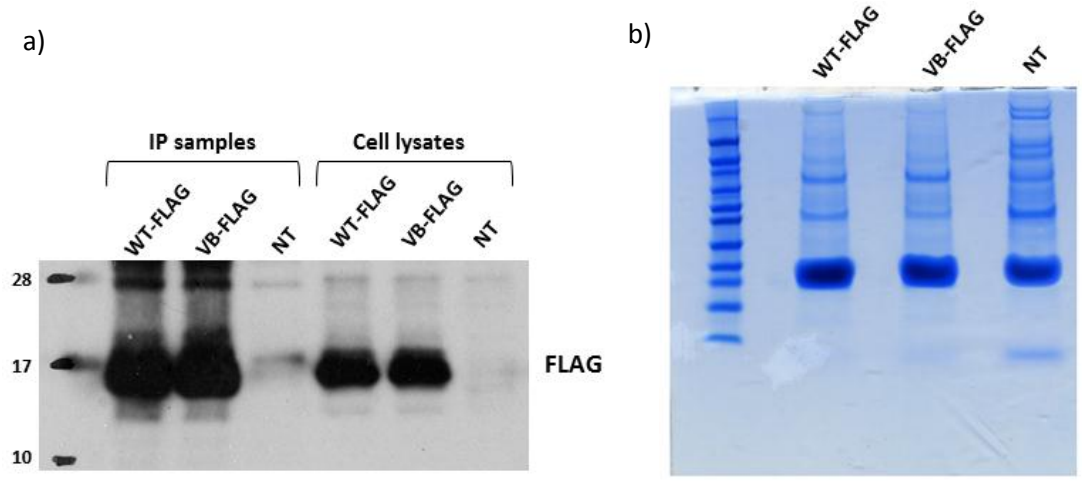

Figure 6.10 - Detection of protein pull-downs prior to mass spectrometry analysis. a) immunodetection of FLAG-tagged cystatin C constructs after protein pull-down from D4O7 cell lysates expressing FLAG-tagged wild-type or variant B cystatin C. Blot was probed with anti-FLAG antibody. Non-transfected cells (NT) were also used as negative control. Cell lysates prior to immunoprecipitation were also loaded. b) Coomassie blue staining of same pull-down samples. Entire lanes for the three samples were cut from the gel for subsequent mass spectrometry analysis.

Table 9 - Mass spectrometry analysis for identification of cystatin C interacting proteins. Entire lanes were extracted from the gel in figure, subjected to in-gel digestion using trypsin and analysed by mass spectrometry. Proteins were identified in each sample (WT cysC, VB cysC and NT), from two independent experiments, by using Mascott and reported in the table below, displaying number of exclusive unique spectra.

			Exp1			**Exp2**		
	Identified Proteins	Molecular Weight	WT cysC	VB cysC	NT	WT cysC	VB cysC	NT
1	**Cystatin-C**	**16 kDa**	**41**	**34**	**4**	**44**	**41**	**4**
2	**Dipeptidyl peptidase 1 (Cathepsin C)**	**52 kDa**	**22**	**20**	**0**	**16**	**19**	**0**
3	**Cathepsin B**	**38 kDa**	**11**	**7**	**0**	**9**	**10**	**0**
4	**Cathepsin L1**	**38 kDa**	**9**	**6**	**0**	**8**	**7**	**0**
5	E3 ubiquitin-protein ligase HUWE1	482 kDa	21	18	2	8	22	5
6	Leucyl-cystinyl aminopeptidase	117 kDa	53	34	0	49	53	0
7	Heat shock 70 kDa protein 4L	95 kDa	17	14	0	27	23	8
8	Heat shock 70 kDa protein 4	94 kDa	22	18	3	42	40	18
9	Heat shock protein 105 kDa	97 kDa	18	11	3	29	22	9

10	Calnexin	68 kDa	32	32	6	30	37	8
11	Endoplasmin	92 kDa	18	15	3	17	17	9
12	Nodal modulator 2	139 kDa	22	24	0	19	33	1
13	Dolichyl-diphosphooligosaccharide-protein glycosyltransferase subunit 2	69 kDa	8	17	3	15	19	0
14	Dolichyl-diphosphooligosaccharide--protein glycosyltransferase subunit 1	69 kDa	16	21	4	18	16	4
15	Sequestosome-1	48 kDa	10	11	0	21	20	1
16	Protein zer-1 homolog	88 kDa	8	15	0	20	21	0
17	Calreticulin	48 kDa	7	8	0	11	12	7
18	Protein ERGIC-53	58 kDa	7	4	0	12	11	0
19	Integrin beta-1	88 kDa	9	8	0	9	11	0
20	Procollagen-lysine,2-oxoglutarate 5-dioxygenase 3	85 kDa	8	11	0	9	15	0
21	Baculoviral IAP repeat-containing protein 6	530 kDa	53	40	0	13	36	0
22	Stress-70 protein, mitochondrial	74 kDa	61	61	20	85	81	42
23	78 kDa glucose-regulated protein	72 kDa	54	59	20	74	67	38
24	Heat shock cognate 71 kDa protein	71 kDa	48	48	21	68	60	38
25	Nuclear pore membrane glycoprotein 210	205 kDa	20	23	0	16	23	0
26	Cation-independent mannose-6-phosphate receptor	274 kDa	20	15	0	6	11	1
27	Nicalin	63 kDa	7	4	0	13	9	0
28	dCTP pyrophosphatase 1	19 kDa	7	7	0	10	11	0
29	Laminin subunit gamma-1	178 kDa	8	4	0	7	11	0

Table 10 - Description of proteins identified in mass spectrometry analysis.

Identified Proteins	UniProt Code	Description
Leucyl-cystinyl aminopeptidase	Q9UIQ6	Exopeptidase responsible for the degradation of several hormones mainly involved in maintenance of cardiovascular homeostasis as well as in the inactivation of neuronal peptides. It is not known if this protease is regulated by cystatin C
E3 ubiquitin-protein ligase HUWE1	Q7Z6Z7	Enzyme that mediates ubiquitination of proteins for their proteasomal degradation
Protein zer-1 homolog	Q7Z7L7	Subunit of the E3 ligase
Heat shock 70 kDa protein 4, 4L	P34932 and O95757	Molecular chaperone involved in the protein folding and assembly, protein transport and response to unfolded proteins
Heat shock protein 105 kDa	Q92598	Chaperone involved in protein folding and that prevents aggregation of misfolded protein under stress condition
Heat shock cognate 71 kDa protein	P11142	Role in transcriptional regulation in inflammatory response and in the ERAD pathway for degradation of misfolded proteins
Calnexin and Calreticulin	P27824 and P27797	ER chaperones that mediate the proper folding of N-linked glycoproteins targeted to the secretory pathway. Also involved in the retention of misfolded proteins in the ER for subsequent degradation
Endoplasmin	P14625	ER chaperone involved in the correct processing and transport of secretory proteins and in ERAD pathway
Protein ERGIC-53	P49257	Mannose-binding protein for transport of glycoproteins from ER to the ERGIC compartment
Dolichyl-diphosphooligosaccharide-protein glycosyltransferase subunit 1, 2	P04843 and P04844	Enzyme that mediates the transfer of an oligosaccharide precursor to a nascent polypeptide chain, essential step for N-glycosylation of proteins
Sequestosome-1	Q13501	Involved in targeting proteins and aggregates for autophagy
Baculoviral IAP repeat-containing protein 6	Q9NR09	Anti-apoptotic protein that regulates caspases and promotes degradation of pro-apoptotic molecules
Stress-70 protein, mitochondrial	P38646	Heat shock protein present in mitochondria, ER, nuclei and cytosol involved in controlling cell proliferation and cellular aging
78 kDa glucose-regulated protein	P11021	Also known as BiP, is involved in mediating the efficient ER translocation of proteins and their subsequent correct folding and assembly in the ER as well as in the degradation of misfolded proteins
Cation-independent mannose-6-phosphate receptor	P11717	It targets glycoproteins from the TGN compartment to the lysosomes, as occurs for the lysosomal cathepsins

6.6. Discussion

Cystatin C levels and activity are controlled by several mechanisms including degradation, dimerization and internalization (described in section 1.2.2). The aim of the work presented in this chapter was to investigate whether the variant B is differently regulated compared to the wild-type. Deregulation of any of these mechanisms could lead to a change of protein activity in the intracellular and/or extracellular compartment. This could lead to an imbalance in proteolytic activity, affecting several other cellular processes in which cystatin C might be involved in RPE, such as inflammation, apoptosis, ECM remodelling and angiogenesis.

Inhibition of ALP or UPS degradative pathways was shown to affect cystatin C protein levels, but influencing the wild-type and variant B in the same way. Therefore, no difference in variant B protein stability and degradation seems to occur.

Analysis in section 6.3 showed that dimerization of cystatin C occurs in RPE cells in both intracellular and extracellular compartments. However, it appears to involve a relatively small fraction of the total protein. A precise quantification of the extent of this process cannot be evaluated with the experimental approach used in this study, as only levels of HA-tagged constructs dimerizing/multimerizing with the FLAG-tagged constructs could be evaluated. This approach does not detect the fraction of FLAG-tagged cystatin C that also forms dimers with the same constructs as well as HA-constructs with themselves. Furthermore, this approach cannot tell us if the proteins detected are part of dimers, multimers or aggregates. As cystatin C has been reported to only form dimers in physiological conditions (Janowski et al. 2001), we can therefore assume that this is the only species present. However, no difference in dimerization was identified for the variant B compared to the wild-type.

Analysis of cystatin C internalization showed protein uptake to occur in D4O7 cells. However, it was not observed with the ARPE19 cell line. This might be due to cell line differences and more time may be needed to allow the cystatin C uptake in

ARPE19 cells. However, these results indicate that the process of internalization occurs in RPE cells and no difference was again identified between wild-type and variant B.

Results obtained from mass spectrometry in section 6.5 also showed no difference in the potential proteins interacting with cystatin C wild-type and variant B. The presence of the known target cathepsins for both forms of cystatin C suggests that variant B maintains its protease inhibitory activity. No additional proteins were found interacting with the variant B that could suggest its involvement in different cellular processes or its presence in other cellular compartments. In this regard, the lack of mitochondrial proteins further confirms that no mislocalization to the mitochondria occurs for variant B. Most of the proteins identified are enzymes and molecular chaperones mainly present in the ER/Golgi compartments implicated in the process of protein folding to ensure appropriate transport through the secretory pathway. Their presence is therefore not surprising. Interestingly, several proteins implicated in the glycosylation of nascent polypeptides were identified to interact with both wild-type and variant B, supporting the presence of cystatin C glycoforms described in chapter 5. Proteins involved in ERAD pathway and proteasomal degradation as well as autophagy were also detected. This supports the hypothesis of the presence of misfolded precursor or alternatively processed fractions, which activate these degradative pathways. In this study this occurred for both wild-type and variant B, possibly because of the protein over-expression overwhelming the system, as described previously. Proteins involved in cell proliferation and apoptosis are also consistent with the role of cystatin C found in earlier reports (as described in section 1.2.3). These potential binding candidates, however, need to be further investigated to confirm their interaction with cystatin C.

Overall, results presented in this chapter indicate that no difference occurs in any of the investigated mechanisms of regulation between the wild-type and the variant B mature cystatin C, therefore excluding, most probably, their involvement in variant B association with diseases. Furthermore, mass spectrometry analysis did

not suggest any other mechanisms involving exclusively the variant B based on a similar set of interacting proteins. However, as this analysis is only qualitative, it cannot tell us whether there is a quantitative difference that could be of functional relevance.

In the analysis of degradation (section 6.2), although no difference was found between wild-type and variant B proteins, significant effects on cystatin C protein expression were observed, consisting in a profound decrease of its level after UPS inhibition and, conversely, an increase after ALP inhibition. These findings were similar for both wild-type and variant B transfected proteins as well as for the endogenous protein, thus indicating a general effect on cystatin C mediated by both degradation pathways.

The ALP inhibitor, chloroquine, specifically increases the pH within the lysosome compartment (Solomon, Lee 2009), which suppresses the lysosomal proteases activity, and inhibits the fusion of autophagosomes and endosomes with the lysosome, preventing removal of cellular debris, damaged proteins and aggregates engulfed in such compartments (Chen, Gombart & Chen 2011, Yoon et al. 2010). Previous studies have also investigated the effect of chloroquine on ARPE19 cells. Consistently, chloroquine caused lysosome dilation and accumulation of intracellular vacuoles leading to progressive accumulation of debris and impairment of the phagocytic activity (Chen, Gombart & Chen 2011, Yoon et al. 2010), thus simulating the effect of impaired autophagy that occurs in the RPE in age-related conditions (Kaarniranta et al. 2013, Guha et al. 2014). Therefore, the increase of cystatin C levels, observed after ALP inhibition in this study, may be due to its accumulation in the autophagosomes and/or lysosomes, as it cannot be degraded. In particular, its presence in the endosomal-lysosome compartment, occurring upon internalization, reflects its physiological function in these cellular organelles, where it regulates cysteine-cathepsin activity and where cystatin C is itself degraded (Watanabe et al. 2014, Wallin, Abrahamson & Ekstrom 2013, Wallin et al. 2010). If the lysosomal activity is suppressed, the turnover of cystatin C would be therefore impaired, thus causing an increase of its level in these compartments.

In particular, down-regulation of aspartic-cathepsin D has been reported to occur due to lysosomal alkalinisation, causing impairment in photoreceptor outer segment (POS) degradation in RPE, during aging and AMD (Chen et al. 2009, Guha et al. 2014). Interestingly, cathepsin D is also known to be one of the proteases involved in cystatin C inactivation (Lenarčič et al. 1991). Therefore, reduced activity of cathepsin D after CQ treatment may determine the increased cystatin C level observed in this study. However, considering the low extent of internalization after 24-hours, observed in RPE cells in this study, it seems unlikely that such increase of cystatin C occurs in the lysosomes, where its presence is due to re-uptake from the extracellular space, unless a very rapid degradation/turnover of cystatin C normally occurs within the lysosome, or there is a significant increase in the process of internalization in response to the ALP inhibition.

The presence of cystatin C in the autophagosomes can be also due to the formation of cystatin C protein aggregates, as it is an aggregation-prone protein (Janowski et al. 2001, Tsiolaki et al. 2015) and this condition was hypothesized to particularly occur for the variant B (as discussed in chapter 4). Such protein aggregates, normally removed by the autophagy system, may accumulate in the autophagosomes because of the CQ-mediated ALP dysfunction, which could explain the increase of cystatin C protein levels. However, this second scenario is unlikely since it occurs not only for the over-expressed wild-type and variant B proteins but also for the endogenous cystatin C. Furthermore, based on the hypothesis, it is the precursor fraction that has been suggested to generate aggregates and not the mature cystatin C.

In addition, cystatin C has been also reported to promote autophagy via inhibition of the AMPK-mTOR pathway with a mechanism independent of its protease inhibitory activity (section 1.3.2) (Tizon et al. 2010b). Activation of the autophagy pathway by increasing cystatin C levels has been shown to occur particularly under stress conditions, such as starvation and oxidative stress, and to be protective in several neurological disease conditions and atherosclerosis (Liu et al. 2014, Liu et al. 2013, Tizon et al. 2010b, Watanabe et al. 2014, Li et al. 2016), enhancing protein degradation and preventing apoptosis of neuronal cells. Therefore, through

mechanisms still unknown, possibly involving regulation of cystatin C gene expression, it is possible that the increase of cystatin C observed in this study after ALP-inhibition occurs as cellular response to activate the down-regulated ALP degradation system. However, since lysosomal degradation is not functional, accumulation of autophagosomes and debris would progressively increase. It is not known whether this sort of regulation occurs and whether it modulates cystatin C at transcriptional or translational level. These aspects therefore need further investigation.

Interestingly, autophagy is particularly activated in several degenerative diseases characterised by lysosome dysfunction, including Alzheimer, Parkinson, Huntington and AMD (Cheung, Ip 2011, Kaarniranta et al. 2013, Kaarniranta et al. 2010), due to increased debris accumulation and protein aggregation. However, excessive activation of the autophagic pathway as a consequence of lysosomal dysfuntion has been suggested to further contribute to protein aggregation and ultimately lead to cell death (Wang et al. 2009, Watanabe et al. 2014, Cheung, Ip 2011).

Finally, oxidative stress conditions and lysosome dysfunction can also lead to lysosomal membrane permeabilization (LMP) with consequent release of lysosomal enzymes (Zdolsek, Svensson 1993, Watanabe et al. 2014). In addition to the consequent decreased proteolytic activity, lysosomal components and debris released from the lysosomes may form aggregates in the cytosol and induce inflammation and apoptosis. Cystatin C has been also found in the cytosol upon LMP and consequently aggregates under oxidative stress conditions (Watanabe et al. 2014). This could also explain the increase of intracellular cystatin C after CQ treatment.

Regarding the effect of inhibition of the proteasomal system on cystatin C, a very significant reduction in the protein level of the mature form was observed. UPS is mainly responsible for the removal of misfolded/damaged protein (Amm, Sommer & Wolf 2014). Based on the hypothesis, the variant B cystatin C may not be properly processed, resulting in a misfolded uncleaved or miscleaved fraction,

which is sent to the proteasome for degradation. Also the O-glycosylation may render the alternative form of cystatin C less stable and therefore susceptible to UPS degradation. Furthermore, in this study the protein over-expression, per se, may cause an accumulation of misfolded precursor proteins, which can therefore be sent to ERAD for degradation (as discussed in chapter 4). It was therefore expected that the inhibition of the proteasomal activity would cause an increase of the intracellular level of cystatin C, and of the variant B in particular. Surprisingly, a highly significant reduction of mature cystatin C levels was observed instead.

However, the unprocessed form of cystatin C was hypothesised to be misfolded and therefore sent for degradation. In support of this, one of the blots (figure 6.1) seems to display a higher fraction of uncleaved precursor after MG132 treatment in both wild-type and variant B compared to the non-treated, meaning that a fraction of accumulated misfolded precursor might be present and sent for degradation, a mechanism that is disrupted after proteasome inhibition. This occurred for both wild-type and variant B because of the overexpression of the exogenous proteins, but it would likely occur only for the variant B in normal conditions if its cleavage is impaired, as hypothesized and discussed earlier. In support of this hypothesis, the identification by mass spectrometry analysis of several proteins involved in ERAD pathway as well as the granule-like structures found occasionally for the precursor protein during imaging, likely representing protein aggregates, also suggests the presence of accumulated misfolded proteins and an active involvement of UPS for their removal. The response to MG132 treatment was not consistent, however, possibly because of the very low protein levels of the precursor fraction that is difficult to detect by immunoblotting.

The reduction in the general level of mature cystatin C could be due to a mechanism of regulation indirectly mediated by proteasomal activity. Levels of cystatin C could be regulated by transcriptional or translational mechanisms involving factors that might, in turn, be modulated by the UPS system. At the transcriptional level, specific transcription factors that can be modulated by several stimuli, including inflammatory cytokines, hormones, growth factors, stress and pathogens, have been identified to regulate cystatin C gene expression (Xu et al.

2015). In particular, in the promoter region of cystatin C, an androgen-responsive element sequence, two activator protein 1 binding sites and an IRF-binding motif, which represent transcription factor binding sites, have been described (Xu et al. 2015). As a result, modulation of the rate of transcription and of the processing and stability of mRNA can occur under certain conditions. Regulation at the level of cystatin C translation has not been explored. Most common mechanisms that control protein synthesis involve the presence of repressor proteins, which can bind specific sequences within mRNAs, preventing the recruitment of the ribosome on the initiation codon (Kozak 1992, Sonenberg, Hinnebusch 2009). This critical step for the initiation of translation can be also suppressed by specific secondary structure of the transcript or by antisense microRNA binding (Kozak 1992, Sonenberg, Hinnebusch 2009). As a result, mRNA translation is repressed. Another common mechanism involves the modulation of initiation factors or other translation components by phosphorylation, which can suppress protein translation. These and other mechanisms of regulation are reviewed elsewhere (Kozak 1992, Sonenberg, Hinnebusch 2009).

Results obtained by qPCR in section 6.1 showed that the proteasome inhibition does not alter the level of cystatin C mRNA, thus excluding a modulation at the transcriptional level. An increased degradation of cystatin C is also unlikely as it occurs in the lysosome by proteinases, which are themselves degraded in this cellular compartment (Turk et al. 2012), and so are independent from the proteasome pathway. Therefore, it is most likely that the effect on cystatin C protein level is mediated by the accumulation of a protein repressor that is under proteasomal regulation. As a result of the proteasome inhibition, accumulation of this repressor and consequent suppression of cystatin C translation may therefore occur.

Interestingly, reduction of serum levels of cystatin C, characterising patients affected by multiple myeloma, has been observed after treatment with bortezomib, a proteasome-inhibitor used in therapy for its anti-myeloma activity (Terpos et al. 2009). This further suggests a role of UPS in cystatin C regulation.

Impairment of the proteolytic mechanisms is observed during aging and under several age-related pathologic conditions such as neurodegenerative diseases, where accumulation and detrimental aggregation of misfolded proteins represent a hallmark (Hipp, Park & Hartl 2014, Vilchez, Saez & Dillin 2014, Cheung, Ip 2011). Dysfunction of ALP and UPS pathways in this study may simulate the conditions occurring in ageing and disease. Further studies are required to understand such mechanisms of regulation of cystatin C and how the altered higher or lower level of cystatin C may affect cell functionality, which could highlight a potential role of the protease inhibitor in the detrimental effects observed in age-related conditions, including the effects on the RPE in the AMD.

In RPE, impairment of both degradative pathways has been reported to play a role in AMD pathogenesis (Kinnunen et al. 2012, Ferrington, Sinha & Kaarniranta 2016).

Regarding the proteasome, a decrease in its functionality has been described to occur in ageing RPE, leading to accumulation of damaged oxidized and cross-linked proteins that can block or overwhelm the proteasomal system (Salminen et al. 2010, Kinnunen et al. 2012). As a consequence, misfolded ubiquitinated proteins can accumulate intracellularly, forming aggregates and causing ER stress. This condition can trigger inflammatory responses, ultimately causing chronic inflammation and formation of drusen, which contributes toward AMD development (Salminen et al. 2010).

Interestingly, a reduction of cystatin C level has been reported to occur in aging RPE cells (Kay et al. 2014). Therefore, based on my findings, the age-related decrease of cystatin C might be due to the reduced activity of the proteasome system that occurs in aged RPE cells. This alteration of cystatin C levels may play role in the age-related structural and functional changes observed in RPE cells during aging as well as in AMD development.

Autophagy also represents one of the most active mechanisms in RPE. Due to its function, RPE is constantly subjected to oxidative stress and therefore damaged proteins need to be constantly removed (Chang et al. 2015). Moreover, as

described in section 1.3, the RPE is also involved in phagocytosis and subsequent intra-lysosomal degradation of photorecepotor outer segment (POS) by the aspartic-cathepsin D, a mechanism fundamental for photoreceptor turnover (Ferrington, Sinha & Kaarniranta 2016). Also mitophagy, a form of autophagy responsible for removal of damaged mitochondria, is a highly active process in the RPE cells, considering the high metabolic activity occurring in this tissue (Thumann, Hoffmann & Hinton 2006). It therefore represents an essential mechanism for the maintenance of the RPE cell homeostasis (Chang et al. 2015, Ferrington, Sinha & Kaarniranta 2016). Oxidative stress has been shown to increase in ageing RPE causing lysosomal alkalinisation and reduced phagocytosis (Chen et al. 2009, Guha et al. 2014), contributing to AMD development (Jarrett, Boulton 2012). In response to oxidative stress, the autophagic activity also increases with age (Mitter et al. 2014, Flores-Bellver et al. 2014). However, if lysosomal function is suppressed, the system is not able to degrade phagocytised POS and damaged cellular components, leading to progressive debris accumulation in the lysosome such as lipofuscin accumulation, impairment in photoreceptor degradation/renewal, activation of inflammatory response via cathepsin B and formation of intra- and extracellular deposits, such as drusen, ultimately causing RPE cell degeneration. (Ferrington, Sinha & Kaarniranta 2016, Kaarniranta et al. 2010, Kinnunen et al. 2012, Klettner et al. 2013, Kaarniranta et al. 2013). Autophagy has also been suggested to directly contribute to drusen formation in aged RPE (Wang et al. 2009). Therefore, altered levels of cystatin C, as a result of impaired ALP, has the potential to play a role in the proteolytic dysfunction described above during aging and AMD.

Autophagy plays an important role also in AD, where it is implicated in the degradation of amyloid precursor protein (APP) and β-amyloid (Aβ). The toxic Aβ peptide is generated in the autophagic vacuoles, thus accumulating in AD brain (Cheung, Ip 2011). Impaired vacuole clearance and lysosomal activity dysfunction contribute to Aβ toxicity. Interestingly, this can be corrected by enhancing lysosomal cathepsin activity (Cheung, Ip 2011, Tizon et al. 2010b, Kaur, Levy 2012). Therefore, reduction of lysosomal activity may increase cystatin C levels, as observed after CQ treatment in this study. This would reduce cathepsin activity,

potentially contributing to Aβ accumulation and toxicity, as described in previous reports (Tizon et al. 2010b, Tizon et al. 2010a, Wang et al. 2012). This may indicate a role for cystatin C in promoting Aβ formation when ALP is non-functional.

On the contrary, in other disease conditions it is the low level of cystatin C and the increased cathepsin activity that causes a detrimental proteolytic imbalance in the cell. For instance, the resulting excessive activity of cathepsins has been reported to degrade ECM of aneurysm walls causing rupture of cerebral aneurysms (Wu et al. 2016), or to promote invasion and metastasis in cancer also by ECM degradation (Keppler 2006, Schulte et al. 2010, Mori et al. 2016, Laurent-Matha et al. 2012, Wallin, Abrahamson & Ekstrom 2013). In RPE such proteolytic imbalance in the extracellular matrix may contribute to drusen formation, Bruch's membrane disruption and abnormal neovascularization, typical of the exudative AMD.

In conclusion, results indicate that cystatin C levels can be modulated by ALP and UPS pathways. Considering the established role of these degradative pathways and the involvement of cystatin C and its target cathepsins in several age-related diseases, including cancer, atherosclerosis and age-related degenerative disorders, further studies to determine the factors responsible for cystatin C regulation mediated by UPS and ALP could be of clinical interest in order to modulate its level to restore the physiological proteolytic balance within cells.

Chapter 7 - Conclusions and Future Work

Results obtained in this study showed no major difference in protein trafficking, stability and regulation between wild-type and variant B cystatin C.

In particular, in contrast to the main accredited theory (Benussi et al. 2003, Paraoan et al. 2004), the outcomes of this study do not support a significant influence of the variant B mutation on protein targeting and localization as well as levels of protein secretion. Indeed, the variant B cystatin C was not found to divert from the conventional secretory pathway or interact with distinct cellular proteins, therefore excluding its involvement in other cellular pathways. Accordingly, this study provides strong evidence against the mitochondrial mislocalization of cystatin C being a factor contributing to AMD/AD pathogenesis. Rather, data obtained indicate that the EGFP tag is responsible for the protein mistrafficking observed in this study and most likely in previous published work (Paraoan et al. 2004). Regarding the secretion, only recently another study also reported no difference in secretion levels between the wild-type and the variant B cystatin C (Nguyen, Hulleman 2016), thus consistent with my findings. In addition, other mechanisms were investigated in this study, including protein degradation, internalization and dimerization, which were also found not to significantly differ between wild-type and variant B.

Overall, these results indicate that the A25T mutation does not affect the targeting of the precursor cystatin C and, consequently, the trafficking and regulation of the mature protein.

However, minor differences in two aspects were found between the wild-type and variant B cystatin C. They consist of the presence of an uncleaved precursor, detected at slightly higher abundance for the variant B, and presence of an alternatively processed, possibly O-glycosylated form, produced and secreted at higher levels for variant B. The presence of both these forms may be due to a decreased efficiency in the signal sequence cleavage, thus indicating that the A25T mutation may affect the precursor processing. The existence of alternative cleaved and glycosylated forms is consistent with previous works (Nguyen, Hulleman 2016,

Nilsson et al. 2009). These events, however, were only observed for a minor fraction of the protein, which are unlikely to produce any significant short-term effects. However, they may prove to be cumulative and affect cell function in the long-term, consistent with the association with age-related disease. As described in detail previously, prolonged accumulation of either the amyloidogenic misfolded uncleaved fraction or the alternative processed O-glycosylated form may result in ER stress, cellular proteolytic imbalance and protein aggregation, which ultimately lead to cell degeneration. Consistent with their possible association with AMD/AD degenerative diseases, their accumulation could further be enhanced in aging, where the functionality of the cellular degradative systems is compromised. In support of this hypothesis, an increase of the precursor fraction was observed in this study to occur in response to proteasome inhibition.

In addition, O-glycans may also be present on a small fraction of wild-type cystatin C. It would be therefore interesting to investigate the role of this alternative form and the effects the glycosylation could have on cystatin C properties, such as function, stability, targeting and regulation. For instance, mechanisms of degradation, internalization and dimerization investigated in this study, did not show any difference in relation to the predominant mature form of cystatin C, but they may be impaired for the alternative cleaved, O-glycosylated form. Depending on the effect of the O-glycan on the protein, it could result in a proteolytic imbalance intra- and extra-cellularly, as described previously. However, because in this study the level of this fraction was very low, it was not possible, to analyse these aspects in relation to this fraction.

Future use of more refined approaches to variant B expression would help to prevent cell stress and reduced viability that overexpression approaches can induce, which therefore did not allow us to study long-term effects, possibly linked with the development of age-related diseases. This factor results to be particularly important considering the very low amounts of both unprocessed and differently processed forms identified in this study, which at these low levels compared to the mature form are unlikely to affect secretion, activity, regulation or cell function. To

overcome these limitations and further exclude effects on different cellular processes due to the overexpression, it would be more suitable to use cystatin C B/B genotyped cells, thus endogenously expressing the variant B protein, which would also avoid the simultaneous presence of the wild-type endogenous cystatin C. Given the unavailability of these cells, generation of cell lines using the CRISPR/Cas9-mediated genome editing technology would provide a valuable approach for this purpose, as it permits to introduce the variant B mutation into the endogenous cystatin C gene. Furthermore, in vivo studies using humanized mice models for wild-type and variant B cystatin C expressed under the endogenous cystatin C promoter for disease modelling could be also an interesting approach to further investigate the cellular and systemic effects of the variant B.

Another aspect of this study, independent from the variant B observations, is the identification of a novel mechanism of regulation of cystatin C concentration and degradation, operated by modulation of the UPS and ALP pathways, which seem to act indirectly at the protein level. It would be therefore interesting to further elucidate these proteasome/autophagy-mediated mechanisms of regulation of cystatin-C and the components that are involved in these pathways. They could be potential targets for clinical intervention, by modulating the level of cystatin C in the several conditions characterised by altered level of cystatin C (see section 1.3).

Furthermore, although the mechanism of cystatin C up-regulation observed in this study upon ALP inhibition is unclear, this event may also determine an increase of the uncleaved precursor and/or the alternatively cleaved glycosylated form of cystatin C, especially in the case of the variant B. Considering ALP deregulation to be a hallmark of age-related degenerative diseases, this event may therefore contribute to the increased risk of developing AMD/AD disorders in presence of the variant B.

In conclusion, although my study did not uncover significant differences between wild-type and variant B, a long term dysregulation of proteolytic balance and, as a

consequence, impairment of cell function or viability by the presence of a higher proportion of the miscleaved cystatin C variant B cannot be excluded. These events, if confirmed, may explain the association of variant B with AMD and AD pathogenesis.

However, it also has to be noted that association of variant B with both AD and AMD diseases is still a controversial issue. Studies reported association only in certain ethnic populations and under specific biological conditions (Finckh et al. 2000, Chuo et al. 2007, Hua et al. 2012, Wang et al. 2008, Nacmias et al. 2006, Maruyama et al. 2001, Helisalmi et al. 2009, Roks et al. 2001). This suggests that genetic factors as well as the status of cellular regulatory components in age-related conditions may play a more important role and the variant B may be, for unknown reasons, more susceptible to altered conditions, thus linking it to the disease pathogenesis. Alternatively, since AMD and AD are both complex multifactorial disorders, depending of several genetic and environmental factors (Horie-Inoue, Inoue 2014, Bettens, Sleegers & Van Broeckhoven 2013, Logue et al. 2014), one or more of these factors could differentially affect variant B. Further investigation are therefore required to shed light on such mechanisms of age-related diseases that can help us understand the possible role of cystatin C in their pathogenesis.

References

Abrahamson, M., Islam, M.Q., Szpirer, J., Szpirer, C. & Levan, G. 1989, "The human cystatin C gene (CST3), mutated in hereditary cystatin C amyloid angiopathy, is located on chromosome 20", *Human genetics,* vol. 82, no. 3, pp. 223-226.

Abrahamson, M., Mason, R.W., Hansson, H., Buttle, D.J., Grubb, A. & Ohlsson, K. 1991, "Human cystatin C. role of the N-terminal segment in the inhibition of human cysteine proteinases and in its inactivation by leucocyte elastase", *The Biochemical journal,* vol. 273 (Pt 3), no. Pt 3, pp. 621-626.

Ahuja, S., Ahuja-Jensen, P., Johnson, L.E., Caffé, A.R., Abrahamson, M., Ekström, P.A. & van Veen, T. 2008, "rd1 Mouse retina shows an imbalance in the activity of cysteine protease cathepsins and their endogenous inhibitor cystatin C", *Investigative ophthalmology & visual science,* vol. 49, no. 3, pp. 1089-1096.

Åkerblom, A., Eriksson, N., Wallentin, L., Siegbahn, A., Barratt, B.J., Becker, R.C., Budaj, A., Himmelmann, A., Husted, S. & Storey, R.F. 2014, "Polymorphism of the cystatin C gene in patients with acute coronary syndromes: Results from the PLATelet inhibition and patient Outcomes study", *American Heart Journal,* vol. 168, no. 1, pp. 96-102. e2.

Alberts, B., Johnson, A., Lewis, J., Raff, M., Roberts, K. & Walter, P. 2008, *Molecular Biology of the Cell,* 5th edn, Garland Science, New York.

Alder, N.N., Shen, Y., Brodsky, J.L., Hendershot, L.M. & Johnson, A.E. 2005, "The molecular mechanisms underlying BiP-mediated gating of the Sec61 translocon of the endoplasmic reticulum", *The Journal of cell biology,* vol. 168, no. 3, pp. 389-399.

Amm, I., Sommer, T. & Wolf, D.H. 2014, "Protein quality control and elimination of protein waste: The role of the ubiquitin–proteasome system", *Biochimica et Biophysica Acta (BBA)-Molecular Cell Research,* vol. 1843, no. 1, pp. 182-196.

Anandatheerthavarada, H.K., Biswas, G., Robin, M.-. & Avadhani, N.G. 2003, "Mitochondrial targeting and a novel transmembrane arrest of Alzheimer's amyloid precursor protein impairs mitochondrial function in neuronal cells", *Journal of Cell Biology,* vol. 161, no. 1, pp. 41-54.

Anandatheerthavarada, H.K. & Devi, L. 2007, "Mitochondrial translocation of amyloid precursor protein and its cleaved products: Relevance to mitochondrial dysfunction in Alzheimer's disease", *Reviews in the neurosciences,* vol. 18, no. 5, pp. 343-354.

Andresen, M., Schmitz-Salue, R. & Jakobs, S. 2004, "Short tetracysteine tags to beta-tubulin demonstrate the significance of small labels for live cell imaging", *Molecular biology of the cell,* vol. 15, no. 12, pp. 5616-5622.

Antonin, W., Meyer, H.A. & Hartmann, E. 2000, "Interactions between Spc2p and other components of the endoplasmic reticulum translocation sites of the yeast Saccharomyces cerevisiae", *The Journal of biological chemistry,* vol. 275, no. 44, pp. 34068-34072.

Arluison, V. & Taghbalout, A. 2015, "Cellular localization of RNA degradation and processing components in Escherichia coli", *RNA Remodeling Proteins: Methods and Protocols,* , pp. 87-101.

Arnold, A., Horst, S.A., Gardella, T.J., Baba, H., Levine, M.A. & Kronenberg, H.M. 1990, "Mutation of the signal peptide-encoding region of the preproparathyroid hormone gene in familial isolated hypoparathyroidism", *The Journal of clinical investigation,* vol. 86, no. 4, pp. 1084-1087.

Ast, T., Cohen, G. & Schuldiner, M. 2013, "A network of cytosolic factors targets SRP-independent proteins to the endoplasmic reticulum", *Cell,* vol. 152, no. 5, pp. 1134-1145.

Auclair, S.M., Bhanu, M.K. & Kendall, D.A. 2012, "Signal peptidase I: cleaving the way to mature proteins", *Protein Science,* vol. 21, no. 1, pp. 13-25.

Balbín, M. & Abrahamson, M. 1991, "SstII polymorphic sites in the promoter region of the human cystatin C gene", *Human genetics,* vol. 87, no. 6, pp. 751-752.

Balbín, M., Grubb, A. & Abrahamson, M. 1993, "An Ala/Thr variation in the coding region of the human cystatin C gene (CST3) detected as a SstII polymorphism", *Human genetics,* vol. 92, no. 2, pp. 206-207.

Barlowe, C.K. & Miller, E.A. 2013, "Secretory protein biogenesis and traffic in the early secretory pathway", *Genetics,* vol. 193, no. 2, pp. 383-410.

Barrett, A.J., Davies, M.E. & Grubb, A. 1984, "The place of human γ-trace (cystatin C) amongst the cysteine proteinase inhibitors", *Biochemical and biophysical research communications,* vol. 120, no. 2, pp. 631-636.

Becker, T., Böttinger, L. & Pfanner, N. 2012, "Mitochondrial protein import: from transport pathways to an integrated network", *Trends in biochemical sciences,* vol. 37, no. 3, pp. 85-91.

Bejarano, L.A. & Gonzalez, C. 1999, "Motif trap: a rapid method to clone motifs that can target proteins to defined subcellular localisations", *Journal of cell science,* vol. 112 (Pt 23), no. Pt 23, pp. 4207-4211.

Bektas, M. & Rubenstein, D.S. 2011, "The role of intracellular protein O-glycosylation in cell adhesion and disease", *Journal of biomedical research,* vol. 25, no. 4, pp. 227-236.

Bengtsson, E., Nilsson, J. & Jovinge, S. 2008, "Cystatin C and cathepsins in cardiovascular disease", *Frontiers in bioscience : a journal and virtual library,* vol. 13, pp. 5780-5786.

Benussi, L., Ghidoni, R., Galimberti, D., Boccardi, M., Fenoglio, C., Scarpini, E., Frisoni, G.B. & Binetti, G. 2010, "The CST3 B haplotype is associated with frontotemporal lobar degeneration", *European Journal Of Neurology: The Official Journal Of The European Federation Of Neurological Societies,* vol. 17, no. 1, pp. 143-146.

Benussi, L., Ghidoni, R., Steinhoff, T., Alberici, A., Villa, A., Mazzoli, F., Nicosia, F., Barbiero, L., Broglio, L., Feudatari, E., Signorini, S., Finckh, U., Nitsch, R.M. & Binetti, G. 2003, "Alzheimer disease-associated cystatin C variant undergoes impaired secretion", *Neurobiology of disease,* vol. 13, no. 1, pp. 15-21.

Bertram, L., McQueen, M.B., Mullin, K., Blacker, D. & Tanzi, R.E. 2007, "Systematic meta-analyses of Alzheimer disease genetic association studies: the AlzGene database", *Nature genetics,* vol. 39, no. 1, pp. 17-23.

Bettens, K., Sleegers, K. & Van Broeckhoven, C. 2013, "Genetic insights in Alzheimer's disease", *The Lancet Neurology,* vol. 12, no. 1, pp. 92-104.

Bhattacharya, A., Prakash, Y. & Eissa, N.T. 2014, "Secretory function of autophagy in innate immune cells", *Cellular microbiology,* vol. 16, no. 11, pp. 1637-1645.

Birk, J., Friberg, M.A., Prescianotto-Baschong, C., Spiess, M. & Rutishauser, J. 2009, "Dominant pro-vasopressin mutants that cause diabetes insipidus form disulfide-linked fibrillar aggregates in the endoplasmic reticulum", *Journal of cell science,* vol. 122, no. Pt 21, pp. 3994-4002.

Bode, W., Engh, R., Musil, D., Thiele, U., Huber, R., Karshikov, A., Brzin, J., Kos, J. & Turk, V. 1988, "The 2.0 A X-ray crystal structure of chicken egg white cystatin and its possible mode of interaction with cysteine proteinases", *The EMBO journal,* vol. 7, no. 8, pp. 2593-2599.

Bradke, F. & Dotti, C.G. 1998, "Membrane traffic in polarized neurons", *Biochimica et Biophysica Acta (BBA)-Molecular Cell Research,* vol. 1404, no. 1, pp. 245-258.

Braulke, T. & Bonifacino, J.S. 2009, "Sorting of lysosomal proteins", *Biochimica et Biophysica Acta (BBA)-Molecular Cell Research,* vol. 1793, no. 4, pp. 605-614.

Brix, K. 2005, "Lysosomal proteases" in *Lysosomes* Springer, , pp. 50-59.

Brodsky, J.L. & Schekman, R. 1993, "A Sec63p-BiP complex from yeast is required for protein translocation in a reconstituted proteoliposome", *The Journal of cell biology,* vol. 123, no. 6 Pt 1, pp. 1355-1363.

Brodsky, J.L., Schekman, R. & Goeckeler, J. 1995, "BiP and Sec63p are required for both co- and posttranslational protein translocation into the yeast endoplasmic reticulum", *Proceedings of the National Academy of Sciences of the United States of America,* vol. 92, no. 21, pp. 9643-9646.

Brown, J.D., Hann, B.C., Medzihradszky, K.F., Niwa, M., Burlingame, A.L. & Walter, P. 1994, "Subunits of the Saccharomyces cerevisiae signal recognition particle required for its functional expression", *The EMBO journal,* vol. 13, no. 18, pp. 4390-4400.

Buchberger, A., Bukau, B. & Sommer, T. 2010, "Protein quality control in the cytosol and the endoplasmic reticulum: brothers in arms", *Molecular cell,* vol. 40, no. 2, pp. 238-252.

Butler, J.M., Sharif, U., Ali, M., McKibbin, M., Thompson, J.P., Gale, R., Yang, Y.C., Inglehearn, C. & Paraoan, L. 2015, "A missense variant in CST3 exerts a recessive effect on susceptibility to age-related macular degeneration resembling its association with Alzheimer's disease", *Human genetics,* vol. 134, no. 7, pp. 705-715.

Calero, M., Pawlik, M., Soto, C., Castaño, E.M., Sigurdsson, E.M., Kumar, A., Gallo, G., Frangione, B. & Levy, E. 2001, "Distinct properties of wild-type and the amyloidogenic human cystatin C variant of hereditary cerebral hemorrhage with amyloidosis, Icelandic type", *Journal of neurochemistry,* vol. 77, no. 2, pp. 628-637.

Cappello, F., Gatti, E., Camossetto, V., David, A., Lelouard, H. & Pierre, P. 2004, "Cystatin F is secreted, but artificial modification of its C-terminus can induce its endocytic targeting", *Experimental cell research,* vol. 297, no. 2, pp. 607-618.

Chacinska, A., Koehler, C.M., Milenkovic, D., Lithgow, T. & Pfanner, N. 2009, "Importing Mitochondrial Proteins: Machineries and Mechanisms", *Cell,* vol. 138, no. 4, pp. 628-644.

Chang, Y., Ho, J.A., Hsu, S. & Wu, L. 2015, "Autophagic Regulation of Retinal Pigment Epithelium Homeostasis", *Journal of Pigmentary Disorders,* vol. 2015.

Chavan, M., Yan, A. & Lennarz, W.J. 2005, "Subunits of the translocon interact with components of the oligosaccharyl transferase complex", *The Journal of biological chemistry,* vol. 280, no. 24, pp. 22917-22924.

Chazotte, B. 2011, "Labeling mitochondria with MitoTracker dyes", *Cold Spring Harbor protocols,* vol. 2011, no. 8, pp. 990-992.

Chen, H., Lukas, T.J., Du, N., Suyeoka, G. & Neufeld, A.H. 2009, "Dysfunction of the retinal pigment epithelium with age: increased iron decreases phagocytosis

and lysosomal activity", *Investigative ophthalmology & visual science,* vol. 50, no. 4, pp. 1895-1902.

Chen, P.M., Gombart, Z.J. & Chen, J.W. 2011, "Chloroquine treatment of ARPE-19 cells leads to lysosome dilation and intracellular lipid accumulation: possible implications of lysosomal dysfunction in macular degeneration", *Cell & bioscience,* vol. 1, no. 1, pp. 1.

Chen, W., Cheng, X., Zhang, X., Zhang, Q., Sun, H., Huang, W. & Xie, Z. 2015, "The expression features of serum Cystatin C and homocysteine of Parkinson's disease with mild cognitive dysfunction", *Eur Rev Med Pharmacol Sci,* vol. 19, no. 16, pp. 2957-2963.

Chen, X., VanValkenburgh, C., Liang, H., Fang, H. & Green, N. 2001, "Signal peptidase and oligosaccharyltransferase interact in a sequential and dependent manner within the endoplasmic reticulum", *The Journal of biological chemistry,* vol. 276, no. 4, pp. 2411-2416.

Cheung, Z.H. & Ip, N.Y. 2011, "Autophagy deregulation in neurodegenerative diseases–recent advances and future perspectives", *Journal of neurochemistry,* vol. 118, no. 3, pp. 317-325.

Chirico, W.J., Waters, M.G. & Blobel, G. 1988, "70K heat shock related proteins stimulate protein translocation into microsomes", *Nature,* vol. 332, no. 6167, pp. 805-810.

Chuo, L.J., Sheu, W.H., Pai, M.C. & Kuo, Y.M. 2007, "Genotype and plasma concentration of cystatin C in patients with late-onset Alzheimer disease", *Dementia and geriatric cognitive disorders,* vol. 23, no. 4, pp. 251-257.

Cimerman, N. 2007, "Human cystatin C", *Türk Biyokimya Dergisi [Turkish Journal of Biochemistry–Turk J Biochem],* vol. 32, no. 3, pp. 95-103.

Cimerman, N., Prebanda, M.T., Turk, B., Popovič, T., Dolenc, I. & Turk, V. 1999, "Interaction of cystatin C variants with papain and human cathepsins B, H and L", *Journal of enzyme inhibition,* vol. 14, no. 2, pp. 167-174.

Conus, S. & Simon, H. 2008, "Cathepsins: key modulators of cell death and inflammatory responses", *Biochemical pharmacology,* vol. 76, no. 11, pp. 1374-1382.

Cottet, S. & Corthésy, B. 1997, "Cellular processing limits the heterologous expression of secretory component in mammalian cells", *European Journal of Biochemistry,* vol. 246, no. 1, pp. 23-31.

Coutinho, M.F., Prata, M.J. & Alves, S. 2012, "Mannose-6-phosphate pathway: a review on its role in lysosomal function and dysfunction", *Molecular genetics and metabolism,* vol. 105, no. 4, pp. 542-550.

Craven, R.A., Egerton, M. & Stirling, C.J. 1996, "A novel Hsp70 of the yeast ER lumen is required for the efficient translocation of a number of protein precursors", *The EMBO journal,* vol. 15, no. 11, pp. 2640-2650.

Crawford, F., Freeman, M., Schinka, J., Abdullah, L., Gold, M., Hartman, R., Krivian, K., Morris, M., Richards, D. & Duara, R. 2000, "A polymorphism in the cystatin C gene is a novel risk factor for late-onset Alzheimer's disease", *Neurology,* vol. 55, no. 6, pp. 763-768.

Dahl, A., Eriksson, P., Davidsson, P., Persson, A., Ekman, R. & Westman-Brinkmalm, A. 2004, "Demonstration of multiple novel glycoforms of the stem cell survival factor CCg", *Journal of neuroscience research,* vol. 77, no. 1, pp. 9-14.

Dalton, A.C. & Barton, W.A. 2014, "Over-expression of secreted proteins from mammalian cell lines", *Protein Science,* vol. 23, no. 5, pp. 517-525.

Davis, A.A., Bernstein, P.S., Bok, D., Turner, J., Nachtigal, M. & Hunt, R.C. 1995, "A human retinal pigment epithelial cell line that retains epithelial characteristics after prolonged culture", *Investigative ophthalmology & visual science,* vol. 36, no. 5, pp. 955-964.

Dean, R.A., Butler, G.S., Hamma-Kourbali, Y., Delbe, J., Brigstock, D.R., Courty, J. & Overall, C.M. 2007, "Identification of candidate angiogenic inhibitors processed by matrix metalloproteinase 2 (MMP-2) in cell-based proteomic screens: disruption of vascular endothelial growth factor (VEGF)/heparin affin regulatory peptide (pleiotrophin) and VEGF/Connective tissue growth factor angiogenic inhibitory complexes by MMP-2 proteolysis", *Molecular and cellular biology,* vol. 27, no. 24, pp. 8454-8465.

Deshaies, R.J., Sanders, S.L., Feldheim, D.A. & Schekman, R. 1991, "Assembly of yeast Sec proteins involved in translocation into the endoplasmic reticulum into a membrane-bound multisubunit complex", .

Deshaies, R.J., Koch, B.D., Werner-Washburne, M., Craig, E.A. & Schekman, R. 1988, "A subfamily of stress proteins facilitates translocation of secretory and mitochondrial precursor polypeptides", *Nature,* vol. 332, no. 6167, pp. 800-805.

Devi, L. & Anandatheerthavarada, H.K. 2010, "Mitochondrial trafficking of APP and alpha synuclein: Relevance to mitochondrial dysfunction in Alzheimer's and Parkinson's diseases", *Biochimica et Biophysica Acta - Molecular Basis of Disease,* vol. 1802, no. 1, pp. 11-19.

Devi, L., Raghavendran, V., Prabhu, B.M., Avadhani, N.G. & Anandatheerthavarada, H.K. 2008, "Mitochondrial import and accumulation of a-synuclein impair complex I in human dopaminergic neuronal cultures and Parkinson disease brain", *Journal of Biological Chemistry,* vol. 283, no. 14, pp. 9089-9100.

Dierks, T., Volkmer, J., Schlenstedt, G., Jung, C., Sandholzer, U., Zachmann, K., Schlotterhose, P., Neifer, K., Schmidt, B. & Zimmermann, R. 1996, "A microsomal ATP-binding protein involved in efficient protein transport into the mammalian endoplasmic reticulum", *The EMBO journal,* vol. 15, no. 24, pp. 6931-6942.

Doherty, G.J. & McMahon, H.T. 2009, "Mechanisms of endocytosis", *Annual Review of Biochemistry,* vol. 78, pp. 857-902.

Droga-Mazovec, G., Bojic, L., Petelin, A., Ivanova, S., Romih, R., Repnik, U., Salvesen, G.S., Stoka, V., Turk, V. & Turk, B. 2008, "Cysteine cathepsins trigger caspase-dependent cell death through cleavage of bid and antiapoptotic Bcl-2 homologues", *The Journal of biological chemistry,* vol. 283, no. 27, pp. 19140-19150.

Dunn, K., Aotaki-Keen, A., Putkey, F. & Hjelmeland, L. 1996, "ARPE-19, a human retinal pigment epithelial cell line with differentiated properties", *Experimental eye research,* vol. 62, no. 2, pp. 155-170.

Eckmann, J., Eckert, S.H., Leuner, K., Muller, W.E. & Eckert, G.P. 2013, "Mitochondria: Mitochondrial membranes in brain ageing and neurodegeneration", *International Journal of Biochemistry and Cell Biology,* vol. 45, no. 1, pp. 76-80.

Ekiel, I. & Abrahamson, M. 1996, "Folding-related dimerization of human cystatin C", *Journal of Biological Chemistry,* vol. 271, no. 3, pp. 1314-1321.

Ekström, U., Wallin, H., Lorenzo, J., Holmqvist, B., Abrahamson, M. & Avilés, F.X. 2008, "Internalization of cystatin C in human cell lines", *FEBS journal,* vol. 275, no. 18, pp. 4571-4582.

Eskelinen, E. & Saftig, P. 2009, "Autophagy: a lysosomal degradation pathway with a central role in health and disease", *Biochimica et Biophysica Acta (BBA)-Molecular Cell Research,* vol. 1793, no. 4, pp. 664-673.

Evans, E.A., Gilmore, R. & Blobel, G. 1986, "Purification of microsomal signal peptidase as a complex", *Proceedings of the National Academy of Sciences of the United States of America,* vol. 83, no. 3, pp. 581-585.

Feher, J., Kovacs, I., Artico, M., Cavallotti, C., Papale, A. & Balacco Gabrieli, C. 2006, "Mitochondrial alterations of retinal pigment epithelium in age-related macular degeneration", *Neurobiology of aging,* vol. 27, no. 7, pp. 983-993.

Feng, L. & Wang, F. 2016, "Detecting A-beta Deposition and RPE Cell Senescence in the Retinas of SAMP8 Mice", *Discovery medicine,* vol. 21, no. 115, pp. 149-158.

Ferrington, D.A., Sinha, D. & Kaarniranta, K. 2016, "Defects in retinal pigment epithelial cell proteolysis and the pathology associated with age-related macular degeneration", *Progress in retinal and eye research,* vol. 51, pp. 69-89.

Finckh, U., Von Der Kammer, H., Velden, J., Michel, T., Andresen, B., Deng, A., Zhang, J., Müller-Thomsen, T., Zuchowski, K., Menzer, G., Mann, U., Papassotiropoulos, A., Heun, R., Zurdel, J., Holst, F., Benussi, L., Stoppe, G., Reiss, J., Miserez, A.R., Staehelin, H.B., Rebeck, G.W., Hyman, B.T., Binetti, G., Hock, C., Growdon, J.H. & Nitsch, R.M. 2000, "Genetic association of a cystatin C gene polymorphism with late-onset Alzheimer disease", *Archives of Neurology,* vol. 57, no. 11, pp. 1579-1583.

Flanagan, J.J., Chen, J.C., Miao, Y., Shao, Y., Lin, J., Bock, P.E. & Johnson, A.E. 2003, "Signal recognition particle binds to ribosome-bound signal sequences with fluorescence-detected subnanomolar affinity that does not diminish as the nascent chain lengthens", *The Journal of biological chemistry,* vol. 278, no. 20, pp. 18628-18637.

Flores-Bellver, M., Bonet-Ponce, L., Barcia, J., Garcia-Verdugo, J., Martinez-Gil, N., Saez-Atienzar, S., Sancho-Pelluz, J., Jordan, J., Galindo, M. & Romero, F. 2014, "Autophagy and mitochondrial alterations in human retinal pigment epithelial cells induced by ethanol: implications of 4-hydroxy-nonenal", *Cell death & disease,* vol. 5, no. 7, pp. e1328.

Fons, R.D., Bogert, B.A. & Hegde, R.S. 2003, "Substrate-specific function of the translocon-associated protein complex during translocation across the ER membrane", *The Journal of cell biology,* vol. 160, no. 4, pp. 529-539.

García-Arencibia, M., Hochfeld, W.E., Toh, P.P. & Rubinsztein, D.C. 2010, "Autophagy, a guardian against neurodegeneration", *Seminars in cell & developmental biology*Elsevier, , pp. 691.

Gauthier, S., Kaur, G., Mi, W., Tizon, B. & Levy, E. 2011, "Protective mechanisms by cystatin C in neurodegenerative diseases", *Frontiers in bioscience (Scholar edition),* vol. 3, pp. 541-554.

Gehrs, K.M., Anderson, D.H., Johnson, L.V. & Hageman, G.S. 2006, "Age-related macular degeneration—emerging pathogenetic and therapeutic concepts", *Annals of Medicine,* vol. 38, no. 7, pp. 450-471.

Ghidoni, R., Benussi, L., Paterlini, A., Missale, C., Usardi, A., Rossi, R., Barbiero, L., Spano, P. & Binetti, G. 2007, "Presenilin 2 mutations alter cystatin C trafficking in mouse primary neurons", *Neurobiology of aging,* vol. 28, no. 3, pp. 371-376.

Ghidoni, R., Benussi, L., Glionna, M., Desenzani, S., Albertini, V., Levy, E., Emanuele, E. & Binetti, G. 2010, "Plasma cystatin c and risk of developing Alzheimer's disease in subjects with mild cognitive impairment", *Journal of Alzheimer's Disease,* vol. 22, no. 3, pp. 985-991.

Ghidoni, R., Benussi, L., Paterlini, A., Albertini, V., Binetti, G. & Emanuele, E. 2011a, "Cerebrospinal fluid biomarkers for Alzheimer's disease: The present and the future", *Neurodegenerative Diseases,* vol. 8, no. 6, pp. 413-420.

Ghidoni, R., Paterlini, A., Albertini, V., Glionna, M., Monti, E., Schiaffonati, L., Benussi, L., Levy, E. & Binetti, G. 2011b, "Cystatin C is released in association with exosomes: A new tool of neuronal communication which is unbalanced in Alzheimer's disease", *Neurobiology of aging,* vol. 32, no. 8, pp. 1435-1442.

Giepmans, B.N., Adams, S.R., Ellisman, M.H. & Tsien, R.Y. 2006, "The fluorescent toolbox for assessing protein location and function", *Science (New York, N.Y.),* vol. 312, no. 5771, pp. 217-224.

Glenn, J.V., Mahaffy, H., Wu, K., Smith, G., Nagai, R., Simpson, D.A., Boulton, M.E. & Stitt, A.W. 2009, "Advanced glycation end product (AGE) accumulation on Bruch's membrane: links to age-related RPE dysfunction", *Investigative ophthalmology & visual science,* vol. 50, no. 1, pp. 441-451.

Goder, V. & Spiess, M. 2003, "Molecular mechanism of signal sequence orientation in the endoplasmic reticulum", *The EMBO journal,* vol. 22, no. 14, pp. 3645-3653.

Gong, X., Harrell, M., Mitchell, D., Sundin, O. & Rubin, L. 2014, "A new human retinal pigment epithelial cell model for interrogating the protective functions of xanthophylls in retinopathies (39.2)", *The FASEB Journal,* vol. 28, no. 1 Supplement, pp. 39.2.

González, C. & Bejarano, L.A. 2000, "Protein traps: using intracellular localization for cloning", *Trends in cell biology,* vol. 10, no. 4, pp. 162-165.

Görlich, D., Prehn, S., Hartmann, E., Kalies, K. & Rapoport, T.A. 1992, "A mammalian homolog of SEC61p and SECYp is associated with ribosomes and nascent polypeptides during translocation", *Cell,* vol. 71, no. 3, pp. 489-503.

Görlich, D. & Rapoport, T.A. 1993, "Protein translocation into proteoliposomes reconstituted from purified components of the endoplasmic reticulum membrane", *Cell,* vol. 75, no. 4, pp. 615-630.

Grant, S.M., Shankar, S.L., Chalmers-Redman, R.M.E., Tatton, W.G., Szyf, M. & Cuello, A.C. 1999, "Mitochondrial abnormalities in neuroectodermal cells stably expressing human amyloid precursor protein (hAPP751)", *Neuroreport,* vol. 10, no. 1, pp. 41-46.

Gu, F., Crump, C. & Thomas, G. 2001, "Trans-Golgi network sorting", *Cellular and Molecular Life Sciences CMLS,* vol. 58, no. 8, pp. 1067-1084.

Guha, S., Liu, J., Baltazar, G., Laties, A.M. & Mitchell, C.H. 2014, "Rescue of compromised lysosomes enhances degradation of photoreceptor outer segments and reduces lipofuscin-like autofluorescence in retinal pigmented epithelial cells" in *Retinal Degenerative Diseases* Springer, , pp. 105-111.

Guha, S. & Padh, H. 2008, "Cathepsins: fundamental effectors of endolysosomal proteolysis", *Indian Journal of Biochemistry and Biophysics,* vol. 45, no. 2, pp. 75.

Halic, M., Becker, T., Pool, M.R., Spahn, C.M., Grassucci, R.A., Frank, J. & Beckmann, R. 2004, "Structure of the signal recognition particle interacting with the elongation-arrested ribosome", *Nature,* vol. 427, no. 6977, pp. 808-814.

Hamilton, G., Colbert, J.D., Schuettelkopf, A.W. & Watts, C. 2008, "Cystatin F is a cathepsin C-directed protease inhibitor regulated by proteolysis", *The EMBO journal,* vol. 27, no. 3, pp. 499-508.

Han, Y.H., Moon, H.J., You, B.R. & Park, W.H. 2009, "The effect of MG132, a proteasome inhibitor on HeLa cells in relation to cell growth, reactive oxygen species and GSH.", *Oncology reports,* vol. 22, no. 1, pp. 215.

Hatsuzawa, K., Tagaya, M. & Mizushima, S. 1997, "The hydrophobic region of signal peptides is a determinant for SRP recognition and protein translocation across the ER membrane", *Journal of Biochemistry,* vol. 121, no. 2, pp. 270-277.

He, R., Shen, J., Zhao, J., Zeng, H., Li, L., Zhao, J., Liu, F. & Jia, W. 2013, "High cystatin C levels predict severe retinopathy in type 2 diabetes patients", *European journal of epidemiology,* vol. 28, no. 9, pp. 775.

Hegde, R.S. & Bernstein, H.D. 2006, "The surprising complexity of signal sequences", *Trends in biochemical sciences,* vol. 31, no. 10, pp. 563-571.

Hegde, R.S. & Ploegh, H.L. 2010, "Quality and quantity control at the endoplasmic reticulum", *Current opinion in cell biology,* vol. 22, no. 4, pp. 437-446.

Heijne, G. 1983, "Patterns of amino acids near signal-sequence cleavage sites", *European journal of biochemistry,* vol. 133, no. 1, pp. 17-21.

Helisalmi, S., Vakeva, A., Hiltunen, M. & Soininen, H. 2009, "Flanking markers of cystatin c (CST3) gene do not show association with Alzheimer's disease", *Dementia and geriatric cognitive disorders,* vol. 27, no. 4, pp. 318-321.

High, S. & Dobberstein, B. 1991, "The signal sequence interacts with the methionine-rich domain of the 54-kD protein of signal recognition particle", *The Journal of cell biology,* vol. 113, no. 2, pp. 229-233.

Hipp, M.S., Park, S. & Hartl, F.U. 2014, "Proteostasis impairment in protein-misfolding and-aggregation diseases", *Trends in cell biology,* vol. 24, no. 9, pp. 506-514.

Hirai, K., Aliev, G., Nunomura, A., Fujioka, H., Russell, R.L., Atwood, C.S., Johnson, A.B., Kress, Y., Vinters, H.V., Tabaton, M., Shimohama, S., Cash, A.D., Siedlak, S.L., Harris, P.L.R., Jones, P.K., Petersen, R.B., Perry, G. & Smith, M.A. 2001, "Mitochondrial abnormalities in Alzheimer's disease", *Journal of Neuroscience,* vol. 21, no. 9, pp. 3017-3023.

Horie-Inoue, K. & Inoue, S. 2014, "Genomic aspects of age-related macular degeneration", *Biochemical and biophysical research communications,* vol. 452, no. 2, pp. 263-275.

Hu, Y., Hung, A.C., Cui, H., Dawkins, E., Bolos, M., Foa, L., Young, K.M. & Small, D.H. 2013, "Role of cystatin C in amyloid precursor protein-induced proliferation of neural stem/progenitor cells", *The Journal of biological chemistry,* vol. 288, no. 26, pp. 18853-18862.

Hua, Y., Zhao, H., Lu, X., Kong, Y. & Jin, H. 2012, "Meta-analysis of the cystatin C (CST3) gene G73A polymorphism and susceptibility to Alzheimer's disease", *International Journal of Neuroscience,* vol. 122, no. 8, pp. 431-438.

Huotari, J. & Helenius, A. 2011, "Endosome maturation", *The EMBO journal,* vol. 30, no. 17, pp. 3481-3500.

Ito, M., Oiso, Y., Murase, T., Kondo, K., Saito, H., Chinzei, T., Racchi, M. & Lively, M.O. 1993, "Possible involvement of inefficient cleavage of preprovasopressin by signal peptidase as a cause for familial central diabetes insipidus", *The Journal of clinical investigation,* vol. 91, no. 6, pp. 2565-2571.

Ito, M., Yu, R.N. & Jameson, J.L. 1999, "Mutant vasopressin precursors that cause autosomal dominant neurohypophyseal diabetes insipidus retain dimerization and impair the secretion of wild-type proteins", *The Journal of biological chemistry,* vol. 274, no. 13, pp. 9029-9037.

Jager, R.D., Mieler, W.F. & Miller, J.W. 2008, "Age-related macular degeneration", *New England Journal of Medicine,* vol. 358, no. 24, pp. 2606-2617.

Jaiswal, J.K., Andrews, N.W. & Simon, S.M. 2002, "Membrane proximal lysosomes are the major vesicles responsible for calcium-dependent exocytosis in nonsecretory cells", *The Journal of cell biology,* vol. 159, no. 4, pp. 625-635.

Janowski, R., Abrahamson, M., Grubb, A. & Jaskolski, M. 2004, "Domain swapping in N-truncated human cystatin C", *Journal of Molecular Biology,* vol. 341, no. 1, pp. 151-160.

Janowski, R., Kozak, M., Abrahamson, M., Grubb, A. & Jaskolski, M. 2005, "3D domain-swapped human cystatin C with amyloidlike intermolecular ß-sheets", *Proteins: Structure, Function and Genetics,* vol. 61, no. 3, pp. 570-578.

Janowski, R., Kozak, M., Jankowska, E., Grzonka, Z., Grubb, A., Abrahamson, M. & Jaskolski, M. 2001, "Human cystatin C, an amyloidogenic protein, dimerizes through three-dimensional domain swapping", *Nature structural biology,* vol. 8, no. 4, pp. 316-320.

Jarjanazi, H., Savas, S., Pabalan, N., Dennis, J.W. & Ozcelik, H. 2008, "Biological implications of SNPs in signal peptide domains of human proteins", *Proteins: Structure, Function, and Bioinformatics,* vol. 70, no. 2, pp. 394-403.

Jarrett, S.G. & Boulton, M.E. 2012, "Consequences of oxidative stress in age-related macular degeneration", *Molecular aspects of medicine,* vol. 33, no. 4, pp. 399-417.

Jarrett, S.G., Lin, H., Godley, B.F. & Boulton, M.E. 2008, "Mitochondrial DNA damage and its potential role in retinal degeneration", *Progress in retinal and eye research,* vol. 27, no. 6, pp. 596-607.

Johnson, N., Vilardi, F., Lang, S., Leznicki, P., Zimmermann, R. & High, S. 2012, "TRC40 can deliver short secretory proteins to the Sec61 translocon", *Journal of cell science,* vol. 125, no. Pt 15, pp. 3612-3620.

Joshi, P., Benussi, L., Furlan, R., Ghidoni, R. & Verderio, C. 2015, "Extracellular vesicles in Alzheimer's disease: friends or foes? Focus on aβ-vesicle interaction", *International journal of molecular sciences,* vol. 16, no. 3, pp. 4800-4813.

Kaarniranta, K., Salminen, A., Haapasalo, A., Soininen, H. & Hiltunen, M. 2011, "Age-related macular degeneration (AMD): Alzheimer's disease in the eye?", *Journal of Alzheimer's Disease,* vol. 24, no. 4, pp. 615-631.

Kaarniranta, K., Sinha, D., Blasiak, J., Kauppinen, A., Veréb, Z., Salminen, A., Boulton, M.E. & Petrovski, G. 2013, "Autophagy and heterophagy dysregulation leads to retinal pigment epithelium dysfunction and development of age-related macular degeneration", *Autophagy,* vol. 9, no. 7, pp. 973-984.

Kaarniranta, K., Hyttinen, J., Ryhanen, T., Viiri, J., Paimela, T., Toropainen, E., Sorri, I. & Salminen, A. 2010, "Mechanisms of protein aggregation in the retinal

pigment epithelial cells", *Frontiers in bioscience (Elite edition),* vol. 2, pp. 1374-1384.

Kaeser, S.A., Herzig, M.C., Coomaraswamy, J., Kilger, E., Selenica, M., Winkler, D.T., Staufenbiel, M., Levy, E., Grubb, A. & Jucker, M. 2007, "Cystatin C modulates cerebral β-amyloidosis", *Nature genetics,* vol. 39, no. 12, pp. 1437-1439.

Karunadharma, P.P., Nordgaard, C.L., Olsen, T.W. & Ferrington, D.A. 2010, "Mitochondrial DNA damage as a potential mechanism for Age-Related macular Degeneration", *Investigative Ophthalmology and Visual Science,* vol. 51, no. 11, pp. 5470-5479.

Kaseda, R., Iino, N., Hosojima, M., Takeda, T., Hosaka, K., Kobayashi, A., Yamamoto, K., Suzuki, A., Kasai, A. & Suzuki, Y. 2007, "Megalin-mediated endocytosis of cystatin C in proximal tubule cells", *Biochemical and biophysical research communications,* vol. 357, no. 4, pp. 1130-1134.

Kaur, G. & Levy, E. 2012, "Cystatin C in Alzheimer's disease", *Frontiers in Molecular Neuroscience,* , no. JULY 2012.

Kaur, G., Mohan, P., Pawlik, M., DeRosa, S., Fajiculay, J., Che, S., Grubb, A., Ginsberg, S.D., Nixon, R.A. & Levy, E. 2010, "Cystatin C rescues degenerating neurons in a cystatin B-knockout mouse model of progressive myoclonus epilepsy", *The American Journal Of Pathology,* vol. 177, no. 5, pp. 2256-2267.

Kay, P., Yang, Y.C., Hiscott, P., Gray, D., Maminishkis, A. & Paraoan, L. 2014, "Age-Related Changes of Cystatin C Expression and Polarized Secretion by Retinal Pigment Epithelium: Potential Age-Related Macular Degeneration LinksAge-Related Decline of Cystatin C Secretion by RPE", *Investigative ophthalmology & visual science,* vol. 55, no. 2, pp. 926-934.

Kay, P., Yang, Y.C. & Paraoan, L. 2013, "Directional protein secretion by the retinal pigment epithelium: roles in retinal health and the development of age-related macular degeneration", *Journal of Cellular and Molecular Medicine,* vol. 17, no. 7, pp. 833-843.

Keppler, D. 2006, "Towards novel anti-cancer strategies based on cystatin function", *Cancer letters,* vol. 235, no. 2, pp. 159-176.

Kim, D.H. & Hwang, I. 2013, "Direct targeting of proteins from the cytosol to organelles: the ER versus endosymbiotic organelles", *Traffic,* vol. 14, no. 6, pp. 613-621.

Kim, R., Emi, M., Tanabe, K. & Murakami, S. 2006, "Role of the unfolded protein response in cell death", *Apoptosis,* vol. 11, no. 1, pp. 5-13.

Kinnunen, K., Petrovski, G., Moe, M.C., Berta, A. & Kaarniranta, K. 2012, "Molecular mechanisms of retinal pigment epithelium damage and development of age-related macular degeneration", *Acta Ophthalmologica,* vol. 90, no. 4, pp. 299-309.

Klausner, R.D., Donaldson, J.G. & Lippincott-Schwartz, J. 1992, "Brefeldin A: insights into the control of membrane traffic and organelle structure", *J.Cell Biol,* vol. 116, no. 5, pp. 1071-1080.

Klein, R., Knudtson, M.D., Lee, K.E. & Klein, B.E.K. 2009, "Serum cystatin C level, kidney disease markers, and incidence of age-related macular degeneration: the Beaver Dam Eye Study", *Archives of Ophthalmology,* vol. 127, no. 2, pp. 193-199.

Klettner, A., Kauppinen, A., Blasiak, J., Roider, J., Salminen, A. & Kaarniranta, K. 2013, "Cellular and molecular mechanisms of age-related macular degeneration: from impaired autophagy to neovascularization", *The international journal of biochemistry & cell biology,* vol. 45, no. 7, pp. 1457-1467.

Kocik, L., Junne, T. & Spiess, M. 2012, "Orientation of internal signal-anchor sequences at the Sec61 translocon", *Journal of Molecular Biology,* vol. 424, no. 5, pp. 368-378.

Kornmann, B., Currie, E., Collins, S.R., Schuldiner, M., Nunnari, J., Weissman, J.S. & Walter, P. 2009, "An ER-mitochondria tethering complex revealed by a synthetic biology screen", *Science (New York, N.Y.),* vol. 325, no. 5939, pp. 477-481.

Kozak, M. 1992, "Regulation of translation in eukaryotic systems", *Annual Review of Cell Biology,* vol. 8, no. 1, pp. 197-225.

Kozak, M., Jankowska, E., Janowski, R., Grzonka, Z., Grubb, A., Fernandez, M.A., Abrahamson, M. & Jaskolski, M. 1999, "Expression of a selenomethionyl derivative and preliminary crystallographic studies of human cystatin C", *Acta Crystallographica Section D: Biological Crystallography,* vol. 55, no. 11, pp. 1939-1942.

Lakkaraju, A.K., Thankappan, R., Mary, C., Garrison, J.L., Taunton, J. & Strub, K. 2012, "Efficient secretion of small proteins in mammalian cells relies on Sec62-dependent posttranslational translocation", *Molecular biology of the cell,* vol. 23, no. 14, pp. 2712-2722.

Laurent-Matha, V., Huesgen, P.F., Masson, O., Derocq, D., Prebois, C., Gary-Bobo, M., Lecaille, F., Rebiere, B., Meurice, G., Orear, C., Hollingsworth, R.E., Abrahamson, M., Lalmanach, G., Overall, C.M. & Liaudet-Coopman, E. 2012, "Proteolysis of cystatin C by cathepsin D in the breast cancer

microenvironment", *FASEB journal : official publication of the Federation of American Societies for Experimental Biology,* vol. 26, no. 12, pp. 5172-5181.

Lecker, S.H., Goldberg, A.L. & Mitch, W.E. 2006, "Protein degradation by the ubiquitin-proteasome pathway in normal and disease states", *Journal of the American Society of Nephrology : JASN,* vol. 17, no. 7, pp. 1807-1819.

Lenarčič, B., Krašovec, M., Ritonja, A., Olafsson, I. & Turk, V. 1991, "Inactivation of human cystatin C and kininogen by human cathepsin D", *FEBS letters,* vol. 280, no. 2, pp. 211-215.

Levy, E., Sastre, M., Kumar, A., Gallo, G., Piccardo, P., Ghetti, B. & Tagliavini, F. 2001, "Codeposition of Cystatin C with Amyloid-[beta] Protein in the Brain of Alzheimer Disease Patients", *Journal of Neuropathology & Experimental Neurology,* vol. 60, no. 1, pp. 94-104.

Li, W., Sultana, N., Siraj, N., Ward, L.J., Pawlik, M., Levy, E., Jovinge, S., Bengtsson, E. & Yuan, X. 2016, "Autophagy dysfunction and regulatory cystatin C in macrophage death of atherosclerosis", *Journal of Cellular and Molecular Medicine,* .

Liang, X., Nagai, A., Terashima, M., Sheikh, A.M., Shiota, Y., Mitaki, S., Kim, S.U. & Yamaguchi, S. 2011, "Cystatin C induces apoptosis and tyrosine hydroxylase gene expression through JNK-dependent pathway in neuronal cells", *Neuroscience letters,* vol. 496, no. 2, pp. 100-105.

Lisenbee, C.S., Karnik, S.K. & Trelease, R.N. 2003, "Overexpression and mislocalization of a Tail-Anchored GFP redefines the identity of peroxisomal ER", *Traffic,* vol. 4, no. 7, pp. 491-501.

Liu, K. & Xie, B. 2012, "Today and future of age-related macular degeneration", *ISRN ophthalmology,* vol. 2012.

Liu, Y., Cai, H., Wang, Z., Li, J., Wang, K., Yu, Z. & Chen, G. 2013, "Induction of autophagy by cystatin C: a potential mechanism for prevention of cerebral vasospasm after experimental subarachnoid hemorrhage", *European journal of medical research,* vol. 18, no. 1, pp. 1.

Liu, Y., Li, J., Wang, Z., Yu, Z. & Chen, G. 2014, "Attenuation of early brain injury and learning deficits following experimental subarachnoid hemorrhage secondary to cystatin C: possible involvement of the autophagy pathway", *Molecular neurobiology,* vol. 49, no. 2, pp. 1043-1054.

Liu, G., Zhang, C., Yin, J., Li, X., Cheng, F., Li, Y., Yang, H., Uéda, K., Chan, P. & Yu, S. 2009, "a-Synuclein is differentially expressed in mitochondria from different rat brain regions and dose-dependently down-regulates complex I activity", *Neuroscience letters,* vol. 454, no. 3, pp. 187-192.

Liu, M., Lara-Lemus, R., Shan, S.O., Wright, J., Haataja, L., Barbetti, F., Guo, H., Larkin, D. & Arvan, P. 2012, "Impaired cleavage of preproinsulin signal peptide linked to autosomal-dominant diabetes", *Diabetes,* vol. 61, no. 4, pp. 828-837.

Locke, C.J., Congrove, N.R., Dismuke, W.M., Bowen, T.J., Stamer, W.D. & McKay, B.S. 2014, "Controlled exosome release from the retinal pigment epithelium in situ", *Experimental eye research,* vol. 129, pp. 1-4.

Logue, M.W., Schu, M., Vardarajan, B.N., Farrell, J., Lunetta, K.L., Jun, G., Baldwin, C.T., DeAngelis, M.M. & Farrer, L.A. 2014, "A search for age-related macular degeneration risk variants in Alzheimer disease genes and pathways", *Neurobiology of aging,* vol. 35, no. 6, pp. 1510. e7-1510. e18.

Lyko, F., Martoglio, B., Jungnickel, B., Rapoport, T.A. & Dobberstein, B. 1995, "Signal sequence processing in rough microsomes", *Journal of Biological Chemistry,* vol. 270, no. 34, pp. 19873-19878.

Maetzler, W., Schmid, B., Synofzik, M., Schulte, C., Riester, K., Huber, H., Brockmann, K., Gasser, T., Berg, D. & Melms, A. 2010, "The CST3 BB genotype and low cystatin C cerebrospinal fluid levels are associated with dementia in Lewy body disease", *Journal of Alzheimer's Disease,* vol. 19, no. 3, pp. 937-942.

Maley, F., Trimble, R.B., Tarentino, A.L. & Plummer, T.H. 1989, "Characterization of glycoproteins and their associated oligosaccharides through the use of endoglycosidases", *Analytical Biochemistry,* vol. 180, no. 2, pp. 195-204.

Marques, C., Oliveira, C.S.F., Alves, S., Chaves, S., Coutinho, O., Côrte-Real, M. & Preto, A. 2013, "Acetate-induced apoptosis in colorectal carcinoma cells involves lysosomal membrane permeabilization and cathepsin D release", *Cell death & disease,* vol. 4, no. 2, pp. e507.

Maruyama, H., Izumi, Y., Oda, M., Torii, T., Morino, H., Toji, H., Sasaki, K., Terasawa, H., Nakamura, S. & Kawakami, H. 2001, "Lack of an association between cystatin C gene polymorphisms in Japanese patients with Alzheimer's disease", *Neurology,* vol. 57, no. 2, pp. 337-339.

Massotte, D. 2003, "G protein-coupled receptor overexpression with the baculovirus–insect cell system: a tool for structural and functional studies", *Biochimica et Biophysica Acta (BBA)-Biomembranes,* vol. 1610, no. 1, pp. 77-89.

Mathews, P.M. & Levy, E. 2016, "Cystatin C in aging and in Alzheimer's disease", *Ageing Research Reviews,* .

Matlack, K.E., Misselwitz, B., Plath, K. & Rapoport, T.A. 1999, "BiP acts as a molecular ratchet during posttranslational transport of prepro-α factor across the ER membrane", *Cell,* vol. 97, no. 5, pp. 553-564.

Meléndez, A. & Levine, B. 2005, "Autophagy in C. elegans", .

Merz, G.S., Benedikz, E., Schwenk, V., Johansen, T.E., Vogel, L.K., Rushbrook, J.I. & Wisniewski, H.M. 1997, "Human cystatin C forms an inactive dimer during intracellular trafficking in transfected CHO cells", *Journal of cellular physiology,* vol. 173, no. 3, pp. 423-432.

Meyer, H. & Hartmann, E. 1997, "The yeast SPC22/23 homolog Spc3p is essential for signal peptidase activity", *Journal of Biological Chemistry,* vol. 272, no. 20, pp. 13159-13164.

Meyer, H.A., Grau, H., Kraft, R., Kostka, S., Prehn, S., Kalies, K.U. & Hartmann, E. 2000, "Mammalian Sec61 is associated with Sec62 and Sec63", *The Journal of biological chemistry,* vol. 275, no. 19, pp. 14550-14557.

Mi, W., Jung, S.S., Yu, H., Schmidt, S.D., Nixon, R.A., Mathews, P.M., Tagliavini, F. & Levy, E. 2009, "Complexes of amyloid-β and cystatin C in the human central nervous system", *Journal of Alzheimer's Disease,* vol. 18, no. 2, pp. 273-280.

Mi, W., Pawlik, M., Sastre, M., Jung, S.S., Radvinsky, D.S., Klein, A.M., Sommer, J., Schmidt, S.D., Nixon, R.A. & Mathews, P.M. 2007, "Cystatin C inhibits amyloid-β deposition in Alzheimer's disease mouse models", *Nature genetics,* vol. 39, no. 12, pp. 1440-1442.

Misselwitz, B., Staeck, O., Matlack, K.E. & Rapoport, T.A. 1999, "Interaction of BiP with the J-domain of the Sec63p component of the endoplasmic reticulum protein translocation complex", *The Journal of biological chemistry,* vol. 274, no. 29, pp. 20110-20115.

Mitter, S.K., Song, C., Qi, X., Mao, H., Rao, H., Akin, D., Lewin, A., Grant, M., Dunn Jr, W. & Ding, J. 2014, "Dysregulated autophagy in the RPE is associated with increased susceptibility to oxidative stress and AMD", *Autophagy,* vol. 10, no. 11, pp. 1989-2005.

Miyawaki, A., Sawano, A. & Kogure, T. 2003, "Lighting up cells: labelling proteins with fluorophores", *Nature cell biology,* vol. Suppl, pp. S1-7.

Mollenhauer, H.H., Morré, D.J. & Rowe, L.D. 1990, "Alteration of intracellular traffic by monensin; mechanism, specificity and relationship to toxicity", *Biochimica et Biophysica Acta (BBA)-Reviews on Biomembranes,* vol. 1031, no. 2, pp. 225-246.

Monastero, R., Camarda, C., Cefalu, A.B., Caldarella, R., Camarda, L.K., Noto, D., Averna, M.R. & Camarda, R. 2005, "No association between the cystatin C gene polymorphism and Alzheimer's disease: a case-control study in an Italian population", *Journal of Alzheimer's Disease,* vol. 7, no. 4, pp. 291-295.

Moreira, P.I., Zhu, X., Wang, X., Lee, H., Nunomura, A., Petersen, R.B., Perry, G. & Smith, M.A. 2010, "Mitochondria: A therapeutic target in neurodegeneration", *Biochimica et Biophysica Acta (BBA) - Molecular Basis of Disease,* vol. 1802, no. 1, pp. 212-220.

Mori, J., Tanikawa, C., Funauchi, Y., Lo, P.H.Y., Nakamura, Y. & Matsuda, K. 2016, "Cystatin C as a p53-inducible apoptotic mediator that regulates cathepsin L activity", *Cancer science,* .

Mueller-Steiner, S., Zhou, Y., Arai, H., Roberson, E.D., Sun, B., Chen, J., Wang, X., Yu, G., Esposito, L. & Mucke, L. 2006, "Antiamyloidogenic and neuroprotective functions of cathepsin B: implications for Alzheimer's disease", *Neuron,* vol. 51, no. 6, pp. 703-714.

Nacmias, B., Bagnoli, S., Tedde, A., Cellini, E., Guarnieri, B.M., Bartoli, A., Serio, A., Piacentini, S. & Sorbi, S. 2006, "Cystatin C and apoe polymorphisms in Italian Alzheimer's disease", *Neuroscience letters,* vol. 392, no. 1, pp. 110-113.

Nagai, A., Ryu, J.K., Terashima, M., Tanigawa, Y., Wakabayashi, K., McLarnon, J.G., Kobayashi, S., Masuda, J. & Kim, S.U. 2005, "Neuronal cell death induced by cystatin C in vivo and in cultured human CNS neurons is inhibited with cathepsin B", *Brain research,* vol. 1066, no. 1, pp. 120-128.

Nedelsky, N.B., Todd, P.K. & Taylor, J.P. 2008, "Autophagy and the ubiquitin-proteasome system: collaborators in neuroprotection", *Biochimica et Biophysica Acta (BBA)-Molecular Basis of Disease,* vol. 1782, no. 12, pp. 691-699.

Nejsum, L.N. & Nelson, W.J. 2009, "Epithelial cell surface polarity: the early steps", *Frontiers in bioscience (Landmark edition),* vol. 14, pp. 1088-1098.

Ng, D.T., Brown, J.D. & Walter, P. 1996, "Signal sequences specify the targeting route to the endoplasmic reticulum membrane", *The Journal of cell biology,* vol. 134, no. 2, pp. 269-278.

Nguyen, A. & Hulleman, J.D. 2016, "Evidence of alternative cystatin c signal sequence cleavage which is influenced by the A25T polymorphism", *PloS one,* vol. 11, no. 2, pp. e0147684.

Ni, J., Fernandez, M.A., Danielsson, L., Chillakuru, R.A., Zhang, J., Grubb, A., Su, J., Gentz, R. & Abrahamson, M. 1998, "Cystatin F is a glycosylated human low molecular weight cysteine proteinase inhibitor", *Journal of Biological Chemistry,* vol. 273, no. 38, pp. 24797-24804.

Nickel, W. & Wieland, F.T. 1998, "Biosynthetic protein transport through the early secretory pathway", *Histochemistry and cell biology,* vol. 109, no. 5-6, pp. 477-486.

Nickel, W. 2005, "Unconventional secretory routes: direct protein export across the plasma membrane of mammalian cells", *Traffic,* vol. 6, no. 8, pp. 607-614.

Nickel, W. & Rabouille, C. 2009, "Mechanisms of regulated unconventional protein secretion", *Nature Reviews Molecular Cell Biology,* vol. 10, no. 2, pp. 148-155.

Nielsen, J. 2013, "Production of biopharmaceutical proteins by yeast: advances through metabolic engineering", *Bioengineered,* vol. 4, no. 4, pp. 207-211.

Nilsson, I., Lara, P., Hessa, T., Johnson, A.E., von Heijne, G. & Karamyshev, A.L. 2015, "The code for directing proteins for translocation across ER membrane: SRP cotranslationally recognizes specific features of a signal sequence", *Journal of Molecular Biology,* vol. 427, no. 6, pp. 1191-1201.

Nilsson, J., Rüetschi, U., Halim, A., Hesse, C., Carlsohn, E., Brinkmalm, G. & Larson, G. 2009, "Enrichment of glycopeptides for glycan structure and attachment site identification", *Nature methods,* vol. 6, no. 11, pp. 809-811.

Nilsson, M., Wang, X., Rodziewicz-Motowidlo, S., Janowski, R., Lindström, V., Önnerfjord, P., Westermark, G., Grzonka, Z., Jaskolski, M. & Grubb, A. 2004, "Prevention of domain swapping inhibits dimerization and amyloid fibril formation of cystatin C. Use of engineered disulfide bridges, antibodies, and carboxymethylpapain to stabilize the monomeric form of cystatin C", *Journal of Biological Chemistry,* vol. 279, no. 23, pp. 24236-24245.

Nishio, C., Yoshida, K., Nishiyama, K., Hatanaka, H. & Yamada, M. 2000, "Involvement of cystatin C in oxidative stress-induced apoptosis of cultured rat CNS neurons", *Brain research,* vol. 873, no. 2, pp. 252-262.

Nishiyama, K., Konishi, A., Nishio, C., Araki-Yoshida, K., Hatanaka, H., Kojima, M., Ohmiya, Y., Yamada, M. & Koshimizu, H. 2005, "Expression of cystatin C prevents oxidative stress-induced death in PC12 cells", *Brain research bulletin,* vol. 67, no. 1, pp. 94-99.

Nordgaard, C.L., Karunadharma, P.P., Feng, X., Olsen, T.W. & Ferrington, D.A. 2008, "Mitochondrial proteomics of the retinal pigment epithelium at progressive stages of age-related macular degeneration", *Investigative Ophthalmology and Visual Science,* vol. 49, no. 7, pp. 2848-2855.

Nothwehr, S.F. & Gordon, J.I. 1990, "Structural features in the NH2-terminal region of a model eukaryotic signal peptide influence the site of its cleavage by signal peptidase", *The Journal of biological chemistry,* vol. 265, no. 28, pp. 17202-17208.

Noto, D., Cefalu, A.B., Barbagallo, C.M., Pace, A., Rizzo, M., Marino, G., Caldarella, R., Castello, A., Pernice, V. & Notarbartolo, A. 2005, "Cystatin C levels are decreased in acute myocardial infarction: effect of cystatin C G73A gene

polymorphism on plasma levels", *International journal of cardiology,* vol. 101, no. 2, pp. 213-217.

Nyathi, Y., Wilkinson, B.M. & Pool, M.R. 2013, "Co-translational targeting and translocation of proteins to the endoplasmic reticulum", *Biochimica et Biophysica Acta (BBA)-Molecular Cell Research,* vol. 1833, no. 11, pp. 2392-2402.

Nycander, M., Estrada, S., Mort, J.S., Abrahamson, M. & Björk, I. 1998, "Two-step mechanism of inhibition of cathepsin B by cystatin C due to displacement of the proteinase occluding loop", *FEBS letters,* vol. 422, no. 1, pp. 61-64.

Obrig, T.G., Culp, W.J., McKeehan, W.L. & Hardesty, B. 1971, "The mechanism by which cycloheximide and related glutarimide antibiotics inhibit peptide synthesis on reticulocyte ribosomes", *The Journal of biological chemistry,* vol. 246, no. 1, pp. 174-181.

Ochieng, J. & Chaudhuri, G. 2010, "Cystatin superfamily", *Journal of health care for the poor and underserved,* vol. 21, no. 1 Suppl, pp. 51-70.

Ohno-Matsui, K. 2011, "Parallel findings in age-related macular degeneration and Alzheimer's disease", *Progress in retinal and eye research,* vol. 30, no. 4, pp. 217-238.

Pagano, R.E., Martin, O.C., Kang, H.C. & Haugland, R.P. 1991, "A novel fluorescent ceramide analogue for studying membrane traffic in animal cells: accumulation at the Golgi apparatus results in altered spectral properties of the sphingolipid precursor", *J Cell Biol,* vol. 113, no. 6, pp. 1267-1279.

Panzner, S., Dreier, L., Hartmann, E., Kostka, S. & Rapoport, T.A. 1995, "Article: Posttranslational protein transport in yeast reconstituted with a purified complex of Sec proteins and Kar2p", *Cell,* vol. 81, pp. 561-570.

Paraoan, L. & Grierson, I. 2007, "Focus on Molecules: Cystatin C", *Experimental eye research,* vol. 84, no. 6, pp. 1019-1020.

Paraoan, L., Grierson, I. & Maden, B.E.H. 2003, "Fate of cystatin C lacking the leader sequence in RPE cells", *Experimental eye research,* vol. 76, no. 6, pp. 753-756.

Paraoan, L., Grierson, I. & Maden, B.E.H. 2000, "Analysis of expressed sequence tags of retinal pigment epithelium: Cystatin C is an abundant transcript", *International Journal of Biochemistry and Cell Biology,* vol. 32, no. 4, pp. 417-426.

Paraoan, L., Hiscott, P., Gosden, C. & Grierson, I. 2010, "Cystatin C in macular and neuronal degenerations: Implications for mechanism(s) of age-related macular degeneration", *Vision research,* vol. 50, no. 7, pp. 737-742.

Paraoan, L., Ratnayaka, A., Spiller, D.G., Hiscott, P., White, M.R.H. & Grierson, I. 2004, "Unexpected intracellular localization of the AMD-associated cystatin C variant", *Traffic,* vol. 5, no. 11, pp. 884-895.

Paraoan, L., White, M.R.H., Spiller, D.G., Grierson, I. & Maden, B.E.H. 2001, "Precursor cystatin C in cultured retinal pigment epithelium cells: Evidence for processing through the secretory pathway", *Molecular membrane biology,* vol. 18, no. 3, pp. 229-236.

Peterson, J.H., Woolhead, C.A. & Bernstein, H.D. 2003, "Basic amino acids in a distinct subset of signal peptides promote interaction with the signal recognition particle", *The Journal of biological chemistry,* vol. 278, no. 46, pp. 46155-46162.

Pfanner, N., Craig, E.A. & Hönlinger, A. 1997, "Mitochondrial preprotein translocase", *Annual Review of Cell and Developmental Biology,* vol. 13, no. 1, pp. 25-51.

Phillips, M.J. & Voeltz, G.K. 2015, "Structure and function of ER membrane contact sites with other organelles", *Nature Reviews Molecular Cell Biology,* .

Pirttilä, T.J., Lukasiuk, K., Håkansson, K., Grubb, A., Abrahamson, M. & Pitkänen, A. 2005, "Cystatin C modulates neurodegeneration and neurogenesis following status epilepticus in mouse", *Neurobiology of disease,* vol. 20, no. 2, pp. 241-253.

Plath, K., Mothes, W., Wilkinson, B.M., Stirling, C.J. & Rapoport, T.A. 1998, "Signal sequence recognition in posttranslational protein transport across the yeast ER membrane", *Cell,* vol. 94, no. 6, pp. 795-807.

Ponchel, F., Toomes, C., Bransfield, K., Leong, F.T., Douglas, S.H., Field, S.L., Bell, S.M., Combaret, V., Puisieux, A. & Mighell, A.J. 2003, "Real-time PCR based on SYBR-Green I fluorescence: an alternative to the TaqMan assay for a relative quantification of gene rearrangements, gene amplifications and micro gene deletions", *BMC biotechnology,* vol. 3, no. 1, pp. 18.

Pool, M.R. 2009, "A trans-membrane segment inside the ribosome exit tunnel triggers RAMP4 recruitment to the Sec61p translocase", *The Journal of cell biology,* vol. 185, no. 5, pp. 889-902.

Popovič, T., Cimerman, N., Dolenc, I., Ritonja, A. & Brzin, J. 1999, "Cathepsin L is capable of truncating cystatin C of 11 N-terminal amino acids", *FEBS letters,* vol. 455, no. 1-2, pp. 92-96.

Racchi, M., Watzke, H.H., High, K.A. & Lively, M.O. 1993, "Human coagulation factor X deficiency caused by a mutant signal peptide that blocks cleavage by signal

peptidase but not targeting and translocation to the endoplasmic reticulum", *The Journal of biological chemistry,* vol. 268, no. 8, pp. 5735-5740.

Rakoczy, P.E., Zhang, D., Robertson, T., Barnett, N.L., Papadimitriou, J., Constable, I.J. & Lai, C. 2002, "Progressive age-related changes similar to age-related macular degeneration in a transgenic mouse model", *The American journal of pathology,* vol. 161, no. 4, pp. 1515-1524.

Rao, X., Huang, X., Zhou, Z. & Lin, X. 2013, "An improvement of the 2^(-delta delta CT) method for quantitative real-time polymerase chain reaction data analysis", *Biostatistics, bioinformatics and biomathematics,* vol. 3, no. 3, pp. 71-85.

Raposo, G. & Stoorvogel, W. 2013, "Extracellular vesicles: exosomes, microvesicles, and friends", *The Journal of cell biology,* vol. 200, no. 4, pp. 373-383.

Ratnayaka, A., Paraoan, L., Spiller, D.G., Hiscott, P., Nelson, G., White, M.R.H. & Grierson, I. 2007, "A dual Golgi- and mitochondria-localised Ala25Ser precursor cystatin C: An additional tool for characterising intracellular mis-localisation leading to increased AMD susceptibility", *Experimental eye research,* vol. 84, no. 6, pp. 1135-1139.

Repnik, U., Cesen, M.H. & Turk, B. 2013, "The endolysosomal system in cell death and survival", *Cold Spring Harbor perspectives in biology,* vol. 5, no. 1, pp. a008755.

Rodriguez, A., Webster, P., Ortego, J. & Andrews, N.W. 1997, "Lysosomes behave as Ca2+-regulated exocytic vesicles in fibroblasts and epithelial cells", *The Journal of cell biology,* vol. 137, no. 1, pp. 93-104.

Rodziewicz-Motowidlo, S., Wahlbom, M., Wang, X., La˛giewka, J., Janowski, R., Jaskólski, M., Grubb, A. & Grzonka, Z. 2006, "Checking the conformational stability of cystatin C and its L68Q variant by molecular dynamics studies: Why is the L68Q variant amyloidogenic?", *Journal of structural biology,* vol. 154, no. 1, pp. 68-78.

Roks, G., Cruts, M., Slooter, A.J., Dermaut, B., Hofman, A., Van Broeckhoven, C. & Van Duijn, C.M. 2001, "The cystatin C polymorphism is not associated with early onset Alzheimer's disease", *Neurology,* vol. 57, no. 2, pp. 366-367.

Rosch, K., Naeher, D., Laird, V., Goder, V. & Spiess, M. 2000, "The topogenic contribution of uncharged amino acids on signal sequence orientation in the endoplasmic reticulum", *The Journal of biological chemistry,* vol. 275, no. 20, pp. 14916-14922.

Rutishauser, J.a. & Spiess, M. 2002, "Endoplasmic reticulum storage diseases", *Swiss medical weekly,* vol. 132, no. 17/18, pp. 211-222.

Rutkowski, D.T., Ott, C.M., Polansky, J.R. & Lingappa, V.R. 2003, "Signal sequences initiate the pathway of maturation in the endoplasmic reticulum lumen", *The Journal of biological chemistry,* vol. 278, no. 32, pp. 30365-30372.

Salminen, A., Kauppinen, A., Hyttinen, J., Toropainen, E. & Kaarniranta, K. 2010, "Endoplasmic reticulum stress in age-related macular degeneration: trigger for neovascularization", *Mol Med,* vol. 16, no. 11-12, pp. 535-542.

Sant'Anna, R., Navarro, S., Ventura, S., Paraoan, L. & Foguel, D. 2016, "Amyloid properties of the leader peptide of variant B cystatin C: implications for Alzheimer and macular degeneration", *FEBS letters,* vol. 590, no. 5, pp. 644-654.

Sastre, M., Calero, M., Pawlik, M., Mathews, P.M., Kumar, A., Danilov, V., Schmidt, S.D., Nixon, R.A., Frangione, B. & Levy, E. 2004, "Binding of cystatin C to Alzheimer's amyloid ß inhibits in vitro amyloid fibril formation", *Neurobiology of aging,* vol. 25, no. 8, pp. 1033-1043.

Schedin-Weiss, S., Winblad, B. & Tjernberg, L.O. 2014, "The role of protein glycosylation in Alzheimer disease", *FEBS Journal,* vol. 281, no. 1, pp. 46-62.

Scherer, W.F., Syverton, J.T. & Gey, G.O. 1953, "Studies on the propagation in vitro of poliomyelitis viruses. IV. Viral multiplication in a stable strain of human malignant epithelial cells (strain HeLa) derived from an epidermoid carcinoma of the cervix", *The Journal of experimental medicine,* vol. 97, no. 5, pp. 695-710.

Schmidt, O., Pfanner, N. & Meisinger, C. 2010, "Mitochondrial protein import: from proteomics to functional mechanisms", *Nature reviews Molecular cell biology,* vol. 11, no. 9, pp. 655-667.

Schrul, B., Kapp, K., Sinning, I. & Dobberstein, B. 2010, "Signal peptide peptidase (SPP) assembles with substrates and misfolded membrane proteins into distinct oligomeric complexes", *The Biochemical journal,* vol. 427, no. 3, pp. 523-534.

Schulte, S., Sun, J., Libby, P., MacFarlane, L., Sun, C., Lopez-Ilasaca, M., Shi, G. & Sukhova, G.K. 2010, "Cystatin C deficiency promotes inflammation in angiotensin II–induced abdominal aortic aneurisms in atherosclerotic mice", *The American journal of pathology,* vol. 177, no. 1, pp. 456-463.

Searle, B.C. 2010, "Scaffold: a bioinformatic tool for validating MS/MS-based proteomic studies", *Proteomics,* vol. 10, no. 6, pp. 1265-1269.

Seibel, N.M., Eljouni, J., Nalaskowski, M.M. & Hampe, W. 2007, "Nuclear localization of enhanced green fluorescent protein homomultimers", *Analytical Biochemistry,* vol. 368, no. 1, pp. 95-99.

Shah, N., Kuntz, D.A. & Rose, D.R. 2008, "Golgi alpha-mannosidase II cleaves two sugars sequentially in the same catalytic site", *Proceedings of the National Academy of Sciences of the United States of America,* vol. 105, no. 28, pp. 9570-9575.

Shao, S. & Hegde, R.S. 2011, "A calmodulin-dependent translocation pathway for small secretory proteins", *Cell,* vol. 147, no. 7, pp. 1576-1588.

Shaw, A.S., Peter, J.M.R. & Rose, J.K. 1988, *Evidence for the Loop Model of Signal-Sequence Insertion into the Endoplasmic Reticulum*, National Academy of Sciences of the United States of America.

Shlipak, M.G., Matsushita, K., Ärnlöv, J., Inker, L.A., Katz, R., Polkinghorne, K.R., Rothenbacher, D., Sarnak, M.J., Astor, B.C. & Coresh, J. 2013, "Cystatin C versus creatinine in determining risk based on kidney function", *New England Journal of Medicine,* vol. 369, no. 10, pp. 932-943.

Singh, P., Sharma, L., Kulothungan, S.R., Adkar, B.V., Prajapati, R.S., Ali, P.S.S., Krishnan, B. & Varadarajan, R. 2013, "Effect of signal peptide on stability and folding of Escherichia coli thioredoxin", *PloS one,* vol. 8, no. 5, pp. e63442.

Soh, H., Venkatesan, N., Veena, M.S., Ravichandran, S., Zinabadi, A., Basak, S.K., Parvatiyar, K., Srivastava, M., Liang, L.J., Gjertson, D.W., Torres, J.Z., Moatamed, N.A. & Srivatsan, E.S. 2016, "Cystatin E/M Suppresses Tumor Cell Growth through Cytoplasmic Retention of NF-kappaB", *Molecular and cellular biology,* vol. 36, no. 12, pp. 1776-1792.

Sokol, J.P. & Schiemann, W.P. 2004, "Cystatin C antagonizes transforming growth factor beta signaling in normal and cancer cells", *Molecular cancer research : MCR,* vol. 2, no. 3, pp. 183-195.

Solomon, V.R. & Lee, H. 2009, "Chloroquine and its analogs: a new promise of an old drug for effective and safe cancer therapies", *European journal of pharmacology,* vol. 625, no. 1, pp. 220-233.

Sonenberg, N. & Hinnebusch, A.G. 2009, "Regulation of translation initiation in eukaryotes: mechanisms and biological targets", *Cell,* vol. 136, no. 4, pp. 731-745.

Stanley, P. 2011, "Golgi glycosylation", *Cold Spring Harbor perspectives in biology,* vol. 3, no. 4, pp. 10.1101/cshperspect.a005199.

Steen, P.V.d., Rudd, P.M., Dwek, R.A. & Opdenakker, G. 1998, "Concepts and principles of O-linked glycosylation", *Critical reviews in biochemistry and molecular biology,* vol. 33, no. 3, pp. 151-208.

Stirling, C.J., Rothblatt, J., Hosobuchi, M., Deshaies, R. & Schekman, R. 1992, "Protein translocation mutants defective in the insertion of integral membrane proteins into the endoplasmic reticulum", *Molecular biology of the cell,* vol. 3, no. 2, pp. 129-142.

Strauss, O. 2005, "The retinal pigment epithelium in visual function", *Physiological Reviews,* vol. 85, no. 3, pp. 845-881.

Sun, B., Zhou, Y., Halabisky, B., Lo, I., Cho, S., Mueller-Steiner, S., Devidze, N., Wang, X., Grubb, A. & Gan, L. 2008, "Cystatin C-cathepsin B axis regulates amyloid beta levels and associated neuronal deficits in an animal model of Alzheimer's disease", *Neuron,* vol. 60, no. 2, pp. 247-257.

Sundelöf, J., Sundström, J., Hansson, O., Eriksdotter-Jönhagen, M., Giedraitis, V., Larsson, A., Degerman-Gunnarsson, M., Ingelsson, M., Minthon, L., Blennow, K., Kilander, L., Basun, H. & Lannfelt, L. 2010, "Cystatin C Levels are Positively Correlated with both Aβ42 and Tau Levels in Cerebrospinal Fluid in Persons with Alzheimer's Disease, Mild Cognitive Impairment, and Healthy Controls", *Journal of Alzheimer's Disease,* vol. 21, no. 2, pp. 471-478.

Sundelof, J., Arnlov, J., Ingelsson, E., Sundstrom, J., Basu, S., Zethelius, B., Larsson, A., Irizarry, M.C., Giedraitis, V., Ronnemaa, E., Degerman-Gunnarsson, M., Hyman, B.T., Basun, H., Kilander, L. & Lannfelt, L. 2008, "Serum cystatin C and the risk of Alzheimer disease in elderly men", *Neurology,* vol. 71, no. 14, pp. 1072-1079.

Suzuki, Y., Jin, C. & Yazawa, I. 2014, "Cystatin C triggers neuronal degeneration in a model of multiple system atrophy", *The American journal of pathology,* vol. 184, no. 3, pp. 790-799.

Szymańska, A., Radulska, A., Czaplewska, P., Grubb, A., Grzonka, Z. & Rodziewicz-Motowidło, S. 2009, "Governing the monomer-dimer ratio of human cystatin c by single amino acid substitution in the hinge region", *Acta Biochim.Pol,* vol. 56, no. 3, pp. 455-463.

Takeyama, N., Miki, S., Hirakawa, A. & Tanaka, T. 2002, "Role of the mitochondrial permeability transition and cytochrome C release in hydrogen peroxide-induced apoptosis", *Experimental cell research,* vol. 274, no. 1, pp. 16-24.

Terpos, E., Katodritou, E., Tsiftsakis, E., Kastritis, E., Christoulas, D., Pouli, A., Michalis, E., Verrou, E., Anargyrou, K., Tsionos, K., Dimopoulos, M.A., Zervas, K. & Greek Myeloma Study Group 2009, "Cystatin-C is an independent prognostic factor for survival in multiple myeloma and is reduced by bortezomib administration", *Haematologica,* vol. 94, no. 3, pp. 372-379.

Thumann, G., Hoffmann, S. & Hinton, D. 2006, "Cell biology of the retinal pigment epithelium", *Retina,* vol. 1, pp. 137-152.

Thyberg, J. & Moskalewski, S. 1999, "Role of microtubules in the organization of the Golgi complex", *Experimental cell research,* vol. 246, no. 2, pp. 263-279.

Tizon, B., Ribe, E.M., Mi, W., Troy, C.M. & Levy, E. 2010a, "Cystatin C protects neuronal cells from amyloid-β-induced toxicity", *Journal of Alzheimer's Disease,* vol. 19, no. 3, pp. 885-894.

Tizon, B., Sahoo, S., Yu, H., Gauthier, S., Kumar, A.R., Mohan, P., Figliola, M., Pawlik, M., Grubb, A., Uchiyama, Y., Bandyopadhyay, U., Cuervo, A.M., Nixon, R.A. & Levy, E. 2010b, "Induction of Autophagy by Cystatin C: A Mechanism That Protects Murine Primary Cortical Neurons and Neuronal Cell Lines", *PLoS ONE,* vol. 5, no. 3, pp. 1-12.

Tong, Y., Zhou, Y., Wang, Y., Zhao, P. & Wang, Z. 2016, "Retinal Pigment Epithelium Cell-derived Exosomes: Possible Relevance to CNV in Wet-age Related Macular Degeneration", *Medical hypotheses,* .

Trucco, A., Polishchuk, R.S., Martella, O., Di Pentima, A., Fusella, A., Di Giandomenico, D., San Pietro, E., Beznoussenko, G.V., Polishchuk, E.V. & Baldassarre, M. 2004, "Secretory traffic triggers the formation of tubular continuities across Golgi sub-compartments", *Nature cell biology,* vol. 6, no. 11, pp. 1071-1081.

Tsai, B., Ye, Y. & Rapoport, T.A. 2002, "Retro-translocation of proteins from the endoplasmic reticulum into the cytosol", *Nature reviews Molecular cell biology,* vol. 3, no. 4, pp. 246-255.

Tseng, W.A., Thein, T., Kinnunen, K., Lashkari, K., Gregory, M.S., D'Amore, P.A. & Ksander, B.R. 2013, "NLRP3 Inflammasome Activation in Retinal Pigment Epithelial Cells by Lysosomal Destabilization: Implications for Age-Related Macular DegenerationNLRP3 Inflammasome Activity in RPE Cells", *Investigative ophthalmology & visual science,* vol. 54, no. 1, pp. 110-120.

Tsien, R.Y. 1998, "The green fluorescent protein", *Annual Review of Biochemistry,* vol. 67, no. 1, pp. 509-544.

Tsiolaki, P.L., Louros, N.N., Hamodrakas, S.J. & Iconomidou, V.A. 2015, "Exploring the 'aggregation-prone'core of human Cystatin C: A structural study", *Journal of structural biology,* vol. 191, no. 3, pp. 272-280.

Turk, V. & Bode, W. 1991, "The cystatins: protein inhibitors of cysteine proteinases", *FEBS letters,* vol. 285, no. 2, pp. 213-219.

Turk, V., Stoka, V. & Turk, D. 2008, "Cystatins: biochemical and structural properties, and medical relevance", *Front Biosci,* vol. 13, no. 5, pp. 5780-5786.

Turk, V., Stoka, V., Vasiljeva, O., Renko, M., Sun, T., Turk, B. & Turk, D. 2012, "Cysteine cathepsins: from structure, function and regulation to new frontiers", *Biochimica et Biophysica Acta (BBA)-Proteins and Proteomics,* vol. 1824, no. 1, pp. 68-88.

Tyedmers, J., Lerner, M., Wiedmann, M., Volkmer, J. & Zimmermann, R. 2003, "Polypeptide-binding proteins mediate completion of co-translational protein translocation into the mammalian endoplasmic reticulum", *EMBO reports,* vol. 4, no. 5, pp. 505-510.

Urbizu, A., Canet-Pons, J., Munoz-Marmol, A.M., Aldecoa, I., Lopez, M.T., Compta, Y., Alvarez, R., Ispierto, L., Tolosa, E. & Ariza, A. 2015, "Cystatin C is differentially involved in multiple system atrophy phenotypes", *Neuropathology and applied neurobiology,* vol. 41, no. 4, pp. 507-519.

Vella, L.J., Sharples, R.A., Nisbet, R.M., Cappai, R. & Hill, A.F. 2008, "The role of exosomes in the processing of proteins associated with neurodegenerative diseases", *European Biophysics Journal,* vol. 37, no. 3, pp. 323-332.

Vilchez, D., Saez, I. & Dillin, A. 2014, "The role of protein clearance mechanisms in organismal ageing and age-related diseases", *Nature communications,* vol. 5.

Voigt, S., Jungnickel, B., Hartmann, E. & Rapoport, T.A. 1996, "Signal sequence-dependent function of the TRAM protein during early phases of protein transport across the endoplasmic reticulum membrane", *The Journal of cell biology,* vol. 134, no. 1, pp. 25-35.

von Heijne, G. 1985, "Signal sequences: the limits of variation", *Journal of Molecular Biology,* vol. 184, no. 1, pp. 99-105.

von Heijne, G. 1984, "Analysis of the distribution of charged residues in the N-terminal region of signal sequences: implications for protein export in prokaryotic and eukaryotic cells", *The EMBO journal,* vol. 3, no. 10, pp. 2315-2318.

Wallin, H., Bjarnadottir, M., Vogel, L.K., Wassélius, J., Ekström, U. & Abrahamson, M. 2010, "Cystatins–Extra-and intracellular cysteine protease inhibitors: High-level secretion and uptake of cystatin C in human neuroblastoma cells", *Biochimie,* vol. 92, no. 11, pp. 1625-1634.

Wallin, H., Abrahamson, M. & Ekstrom, U. 2013, "Cystatin C properties crucial for uptake and inhibition of intracellular target enzymes", *The Journal of biological chemistry,* vol. 288, no. 23, pp. 17019-17029.

Walter, P. & Blobel, G. 1981, "Translocation of proteins across the endoplasmic reticulum. II. Signal recognition protein (SRP) mediates the selective binding to

microsomal membranes of in-vitro-assembled polysomes synthesizing secretory protein", *The Journal of cell biology,* vol. 91, no. 2 Pt 1, pp. 551-556.

Wang, A.L., Lukas, T.J., Yuan, M., Du, N., Tso, M.O. & Neufeld, A.H. 2009, "Autophagy and exosomes in the aged retinal pigment epithelium: possible relevance to drusen formation and age-related macular degeneration", *PloS one,* vol. 4, no. 1, pp. e4160.

Wang, B., Xie, Y.C., Yang, Z., Peng, D., Wang, J., Zhou, S., Li, S. & Ma, X. 2008, "Lack of an association between Alzheimer's disease and the cystatin C (CST3) gene G73A polymorphism in Mainland Chinese", *Dementia and geriatric cognitive disorders,* vol. 25, no. 5, pp. 461-464.

Wang, C., Sun, B., Zhou, Y., Grubb, A. & Gan, L. 2012, "Cathepsin B degrades amyloid-beta in mice expressing wild-type human amyloid precursor protein", *The Journal of biological chemistry,* vol. 287, no. 47, pp. 39834-39841.

Wasselius, J., Håkansson, K., Abrahamson, M. & Ehinger, B. 2004, "Cystatin C in the anterior segment of rat and mouse eyes", *Acta Ophthalmologica Scandinavica,* vol. 82, no. 1, pp. 68-75.

Wassélius, J., Håkansson, K., Johansson, K., Abrahamson, M. & Ehinger, B. 2001, "Identification and localization of retinal cystatin C", *Investigative ophthalmology & visual science,* vol. 42, no. 8, pp. 1901-1906.

Wassélius, J., Johansson, K., Håkansson, K., Abrahamson, M. & Ehinger, B. 2005, "Cystatin C uptake in the eye", *Graefe's Archive for Clinical and Experimental Ophthalmology,* vol. 243, no. 6, pp. 583-592.

Watanabe, S., Hayakawa, T., Wakasugi, K. & Yamanaka, K. 2014, "Cystatin C protects neuronal cells against mutant copper-zinc superoxide dismutase-mediated toxicity", *Cell death & disease,* vol. 5, no. 10, pp. e1497.

Wei, L., Berman, Y., Castano, E.M., Cadene, M., Beavis, R.C., Devi, L. & Levy, E. 1998, "Instability of the amyloidogenic cystatin C variant of hereditary cerebral hemorrhage with amyloidosis, Icelandic type", *The Journal of biological chemistry,* vol. 273, no. 19, pp. 11806-11814.

Wilson, M.E., Boumaza, I., Lacomis, D. & Bowser, R. 2010, "Cystatin C: A Candidate Biomarker for Amyotrophic Lateral Sclerosis", *PLoS ONE,* vol. 5, no. 12.

Wu, H., Niu, H., Wu, C., Li, Y., Wang, K., Zhang, J., Wang, Y. & Yang, S. 2016, "The autophagy–lysosomal system in subarachnoid haemorrhage", *Journal of Cellular and Molecular Medicine,* .

Xie, L., Terrand, J., Xu, B., Tsaprailis, G., Boyer, J. & Chen, Q.M. 2010, "Cystatin C increases in cardiac injury: a role in extracellular matrix protein modulation", *Cardiovascular research,* vol. 87, no. 4, pp. 628-635.

Xu, L., Sheng, J., Tang, Z., Wu, X., Yu, Y., Guo, H., Shen, Y., Zhou, C., Paraoan, L. & Zhou, J. 2005, "Cystatin C prevents degeneration of rat nigral dopaminergic neurons: in vitro and in vivo studies", *Neurobiology of disease,* vol. 18, no. 1, pp. 152-165.

Xu, Y., Ding, Y., Li, X. & Wu, X. 2015, "Cystatin C is a disease-associated protein subject to multiple regulation", *Immunology and cell biology,* vol. 93, no. 5, pp. 442-451.

Xu, Y., Lindemann, P., Vega-Ramos, J., Zhang, J.G. & Villadangos, J.A. 2014, "Developmental regulation of synthesis and dimerization of the amyloidogenic protease inhibitor cystatin C in the hematopoietic system", *The Journal of biological chemistry,* vol. 289, no. 14, pp. 9730-9740.

Yamamoto-Watanabe, Y., Watanabe, M., Jackson, M., Akimoto, H., Sugimoto, K., Yasujima, M., Wakasaya, Y., Matsubara, E., Kawarabayashi, T. & Harigaya, Y. 2010, "Quantification of cystatin C in cerebrospinal fluid from various neurological disorders and correlation with G73A polymorphism in CST3", *Brain research,* vol. 1361, pp. 140-145.

Yoon, Y.H., Cho, K.S., Hwang, J.J., Lee, S., Choi, J.A. & Koh, J. 2010, "Induction of lysosomal dilatation, arrested autophagy, and cell death by chloroquine in cultured ARPE-19 cells", *Investigative ophthalmology & visual science,* vol. 51, no. 11, pp. 6030-6037.

Young, B.P., Craven, R.A., Reid, P.J., Willer, M. & Stirling, C.J. 2001, "Sec63p and Kar2p are required for the translocation of SRP-dependent precursors into the yeast endoplasmic reticulum in vivo", *The EMBO journal,* vol. 20, no. 1-2, pp. 262-271.

Zdolsek, J.M. & Svensson, I. 1993, "Effect of reactive oxygen species on lysosomal membrane integrity", *Virchows Archiv B,* vol. 64, no. 1, pp. 401-406.

Žerovnik, E. 2009, "The emerging role of cystatins in Alzheimer's disease", *Bioessays,* vol. 31, no. 6, pp. 597-599.

Zhan, J., He, J., Zhou, Y., Wu, M., Liu, Y., Shang, F. & Zhang, X. 2016, "Crosstalk Between the Autophagy-Lysosome Pathway and the Ubiquitin-Proteasome Pathway in Retinal Pigment Epithelial Cells", *Current Molecular Medicine,* vol. 16, no. 5, pp. 487-495.

Zhang, J., Campbell, R.E., Ting, A.Y. & Tsien, R.Y. 2002, "Creating new fluorescent probes for cell biology", *Nature reviews Molecular cell biology,* vol. 3, no. 12, pp. 906-918.

Zhao, Y., Bhattacharjee, S., Jones, B.M., Hill, J.M., Clement, C., Sambamurti, K., Dua, P. & Lukiw, W.J. 2015, "Beta-amyloid precursor protein (βAPP) processing in Alzheimer's disease (AD) and age-related macular degeneration (AMD)", *Molecular neurobiology,* vol. 52, no. 1, pp. 533-544.

Zhong, X., Hou, L., Luo, X., Shi, H., Hu, G., He, H., Chen, X., Zheng, D., Zhang, Y. & Tan, Y. 2013, "Alterations of CSF Cystatin C Levels and Their Correlations with CSF Aβ40 and Aβ42 Levels in Patients with Alzheimer's Disease, Dementia with Lewy Bodies and the Atrophic Form of General Paresis", *PloS one,* vol. 8, no. 1, pp. e55328.

Zhu, M., Ni, W., Dong, Y. & Wu, Z. 2013, "EGFP tags affect cellular localization of ATP7B mutants", *CNS neuroscience & therapeutics,* vol. 19, no. 5, pp. 346-351.

Zipper, H., Brunner, H., Bernhagen, J. & Vitzthum, F. 2004, "Investigations on DNA intercalation and surface binding by SYBR Green I, its structure determination and methodological implications", *Nucleic acids research,* vol. 32, no. 12, pp. e103.

Zopf, D., Bernstein, H.D. & Walter, P. 1993, "GTPase domain of the 54-kD subunit of the mammalian signal recognition particle is required for protein translocation but not for signal sequence binding", *The Journal of cell biology,* vol. 120, no. 5, pp. 1113-1121.

Zurdel, J., Finckh, U., Menzer, G., Nitsch, R.M. & Richard, G. 2002, "CST3 genotype associated with exudative age related macular degeneration", *British Journal of Ophthalmology,* vol. 86, no. 2, pp. 214-219.

APPENDIX 1: Buffer Recipes

- 1x TAE buffer:

  40 mM Tris (pH 7.6), 20 mM acetic acid, 1 mM EDTA

- Resolving buffer:

  3 M Tris (pH 8.85)

- Stacking buffer:

  0.25 M Tris (pH 6.8)

- 5X Running buffer

  0.125 M Tris, 1.25 M Glycine, 0.5% SDS

- Transfer buffer

  0.0125 M Tris, 0.125 M Glycine, 0.05% SDS, 23.3% Ethanol

- RIPA buffer

  50 mM Tris, 150 mM NaCl, 1mM EDTA, 1%NP-40, 0.25% Sodium-deoxycholate, protease inhibitors

- 5X Laemmli buffer (loading buffer)

  125 mM Tris (pH 6.8), 20% Glycerol, 4% SDS, 0.625 M β-mercaptoethanol, bromophenol blue

- Mitochondrial Isolation Buffer (MIB)

  20 mM Hepes-KOH, 15 mM KCl, 1.5 mM MgCl2, 250 mM Sucrose, 1 mM EDTA, protease inhibitors